Ferrochrome waste management - addressing current gaps

SP du Preez

orcid.org/ 0000-0001-5214-3693

Thesis submitted for the degree *Doctor of Philosophy in Chemistry* at the North-West University

Promoter: Prof JP Beukes

Co-promoter: Prof PG van Zyl

Graduation May 2018

21220212

NWU®

NORTH-WEST UNIVERSITY
NOORDWES-UNIVERSITEIT
UNIBESITI YA BOKONE-BOPHIRIMA

SOLEM DECLARATION

I, ***Stephanus Petrus du Preez***, declare herewith that the thesis entitled:

Ferrochrome waste management - addressing current gaps,

which I herewith submit to the North-West University (NWU) as completion of the requirement set for the ***Doctor in Philosophiae in Chemistry*** degree, is my own work, unless specifically indicated otherwise, has been text edited as required, and has not been submitted to any other tertiary institution other than the NWU.

Signature of the candidate:  University number: **21220212**

Signed at **Potchefstroom** on **20 November 2017**

ACKNOWLEDGMENTS

"A sluggard's appetite is never filled, but the desires of the diligent are fully satisfied"

Proverbs 12:4

God Almighty, thank you for the strength and perseverance to undertake each task that came across my path. Without your grace and love, I am nothing.

I would sincerely like to thank and convey my most genuine gratitude towards the following people for their support, assistance and guidance during the past three years. They played a vital role in the completion of my thesis and helped me to grow both academically and as a person.

My supervisor Prof Paul Beukes, and co-supervisor Dr Pieter van Zyl. I am endlessly thankful for your excellent guidance, patience, and the critical roles that both of you played in my personal and academical growth.

Prof Dogan Paktunc. Your expertise and willingness to assist contributed significantly toward the success of my thesis.

My parents, Faan and Yvonne, and siblings Johan, Bennie and Yolandi, thank you for your support and encouragement.

My better half, Michelle Eagleton. Thank you for your unconditional love, and support. You kept me focused and helped me to persevere throughout my PhD studies. I am truly grateful for having you in my life.

The National Research Foundation (NRF) for financial assistance towards this research (grant number: 101345).

PREFACE

Introduction

This thesis was submitted in article format, as allowed by the North-West University (NWU) under the General Academic Rules (A-rules) set for post-graduate curricula. The A-rules prescribed that "...where a candidate is permitted to submit a thesis in the form of a published research article or articles or as an unpublished manuscript or manuscripts in article format and more than one such article or manuscript is used, the thesis must still be presented as a unit, supplemented with an inclusive problem statement, a focused literature analysis and integration and with a synoptic conclusion….". Thus, due to the aforementioned, the articles included in this PhD thesis were added as they were published/submitted/drafted in/for a specific journal, depending at which stage the specific article was at the time the thesis was submitted for examination. Some conventional chapters, i.e. experimental, as well as results and discussions, were therefore excluded from the thesis, since the relevant information is presented in each respective article (Chapters 3 to 5). Separate motivation and objectives (Chapter 1), literature survey (Chapter 2), as well as conclusions and project evaluation (Chapter 6) chapters, were included along with the articles. Some repetition of ideas and similar text in some of the chapters and articles do occur, as some information presented in the motivation and objectives, literature survey, as well as conclusions and project evaluation chapters were summarized in the articles. This repetition is therefore a result of the format in which the thesis is submitted and is beyond the candidate's control. Furthermore, the fonts, numbering, and layout of Chapters 3, 4 and 5 (containing the research articles) are not consistent with the rest of the thesis, since they were included as published (Chapter 3), or in generic article format (Chapter 4 and 5, in preparation for submission to accredited peer reviewed journals).

Rationale in submitting thesis in article format

Submitting a PhD thesis in article format is allowed by the NWU, however, it is not a requirement of the NWU's A-rules. It is prescribed in the A-rules that with the submission of a non-article format thesis, the faculty may require proof that at the time of submitting the thesis for examination, the candidate has prepared a draft article ready for submission, or submit proof that a research article has already been submitted to an accredited journal. However, in practice, many of these draft articles are never submitted to accredited peer-reviewed journals.

Some advantages of submitting a PhD thesis in article format include: (i) it increases the likelihood that the conducted work will be published, which is advantageous to the candidate, supervisor(s), and the university in general, (ii) articles submitted for publication are reviewed by experts in the respective field, which is implemented by the candidate to improve the article(s). This not only improves the thesis's quality, but also gives the candidate (as well as supervisors and examiners) greater confidence in the conducted work, and (iii) it resolves the conflict between preparing articles for publication and the thesis for examination, as the writing of the thesis often enjoys priority, resulting in a lot of research results not getting published in the peer-reviewed public domain.

At the time when his thesis was submitted for examination, two articles presented in Chapter 3 and Appendix A had already been published in *Water SA* (ISSN: 1816-7950) and *Journal of Cleaner Production* (ISSN: 0959-6526), respectively. The articles included in Chapter 4 and 5 were ready for submission to *Resources, Conservation and Recycling* (ISSN: 0921-3449) and *Metallurgical and Materials Transactions B* (ISSN: 1073-5615), respectively.

Declaration by co-authors

All of the co-authors, i.e. J.P. Beukes, P.G. van Zyl, D. Paktunc, L.R. Tiedt, A. Jordaan, M.M. Loock-Hatting, and W.P.J. van Dalen, which contributed towards the various articles included in this thesis, have been informed that the respective articles will form part of the candidate's PhD, submitted in article format, and have granted permission that the articles may be used for the purpose stated.

ABSTRACT

Various chromium (Cr) compounds, Cr metal and/or Cr-containing alloys are used in modern society. By volume the largest application for Cr is in the production of stainless steel, which owes its corrosion resistance mainly to the inclusion of Cr. Stainless steel is mostly produced from recycled scrap and ferrochrome (FeCr), a relatively crude alloy between Cr and iron (Fe). FeCr is mainly produced by the carbothermic reduction of chromite in submerged arc furnaces (SAFs) and direct current (DC) arc furnaces. Various wastes are generated during FeCr production, depending on the production route used. By reviewing the production routes, three currently applied wastes handling strategies were identified as requiring improvement, which were subsequently investigated.

The first waste handling strategy investigated was the leaching of Cr(VI) from bag filter dust (BFD), originating from semi-closed SAF off-gas cleaning (results presented in Chapter 3). Small amounts of Cr(VI) are unintentionally formed during FeCr production. BFD contains the highest concentration of Cr(VI) of all FeCr wastes. Currently, BFD is contacted with water and treated to chemically reduce Cr(VI) before it is disposed in fit-for-purpose slimes dams. A major concern for FeCr producers is the presence of relatively high Cr(VI) concentrations in slimes dams, notwithstanding the treatment prior to disposal. The results presented in this study proved that the currently applied Cr(VI) treatment strategies of FeCr producer (with process water pH $\leq$ 9) only effectively extract and treat the water-soluble Cr(VI) compounds, which merely represent approximately 31% of the total Cr(VI) present in BFD. Extended extraction time, within the afore-mentioned pH range (pH $\leq$ 9), proved futile in extracting sparingly and water-insoluble Cr(VI) species, which represented approximately 34 and 35% of the total Cr(VI), respectively. Due to the deficiencies of the current treatment strategies, it is highly likely that sparingly water-soluble Cr(VI) compounds will leach from

waste storage facilities (e.g. slimes dams) over time. Therefore, it is critical that improved Cr(VI) treatment strategies be formulated, which should be an important future perspective for FeCr producers and researchers alike.

The second waste handling strategy investigated was the flaring of CO-rich off-gas (results presented in Chapter 4). The majority of cleaned CO-rich off-gas (after most of the particles have been removed) generated by closed SAF and DC furnace is flared on stacks. This is done, since the storing of large volumes thereof is problematic due to the toxic and explosive risks associated with it. However, flaring CO-rich off-gas wastes massive quantities of energy. In this study an alternative approach to the use of closed SAF CO-rich off-gas was explored. It is suggested that the thermal energy associated with the combustion of such off-gas can at least partially be stored in the form of chemical energy, i.e. production of silicon carbide (SiC) from quartz and anthracite fines (partially classified as waste materials, which are generated on-site). SiC can partially replace conventional reductants used during FeCr production. The influences of quartz and anthracite particle size, treatment temperature and gaseous atmosphere (nitrogen or air) on SiC formation were investigated. A quartz-anthracite mixture with 90% of the particles <350.9 μm carbothermically treated at 1600°C resulted in almost complete conversion of quartz to SiC in both nitrogen and air atmospheres. These results indicated significant potential for industrial application of the process.

The third waste handling strategy investigated was the recycling of pre-oxidised chromite fines in the oxidative sintered pellet production process (Outotec steel belt sintering) (results presented in Chapter 5). Currently, recycling of such pre-oxidised chromite fines, collected from the pellet sintering off-gas and fines screened out from the sintered pellets, are limited to a maximum of 4 wt% of the total pellet composition since it is believed to adversely affect pellet quality. This limitation has resulted in the accumulation of pre-oxidised fine chromite stockpiles at some FeCr producers. According to literature, pre-oxidized chromite ore

requires less energy to metallize if compared to normal chromite. Additionally, pre-oxidized chromite fines significantly improve chromite pre-reduction (solid state reduction). Considering these energy related benefits, the recycling of pre-oxidized fines beyond the current limitation of 4 wt% pellet composition was investigated. The results presented in this study proved that re-cycling of such fines, up to a limit of 32 wt% of the total pellet composition, improved cured pellet compressive and abrasions strengths. In addition, electron microprobe and quantitative X-ray diffraction (XRD) analyses demonstrated that chromite grains present in the pre-oxidized chromite fines at least partially consist of crystalline phases/compounds that will improve the metallurgical efficiency and specific electricity consumption (i.e. MWh/ton FeCr produced) of the smelting process.

Keywords: chromite, chromium (Cr), ferrochromium/ferrochrome (FeCr), waste management, waste materials, hexavalent Cr, Cr(VI), off-gas combustion, carbon monoxide (CO), silicon carbide (SiC), under-sized material, pre-oxidized chromite.

TABLE OF CONTENTS

LIST OF TABLES

The tables in the articles and appendixes are no listed here

LIST OF FIGURES

The figures in the articles and appendixes are no listed here

CHAPTER 1: MOTIVATION AND OBJECTIVES

An overview of the project motivation is briefly discussed in Section 1.1, while general aims and specific objectives are listed in Section 1.2.

1.1 Background and motivation

The corrosion-, oxidation-, and heat resistance of many alloys may be ascribed to the presence of chromium (Cr) therein. Generally, the higher the Cr content of an alloy, the more corrosion-, oxidation-, and heat resistant the alloy becomes. The Cr content of alloys range between 12 to 35% and is truly an essential element in modern day society. The only commercially viable source of new Cr units is chromite ore, which contains Cr in the characteristic spinel mineral form. The majority of mined chromite (approximately 90 to 95%) is utilized in the production of various grades of ferrochrome (FeCr), typically containing >48% to 65% Cr, 4 to 8% C, <8% Si, various trace compounds, and Fe the balance. Subsequently, 80 to 90% of produced FeCr is consumed by the stainless steel industry. Thus, the demand for chromite and FeCr is driven by the demand for stainless steel. Global stainless steel production is expected to grow by an average 5.5% per annum (Murthy et al., 2011; ICDA, 2013a; b).

FeCr is mainly produced by the carbothermic reduction of chromite in alternating current (AC) submerged arc furnaces (SAFs) and direct current (DC) arc furnaces (Beukes et al., 2010; Neizel et al., 2013). Chromite smelting is very endothermic and a high temperature is continuously required in the furnace (Eksteen et al., 2002). The energy required for heating, and reducing chromite to its metallic state is supplied by electrical energy (Pan, 2013). In addition, very high operating temperatures are required to separate the Cr-containing alloy from the slag phase (Barnes et al. 2015).

It is generally accepted that South Africa holds approximately >70% of the world's viable chromite ore reserves (Riekkola-Vanhanen, 1999; Cramer et al., 2004; Murthy et al., 2011; Beukes et al., 2012). The entire reserve is located in the Bushveld Complex, which is a geological structure in the northern part of South Africa (Howat, 1994). Large increases in chromite mining have led to a similar growth in the South African FeCr industry. Currently, 14 separate FeCr smelting facilities have a combined estimated production capacity of 5.2 million ton/year (Beukes et al., 2012). South Africa accounted for approximately 41% of globally produced chromite ores in 2012. An estimate of 55% of the approximate 10 million tonnes of South African produced chromite ores were exported, which implies that around 28% of ore consumed world-wide in 2012 originated from South Africa (ICDA, 2013a, b, and c; Kleynhans et al., 2016a).

Four relatively well-defined process combinations are utilized by the South African FeCr industry; (i) closed SAFs mainly consuming pre-reduced chromite pellets, and coarse (typically, 6 mm ≤ size ≤ 150 mm) reductants and fluxes, coupled with venturi off-gas scrubbers, (ii) closed SAFs mainly consuming oxidized sintered chromite pellets, and coarse reductants and fluxes, coupled with venturi off-gas scrubbers, (iii) conventional semi-closed SAFs mainly consuming coarse feed materials, coupled with bag filter off-gas treatment, and (iv) DC arc furnaces that can accommodate exclusively fine materials as a furnace feed, coupled with venturi off-gas scrubbers (Beukes et al., 2012; Beukes et al., 2017).

South African chromite ores are classified as friable and can relatively easily be reduced to the size of a single chromite crystal (Gu and Wills, 1988; Beukes et al., 2010). It is common to recover 10 to 15% lumpy ore (15 to 150mm typical size range), 8 to 12% chip/pebble ore (6 to 15mm typical size range), with the remainder of ores being in the <6mm size fraction (Glastonbury et al., 2010). Such fines are upgraded to render it chemically suitable for smelting. Upgraded ore, referred to as metallurgical grade ore, typically has a Cr_2O_3 content

of ≥45% (Glastonbury et al., 2010), but lower grades are also used. The use of chromite fines (<6mm) is restricted in SAF operations as it may facilitate furnace bed sintering, which traps the evolving process gasses and subsequently increases the risk of dangerous furnace bed turnovers and eruptions (Riekkola-Vanhanen, 1999; Beukes et al., 2010). Consequently, agglomeration is required prior to feeding these ores to SAFs. Agglomerated chromite is usually thermally treated, e.g. pre-reduced or pre-oxidized, to produce mechanically strong pellets, which ensures a permeable furnace bed.

During FeCr production, various wastes are generated, depending on the furnace type used. A relatively detailed investigation of each applied process step used by the FeCr industry, utilizing various production routes and furnace types, are presented in this study. Each process step was discussed in detail and the generated waste identified (where applicable). The wastes considered in this thesis, and the reasoning for considering them, are as follows:

i. Bag filter dust (BFD) originating from semi-closed SAF off-gas cleaning. Off-gas cleaning is achieved by initially passing off-gas through a cyclone or drop-out box to separate coarse material from the off-gas. Thereafter, off-gas passes through a baghouse where the fine particulate matter is collected in baghouse filters. The collected dust is then contacted with water as soon as possible, preventing dry dust spillages or wind dispersal (Beukes et al., 2012). BFD contains significant levels of Cr(VI) and cannot be disposed prior to proper Cr(VI) treatment (Gericke, 1998; Maine et al., 2005; Beukes et al., 2012). After the BFD is treated to reduce Cr(VI), it is typically disposed in fit-for-purpose waste facilities such as slimes dams. However, delayed Cr(VI) leaching from slimes dams were observed by several FeCr producers. This implies that the currently applied Cr(VI) extraction method does not solubilize the entire Cr(VI) content from the solid BFD matrix. Several studies indicated that Cr(VI) extraction from BFD can be achieved by neutral or acidic aqueous extractions.

For instance, Maine et al. (2005) indicated that > 100 h of extraction is required with neutral water to completely extract Cr(VI) from BFD. Gericke (1995) maintained that 24 h leaching with aqueous solutions of pH 2 to 6 is adequate for Cr(VI) extraction from BFD. Bulut et al. (2009) stated that only 30 min was required to dissolve all Cr(VI) present in BFD and that the solution pH did not play a significant role. However, none of these authors used buffers and extraction methods to ensure extraction of sparingly water-soluble and water-insoluble Cr(VI) compounds (Ashley et al., 2003).

ii. Excess CO-rich off-gas originating from closed SAFs, which is not used as an on-site energy source, is typically flared on-top of furnace stacks. Niemelä et al. (2004) estimated that for each ton of FeCr produced, the accompanying generated CO(g) has an energy value of between 2.0 to 2.3 MWh. The volume and composition of closed SAF off-gas depends on various factors, e.g. furnace design, process metallurgical condition, feed pre-treatment methods, feed material, and furnace operating philosophy (Beukes et al. 2010). It has been reported that closed SAF off-gas typically consists of 75 to 90% CO, 2 to 15% H_2, 2 to 10% CO_2 and 2 to 7% N_2 and between 650 to 750 $Nm^3.ton^{-1}$ FeCr is generated (Niemelä et al., 2004). The energy value of off-gas lays primarily within the CO content and to a lesser extent the H_2 content. Several methods to utilize the energies associated with CO(g) do exist, e.g. fermentation of CO-rich off-gasses with bacteria to produce usable chemicals (Molitor et al., 2016), off-gas combustion to generate steam for steam turbine electricity generation (Dos Santos, 2010), and internal combustion engines utilizing closed SAF off-gas as a fuel source to drive electrical power producing alternators (Schubert and Gottschling, 2011). However, each of these methods holds various limitations and are typically not applied by the FeCr industry. A non-appreciable

amount of CO(g) is utilized during drying, heating, and pellet pre-reduction procedures (Schubert and Gottschling, 2011). It is thus essential to develop a novel method to utilize the energy associated with off-gas combustion, without the need to store off-gas. Off-gas is explosive and highly poisonous to humans (Niemelä et al., 2004; Maynard et al. 2015); thus it is essential to consume generated off-gas as it is produced.

iii. Chromite ore, reductants, and fluxes are screened by some FeCr producers to remove the under-sized fractions prior to SAF smelting (Riekkola-Vanhanen, 1999; Beukes et al. 2010). The use of under-sized materials is essentially avoided (or at least limited) during closed SAF and semi-closed SAF smelting due to operational complications arising from furnace bed sintering. Under-sized chromite and reductants are typically used in the pellet production process. Under-sized quartz has been proven to enhance the achievable chromite pre-reduction level (Lekatou and Walker, 1997). However, the last mentioned process has yet to be industrially applied. Consequently, the on-site uses of quartz fines in the FeCr production process are limited.

iv. Under-sized oxidized chromite screened out from the pellets produced by the oxidative sintering process (Outotec steel belt sintering). Currently, such fines can be included as a pellet constituent. However, the addition thereof is believed to adversely affect the quality of sintered pellets (Basson and Daavittila, 2013), which has resulted in a stockpile of such fines building up at some FeCr producers. However, the afore-mentioned assumption, i.e. that limited pre-oxidized chromite fines can be recycled into the pellets, is currently unsubstantiated (at least in the peer reviewed public domain).

1.2 Objectives

The general aim of this study was to contribute towards better waste management/utilization of the FeCr industry. The specific objectives were to:

i. Determine the solubility of Cr(VI) present in bag filter dusts (BFDs) as a function of solution pH, and possibly speciate the respective compounds. Ultimately, the efficiency of currently applied Cr(VI) treatment of BFD will be assessed.

ii. Test if it will not be possible to store thermal energy generated by CO-rich off-gas combustion as chemical energy, which can be used in the FeCr production process. Specifically it was evaluated if under-sized (too fine for SAF smelting) quartz (that is used as a flux) can be carbothermically treated with under-sized anthracite to produce silicon carbide (SiC) within the temperature range achievable by closed SAF CO-rich off-gas combustion. Various authors have previously proven that SiC can be used as a reductant during chromite smelting (Demir, 2001; Pheiffer and Cookson, 2015). SiC formation will be investigated as a function of temperature required to convert quartz to SiC, as well as quartz and anthracite particle size. The reaction mechanism will also be considered and the possible on-site industrial application of such a process will be considered.

iii. Determine the effect of under-sized pre-oxidized chromite inclusion as an oxidative sintered pellet constituent on pellet mechanical properties, i.e. compressive strength and abrasion resistance. Furthermore, the reasons (mechanism) behind the observations will be investigated.

CHAPTER 2: LITERATURE SURVEY

This chapter reviews current, relevant literature related to the thesis topic, i.e. Ferrochrome waste management – identifying current gaps. This chapter consists of general information on chromium (Section 2.1), chromite exploitation and the valuation thereof (Section 2.2), the magnitude and importance of the South African chromite reserves and ferrochrome industry (Section 2.3), the process of chromite smelting (Section 2.4), the main processes and techniques utilized to beneficiate chromite and to produce ferrochrome (Section 2.5) and furnace feed materials preparation process steps (Section 2.6). From the afore-mentioned sections, waste materials that require improved handling were identified (Section 2.7). Finally, a concluding summary is provided (Section 2.8).

2.1 General information on chromium

2.1.1 Chromium properties and initial development

Chromium (Cr) is a group VI-B transition element with a ground-state electronic configuration of Ar $3d^5 4s^1$. The word "chromium" originates from the Greek word "Chroma", meaning colour, due to the various colours of Cr compounds (Mohan and Pittman Jr, 2006; Emsley, 2011). The unique colours of emerald and ruby gemstones are due to the presence of Cr therein (Mukherjee, 1998). Crocoite (lead ore) was the first Cr containing compound discovered in 1766 in the Beresof gold mine, Siberia. The French chemist Louise-Nicolas Vauquelin first synthesized Cr oxide in 1798 by reacting crocoite with hydrochloric acid (Nriagu and Nieboer, 1988; Shanker et al., 2005). In 1821, a French scientist Pierre Berthier, found that Cr inclusion in iron (Fe) formed a corrosion resistant alloy, but it could not be used due to the alloy being too brittle (Roza, 2008). Upon further process refinement, the French scientist Henri Moissan produced an alloy he referred to as ferrochrome (FeCr) in

1893. Subsequently, various scientist experimented on the chromium-to-iron ratio (Cr/Fe) until stainless steel, as we know it today, was developed (Loock-Hatting, 2016 and references therein).

2.1.2 Oxidation state and speciation

Cr has a wide range of oxidation states, which ranges from -2 to +6 (Rai et al., 1987; Rinehart et al., 1997). However, Cr most commonly occurs as Cr^0 (metallic Cr), Cr(II), Cr(III) and Cr(VI). Cr in the +2 oxidation state is relatively unstable and rapidly oxidizes to the +3 state, thus only the trivalent and hexavalent forms are found in nature. Cr^0 is mainly produced by human intervention (Bartlett, 1991; Motzer and Engineers, 2004). Cr(III) is the most stable of all the Cr oxidation states, whereas Cr(VI) is the most oxidized (Fendorf, 1995; Døssing et al., 2011).

Environmental Cr mobility and distribution is controlled by several interactions, such as sorption-desorption, oxidation-reduction, and precipitation-dissolution (Salem et al., 1989). Cr solubility (and mobility) depends on both the oxidation state and chemical form of Cr. Cr(III) compounds are less reactive, mobile and toxic than Cr(VI) due to slow ligand exchange kinetics (Fendorf, 1995). Of the commonly encountered environmental ligands, e.g. OH^-, SO_4^-, CO_3^-, and NO_3^-, Cr(III) only significantly complexes with OH^- (Salem et al., 1989; Loock-Hatting, 2016).

Cr(VI) species predominantly occur under oxidizing (Eh >0) and alkaline (pH >6) conditions (Motzer and Engineers, 2004), and is present in compounds as a oxyanion with a general formula of $H_xCrO_4^{2-x}$ (Rinehart et al., 1997). Cr(VI) commonly occurs as monomeric ions, CrO_4^{2-} (Shanker et al., 2005), $HCrO_4^-$ (Eary and Davis, 2007), H_2CrO_4 (Mohan and Pittman Jr, 2006), and as the dimeric ion $Cr_2O_7^{2-}$ (Namasivayam and Sureshkumar, 2008). In neutral and basic environments, Cr exists predominantly in the Cr(III) phase as $Cr(OH)_3$, and as coprecipitate between Cr(III) and Fe oxides, i.e. $(Cr,Fe)(OH)_3$ (Rai et al., 1984; Sass and Rai,

1987; Apte et al., 2006). $Cr(OH)_3$ has a low solubility between pH values of 6 and 10.5 (Rai et al., 1987), while $(Cr,Fe)(OH)_3$ has an even lower solubility (Sass and Rai, 1987). Hence, Cr has limited mobility in soil if it is in the Cr(III) state. However, Cr(III) may be solubilized, and consequently mobilized by complexing with organic acids originating from root exudates, forming metal ions in the aqueous phases of soil (Jones and Darrah, 1994).

2.1.3 Natural occurrence and properties

Cr is the ninth most abundant compound in the earth's crust. In the natural environment, Cr can occur in approximately 82 different mineral types (Motzer and Engineers, 2004). However, the only ore type that is commercially exploited to obtain new Cr units is chromite (Motzer and Engineers, 2004; Nriagu and Nieboer, 1988). Chromite is primarily found in peridotite of plutonic rocks by the intrusion and subsequent solidification of lava/magma, which contains relatively high contents of heavy, Fe-rich pyroxene and olivine minerals (Nriagu and Nieboer, 1988). Cr occurs within these rocks as a spinel structure with a composition of $AO.B_2O_3$, where the divalent A cation can be Fe^{2+} or Mg^{2+}, and the trivalent cation B can be Fe^{3+}, Cr^{3+}, or Al^{3+} (Kamolpornwijit et al., 2007). The chromite mineral belongs to a spinel mineral group characterized by the formula $[(Mg,Fe^{2+})(Al,Cr,Fe^{3+})_2O_4]$ (Haggerty, 1991). The chromite spinel has a cubic system, as shown in Figure 2-1. In this system, 32 oxygen atoms stack in the central plane of the large cubic cell, subsequently forming 32 octahedral and 64 tetrahedral voids. Amongst these cavities, 16 octahedral and eight tetrahedral sites are occupied by Cr^{3+} and Fe^{2+}, respectively. However, this is only true for pure chromite, i.e. $FeCr_2O_4$. For natural occurring chromite, some of the Cr^{3+} can partially be replaced by Al^{3+}, and the Fe^{2+} by Mg^{2+}. Thus, the Cr-bearing phase, i.e. $(Mg,Fe^{2+})(Al,Cr,Fe^{3+})_2O_4$, may be considered as isomorphic, with Fe^{3+}, Cr^{3+}, or Al^{3+} occupying the octahedral sites, and Fe^{2+} and Mg^{2+} occupying the tetrahedral sites (Zhang et al., 2016).

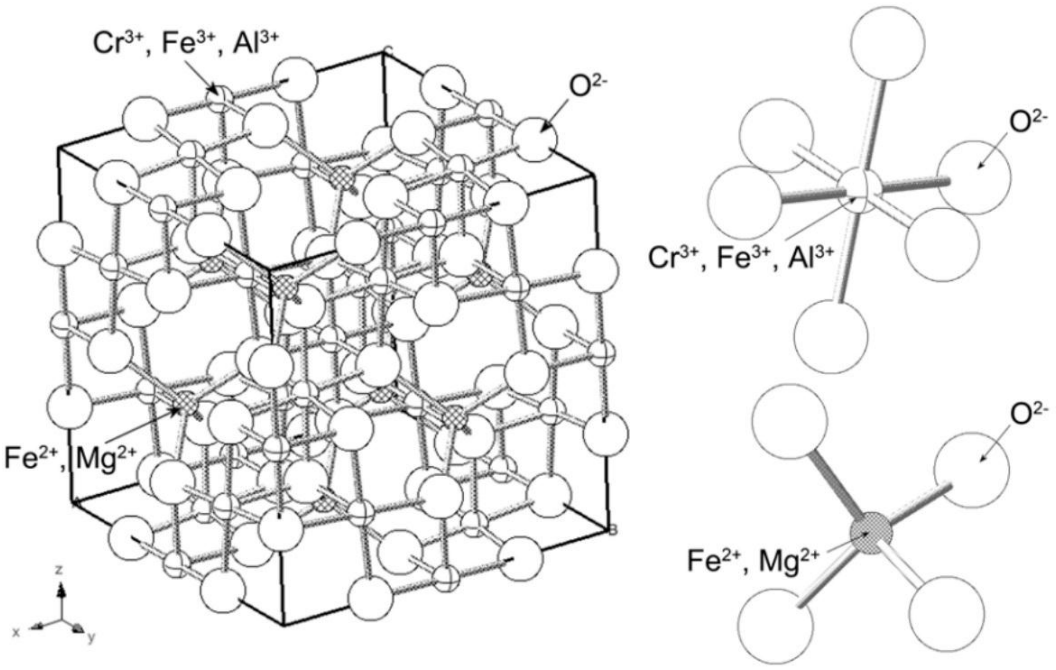

Figure 2-1: The crystalline structure of chromite spinel (Zhang et al., 2016).

The relative Fe and Cr contents in the chromite lattice can vary significantly in different deposits. This affects the ore grade, in terms of Cr_2O_3 contents, and Cr/Fe ratio, which determines the Cr content of the FeCr produced. Furthermore, the variations in chemical composition also affect chromite ore reducibility, i.e. relative ease of metallization/reduction. For example, replacing Al^{3+} with Fe^{3+} in the octahedral sites, and Mg^{2+} with Fe^{2+} in the tetrahedral sites, will greatly increase the spinel reducibility. Chromite ore can be given a refractory index, i.e. relative resistance to reduction. This index is expressed in Equation 2-1 (Guertin, 2005):

$$\text{Refractory index} = \frac{\text{wt.\% } Cr_2O_3 + MgO + Al_2O_3}{(Fe_{total} \text{ as } FeO) + SiO_2} \quad \text{(Equation 2-1)}$$

2.1.4 Use and consumption

Cr has a wide range of applications, e.g. electroplating (Cui et al., 2011), chromate chemical production (Darrie, 2001), leather tanning (Apte et al., 2005), wood preservation (El-Shazly et al., 2005), and colour pigments in textiles and paints (Kassem, 2010). Cr is also included

in non-ferrous alloys such as aluminium, cobalt, titanium, copper, and nickel (Bielicka et al., 2005). More importantly, Cr has excellent resistance to ordinary corrosive agents at room temperature and is therefore used in electroplating processes and in the production of ferrous alloys, primarily stainless steel (Dhal et al., 2013a). Of the total chromite ore production, the refractory and chemical industries each consumes approximately 5% of mined chromite ore (Dhal et al., 2013a), whereas the remaining 90% is consumed by the metallurgical industry in the production of FeCr (Murthy et al., 2011). FeCr is a relatively crude alloy between Fe and Cr. Primarily four different grades of FeCr alloys are produced, i.e. high carbon, medium carbon, low carbon, and charge grade, as indicated in Table 2-1. However, since the development of stainless steel processes such as vacuum oxygen decarburization and argon oxygen decarburization, the demand for low and medium grade carbon FeCr has decreased substantially. These processes allow for the removal of C and Si from stainless steel, with acceptable Cr losses (Beukes et al., 2017 and references therein). Thus, high carbon and charge grade FeCr is the most commonly produced FeCr types (Kleynhans et al., 2016b; ICDA, 2013a and b). High carbon and charge grade FeCr are relatively similar and it is common to refer to these two grades FeCr as high carbon charge grade FeCr (ICDA, 2013c). Approximately 90% of FeCr is consumed in the production of stainless steel (Abubakre et al., 2007; Murthy et al., 2011; ICDA, 2013c).

Table 2-1: **Main commercial grades of FeCr according to ISO-standard 54481-81 (Downing et al., 1986; Kleynhans, 2011)**

FeCr grade	% Cr	% C	% Si	% P	% S
High carbon	45-70	4-10	0-10	<0.05	<0.10
Medium carbon	55-75	0.5-4	<1.5	<0.05	<0.05
Low carbon	55-95	0.1-0.5	<1.5	<0.03	<0.03
Charge grade	53-58	5-8	3-6		

2.2 Exploitation and valuation

Commercially exploitable chromite ore is primarily encountered in three deposit types, i.e. alluvial, podiform and stratiform (Cramer et al., 2004; Murthy et al., 2011; Glastonbury et al., 2015). Alluvial deposits are typically relatively small and of minor commercial interest. Such deposits are formed by the weathering of chromite-bearing rocks and subsequent gravity concentration by means of flowing water (Murthy et al., 2011; Glastonbury et al., 2015). Podiform-type chromite occurs in irregular shapes, i.e. pods or lenses, and exploration and exploitation are usually expensive endeavours. However, economically feasible podiform deposits are located in Albania, Kazakhstan, and Turkey (Cramer et al., 2004). Stratiform-type chromite deposits are found in large, parallel layered igneous rock complexes. These chromite ore deposits are economically feasible to exploit due to regular layering, and large lateral continuity (Cramer et al., 2004).

The value of chromite ores are not determined solely by the Cr_2O_3 contents, but also by the Cr/Fe ratios. Figure 2-2 presents the typical Cr_2O_3 contents and Cr/Fe ratios of selected chromite ores from South Africa, Kazakhstan, India, Zimbabwe, and Turkey. By comparing South African primary metallurgical grade and UG2 ore with typical ores from other countries, it is observed that the Cr_2O_3 contents are similar. However, the Cr/Fe ratios differ.

This is due to the high Fe contents of South African ores. Figure 2-3 presents the various FeCr grades produced from chromite ores with different Cr/Fe ratios. Primarily normal and low grade FeCr is produce from South African metallurgical grade (Cr/Fe = 1.5) and UG2 (Cr/Fe <1.5) ores, respectively. Whereas, high carbon FeCr, that contain a higher Cr content, is produced from for instance Turkish ores (Cr/Fe >3) (Fowkes, 2014; Kleynhans, 2016a).

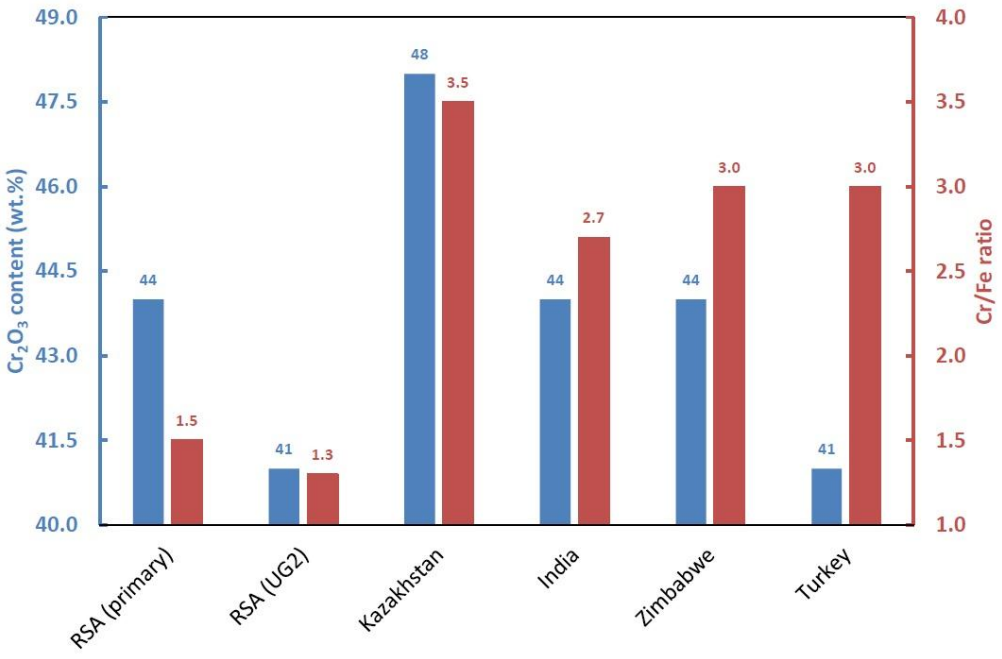

Figure 2-2: Average Cr_2O_3 contents and Cr/Fe ratios of typical chromite ores from various countries (Fowkes, 2014; Kleynhans, 2016a).

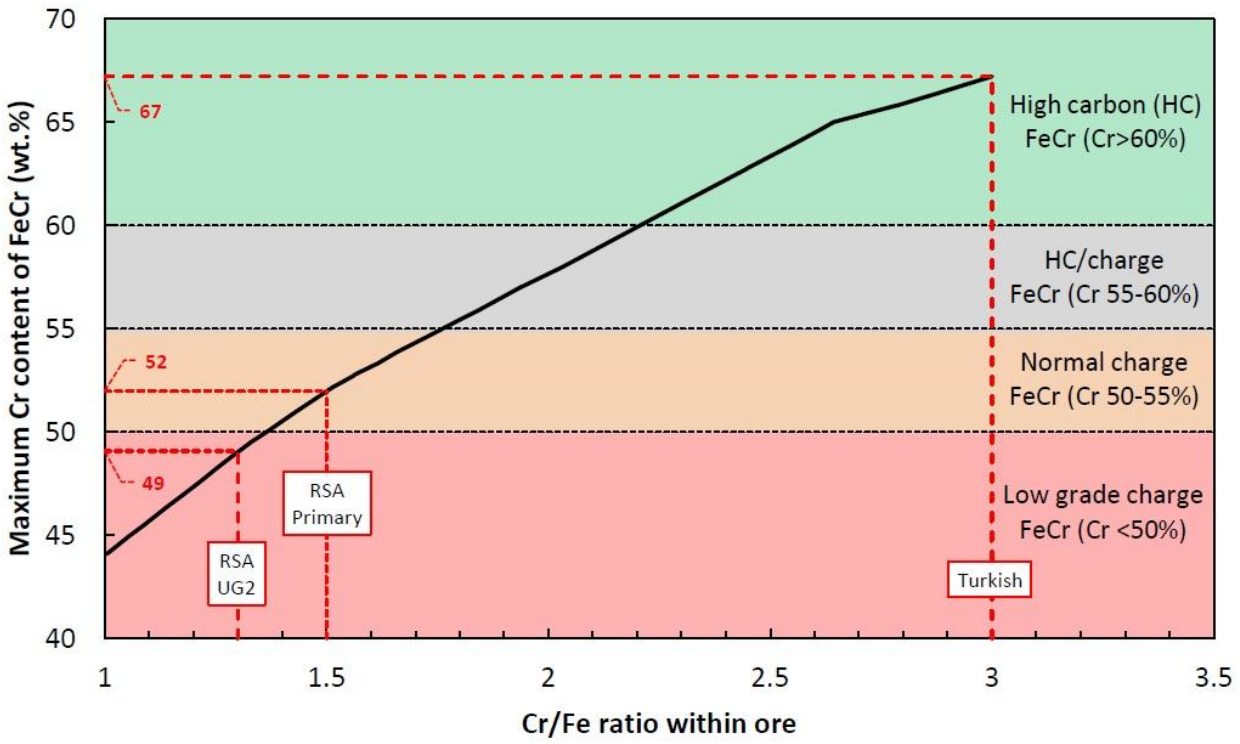

Figure 2-3: Various FeCr grades produces from chromite ores with different Cr/Fe ratios (Fowkes, 2014; Kleynhans, 2016a).

2.3 South African chromite reserves and FeCr industry

It is estimated that South Africa holds approximately three quarters of the world's viable chromite ore reserves (Beukes et al., 2012; Creamer, 2013; Kleynhans et al., 2017), making the exploitation thereof significant for the South African economy. The entire South African chromite reserve occurs in the Bushveld Complex (BC) (Cramer et al., 2004; Cawthorn, 2010). The BC is a geological structure with various limbs, located in the northern part of South Africa (Howat, 1994). Figure 2-4 graphically illustrates the extent of the BC and locations of FeCr smelters (map courtesy of JP Beukes).

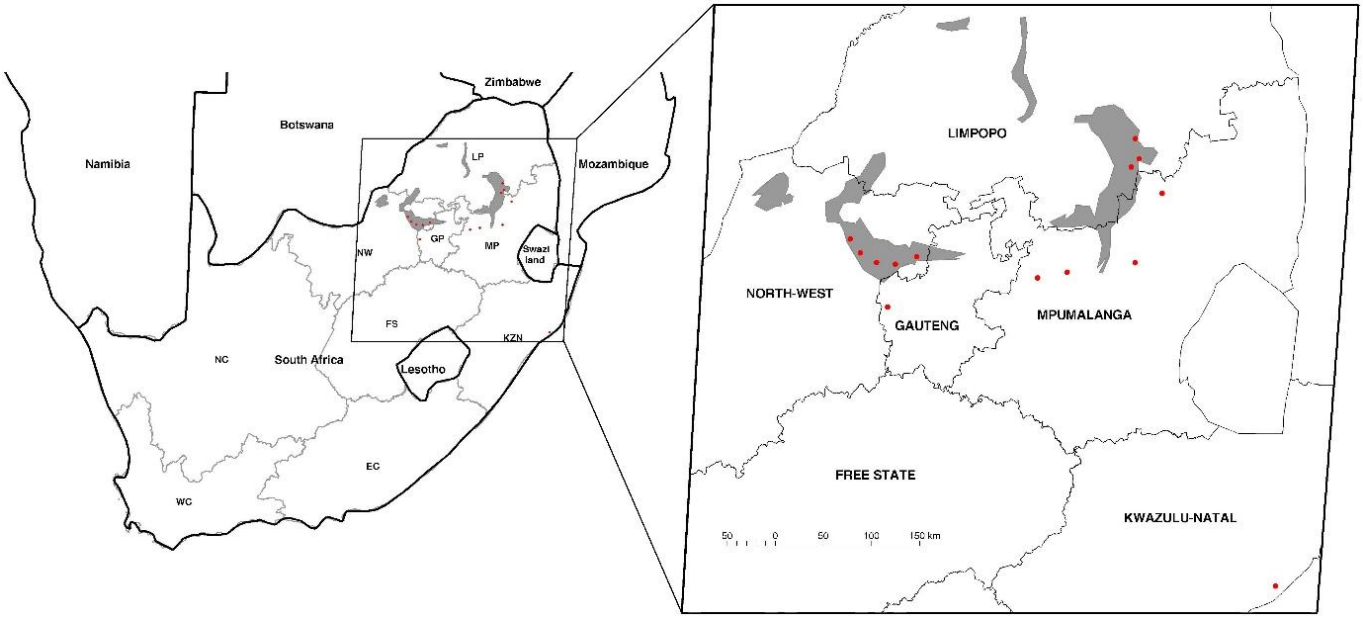

Figure 2-4: Extent of BC (grey areas) and locations of FeCr smelters (red dots) (map courtesy of JP Beukes).

The BC contains several seams, with the ones of economic interest being the lower group 6 (LG6), middle group 1 and 2 (MG1 and MG2), and the upper group (UG2) seams (Cramer et al., 2004; Glastonbury et al., 2015). Each seam has different Cr/Fe ratios. The LG6 seam has a Cr/Fe ratio of 1.5 to 2, MG1 and MG2 seams have ratios of 1.5 to 1.8, and the UG2 seam has a ratio of 1.3 to 1.4 (Soykan et al., 1991; Cramer et al., 2004; Basson et al., 2007; Beukes et al., 2010; Kleynhans, 2011). The UG2 seam is primarily mined as a source of platinum group metals (PGMs) (Xiao and Laplante, 2004). PGM extraction from UG2 ores typically involves sulphide liberation by milling, and subsequent recovery of the PGM concentrate by flotation processes (Xiao and Laplante, 2004). The PGM recovery circuits are specifically designed to reject chromite to the tailings stream. Subsequently, these tailings are upgraded to the required Cr content, and utilized for FeCr production (Glastonbury et al., 2015). UG2 chromite has gained acceptance in the production of charge grade FeCr with the utilization of various technological innovations (Cramer et al., 2004; Basson et al., 2007).

South Africa has at least 14 separate FeCr smelters (see Figure 2-4 for locations), with each of these smelters operating between two to six smelting furnaces. These smelters have a combines production capacity potential of more than five million tons FeCr per annum (updated from Beukes et al., 2012 and Jones, 2011). The production capacities of South African FeCr smelters are summarized in Table 2-2.

Table 2-2: Production capacity of South African FeCr producers adapted from Jones (2011) by Beukes et al. (2012).

Plant	Locality	Production capacity (t/y)
ASA Metals Dilokong	Burgersfort	400 000
Assmang Chrome	Machadodorp	300 000
Ferrometals	Witbank	550 000
Hernic Ferrochrome	Brits	420 000 (updated value)
International Ferro-Metals	Rustenburg-Brits	267 000
Middelburg Ferrochrome	Middelburg	285 000
Mogale Alloys	Krugersdorp	130 000
Tata Ferrochrome	Richards Bay	135 000
Tubatse Ferrochrome	Steelpoort	360 000
Glencore Lydenburg	Lydenburg	400 000
Glencore-Merafe Boshoek	Rustenburg-Sun City	240 000
Glencore-Merafe Lion	Steelpoort	728 000
Glencore Rustenburg	Rustenburg	430 000
Glencore Wonderkop	Rustenburg-Brits	545 000
TOTAL		5 190 000

2.4 Chromite smelting

FeCr is primarily produced by the carbothermal reduction of chromite ore in submerged arc furnaces (SAFs) and direct current (DC) furnaces (Beukes et al., 2010; Neizel et al., 2013; Dwarapudi et al., 2013). The reduction process is very endothermic and a high temperature of approximately 1700°C is continuously required within the furnace (Eksteen et al., 2002; Niemelä and Kauppi, 2007). The energy required for heating, and chromite reduction is mainly supplied by electrical energy (Pan, 2013). Various types of reductants are used as carbon (C) sources during chromite smelting, e.g. coke, coal, and charcoal (Riekkola-Vanhanen, 1999; Niemelä and Kauppi, 2007). A reductant with low ash, low phosphorous, and low sulphur contents is preferred for FeCr production (Basson et al., 2007; Makhoba and Hurman Eric, 2010). Fluxes utilized include quartzite, bauxite, dolomite, olivine, calcite, and limestone, depending on the operation conditions and the chemical composition of the chromite being smelted (Riekkola-Vanhanen, 1999; Niemelä and Kauppi, 2007).

During chromite smelting, Cr and Fe oxides are reduced to their metallic states, i.e. Fe^0 and Cr^0. However, considerable fractions of Fe and Cr are in the carbide form (Riekkola-Vanhanen, 1999). A small fraction of silica (SiO_2) is also reduced, which accounts for the Si-content in produced FeCr. These reactions occur as indicated below (Niemelä and Kauppi, 2007).

In the early stages of chromite smelting, Fe_3O_2 is reduced to FeO:

$$Fe_2O_3 + C \rightarrow 2FeO + CO \qquad \text{(Reaction 2-1)}$$

FeO is then reduced to Fe^0:

$$FeO + C \rightarrow Fe + CO \qquad \text{(Reaction 2-2)}$$

Cr_2O_3 is reduced to Cr^0:

$$Cr_2O_3 + 3C \rightarrow 2Cr + 3CO \qquad \text{(Reaction 2-3)}$$

SiO_2 is reduced to Si^0:

$SiO_2 + C \rightarrow SiO + CO$ (Reaction 2-4)

2.5 Main processes and techniques

2.5.1 Mining and beneficiation of chromite ores

Underground and open-cast mining techniques are used to obtain chromite ores, and the specific technique depends on the local resources and materials (Gediga and Russ, 2007).

The purpose of chromite ore beneficiation is to render ores chemically suitable for subsequent use (e.g. smelting). Beneficiation typically serves to separate valuable minerals from gangue (waste material), prepare ore for subsequent refinements, or to remove impurities. In preparation for FeCr smelting, chromite beneficiation typically consists of reducing the particle size (crushing and grinding) and increasing the Cr_2O_3 content of certain chromite streams.

South African chromite ores are classified as friable and can relatively easily be reduced to the size of a single chromite crystal. South African chromite mines commonly recover 10 to 15% lumpy ore ($15 \leq$ typical size range $\leq$ 150mm), 8 to 12% chip/pebble ore ($6 \leq$ typical size range $\leq$ 15mm), with the remainder of ores being in the <6mm size fraction (Glastonbury et al., 2010). The <6mm fraction requires beneficiation to be rendered chemically suitable for smelting. Figure 2-5 presents a general process flow diagram for chromite ore beneficiation for the production of a typical metallurgical grade chromite concentrate. This diagram consists of two sections, i.e. feed preparation (comminution) and concentration (Abubakre et al., 2007; Murthy et al., 2011).

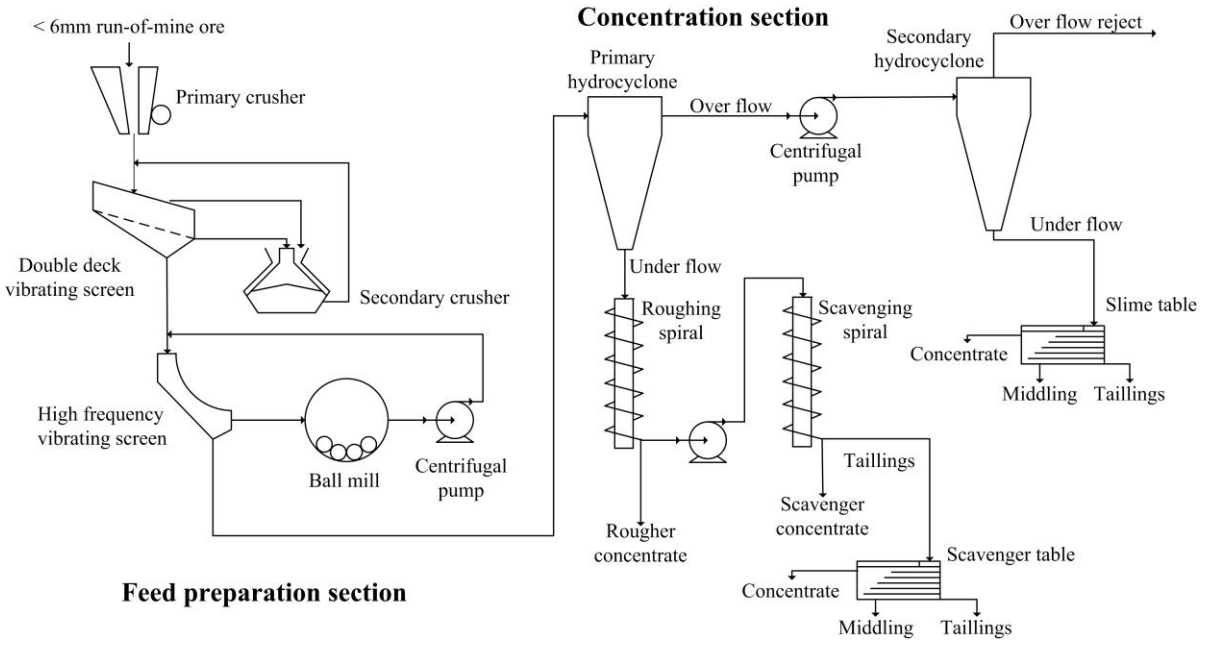

Figure 2-5: Run-of-mine chromite beneficiation process to produce typical metallurgical grade chromite concentrate (adapted from Murthy et al., 2011).

The feed preparation section in Figure 2-5 entails screening the <6 mm fraction from the run-of-mine chromite ores, followed by primary and secondary crushing, separated by screening. The secondary crusher offset is continuously recycled. Crushed ore is then ball milled to <1 mm, and conveyed to the concentration section where the Cr_2O_3 content is upgraded using conventional gravity techniques, e.g. hydrocyclones and/or spiral concentrators (Murthy et al., 2011). This upgraded ore is then referred to as metallurgical grade ore and has a typical Cr_2O_3 content of ≥45% (Glastonbury et al., 2010), although lower grade is also often generated.

Gravity techniques become complex and ineffective when treating particles <75 µm. Each gravity separation technique has an optimal operating efficiency under specific operational conditions and particle size range (Murthy et al., 2011). Gravity concentration of heavy media is the most commonly applied beneficiation process, being the most economical

method operating on coarse particles ranging between 6 to 150 mm. Finer particles require the use of spirals, jigs, and shaking tables, with spirals being the preferred gravity concentrator. More sophisticated beneficiation processes do exist, e.g. flotation, but are usually not economically feasible (Wesseldijk et al., 1999).

2.5.2 FeCr production processes

The most commonly applied smelting technologies utilized by South African FeCr producers are semi-closed and closed SAFs, and DC furnaces. As indicated in Figure 2-6, Beukes et al. (2017) presented simple illustrations, to explain the differences between semi-closed (referred to as "open furnaces" by some authors) and closed furnaces (which include closed SAFs and DC furnaces). As is evident from Figure 2-6 the terms "semi-closed" and "closed" merely refer to the entry (or prevention thereof) of ambient air into the furnaces. For semi-closed furnaces, CO-rich off-gas is combusted above the furnace bed, while in closed furnaces the CO-rich off-gas is extracted without being combusted.

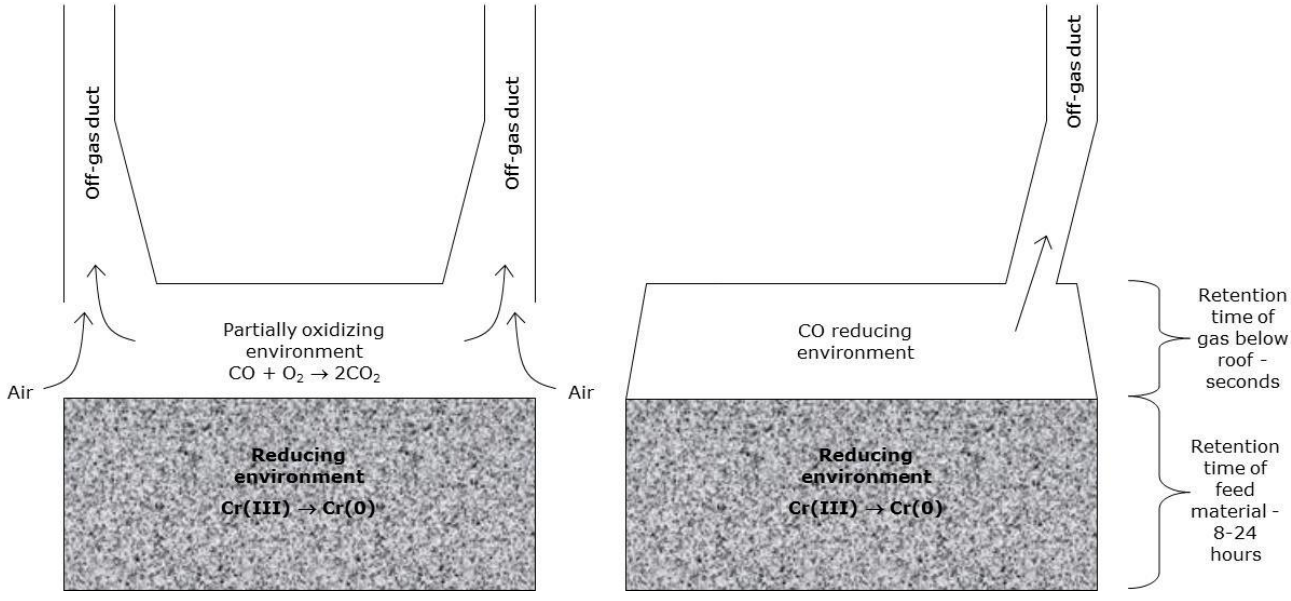

Figure 2-6: Simplified illustration of semi-closed (left) and closed (right) SAF/DC furnace designs, adapted form (Beukes et al., 2017).

A generalised flow diagram, indicating the most common process steps utilized by the South African FeCr industry is shown in Figure 2-7 (Beukes et al., 2010; Beukes et al., 2017). In general, four relatively well defined process combinations are used (Beukes et al., 2010; Beukes et al., 2017):

A. Closed SAFs mainly consuming hot pre-reduced chromite pellets (fed directly after pre-reduction), and coarse (6 mm ≤ typically size ≤ 150 mm) reductants and fluxes, coupled with venturi off-gas scrubbers. Glencore Alloys (previously Xtrata Alloys) apply this process at two smelters (Naiker, 2007). Closed SAFs consuming pre-reduced pelletized feed operates on a basic slag, with a basicity factor (BF) of >1. The BF is defined as (Beukes et al., 2010):

$$BF = \frac{\%CaO+\%MgO}{\%SiO2} \quad \text{(Equation 2-2)}$$

Usually, the carbonaceous reductant content present in SAFs during smelting facilitates the burden conductivity. However, due to some of the Fe and Cr already being reduced/metallized, less carbonaceous reductant is fed to closed SAFs consuming pre-reduced chromite pellets. Thus, the furnace burden lacks conductivity; therefore, a conductive basic slag is used.

B. Closed SAFs mainly consuming oxidized sintered chromite pellets, and coarse reductants and fluxes, coupled with venturi off-gas scrubbers. This has been the technology most commonly employed in South Africa over the last couple of decades, in various green and brownfield developments. This process route is commercially known as the Outotec process (also applied by the Outokompu at Tornio, Finland). These furnaces are typically operated on an acidic slag (BF <1) (Bekues et al. 2010).

C. Conventional semi-closed SAFs mainly consuming coarse chromite, reductants and fluxes, coupled with off-gas bag filter treatment. This is the oldest technology applied

in South Africa, but it still accounts for a substantial fraction of overall FeCr production (Gediga and Russ, 2007). The majority of South African semi-closed SAFs operate on an acid slag regime (BF <1). Coarse materials are utilized as they allow process gasses to permeate through the furnace bed (Dwarapudi e al., 2013). Fine materials (<6mm) are avoided (or at least limited) as it may facilitate furnace bed sintering, which traps the evolving process gasses and subsequently increases the risk of furnace bed turnovers and eruptions (Riekkola-Vanhanen, 1999; Beukes et al., 2010). Nevertheless, a substantial amount of chromite ore fines are fed to these furnaces in South Africa (Beukes et al., 2010). Operation benefits of semi-closed SAFs include simplicity of operation (i.e. option to exclude raw material screening), easily accessible electrode equipment and furnace bed (i.e. easier maintenance compared to closed SAFs), and furnace bed visibility (i.e. visually determine process condition). Furthermore, lack of sophisticated control systems means that less capital is required for FeCr production by semi-closed SAFs. However, these SAFs have lower metallurgical and thermal efficiencies (Basson and Daavittila, 2013). Semi-closed SAFs may also consume pelletized feeds.

D. DC furnaces that can accommodate exclusively fine materials as a furnace feed, coupled with venturi off-gas scrubbers. Currently, three FeCr DC furnaces are in routine commercial operation in South Africa and typically operate on a basic slag regime (BF >1) (Denton et al., 2004; Curr, 2009).

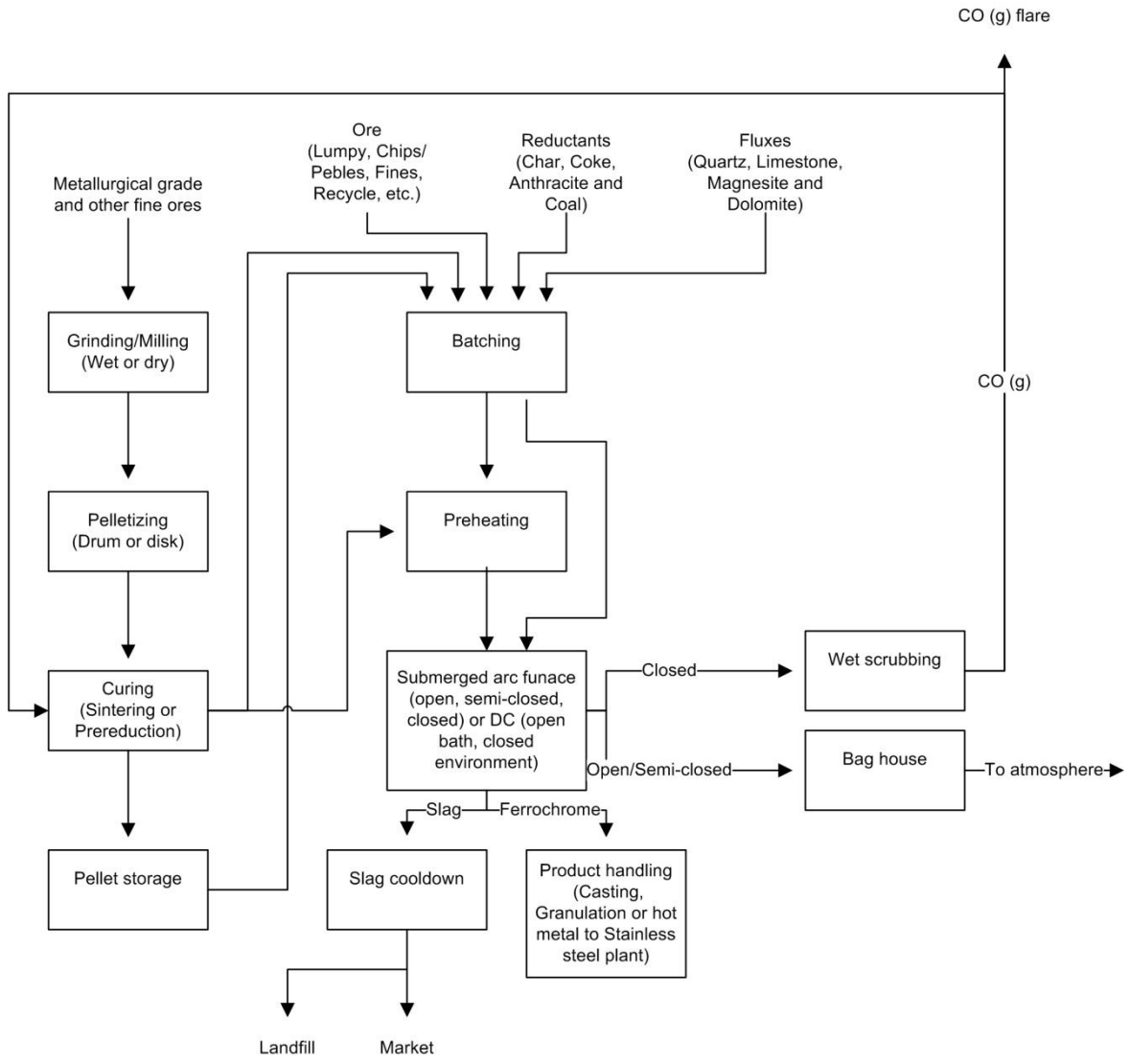

Figure 2-7: A flow diagram adapted by Beukes et al. (2017) from Riekkola-Vanhanen (1999) and Beukes et al. (2010), indicating the most common process steps utilized by the South African FeCr industry

Table 2-3 presents the respective Cr recovery (%), the specific energy consumption (SEC), and economy of scale (EoS) of the four process combinations discussed in the previous paragraphs. Cr recovery refers to the % of Cr recovered from chromite ores (the remaining % Cr remains in waste). SEC is defined as the amount of energy (kWh) required to produce

1 ton FeCr. EoS indicates the maximum size of a furnace with regard to energy consumption relevant to the amount of FeCr producible per annum (Basson and Daavittila, 2013).

Table 2-3: Different high carbon FeCr process route comparisons (Basson and Daavittila, 2013)

Furnace type	Cr recovery (%)	SEC ($kWh.t^{-1}$)	EoS (single furnace maximum size/single furnace output)
Semi-closed SAF (no raw material screening)	70-75	4300	30MVA/50ktpa[#]
Closed SAF (oxidative sintered feed and pre-heating)	83-88	3200	135MVA/240ktpa
Closed SAF (pre-reduced pelletized feed)	88-92	2400*	66MVA/160ktpa
Closed DC furnace	88-92	4200	60MVA/110ktpa

*Excluding pre-reduction associated fuel energy
[#]Although Basson and Daavittila (2013) indicate EoS as 30MVA, 45 MVA furnaces are in routine operation in South Africa (Jones, 2011)

2.6 Furnace feed material preparation and smelting processes

In order to facilitate discussions on the waste materials generated by the FeCr industry, the process steps indicated in Figure 2-7 were discussed in greater detail.

2.6.1 Green pellet generation

Several beneficiated ore (as discussed in Section 2.5.1) agglomeration processes are used by the FeCr industry, i.e. pelletization and briquetting. Pelletization is typically the preferred technique. Briquetting utilizes coarser chromite, and briquettes typically have worse compressive strengths and lower Cr recoveries during smelting, if compared to pelletized chromite (Riekkola-Vanhanen, 1999). Consequently, only pelletization processes were considered in this section.

As indicated in Section 2.5.2, two different pellet types are commonly produced for closed SAF smelting, i.e. pre-reduced and oxidative sintered. These pellet types, and generation process steps, differs substantially from one another. Figure 2-8 presents a flow diagram of green pellet generation processes of pellets destined for pre-reduction and oxidative sintering curing processes. Steps associated with green pellets destined for pre-reductive curing, and oxidative sintering are indicated in red and blue, respectively. Commonly shared process steps are indicated in black.

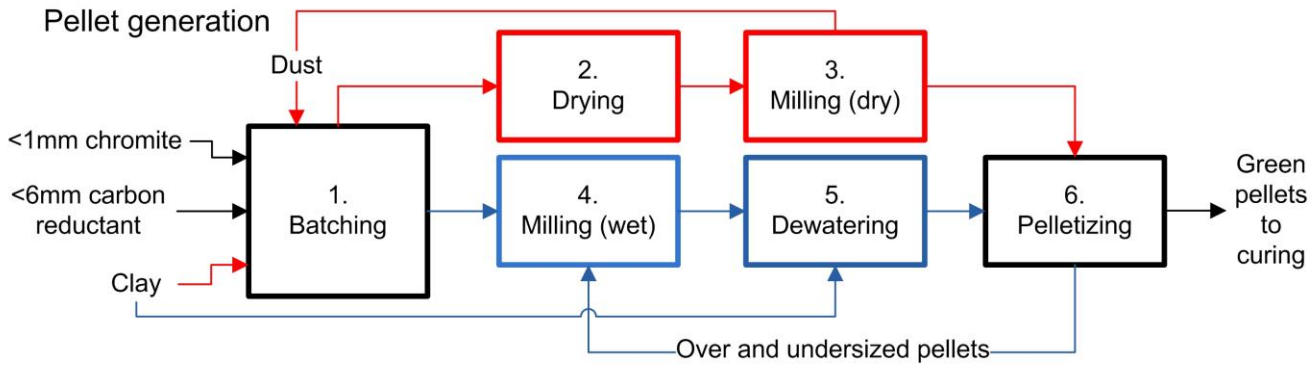

Figure 2-8: A flow diagram of the process steps for green pellet generation, destined for pre-reduction (red) and oxidative sintering (blue) curing. Common process steps are indicated in black.

2.6.1.1 Green pellet generation destined for pre-reduction

Green pellets destined for pre-reduction are generated by combining process Steps 1, 2, 3, and 6 in Figure 2-8. In this process, metallurgical grade ore (or upgraded UG2 ore), <6mm carbon reductant, and a clay binder are weight proportionated (batched) according to a pre-determined metallurgical recipe (Step 1, Figure 2-8). Green pellets typically contain 12 to 14 wt% carbonaceous reductant, and 3 to 4.5 wt% clay, with chromite being the balance. After the batching process, the mixture is dried to remove moisture (Step 2, Figure 2-8). Thereafter, the mixture is dry ball milled (Step 3, Figure 2-8) to obtain a homogeneous

mixture with a particle size distribution of which 90% of the particles are smaller than 75 µm (Basson and Daavittila, 2013). During dry milling, dust is generated, which is collected and re-introduced into the pellet generation process. Thereafter, the mixture is pre-wetted (some water added) and agglomerated into green pellets on pelletizer discs (Step 6, Figure 2-8). To enable the pellet formation process, fine water spray is introduced at various strategic points on the pelletizer disc. Green pellet formation occurs in two steps, i.e. nucleation and growth (Pandey et al., 2012). In this case, nucleation is the process where micro-pellets are formed when the water spray is introduced to the milled mixture. Subsequently, the micro-pellets are grown by the coagulation of drier material onto the wetted surface of the micro-pellets. Nucleation and growth depends on several factors, e.g. pelletization disc slope, material residence time on disc pelletizer, disc rotation speed, feed material size, volume water added, water spray nozzle combination and position, and material feed rate (Pandey et al., 2012). During the pellet generation process, raw material spillages do occur. However, these materials can easily be collected and re-introduced to the pelletization process due to the nature thereof. Green pellets destined for pre-reduction should ideally be between 12 to 18 mm in diameter (Basson and Daavittila, 2013). However, under- and oversized pellets are typically also fed to closed SAFs.

Wastes generated during green pellet generation destined for pre-reductive curing is relatively limited, except for inevitable spillages during material handling. Dust originating from dry milling and bag filter dust (BFD) collected from the material drying off-gas are the only materials that may be partially classified as waste materials. However, these dusts consist exclusively out of feed materials and are therefore easily recycled.

2.6.1.2 Green pellet generation destined for oxidative sintering

Green pellets destined for oxidative sintering are generated by a combination of process Steps 1, 4, 5, and 6 in Figure 2-8. This process starts with weight proportioning of chromite

fines and approximately 1 to 2 wt% reductant fines (Step 1, Figure 2-8). Coke is the preferred carbonaceous material; however gas coke, char and anthracite have also been successfully used (Basson and Daavittila, 2013). Thereafter, the mixture is wet ball milled (Step 4, Figure 2-8) to obtain a homogeneous mixture with a particle size distribution of which 80% of the particles are smaller than 74 µm (Basson and Daavittila, 2013). The wet milled mixture is then dewatered (Step 5, Figure 2-8) using ceramic filters. The process water obtained from the dewatering step is recycled and re-used in the wet milling process. The dewatered material typically contains 8.5 to 9% moisture after dewatering (Basson and Daavittila, 2013). Approximately 1% refined clay (usually bentonite) is then added to the moist mixture and thoroughly mixed to ensure a homogenous blend using a high intensity mixer. Green pellets are then generated in a pelletization drum (Step 6, Figure 2-8) (Visser, 2006). Drum pelletization is the process where wetted material is introduced to a large, long, rotating drum operating at a slight decline. The nucleation and growth mechanism of pellets are very similar to that of disc pelletization. Generated green pellets are then screened (to be between 9 and 13 mm). Oversized pellets are broken down and recycled back into the pelletization process, along with any undersized pellets. Waste generation during green pellet generation destined for oxidative sintering is relatively limited (e.g. material spillages), and no major wastes occur.

2.6.2 Pellet curing and furnace feed material screening

In this section, the green pellet curing processes, i.e. pre-reduction and oxidative sintering, are discussed. These processes are illustrated in Figure 2-9. Pre-reduction and oxidative sintering process steps are indicated in red and blue, respectively. Commonly shared process steps are indicated in black. Furnace raw material screening was also included in Figure 2-9 (indicated in the "material screening" section), since cured pellet screening is currently regarded as compulsory for oxidative sintered pellets fed to closed SAFs. Screening

procedures associated with semi-closed and closed furnaces are indicated in yellow and purple, respectively.

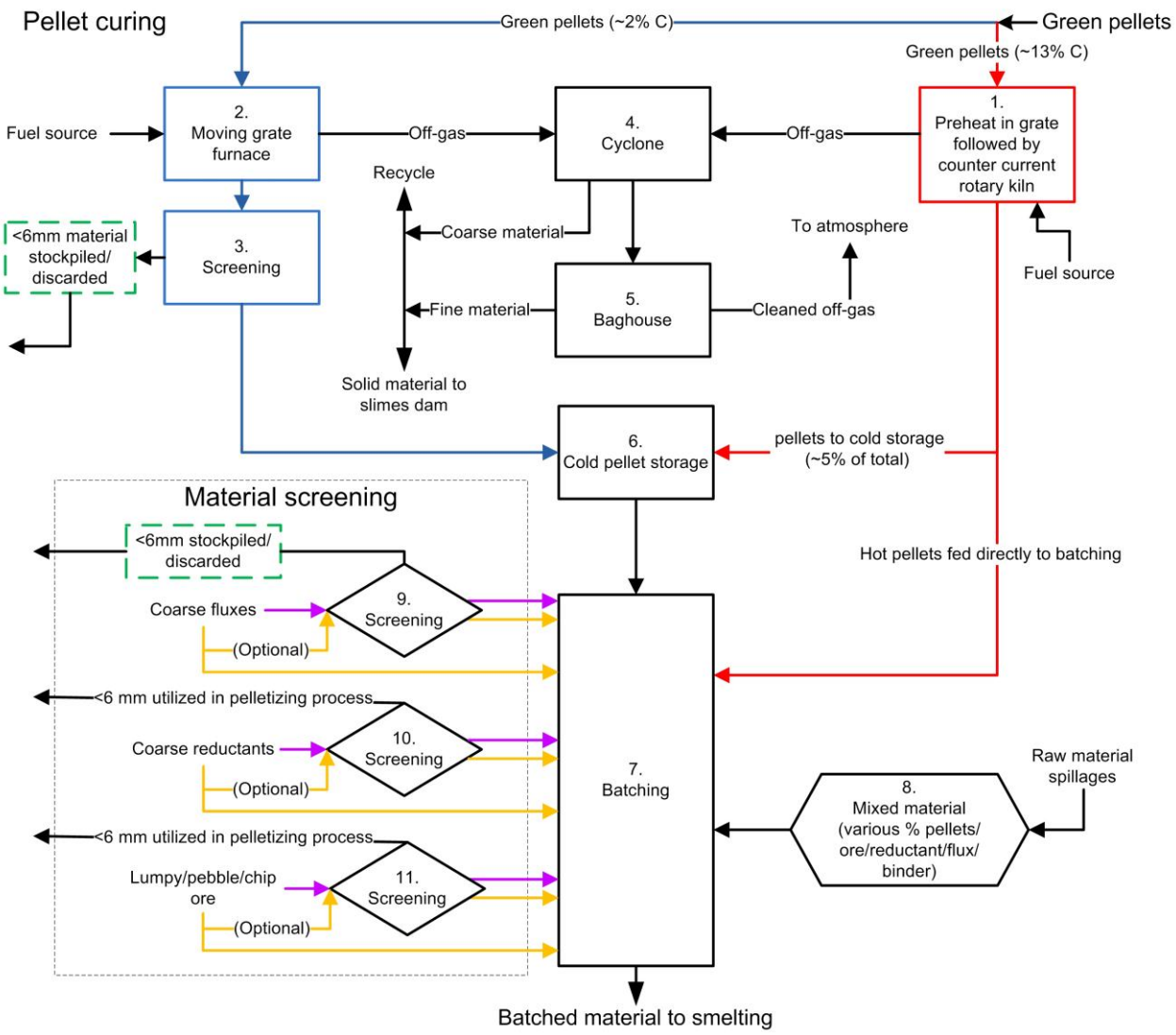

Figure 2-9: A generalized flow diagram of the pre-reduction (indicated in red) and oxidative sintering (indicated in blue) processes, and furnace feed material screening destined for semi-closed (indicated in yellow) and closed (indicated in purple) SAF smelting. Common process steps are indicated in black.

2.6.2.1 Green pellet pre-reduction

Pre-reduction (also known as solid state reduction of chromite) is defined as the process where fractions of Cr and Fe present in the chromite spinel are reduced to lower oxidation states (e.g. Fe(III) reduced to Fe(II)), or their metallic states (Cr(III) reduced to Cr^0 and Fe(II) reduced to Fe^0) prior to closed SAF smelting. The degree of pre-reduction depends on various factors, e.g. kiln temperature, retention time of pellets within the kiln, pellet size, %C present in green pellets and particle size after milling.

The pre-reduction process consists of Steps 1, 4, 5, 6 and 7 in Figure 2-9. Green pellets are dried and preheated in a grate, and fired in counter current rotary kilns (Step 1, Figure 2-9), operating at a temperature of between 1300 to 1400°C (Riekkola-Vanhanen, 1999; Basson and Daavittila, 2013). The kiln is heated by combusting pulverized coal, crude oil, or CO gas (Riekkola-Vanhanen, 1999). Off-gas produced during pellet pre-reduction is subsequently extracted from the kiln, and passes through a cyclone (Step 4, Figure 2-9) to remove coarse material from the off-gas. Such coarse material usually consists of unreacted chromite and/or carbonaceous reductant (Beukes et al., 2010; Van Staden et al., 2014; Du Preez et al., 2017), and is usually re-introduced into the pellet generation process or discarded (e.g. in a slimes dam). Thereafter, the off-gas passes through a baghouse (Step 5, Figure 2-9) where the remaining fine materials are separated from the off-gas. The BFD consist mostly of ash associated with combusted pulverised coal and is usually discarded in a fit-for-propose designed slimes dam. Pre-reduced pellets are fed hot, directly to closed SAFs, without being screened to remove fines (Naiker, 2007; Beukes et al., 2010; Kleynhans et al., 2012). A small percentage (approximately 5%) of pellets are water cooled, and stored as cold pellets (Step 6, Figure 2-9) to be smelted at a later stage.

Hot pre-reduced pellets are conveyed to be batched (Step 7, Figure 2-9) with other furnace feed materials according to a specific metallurgical recipe, which depends on the chemical

compositions of the materials to be smelted and the specific furnace slag regime. In some instances, spilled raw materials are included (Step 8, Figure 2-9), depending on the chemical composition and physical properties thereof.

Wastes generated during the pellet pre-reduction processes are relatively well managed. However, pellets may disintegrate in the pre-drying grate prior to entering the counter current rotary kiln, which may lead to a material build-up inside the kiln in the form of a so-called damrings (Kleynhans et al., 2016c). Combusted pulverised coal ash also contribute significantly to the formation of damrings. Excessive damrings have to be removed intermittently, which is only possible if the entire pre-reduction process is stopped. This entails that pellet production has to be halted, resulting in a decrease in metallurgical efficiency of the associated closed SAFs, if such furnaces are fed lumpy ore instead of pre-reduced pellets.

2.6.2.2 Green pellet oxidative sintering

Green pellet oxidative sintering consists of Steps 2 to 7 (Figure 2-9). Green pellets are introduced to a sintering furnace, i.e. moving steel belt grate furnace (Step 2, Figure 2-9). Here, green pellets are layer on-top a layer of already sintered pellets in order to protect the under-laying steel sintering belt from excessive temperatures. Gas burners are used to gradually increase the sintering temperature to between 1400 to 1500ºC (Basson and Daavittila, 2013). The pellets are subsequently ignited and air is drawn through the pellet bed. The carbon present in the pellets provides a sufficient amount of exothermic energy to allow pellet sintering (Niemelä et al., 2004; Beukes et al., 2010; Kleynhans et al., 2012; Glastonbury et al., 2015). Sintering entails inter-particle binding of chromite grains by molten silicates and produces mechanically strong and porous pellets (Riekkola-Vanhanen, 1999; Zhao and Hayes, 2010). Sintered pellets are then screened (Step 3, Figure 2-9) to remove <6mm particulate material from the pelletized feed. Smaller aperture screening has

also been observed by the candidate. The <6mm material, which contain a significant amount of chromite grains that have undergone alteration due to oxidation, was of interest in this thesis and is therefore further discussed in Section 2.7. Off-gas generated during oxidative pellet sintering is handled in a similar manner than the off-gas generated during pellet pre-reduction (Step 4 and 5, Figure 2-9). Screened, sintered pellets are then stored as cold pellets (Step 6, Figure 2-9).

Cold sintered pellets are then conveyed to be batched (Step 7, Figure 2-9) with other furnace feed materials according to a specific metallurgical recipe, which depends on the chemical compositions of the materials to be smelted and the specific furnace slag regime. In some instances, spilled raw materials are included (Step 8, Figure 2-9), depending on the chemical composition and physical properties thereof.

2.6.2.3 Furnace feed material screening

This section refers to the "material screening" segment included in Figure 2-9 and refers specifically to Steps 9, 10, and 11. Under-sized furnace feed materials may be screened out from raw material streams, depending on the furnace type and the SAF's raw material prerequisites. Each furnace feed material, i.e. coarse flux, coarse reductant and chromite ore, is screened separately. In some cases, lumpy ores are also smelted. However, closed SAFs primarily consumes pre-treated (pre-reduced or oxidative sintering) pelletized chromite. Semi-closed SAF operations (indicated in yellow, Figure 2-9) are more robust than closed-SAFs (indicated in purple, Figure 2-9) with regard to material size prerequisites and may accommodate more fine materials in the furnace feed.

In summary, in some cases materials are screened prior to smelting to remove the under-sized fractions. These under-sized furnace feed materials were partially considered as waste materials, and are further discussed further in Section 2.7.

2.6.3. Specific smelting procedures

As indicated in Section 2.5.2, several FeCr smelting processes are utilized by the South African FeCr industry. This section is dedicated to discussing these processes in greater detail, as well as to identify generated wastes. All of the applied process steps applied during chromite smelting are presented in Figure 2-10. DC furnace smelting was not discussed, since solid wastes associated with it were not considered in this study.

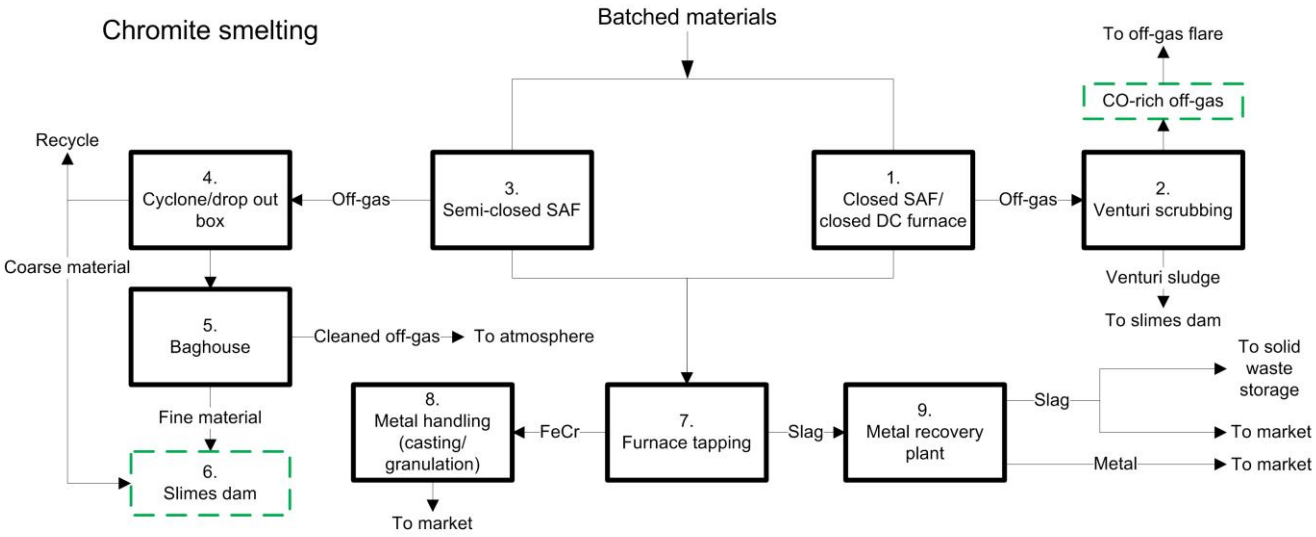

Figure 2-10: A flow diagram of currently applied chromite smelting processes and corresponding off-gas, FeCr, and slag handling procedures.

2.6.3.1 Closed SAF operation consuming a pre-reduced pelletized feed, coupled with venturi off-gas scrubbers

This FeCr smelting process consists of Steps 1, 2, 7, 8, and 9 in Figure 2-10. Mostly, screened furnace feed materials (including ores, fluxes and reductants) and hot pellets (and some cold pellets in certain instances) are fed to closed SAFs (Step 1, Figure 2-10). The *in-situ* generated CO-rich off-gas is continuously extracted from the furnace during smelting. This off-gas contains fine solid particulate matter, which has to be removed prior to the gas being released into the atmosphere. The solid particulate matter is removed by means of wet

venturi scrubbing (Step 2, Figure 2-10) (Gericke, 1995; Beukes et al., 2012; Van Staden et al., 2014). Figure 2-11 presents the schematic illustration of the venturi scrubbing process, as well as the subsequent handling of the venturi scrubber sludge and process water.

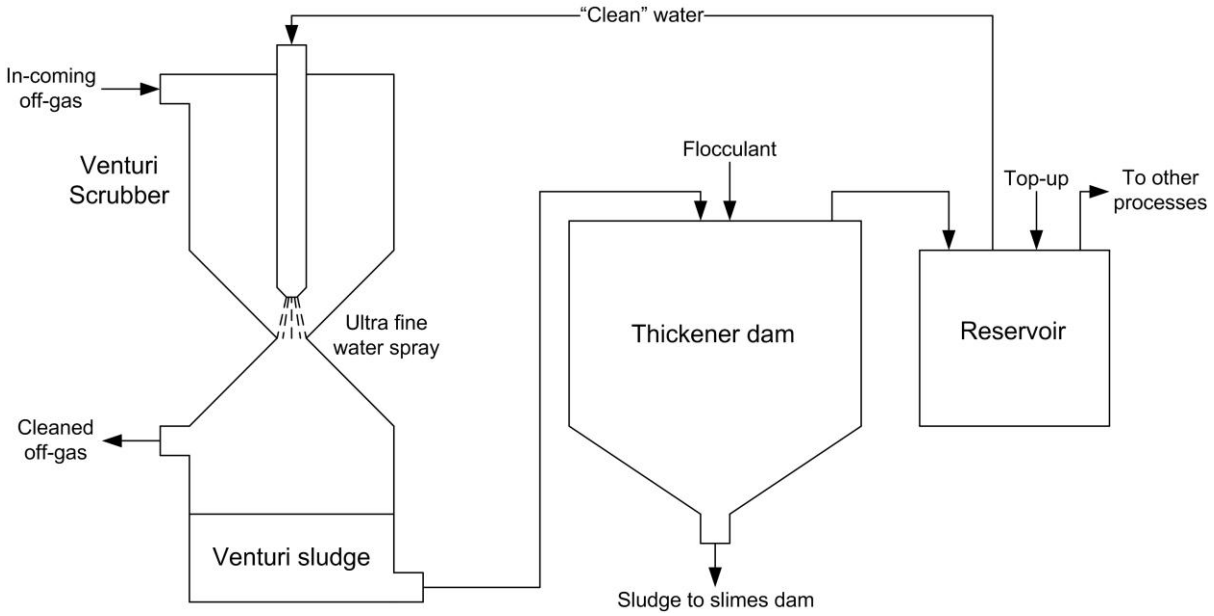

Figure 2-11: Schematic illustration to demonstrate the functioning of off-gas venturi scrubbing.

Prior to the off-gas scrubbing process, the in-coming off-gas is between 600 to 1000°C, and contains between 35 to 45 g.Nm^{-3} of solid material. During off-gas venturi scrubbing (Figure 2-11), 1 Nm^3 of off-gas is sprayed with 3 to 7 L of water at 30 bar (Niemelä et al., 2004). The water undergoes cloud-type atomization and results in the formation of liquid droplets with diameters of <10 µm (Hesketh, 1973). These tiny droplets allows for intimate contact between the droplets and particulate matter present in the off-gas, resulting in 99.9% of particulate matter being removed from the off-gas. Thus, the initial particulate matter content is reduced from 35 to 45 g.Nm^{-3} to between 50 to 100 mg.Nm^{-3}. However, the size of the remaining particles is usually <1 µm, which is difficult to remove from the off-gas stream by venturi scrubbing. This remaining ultra-fine particulate matter can be removed by sintered

filters (Niemelä et al., 2004). However, such filters are usually not used by South African FeCr producers (Beukes et al., 2010). During off-gas scrubbing, the generated venturi sludge collects at the bottom of the venturi scrubber from where it is pumped into a thickener. Here, the venturi sludge is allowed to separate from the scrubber water via settling. This settling process is usually accelerated through the addition of flocculants. The settled venturi sludge is considered as a hazardous waste material and is commonly treated for Cr(VI) (Beukes et al., 2012). Thereafter, the treated venturi sludge is dewatered and discarded in fit-for-purpose slimes dams. The "clean" process water in stored in a reservoir and is topped-up to maintain a certain volume. From here, the process water is either re-used in the scrubbing process, or utilized in other on-site processes.

The cleaned off-gas is used as an energy source on-site (e.g. material drying, pellet sintering, heating of ladles and drying of runners in the tapping area). However, due to the explosive and toxic nature of CO(g), unused cleaned off-gas is flared (burned) on-top of stacks. In doing so, large quantities of energy (in the form of heat released by combustion) are wasted. Closed SAF off-gas was considered in greater detail in Section 2.7.

Closed SAFs are intermittently tapped (Step 7, Figure 2-10) to remove the molten FeCr and slag. Furnace tapping is typically performed at fixed time intervals or when a fixed quantity of electricity has been consumed since the previous tap. Each SAF will have at least one taphole, which is a specially designed refractory inset in the furnace wall with a circular opening. After each tap, the taphole is plugged using specialized refractory clay. Both FeCr and slag are tapped through the same taphole (Riekkola-Vanhanen, 1999).

Molten FeCr is subsequently casted/granulated (Step 8, Figure 2-10) according to clients' prerequisites. Subsequently, the molten slag phase is allowed to solidify either naturally or by means of water spraying. Thereafter, the solid slag is broken into smaller pieces, crushed and conveyed to a metal recovery plant (Step 9, Figure 2-10). Any remaining FeCr is usually

recovered from slag with magnetic separation or jigging. The recovered FeCr is then sold, while the slag is either stockpiled or utilized in various commercial applications. Though, slag is considered the largest waste material by volume (Van Staden et al., 2014), it was not considered further in this study since various uses thereof already exist and it has received significant research attention (Lind et al., 2001; Zelić, 2005; Niemelä and Kauppi, 2007).

2.6.3.2 Closed SAF consuming oxidative sintered pelletized feed, coupled with venturi off-gas scrubbers

This smelting route consists of Steps 1, 2, 7, 8, and 9 in Figure 2-10. Generated off-gas is treated in a similar way (Step 2, Figure 2-10) as described in Section 2.6.3.1. The furnace tapping (Step 7, Figure 2-10), and subsequent FeCr (Step 8, Figure 2-10) and slag (Step 9, Figure 2-10) handling procedures are also similar to procedures discussed in Section 2.6.3.1. In terms of waste generation, the most significant difference between the two process options (Sections 2.6.3.1 and 2.6.3.2) is that screened furnace feed is preferred for SAF consuming oxidative sintered pellets, which results in <6mm materials (pellet fragments, ore, reductants and fluxes) having to be recycled or used in alternative applications. The supplier of the oxidative sintering technology indicated that chromite containing dusts collected from the pellet sintering scrubber and fines screened out from the sintered pellets can be re-introduced into the moist material mixture that is pelletized (Basson and Daavittila, 2013). However, it is specified that this addition must be limited to a maximum of 4 wt% of the total pellet composition, since it is believed to adversely affect pellet quality (Basson and Daavittila, 2013). This has resulted in the build-up of stockpiles of such pre-oxidised chromite fines at some FeCr producers.

2.6.3.3 Semi-closed SAF operations, coupled with bag filter off-gas treatment

This smelting route consists of Steps 3 to 9 in Figure 2-10. During semi-closed SAF smelting (Step 3, Figure 2-10), CO-rich off-gas permeates through the furnace bed and is unavoidably

ignited on top of the furnace bed due to air ingress into these types of furnaces. Thereafter the combusted off-gas is extracted and cleaned with bag filters, before being released into the atmosphere (Riekkola-Vanhanen, 1999; Beukes et al., 2010; Du Preez et al., 2017). Off-gas cleaning is achieved by initially passing off-gas through a cyclone or drop-out box (Step 4, Figure 2-10), where coarse material is separated from the off-gas. This coarse material may be recycled or discarded. Thereafter, the off-gas passes through a baghouse (Step 5, Figure 2-10) where the dry fine material is collected in specially designed bag filters. The collected dust is contacted with water as soon as possible, preventing dry dust spillages or wind dispersal (Beukes et al., 2012). The generated sludge is then treated to reduce Cr(VI) and is thereafter disposed in fit-for-purpose slimes dams (Step 6, Figure 2-10). The off-gas bag filter treatment process is illustrated in Figure 2-12 (Du Preez et al., 2017).

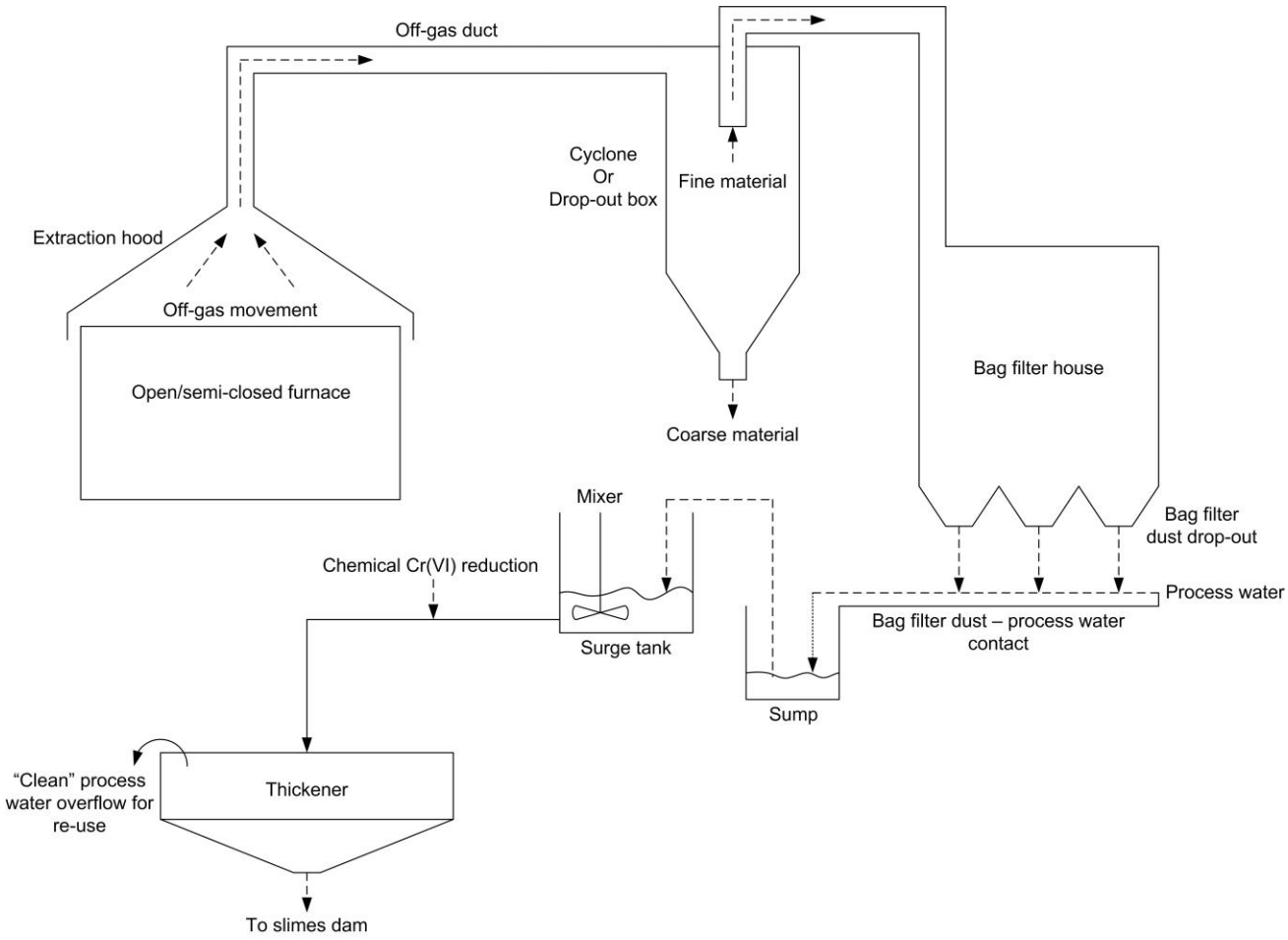

Figure 2-12: Schematic illustration to demonstrate the typical process flow of baghouse filter dust collection and subsequent treatment thereof (Du Preez et al., 2017).

A major concern for FeCr producers is the presence of relatively high Cr(VI) concentrations in slimes dams, since materials discarded in slimes dams, i.e. mainly BFD and/or venturi sludge, have already undergone treatment for Cr(VI) prior to being discarded. This may imply that the currently applied process, as indicated in Figure 2-12, does not extract the total Cr(VI) content present in BFD. The un-extracted Cr(VI) fraction present in BFD, which is stockpiled in slimes dams, may then solubilize and be released into the environment. Cr(VI) released into the environment as a result of FeCr production is extremely detrimental to the

ambient environment (Loock et al., 2014; Loock-Hattingh et al., 2015). Therefore, BFD was considered as a critical waste material in this study and was further discussed in Section 2.7.

Furnace tapping (Step 7, Figure 2-10), and subsequent FeCr (Step 8, Figure 2-10) and slag (Step 9, Figure 2-10) handling procedures are similar to procedures discussed in Section 2.6.3.1.

2.7 Waste materials investigated in this study

This section discusses the FeCr production wastes identified in Section 2.6, which will be investigated in this study. These include:

- BFD. Although Cr(VI) treatment have received significant research attention (Gericke, 1995; Maine et al., 2005; Bulut et al., 2009), it seems that the extraction of Cr(VI) from BFD is problematic in the currently applied treatment process.
- Cleaned CO-rich off-gas. Significant quantities of energy are currently being lost due to the forced flaring of cleaned CO-rich off-gas (Niemelä et al., 2004; Schubert and Gottschling, 2011). Considering the drive for improved energy consumption and reduced carbon footprint, it is important to consider how energy losses via CO flaring can be reduced.
- Fine raw materials (fluxes and reductants), which have been screened out of furnace feed. This "waste" is mainly associated with SAFs consuming oxidative sintered pellets.
- Pre-oxidised chromite fines. Pre-oxidised chromite fines originate from dusts collected from the pellet sintering scrubbers and fines screened out from the sintered pellets (Basson and Daavittila, 2013). Due to the limit specified by the technology supplier for recycling of such fines, stockpiles of this material have build-up at some FeCr producers.

2.7.1 Cr(VI) in the FeCr industry

Though this thesis did not focus in its entirety on Cr(VI), the fact that not all Cr(VI) is currently being extracted from BFD prior to treatment, as indicated in Section 2.6.3.3, highlighted the need for greater understanding of Cr(VI) related issues. Therefore, this section was devoted to contextualising the relevance of Cr speciation, mobility, and toxicity in the FeCr industry. Considering the significant differences in the impact of Cr(VI) on human health and the environment, as opposed to Cr(III) and Cr(0), it is important to consider the current knowledge base and the gaps therein, as well as best practices related to mining and smelting of chromite to produce FeCr. The candidate, as part of his PhD work, co-authored a review paper related to Cr(VI) issues associated with the FeCr industry (Beukes et al., 2017). The text presented in this section (as well as some text already presented) was a synopsis of the afore-mentioned review. The afore-mentioned published Cr(VI) review paper is attached as Appendix A.

2.7.1.1 Cr toxicity

Cr toxicity of the various oxidation states differs substantially. Cr(III) and Cr^0 are not classified as carcinogenic. Cr(III) is in fact an important trace element in a balanced nutritional diet and is in certain circumstances specifically included as a dietary supplement (Hininger et al., 2007). Furthermore, some Cr(III) species are considered as essential micro-nutrient required for protein, lipid, and carbohydrate metabolism in mammals (Berner et al., 2004). Additionally, Cr(III) diminishes low density lipoproteins in blood (Kassem, 2010; Whittleston et al., 2011; Dhal et al., 2013b).

In contrast to Cr(III) and Cr^0, Cr(VI) is considered as a toxic form of Cr (Cervantes et al., 2001). Excessive intake of Cr(VI) exerts toxic effects on biological systems and is associated with potentially deadly pathological changes within cells (Bielicka et al., 2005). Cr(VI) compounds are generally classified as carcinogenic, with specific ailments of the respiratory

system being implicated (Li et al., 2008; Beaver et al., 2009; IARC, 2012). Cr(VI) toxicity is ascribed to how easily Cr(VI) diffuses across cell membranes of organisms, resulting in metabolic reduction. Subsequently, free radicals are released that directly alters double-stranded deoxyribonucleic acid (DNA), affection gene duplication, replication, and repair (Dhal et al., 2013a). Cr(VI) has been shown to have several negative environmental impacts, e.g. reduced germination and growth of some plants (Peralta et al., 2001), increased mortality and reproduction rates in earthworms (Abbasi and Soni, 1983), organ damage in crayfish (Bollinger et al., 1997), detrimental effects on survivability, growth and post-exposure reproduction of marine fish larvae and copepods (Hutchinson et al., 1994), toxic effects on gill, kidney and liver cells of fresh water fish (Mishra and Mohanty, 2008), and possible diatom demise (Loock-Hattingh et al., 2015). The mobility of certain Cr(VI) compounds in aqueous systems exacerbate the hazardousness thereof (Ferreira et al., 1999). Cr(VI) mobility refers to the ability of certain Cr(VI) compounds (likely water-soluble compounds) to solubilize under certain conditions, and be transported into sub-surface soils and groundwater (Sethunathan et al., 2005). Public health related threats arise if drinking water is contaminated with Cr(VI) (Shen et al., 2012), increasing the risk of stomach cancer (Zhang and Li, 1987; Beaumont et al., 2008; IARC, 2012). Therefore, it is important to prevent or at least mitigate the formation of such compounds, and to apply proper treatment strategies to Cr(VI) containing wastes.

2.7.1.2 Cr(VI) natural occurrence and/or formation

In order to contextualize the possible natural occurrence and/or formation of Cr(VI), the basic Cr cycle in soil and water, as presented in Figure 2-13 (Bartlett, 1991; Testa et al., 2004) needs to be considered first. Only a synopsis of this Cr cycle will be considered here, with detailed information available in the original text and references therein (Bartlett, 1991; Testa et al., 2004).

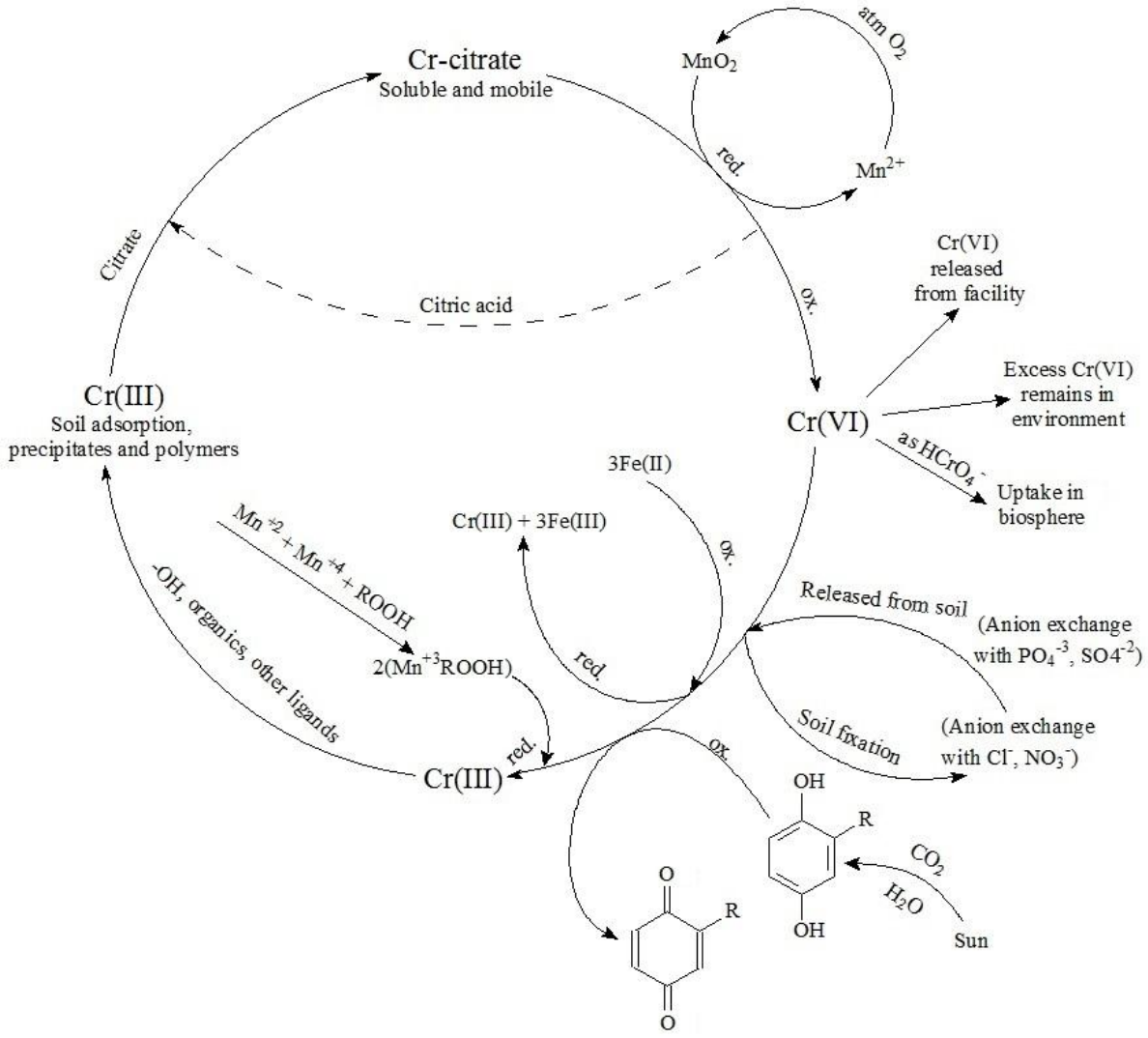

Figure 2-13: The Cr cycle, adapted from Testa et al. (2004) and Bartlett (1991).

In essence, the soil/water Cr cycle (Figure 2-13) indicates that Cr(III) is the dominant species under most near-surface environmental conditions. However, Cr(III) can be oxidized under ambient environmental conditions in the presence of MnO_2, which serves as a catalyst for the atmospheric oxidation of Cr(III) in surface or ground water. However, for this to take place Cr(III) must be in a soluble form (Bartlett, 1991). Cr(III) hydroxides are relatively insoluble over a wide pH range (see Figure 2-14; Rai et al., 1987) and therefore usually do not contribute significantly to such oxidation. Cr(VI) can be reduced by various inorganic species, including aqueous Fe(II) (Eary and Rai, 1988), magnetite (Peterson et al., 1996),

green rust (Williams and Scherer, 2001), and zero valent iron (Chang et al., 2014). Additionally, Cr(VI) can be reduced by numerous organic compounds (both synthetic and natural) and microorganisms (March, 1992; Dong et al., 2014; Miller et al., 2016; Jin et al., 2017; Gupta et al., 2017; Wang et al., 2017). However, some organic compounds could complex Cr(III) and in so doing solubilize it, which could facilitate the formation of Cr(VI) due to natural oxidation in the presence of MnO_2.

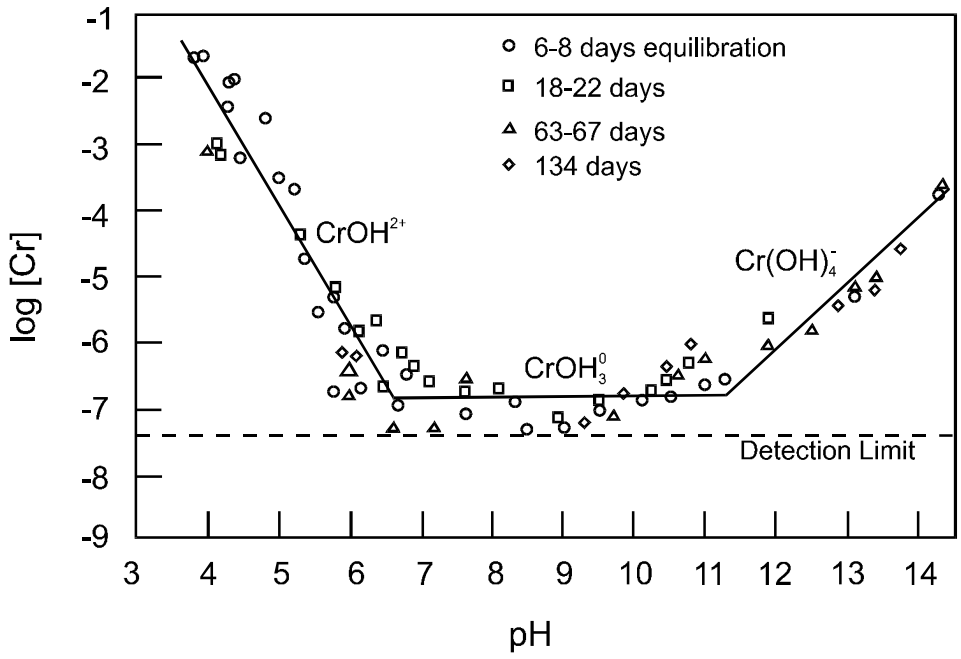

Figure 2-14: The solubility of $Cr(OH)_3(s)$, adapted from (Rai et al., 1987).

In the ambient atmosphere, Cr(VI) is associated exclusively with particulate matter and/or atmospheric water, since the vapour pressure of all Cr compounds at ambient conditions is negligible (Seigneur and Constantinou, 1995; Kimbrough et al., 1999). All atmospheric inter-conversion reactions leading to possible Cr(VI) formation and reduction to Cr(III) are therefore water-phase reactions (Seigneur and Constantinou, 1995; Kimbrough et al., 1999). The basic atmospheric cycle of Cr, as presented in Figure 2-15, has some similarities to the soil/water cycle previously presented (Figure 2-13). Again, Cr(III) is the dominant species, with many compounds able to reduce Cr(VI) to Cr(III). In the atmosphere S(IV) is a

relatively important species that can reduce Cr(VI) to Cr(III). S(IV) is basically SO_2, which is a common atmospheric anthropogenic pollutant, dissolved in water (Seigneur and Constantinou, 1995; Beukes et al., 1999; Beukes et al., 2000). Cr(VI) formation is usually associated with the presence of MnO_2 (Seigneur and Constantinou, 1995; Kimbrough et al., 1999).

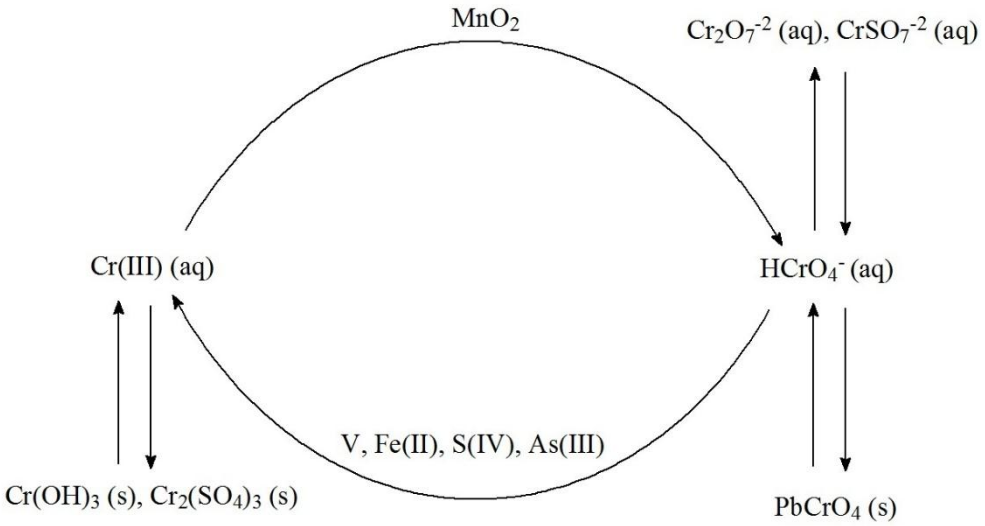

Figure 2-15: The basic atmospheric cycle of Cr, adapted from Seigneur and Constantinou (1995).

Notwithstanding the likely dominance of insoluble Cr(III) in natural environments, naturally occurring Cr(VI) and/or natural formation thereof have been reported for various locations. At least 24 known Cr(VI)-bearing minerals occur (Motzer and Engineers, 2004 and references therein), which could serve as a natural sources of Cr(VI). This includes minerals such as crocoite ($PbCrO_4$) that form in the oxidized zones of lead (Pb) deposits and Cr(VI) minerals in nitrate-rich evaporite deposits in arid environments such as the Chilean nitrate deposits in the Atacama Desert. (Motzer and Engineers, 2004 and references therein), also described Cr(VI) occurring in groundwater due to natural formation/processes at various locations in the USA, including Paradise Valley (Arizona), the Presidio in San Francisco,

Davis (California), the western Mojave Desert (California) and Soquel Water District south of Santa Cruz (California). In general, it is believed that most of these natural occurrences of Cr(VI) in groundwater are linked to the hydrolysis of feldspar, some common mafic minerals such as Cr-bearing pyroxenes and chromite, together with calcite, which cause alkaline groundwater conditions. This, coupled with the absence of natural reducing agents, e.g. Fe(II), organic matter and reducing organisms (see Figure 2-13), may have allowed oxidation of Cr(III) to Cr(VI).

Chromite is a stable non-soluble mineral, in which Cr occurs in the Cr(III) oxidation state. However, Cr(VI) contamination of ground and/or surface water has been reported as a direct result of chromite mining in India. Godgul and Sahu (1995) postulated that serpentinization and magnesium (Mg) ion release during deuteric alteration of ultramafic rocks (peridotites) and associated oxidation (laterization) created alkaline pore water in the chromite deposits of the Sukinda belt of Orissa (India), which resulted in conditions favorable for natural Cr(VI) formation. Dubey et al. (2001), Tiwary et al. (2005) and Dhal et al. (2010) subsequently reported on several aspects related to the Cr(VI) leaching from these deposits and/or mine dumps in the same area.

As far as the authors could ascertain, Cr(VI) has not been reported in surface and/or ground-waters in South Africa (and Canada which was specifically considered in the review by Beukes et al., 2017) as a result of natural occurrence/formation, or chromite mining. Pöykiö et al. (2005) did, however, show that Scots pine (Pinus sylvestris L.) bark used as a passive bio-indicator in the immediate vicinity of the FeCr and stainless steel works at Tornio and near the open-cast chromite mine at Kemi (both in northern Finland) indicated Cr pollution factors (PF i.e. ratio of heavy metal concentrations in the bio-indicators to those in the background area) of 81 and 5.3, respectively. However, this data does not imply that the Cr occurred as Cr(VI).

2.7.1.3 Cr(VI) in BFD

As indicated earlier (text below Figure 2-12, Section 2.6.3.3), a major issue for FeCr producers utilizing semi-closed SAFs is the occurrence of Cr(VI) in slimes dams, even after Cr(VI) treatment was applied. The primary Cr(VI) containing waste material stockpiled in slimes dams is BFD, which originates from semi-closed FeCr SAFs (Basson and Daavittila, 2013). Other materials co-disposed in slimes dams, e.g. venturi sludge (Beukes et al., 2017), do not significantly contribute to the total Cr(VI) content of slimes dams. Cr(VI) leaching from slimes dams indicates that currently applied Cr(VI) extraction procedures applied by FeCr producers may not sufficiently extract Cr(VI) from Cr(VI) containing wastes. However, previous studies indicated that complete Cr(VI) extraction from BFD is achievable by contacting the BFD with neutral water for >100 h (Maine et al., 2005). Gericke (1995) stated that Cr(VI) can be leached from BFD after 24 hrs with a pH 2 to 6 aqueous solution. Bulut et al. (2009) indicated that Cr(VI) is completely solubilized from BFD after 30 min of leaching and that the solution pH did not play a significant role Bulut et al. (2009).

Cr(VI) leachability from BFD was specifically investigated in this study, with the associated results presented in Chapter 3 in the form of a published paper.

2.7.2 CO-rich off-gas

The candidate, as part of his MSc studies, published a paper related to the formation of Cr(VI) in CO-rich off-gas flaring. Although not part of this study *per se* this paper is attached as Appendix B, so that the reader can understand the total contribution the candidate have made to the field of study.

CO-rich off-gas originating from closed SAF smelting and closed DC furnace smelting contains various concentrations of CO(g) and H_2(g) (Schubert and Gottschling, 2011; Niemelä et al., 2004), and is typically flared on top a furnace stack in order to oxidize the CO and H_2 contents thereof (Schubert and Gottschling, 2011). As previously stated, the main

reasons why CO-rich off-gas is usually not stored in large volumes on-site are its toxicity to humans via inhalation (Hall et al., 2015; Maynard et al., 2015) and its explosive risk (Niemelä et al., 2004). Figure 2-16 shows a typical off-gas flare burning on top a purposefully designed closed SAF stack (Du Preez et al., 2015).

Figure 2-16: A typical off-gas flare on top a closed SAF stack, courtesy of (Du Preez et al., 2015).

The volume and composition of off-gas originating from closed SAF operations depends on various factors, e.g. furnace design, process metallurgical condition, feed pre-treatment methods, feed material, and furnace operating philosophy (Beukes et al., 2010). It has been reported that closed SAF off-gas typically consists of 75 to 90% CO, 2 to 15% H_2, 2 to 10% CO_2 and 2 to 7% N_2 and between 650 to 750 Nm^3 of off-gas is generated per ton FeCr produced (Niemelä et al., 2004), whereas closed DC furnace off-gas compositions has been

reported to be 58 to 64% CO, 2 to 6% CO_2, 26 to 34% H_2, 0 to 5% N_2 and <1% O_2 (Schubert and Gottschling, 2011).

Niemelä et al. (2004) estimated that for each ton of FeCr produced in a closed SAF, the accompanying generated CO(g) has an energy value of between 2.0 to 2.3 MWh, depending on the CO(g) and H_2(g) contents. Thus, massive quantities of energy are lost during CO-rich off-gas flaring (Niemelä et al., 2004; Schubert and Gottschling, 2011). Some FeCr producers utilize between 30 to 35% of CO-rich off-gas as an on-site energy source for e.g. heating ladles, raw material drying, pre-heating furnace charge and chromite pellet sintering/pre-reduction (Niemelä et al., 2004). However, it is estimated that the amount of heat utilized by heating/drying procedures may be considered as negligible compared to the potential heat associated with CO-rich off-gas (Schubert and Gottschling, 2011).

Due to increased pressure on profitability (e.g. due to increasing electricity costs) and increased environmental concerns (e.g. reduction in carbon footprint, and carbon tax), methods have been developed in an attempt to utilize CO-rich off-gas. Methods includes the combustion of the cleaned off-gas in so-called CO-gens, which is defined as internal combustion engines utilizing CO- and H_2-rich off-gas as a fuel source to drive electrical power producing alternators (Schubert and Gottschling, 2011), fermentation of CO-rich off-gas with bacteria to produce usable chemicals (Molitor et al., 2016), and off-gas combustion to generate steam for steam turbine electricity generation (Dos Santos, 2010). However, each of the afore-mentioned methods has associated complications, limiting the large scale industrial applications thereof. Additionally, as previously stated, off-gas storage should be avoided due to the toxic and explosive nature thereof. Ideally, off-gas has to be utilized as soon as it is generated. A novel approach to the utilization of energy associated with CO-rich off-gas combustion was investigated in this study and is presented in Chapter 4.

2.7.3 Under-sized raw materials

The term "waste" is used loosely here and primarily refers to carbonaceous reductant and quartz deemed to be too fine (<6mm), which is screened out of furnace feed materials designated for closed SAF smelting. These under-sized materials are usually collected and re-used on-site, or are discarded if a suitable application does not exist. Under-sized chromite and reductants are typically re-used in the pellet production process and therefore do not build-up in significant quantities. However, fine quartz (used as a flux) does not have such a metallurgical recycling route. Limited quantities can be used in ingot sand moulds, wherein hot FeCr metal is casted. Also, it can be used on-site in concrete, but this has finite application.

An alternative, novel approach for the use of several fine feed material wastes (or partially classified as waste) is presented in Chapter 4.

2.7.4 Under-sized pre-oxidized sintered material

Oxidized chromite requires less energy to metallize if compared to normal chromite (Kapure et al., 2010). Additional oxidation of oxidative sintered pellets further decreases the energy required for reduction (Zhao and Hayes, 2010). Furthermore, pre-oxidation of chromite fines significantly improve pre-reduction (solid state reduction) of chromite (Kleynhans et al., 2016b and 2017). Considering these energy related benefits, the candidate believe that all pre-oxidised fine chromite generated during oxidative sintering (Section 2.6.2.2) should be recycled on-site at FeCr producers. With this in mind, the possible recycling of pre-oxidized chromite fines into oxidative sintered pellets beyond the current limitation of 4 wt% pellet composition was investigated (Chapter 5).

2.8 Summary

It is evident from the literature survey presented in this chapter that the management of several wastes generated by the FeCr industry can be improved. Specifically three

aspects/wastes were identified, which was investigated in greater detail in this study. These were:

- The leaching behaviour of Cr(VI) from BFD, with the aim of contributing to improved Cr(VI) treatment strategies – results presented in Chapter 3.
- The development of a novel method to store energy associated with CO-rich off-gas combustion – results presented in Chapter 4.
- The recycling of pre-oxidised chromite fines beyond the current limitation of 4 wt%, which is specified by the technology supplier – results presented in Chapter 5.

CHAPTER 3: ARTICLE 1

Aqueous solubility of Cr(VI) compounds in ferrochrome bag filter dust and the implications thereof

3.1 Author list, contributions, and consent

Authors list

SP du Preez[a], JP Beukes[a*], WPJ van Dalen[a], PG van Zyl[a], D Paktunc[b] and MM Loock-Hattingh[a]

[a]Chemical Resource Beneficiation, North-West University, Potchefstroom Campus, Private Bag X6001, Potchefstroom 2520, South Africa

[b]CanmetMINING, Natural Resources Canada, 555 Booth St., Ottawa, ON, K1A0G1, Canada

Contributions

Contributions of the various co-authors were as follows:

Experimental work, data processing and interpretation, research, and writing of the scientific paper, was performed mainly by the candidate, SP du Preez. WPJ van Dalen conducted some experimental work included in this article as part of his Magister in Chemistry degree at the North-West University, Potchefstroom Campus. Some analytical work and assistance with the interpretation thereof was performed by D Paktunc. JP Beukes (supervisor), PG van Zyl (co-supervisor) and MM Loock-Hatting made conceptual contributions.

Consent

All of the co-authors that contributed to the article presented in this chapter have been informed that the article will form part of the candidate's PhD, submitted in article format, and have granted permission that the article may be used for the purpose stated.

3.2 Formatting and current status of the article

The article presented in Chapter 3 was published by *Water SA* in 2017, Vol. 43(2), pages 298-309 (DOI: http://dx.doi.org/10.4314/wsa.v43i2.13). The journal details can be found at http://www.wrc.org.za/Pages/KH_WaterSA.aspx?dt=5&L0=1&L1=4 (Date of access: 16 November 2017).

Aqueous solubility of Cr(VI) compounds in ferrochrome bag filter dust and the implications thereof

SP du Preez[1], JP Beukes[1]*, WPJ van Dalen[1], PG van Zyl[1], D Paktunc[2] and MM Loock-Hattingh[1]

[1]*Chemical Resource Beneficiation, North-West University, Potchefstroom Campus, Private Bag X6001, Potchefstroom 2520, South Africa*

[2]*CanmetMINING, Natural Resources Canada, 555 Booth St., Ottawa, ON, K1A0G1, Canada*

ABSTRACT

The production of ferrochrome (FeCr) is a reducing process. However, it is impossible to completely exclude oxygen from all of the high-temperature production process steps, which may lead to unintentional formation of small amounts of Cr(VI). The majority of Cr(VI) is associated with particles found in the off-gas of the high-temperature processes, which are cleaned by means of venturi scrubbers or bag filter dust (BFD) systems. BFD contains the highest concentration of Cr(VI) of all FeCr wastes. In this study, the solubility of Cr(VI) present in BFD was determined by evaluating four different BFD samples. The results indicate that the currently applied Cr(VI) treatment strategies of the FeCr producer (with process water pH ≤ 9) only effectively extract and treat the water-soluble Cr(VI) compounds, which merely represented approximately 31% of the total Cr(VI) present in the BFD samples evaluated. Extended extraction time, within the afore-mentioned pH range, proved futile in extracting sparingly-soluble and water-insoluble Cr(VI) species, which represented approximately 34% and 35% of the total Cr(VI), respectively. Due to the deficiencies of the current treatment strategies, it is highly likely that sparingly water-soluble Cr(VI) compounds will leach from waste storage facilities (e.g. slimes dams) over time. Therefore, it is critical that improved Cr(VI) treatment strategies be formulated, which should be an important future perspective for FeCr producers and researchers alike.

Keywords: hexavalent chromium, Cr(VI), ferrochromium, ferrochrome, bag filter dust, smelter waste

INTRODUCTION

Since its discovery in 1798, chromite has remained the only commercially viable source of new chromium (Cr) units (Murthy et al. 2011; Riekkola-Vanhanen, 1999). Approximately 90% to 95% of mined chromite is used in the metallurgical industry for the production of various grades of FeCr, which is produced through the carbo-thermic reduction of chromite ore (Riekkola-Vanhanen, 1999). About 80% to 90% of ferrochrome (FeCr) is consumed by the stainless-steel industry, primarily as high-carbon or charge-grade FeCr (Murthy et al. 2011). Stainless steel is a vital alloy in various applications (Gasik, 2013), with the Cr content of stainless steel increasing its corrosion resistance. South Africa holds the largest chromite deposits and is the second-largest FeCr producing country (ICDA, 2012), with 14 FeCr smelters (Beukes et al., 2012).

Cr is present as Cr(III) in chromite ore, while Cr(0) occurs in the produced FeCr. Although completely unintended, small amounts of Cr(VI) are formed during FeCr production, which may be present in waste materials (Beukes et al., 2010). Cr(VI) is generally regarded as carcinogenic (IARC, 2012), with specifically airborne exposure to Cr(VI) being associated with cancer of the respiratory system (Proctor et al., 2002). In contrast to Cr(VI), Cr(III) and Cr(0) are not classified as carcinogenic. Cr(III) is in fact used a dietary supplement for certain human health abnormalities (Hininger et al., 2007).

*To whom all correspondence should be addressed.
Tel.: +27 (0) 18 299 2337; fax: +27 18 (0) 299 2350;
e-mail: paul.beukes@nwu.ac.za
Received 7 September 2016; accepted in revised form 27 March 2017

The main types of waste generated during FeCr production are slag, sludge from wet venturi scrubbers and bag filter dust (BFD) (Van Staden et al., 2014). Slag-to-FeCr generation ratios of 1.1:1 up to 1.9:1 are common in this industry, with ratios varying according to different production technologies employed (Beukes et al., 2010; Niemelä and Kauppi, 2007). Although the volumes of slag generated are large, the Cr(VI) content of the slag is usually very low (Beukes et al., 2010; Niemelä and Kauppi, 2007). Additionally, FeCr slag can be used in various commercial applications (Niemelä and Kauppi, 2007; Zelić, 2005; Lind et al., 2001; Riekkola-Vanhanen, 1999). Sludge, which is generated during the wet venturi scrubbing of closed furnace off-gas (Beukes et al., 2010; Niemelä et al., 2004) does not usually contain significant Cr(VI) concentrations (Gericke, 1998). However, in contrast to slag and sludge, BFD generated during the cleaning of off-gas from open/semi-closed FeCr furnaces contains significant levels of Cr(VI) (Beukes et al., 2012; Maine et al., 2005; Gericke, 1998), which cannot be disposed without proper Cr(VI) treatment (Beukes et al., 2012). After the BFD is treated to reduce Cr(VI), it is usually disposed in fit-for-purpose waste facilities such as slimes dams.

Treatment of BFD (and indeed any Cr(VI) containing FeCr waste) usually involve the aqueous reduction of Cr(VI) with an appropriate inorganic reducing agent such as Fe(II) (Beukes et al., 2012; Seaman et al., 1999; Buerge and Hug, 1997) and S(IV) (Beukes et al., 2001 and 1999), or bacterial reduction (Dhal et al., 2013; Molokwane et al., 2008). Although Cr(VI) can also be reduced with numerous organic compounds (Kassem, 2010; March, 1992), this is usually avoided due to the potential solubilisation of Cr(III) (Beukes et al., 2012; Apte et al., 2006). In this paper, the leaching potential of Cr(VI) from BFD is investigated and it is proven that this can be a major limitation in the effectiveness of the conventional Cr(VI) treatment used by industry.

http://dx.doi.org/10.4314/wsa.v43i2.13
Available on website http://www.wrc.org.za
ISSN 1816-7950 (Online) = Water SA Vol. 43 No. 2 April 2017

MATERIALS AND METHODS

Materials

Numerous factors can influence the composition of BFD, including the production technology employed (e.g. open or semi-closed furnace technology, type of filters used in the bag filter plant), physical separation in the bag filter plant itself (e.g. some compartments containing finer material than others), metallurgical operating conditions (e.g. basic or acid slag operating conditions) and composition of feed materials (e.g. chemical and physical differences of ores). Therefore, four different BFD samples were obtained from FeCr producers in South Africa. These producers preferred to remain anonymous and therefore the samples are merely referred to as BFD samples A, B, C and D.

All chemicals used were analytical grade reagents. Standard Cr(VI) solutions were prepared from a 1 009 ± 5 mg·mL^{-1} aqueous chromate (CrO_4^{2-}) analytical solution (Spectrascan, distributed by Teknolab AB, Sweden), which were used for calibration and verification of the analytical technique employed. The post-column reagent that was used during Cr(VI) analysis was prepared using 1,5-diphenylcarbazide (DPC) (FLUKA), 98% sulfuric acid (Rochelle Chemicals) and HPLC grade methanol (Ace). Solutions of sodium hydroxide (Merck) and perchloric acid (Merck) were used to adjust the pH of aqueous solutions/mixtures. According to solubility data, Cr(VI) chemicals can be classified as water soluble, sparingly water soluble and water insoluble (IARC, 2012; Ashley et al., 2003). Ammonium sulphate with 99% purity (Merck SA) and 25% ammonia solution (Associated chemical enterprises) were used to prepare a 0.05 M $(NH_4)_2SO_4$ – 0.05 M NH_4OH extraction buffer that is capable of leaching all water-soluble and sparingly water-soluble Cr(VI) compounds (Ashley et al., 2003). Sodium hydroxide (Promark chemicals) and anhydrous sodium carbonate (Merck SA) were used to prepare a 3 wt% Na_2CO_3 – 2 wt% NaOH extraction buffer, to quantitatively extract all Cr(VI) in the BFD samples, including the water-insoluble fraction (Ashley et al., 2003). Ultra-pure deionized water (resistivity, 18.2 MΩcm^{-1}), produced by a Milli-Q water purification system, was used for all dilutions and aqueous extractions. 99.999% pure nitrogen gas (N_2) (AFROX) was used to provide an inert environment during leaching. Hydrophilic PVDF 0.45 µm filters (Millipore Millex, USA) were used for the filtration of solutions.

BFD sample characterisation

A Malvern Mastersizer 2000 was used to determine the particle size distribution of the BFD samples. A diluted suspension of material was ultra-sonicated for 1 min prior to the particle size measurement, in order to disperse the individual particles and to prevent the use of a chemical dispersant. Laser obscuration was kept at 10% to 15%, while mechanical stirring was set to 2 000 r·min^{-1}. Ten measurements were made for each sample and the average taken.

Scanning electron microscopy with energy dispersive x-ray detectors (SEM-EDS) was used to perform morphological and chemical characterisation of the BFD particles. FEI Quanta 250 FEG ESEM incorporating Oxford Inca X-Max 20 EDS system with a 15 kV electron beam at a 10 mm working distance was used. BFD samples were prepared with two different procedures for SEM analysis. Firstly, samples were mounted onto a specimen stub with carbon-coated tape and subsequently gold coated in order to determine the general BFD particle characteristics, e.g., size and shape. In order to determine the chemical compositions of the BFD samples by SEM-EDS, the samples were set in resin and polished before being analysed. The SEM-EDS analysis was performed by scanning a wide rectangular area of the sample surface in a raster-like pattern for 60 s. Spot analyses were also performed to determine the composition of individual particles present in the BFD.

X-ray diffraction (XRD) analyses were performed on BFD samples ground to < 45 µm using a Rigaku D/MAX 2500 rotating-anode powder diffractometer with Cu Kα radiation at 50 kV, 260 mA, a step-scan of 0.02°, and a scan rate at 1 min^{-1} in 2 h from 5° to 70°. Phase identifications were made using JADE v.9.3 coupled with the ICSD and ICDD diffraction databases.

Trace metal analysis

Inductively coupled plasma mass spectroscopy (ICP-MS) (Agilent 7500CE ICP-MS with Octopole Reaction System) was used to determine the total metal concentrations, irrespective of oxidation state, present in aqueous leach solutions. These solutions were obtained as described in the next section.

Cr(VI) extraction and analysis

For each BFD sample, 0.50 g was transferred into a 100 mL glass beaker, which contained 50 mL of deionized water. The initial pH of the deionized water had been adjusted to a predetermined value. Leaching solutions were purged with N_2 for 10 min prior to Cr(VI) extraction to remove dissolved oxygen from the solution, which may cause unwanted Cr(III) oxidation (Ashley et al., 2003). Each beaker and its contents were placed on a magnetic stirrer and agitated for a period of 2 h. A steady stream of N_2 was continually used to purge the suspension, ensuring an inert environment during leaching. After Cr(VI) extraction, the leaching solutions were filtered through hydrophilic Millipore 0.45 µm PVDF filters to remove particulate matter, followed by another pH measurement to ensure that no pH drift occurred. Thereafter the filtrates were transferred to 100 mL A-grade volumetric flasks and diluted to a final volume of 100 mL with pH-adjusted deionized water. 50 mL of each solution was used for aqueous trace metal analyses, while the remaining 50 mL was used for Cr(VI) analysis. All pH measurements were conducted with a HANNA - HI 991001 pH meter with a temperature probe.

In addition to Cr(VI) extraction at specific pH values, Cr(VI) extractions were also performed using hot plate digestion. A buffer of 0.05 M $(NH_4)_2SO_4$ and 0.05 M NH_4OH was used to leach water-soluble and sparingly water-soluble Cr(VI) compounds, while a buffer of 3 wt% Na_2CO_3 and 2 wt% NaOH was used to leach total Cr(VI) (Ashley et al., 2003; NIOSH 7605, 2003). The afore-mentioned buffer (Na_2CO_3 – NaOH) enhances the dissolution of insoluble Cr(VI) compounds at higher pH levels by the addition of carbonate (CO_3^{2-}), as indicated in Eq. 1. In the presence of a large excess of CO_3^{2-} the equilibrium shifts quantitatively to the right of Eq. 1 and insoluble Cr(VI) becomes soluble (Ashley et al., 2003).

$$MCrO_4 + CO_3^{2-} \leftrightarrow MCO_3 + CrO_4^{2-} \quad (1)$$

with M = cation associated with chromate

The Cr(VI) concentrations of aliquots were determined with a Thermo Scientific Dionex ICS 3000 ion chromatograph (IC) according to the procedure described by Loock et al. (2014) and Du Preez et al. (2015), which was derived from Dionex Application Update 179 (2011), Dionex Application Update 144 (2003), and Thomas et al. (2002). The IC system was equipped with a Dionex IonPac AG7 4 x 50 mm guard column

http://dx.doi.org/10.4314/wsa.v43i2.13
Available on website http://www.wrc.org.za
ISSN 1816-7950 (Online) = Water SA Vol. 43 No. 2 April 2017

and a Dionex IonPac AS7 4 x 250 mm analytical separation columns. A 1 000 µL injection coil and a 2 x 375 µL knitted reaction coil coupled to a UV-visible absorbance detector set at a wavelength of 530 nm were used. 250 mM ammonium sulphate was used as an eluent and an isocratic pump carried the eluent and the injected sample through the system. 2 mM DPC solution was used for post column coloration, which was delivered into the system by an AXP pump. The flow rates of the eluent and colorant were 1.0 mL·min^{-1} and 0.5 mL·min^{-1}, respectively. A six-point calibration was performed for Cr(VI), ranging from 5 to 75 µg·L^{-1}. The correlation coefficient of this linear calibration line was > 99.96%. The detection limit of this method at a confidence level of 98.3%, which was calculated according to the method specified by Skoog et al. (2013), was experimentally determined as 0.9 µg·L^{-1} by Loock-Hattingh (2016). The accuracy of the specific analytical method (and the specific instrument used) was recently indicated (Venter et al., 2016) by analysis of a Community Bureau of Reference (former reference materials program of the European Commission) BCR Nº 545 welding dust filter certified reference material (individual identification Nº B7-36, purchased on 25 January 2013), for which a value of 39.7 mg·g^{-1} Cr(VI) was obtained, which was within the uncertainty of the reference material that was defined as the half width of the 95% confidence interval of the mean of 40.2 mg·g^{-1} Cr(VI).

X-ray absorption spectroscopy (XAS)

XAS experiments were carried out at PNC-CAT's bending magnet beam-line 20-BM of the Advanced Photon Source (APS), Argonne, IL, USA. Finely ground and homogenized BFD samples were placed as monolayers on tapes and loaded into Plexiglass sample holders. Experiments were carried out at room temperature both in transmission and fluorescence modes using ion chambers filled with nitrogen and helium gases, and a Canberra 13-element detector. A Cr foil was used for energy calibration. Between 4 and 6 scans were collected from each sample and the reference materials. Data reduction and analysis were performed with ATHENA (Ravel and Newville, 2005). The least squares fitting of the XANES spectra were made with LSFitXAFS (Paktunc, 2004). XAS, including both X-ray absorption near-edge spectroscopy (XANES) and extended X-ray absorption fine structure (EXAFS) regimes, was employed to determine the sources and quantitative speciation of Cr in the BFD samples and possible cation association of CrO_4^{2-} that could be leached and precipitated from the BFD samples. Precipitates were prepared by contacting 50 g of BFD with 1 L of deionized water for 4 consecutive 24 h contacting periods. After 24 h contact, the water was separated from the BFD by means of filtration, after which the BFD were re-contacted with fresh water and the procedure repeated. All four leachates were combined and then allowed to evaporate at room temperature in a fume cupboard circulated with filtered air to prevent contamination, producing a solid residue that was analysed with XAS spectroscopy techniques.

RESULTS AND DISCUSSION

Particle size analysis

The d_{90}, d_{50} and d_{10} of the particle size distribution of the different BFD samples are presented in Table 1. The d_{90} is defined as the equivalent particle size for which 90% of the particles are smaller, with definitions of d_{50} and d_{10} derived similarly. The particle size analyses indicated that the d_{90} of all four BFD samples ranged between 32.8 and 152.2 µm, with the A and B samples being coarser than the C and D samples. The particle sizes reported here are similar to BFD particle sizes reported previously (Van Staden et al., 2014; Beukes et al., 2010).

TABLE 1
The average d_{90}, d_{50} and d_{10} values of BFDs

BFD	Particle size (µm)		
	d_{90}	d_{50}	d_{10}
A	140.6	39.4	4.3
B	152.2	37.6	4.2
C	32.8	10.3	1.7
D	33.3	9.7	1.7

SEM observations

Figures 1(a), 1(b), 1(c) and 1(d) indicate SEM micrographs of BFD samples of A, B, C and D. Each of these figures present combined images, with the larger images indicating cross-sectional polished micrographs. The smaller images (in the bottom right-hand corners) represent micrographs of the BFDs pressed onto stubs with adhesive carbon tape. It is evident from these micrographs that the BFD samples consisted mainly of very small particulate matter (mostly < 40 µm), with some larger particles of up to approx. 200 µm. It was previously shown that the larger unevenly-shaped particles observed in BFD are unreacted or partially-reacted feed materials such as chromite, fluxes or reductants, while the very small spherical particles represent the actual off-gas particulates (Van Staden et al., 2014; Beukes et al., 2010; Beukes et al., 1999). However, to confrim that unreacted/partially-reacted chromite particles were present in the BFD samples, one of the unevenly-shaped grey particles, marked with a white box in Fig. 1(a) (BFD sample A), was analysed with SEM-EDS, which revealed Cr and Fe contents of 30.7 and 20.8 wt%, respectively. These correspond to a Cr/Fe ratio of 1.48 which is comparable to typical South African chromite ore (Cramer et al., 2004). The SEM micrographs also revealed that the BFD samples A and B (Figs. 1(a) and 1(b)) contained more unreacted/partially-reacted larger raw material particles when compared to C and D (Figs. 1(c) and 1(d)). The SEM observations confirmed the particle size analysis results (Table 1), which indicated that the A and B samples were coarser than C and D. As previously indicated, the presence of a greater number of larger raw material particles in the BFD could be ascribed to the differences in the technology applied or the feed materials used at different production facilities. For instance, some FeCr smelters utilize a cyclone to remove larger and denser particles before the off-gas is cleaned in the bag filter plant, while others merely use a drop-out box that is less effective.

SEM-EDS chemical analyses of the BFD samples are presented in Table 2. These results should be considered as semi-quantitative, with O content determined by difference. Carbon (C) was not analysed, since a carbon-based resin was used to set the BFD samples prior to polishing. Cr content of the samples varied between 3.28% (Sample C) and 7.62% (Sample B). As expected, the elements with lower elemental mass that

http://dx.doi.org/10.4314/wsa.v43i2.13
Available on website http://www.wrc.org.za
ISSN 1816-7950 (Online) = Water SA Vol. 43 No. 2 April 2017

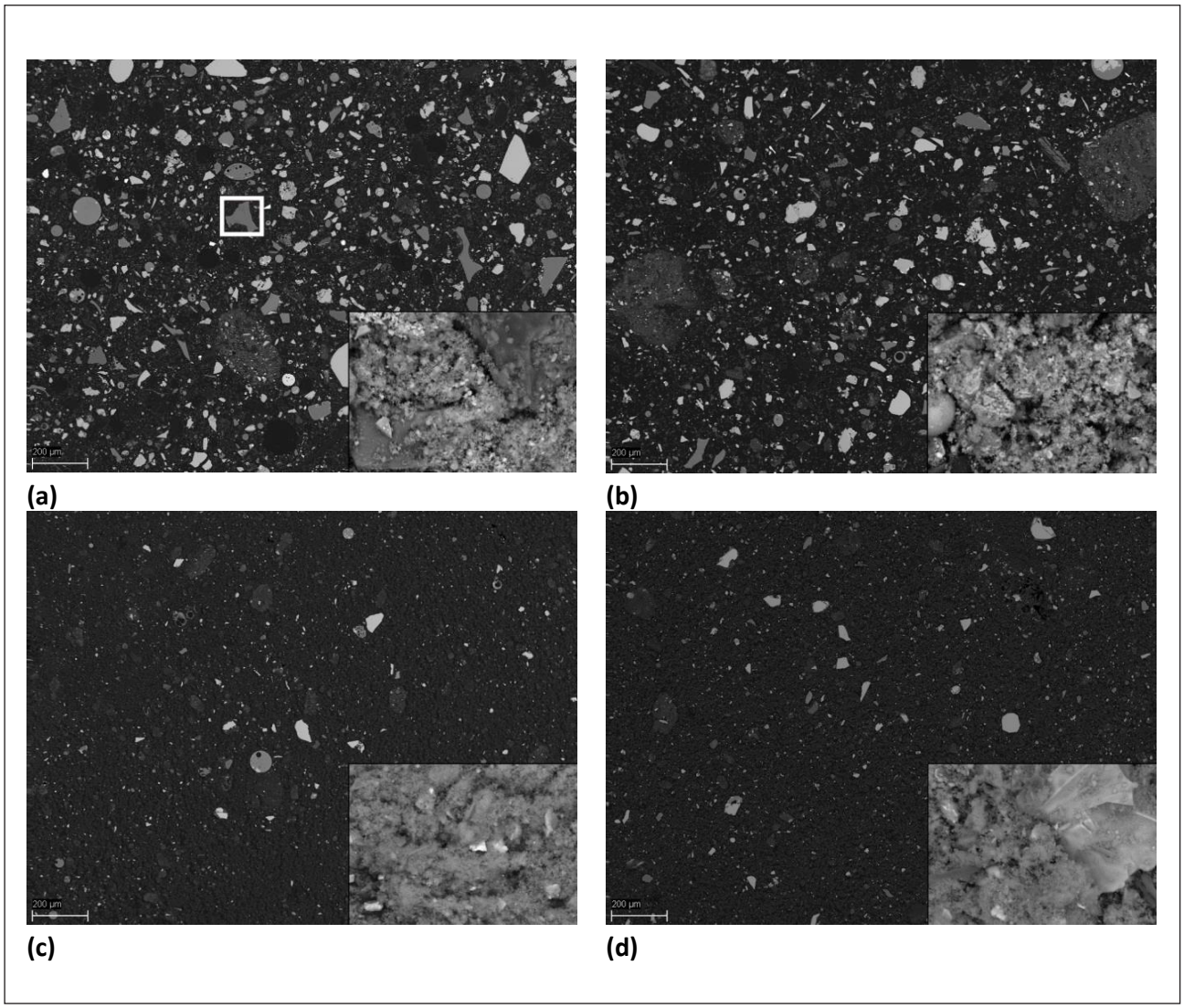

Figure 1

SEM micrographs for BFDs A (a), B (b), C (c) and D (d), at 2 000 (larger image) and 100 (smaller image) times magnification. The larger particle with an uneven morphology, marked by the white box in (a), is an example of an un-reacted chromite particle.

TABLE 2
SEM-EDS analyses of cross-sectional polished BFDs

BFD	Detected elements (%)											Total
	Mg	Al	Si	S	Cl	K	Ca	Cr	Fe	Zn	O	
A	6.24	3.38	11.71	1.55	5.38	3.11	1.29	6.81	7.97	18.66	33.91	100
B	6.66	2.98	11.75	1.63	4.67	3.01	1.06	7.62	8.47	18	34.2	100
C	12.3	2.26	21.77	1.18	1.6	2.66	0.59	3.28	2.85	9.4	42.09	100
D	13.23	2.58	20.12	1.33	1.57	2.36	0.92	3.84	3.76	8.57	41.71	100

http://dx.doi.org/10.4314/wsa.v43i2.13
Available on website http://www.wrc.org.za
ISSN 1816-7950 (Online) = Water SA Vol. 43 No. 2 April 2017

are typically associated with actual off-gas particles, such as magnesium (Mg), aluminium (Al), silicon (Si) and zinc (Zn), were present in significant concentrations in all of the BFD samples. Of particular interest was that no noteworthy amounts of Na were detected in any of the BFD samples. It is well known that alkali roasting of chromite is an industrial process for the production of sodium chromate, the formation efficiency of which depends on the amount of O_2 and alkali present, as well as the temperature during the production process (Antony et al., 2001). Maine et al. (2005) proposed that Cr(VI) could mainly be associated with alkali metals in FeCr BFD, but did not present any evidence to support this statement. However, the lack of Na in the BFD samples cannot be considered as evidence that anionic Cr(VI) (CrO_4^{2-}) is not associated with significant amounts of Na since the SEM-EDS technique has limitations with respect to Na analysis.

XRD analysis

XRD of the BFDs indicated that all of the samples comprised mainly of the same crystalline compounds. In the order of decreasing abundance, they are chromiun spinel ((Fe^{2+},Mg)(Cr,Fe^{3+})$_2O_4$), quartz (SiO_2), halite (NaCl), anorthite ($CaAl_2Si_2O_8$), osakaite ($Zn_4SO_4(OH)_6{\cdot}5H_2O$) and forsterite ($Mg_2SiO_4$). The similarities in crystalline phases of the investigated BFDs indicate that the samples originated from a similar type of process (i.e. FeCr production with BFD off-gas cleaning).

XAS characterisation

As is evident from Fig. 2(a) XAS spectra of the BFD samples collected at Cr K-edge indicate that they are broadly similar. The spectral features at the edge and above are similar to those of chromite from the upgraded upper group 2 (UG2) chromite layer of the Bushveld Complex in South Africa, suggesting that the unreacted chromite is the dominant Cr carrier in the furnaces where the BFD samples A, B and C were collected. BFD sample D was not characterized by XAS. Other important sources of Cr in the BFD samples include ferrochrome and slag. Figure 2(b) presents the least squares fitting of the Cr K-edge XANES spectra, indicating that the BFD samples consists of chromite, FeCr and FeCr slag, as represented by reference materials, i.e., UG2 chromite, FeCr and FeCr slag obtained from a FeCr smelter in South Africa. The BFD samples are dominated by chromite in terms of Cr concentrations, with chromite abundances ranging from 72% to 82% by weight (Table 3). The remaining Cr concentrations are tied to FeCr and slag.

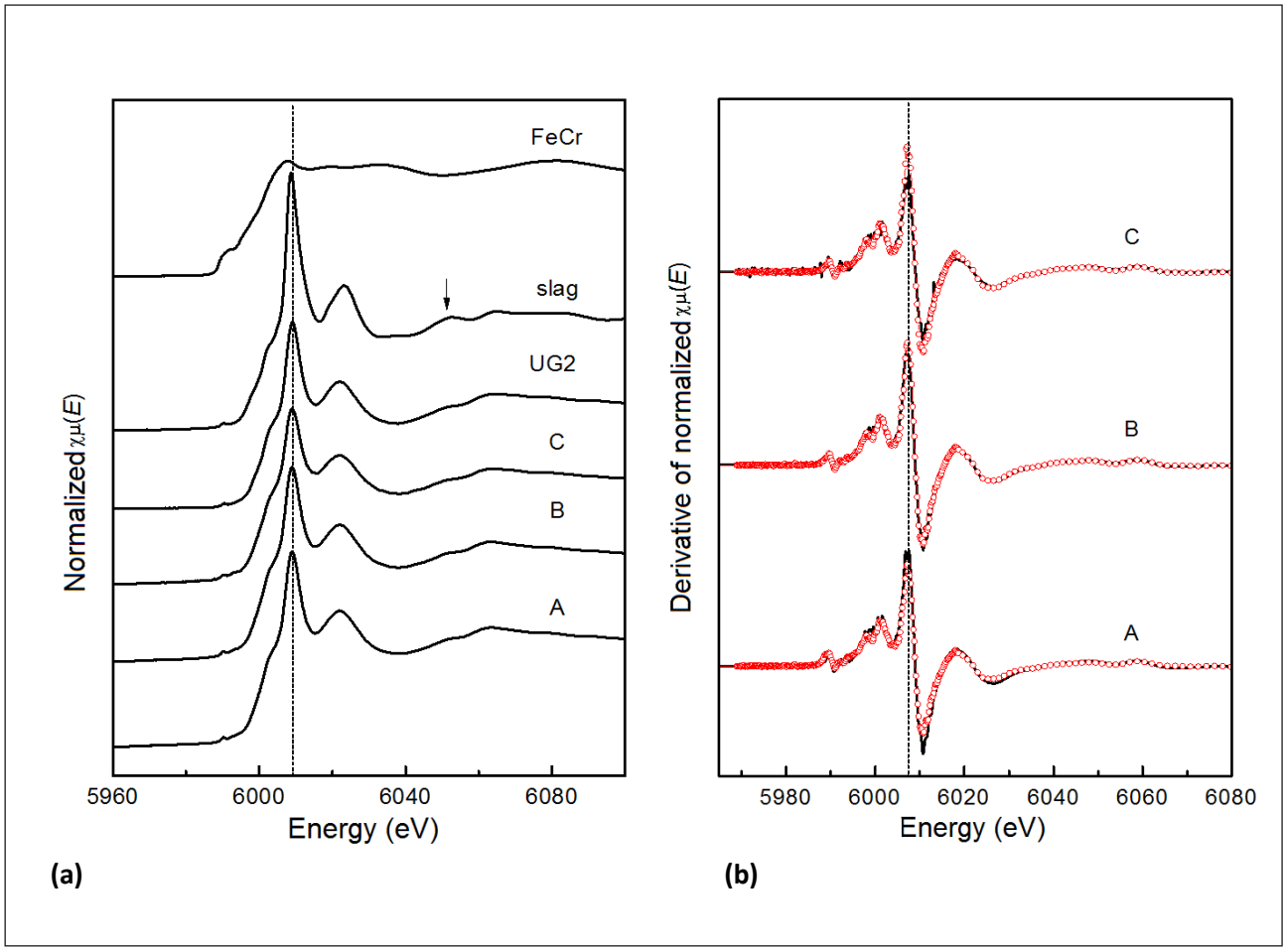

Figure 2

Cr K-edge XANES spectra of the BFD samples and their comparison to the UG2 chromite, slag and FeCr reference samples obtained from a South African FeCr producer (a). Least squares fitting of the derivative of the normalized BFD samples with end member compositions of chromite, slag and FeCr. Measured spectra are shown in black and the fits are indicated by the red circles (b).

http://dx.doi.org/10.4314/wsa.v43i2.13
Available on website http://www.wrc.org.za
ISSN 1816-7950 (Online) = Water SA Vol. 43 No. 2 April 2017

TABLE 3 Cr-containing constituents present in BFD samples determined from least square fitting of the XANES spectra			
BFD	% Cr constituent, compared to reference materials		
	UG2 chromite	FeCr	Slag
A	81.6	10.1	8.3
B	80.6	11.8	7.6
C	71.6	25.4	3.0

Trace metal leachability

It is generally accepted that higher concentrations of most heavy and transitional metals will leach out of a solid matrix (e.g. waste and soil) at low pH values (Ding et al., 2014; Lee et al., 2012). This was also observed experimentally, as indicated in Figs. 3 and 4, which present the log concentrations of alkali and alkali earth (Fig. 3), as well as transition and heavy (Fig. 4) metals as a function of leach solution pH. The higher solubility at lower pH was especially evident at pH ≤ 3. Elements occurring in low concentrations in the BDF samples (< 10 mg·kg^{-1} BFD) were excluded from all figures to prevent congestion of the graphs, and Na contents were excluded from Figs 3(a) and (b) at pH > 7, since NaOH solution was used to increase the pH of the leach solutions.

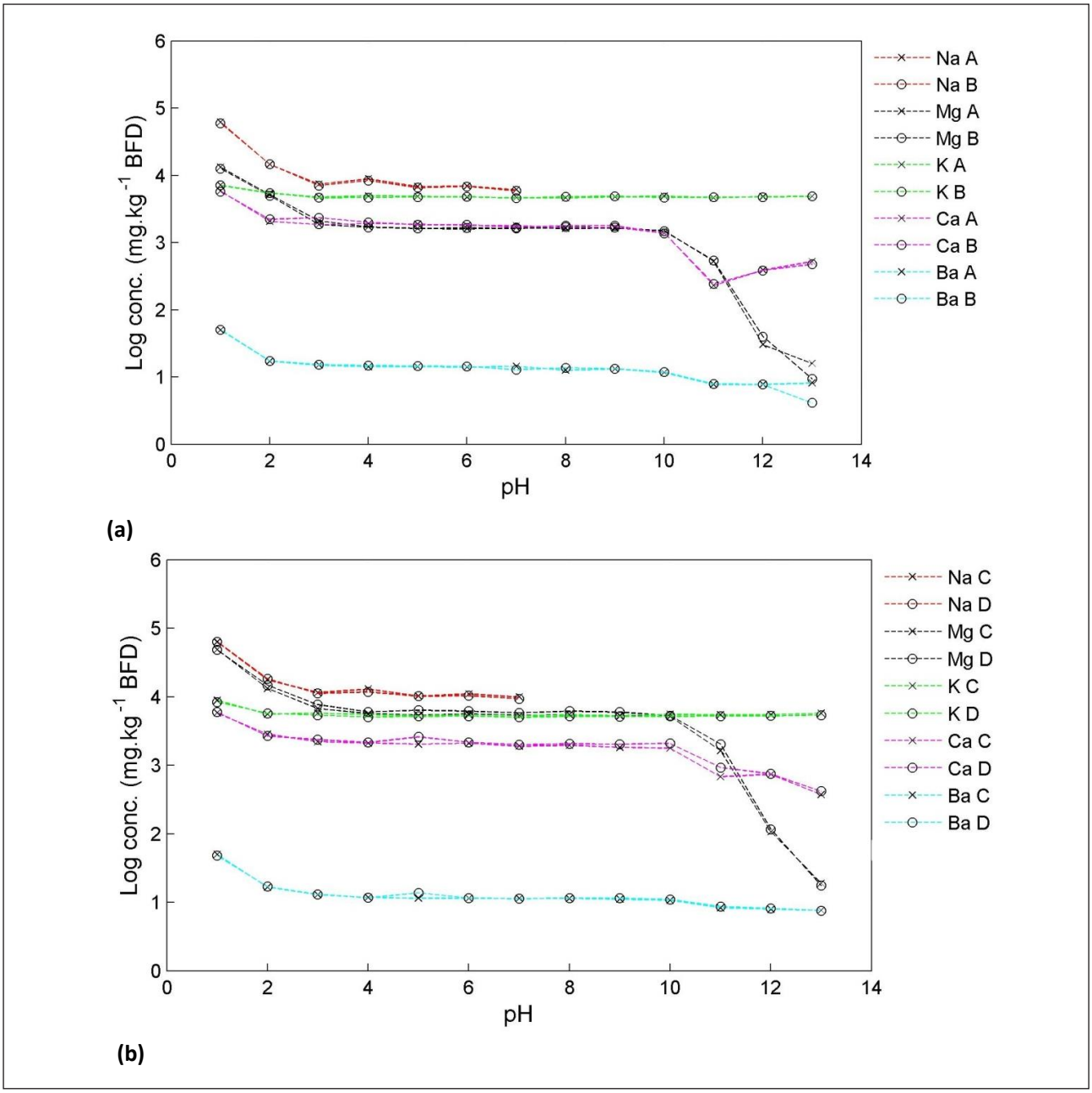

Figure 3

Log concentration of alkali and alkali earth metals in (a) BFDs A and B, as well as (b) BFDs C and D, as a function of leach solution pH.

http://dx.doi.org/10.4314/wsa.v43i2.13
Available on website http://www.wrc.org.za
ISSN 1816-7950 (Online) = Water SA Vol. 43 No. 2 April 2017

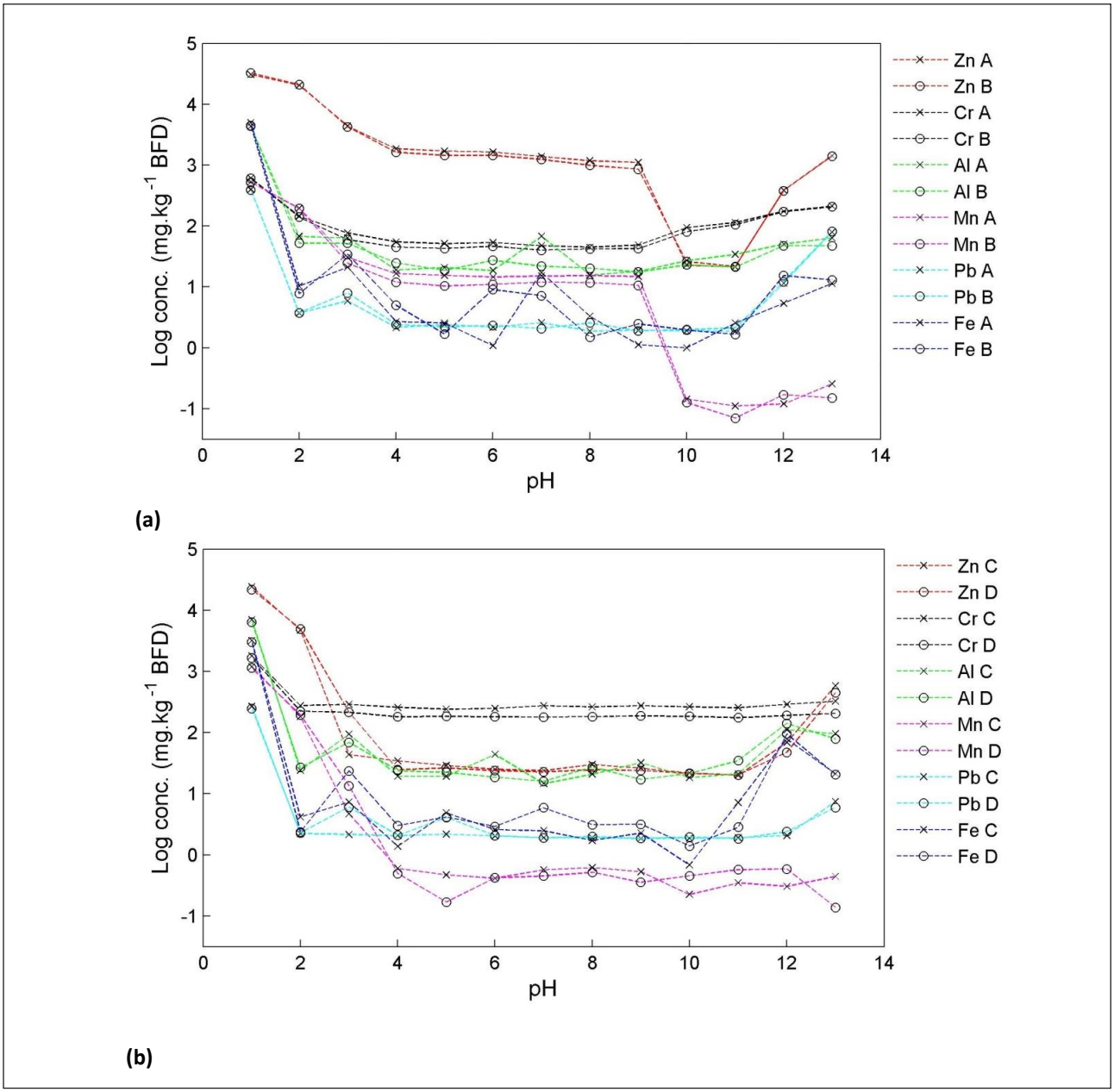

Figure 4

Log concentration of transition and heavy metals present in (a) BFD A and B, as well as (b) C and D as a function of leach solution pH

When comparing metal concentrations presented in Fig. 3 to concentrations presented in Fig. 4, it is evident that most alkali and alkali earth metals, excluding Ba, were present in much higher concentrations than transition and heavy metals, except for Zn that had concentrations comparable to alkali and alkali earth metals, especially at very low pH. The results presented in Figs 3 and 4 will be contextualized further in the following sections.

Cr(VI) leachability

Figure 5(a) presents the leachable Cr(VI) concentrations as a function of leach solution pH, as well as the two solubility fractions, i.e., combined water-soluble and sparingly water-soluble Cr(VI), as well as total Cr(VI) determined. Figure 5(b) indicates the same data normalized to percentage, based on the total extractable Cr(VI) of each sample. From these results, it is evident that the amount and percentage of leachable Cr(VI) increased with an increase in leach solution pH at pH ≥ 9. This is in contrast to the results obtained for all the other metals (Figs 3 and 4) for which the leachability increased as the leach solution pH decreased.

From the data presented in Figs 3, 4 and 5, it is impossible to shed any light on the possible association of anionic CrO_4^{2-} with cations, to indicate the identity of the Cr(VI) compounds that are present in the BFD samples. However, the observed increase of leachable Cr(VI) with an increase in pH (Fig. 5(b)) is an indication that not only water-soluble (e.g. Na_2CrO_4, K_2CrO_4), but also sparingly water-soluble (e.g. $CaCrO_4$, $SrCrO_4$) and waterinsoluble (e.g. $BaCrO_4$, $PbCrO_4$) Cr(VI) compounds occur in the samples evaluated. This data can also be used to estimate the average water-soluble, sparingly water-insoluble and

http://dx.doi.org/10.4314/wsa.v43i2.13
Available on website http://www.wrc.org.za
ISSN 1816-7950 (Online) = Water SA Vol. 43 No. 2 April 2017

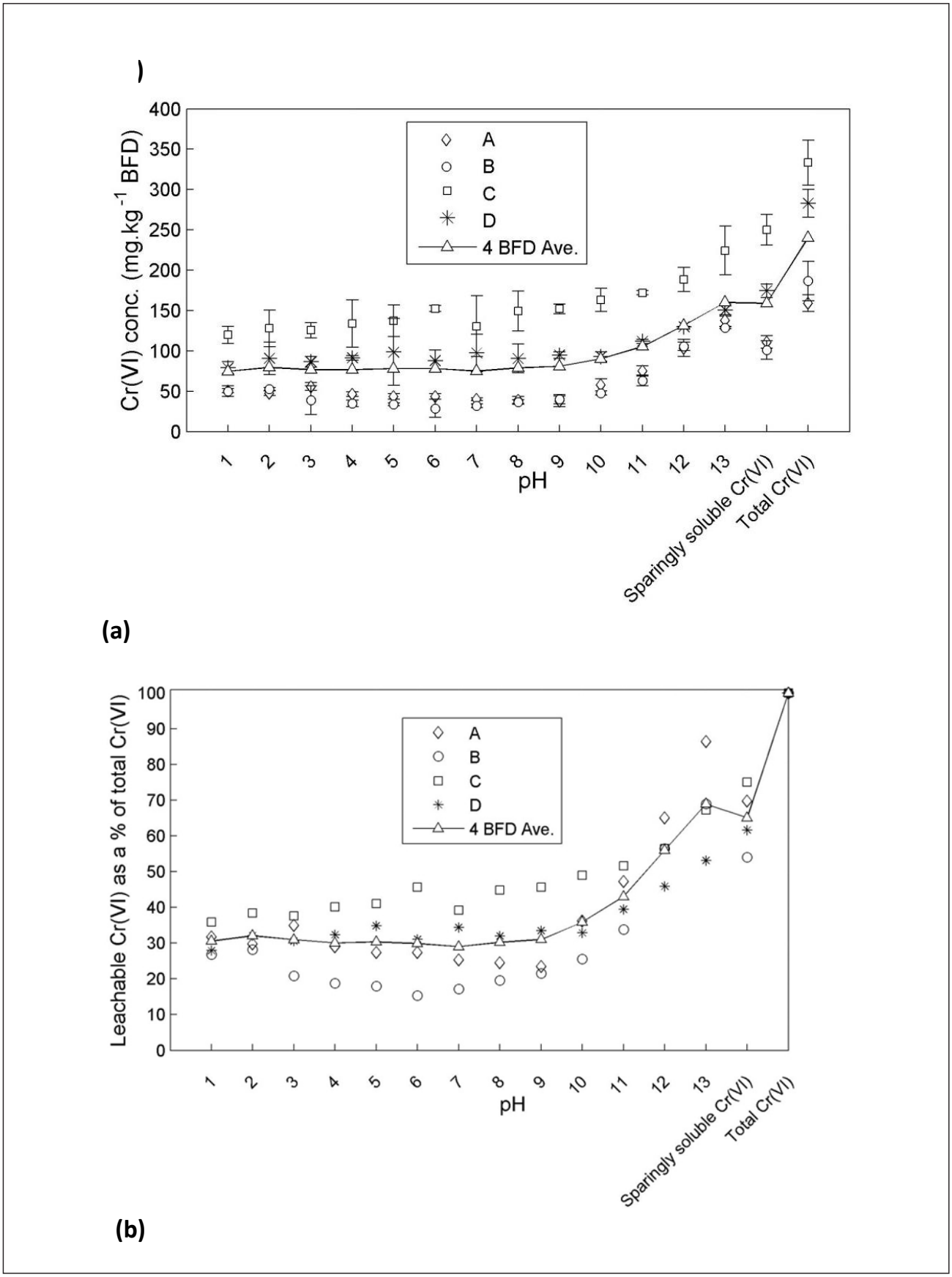

Figure 5

Leachable Cr(VI) as a function of leach solution pH, combined water-soluble and sparingly water-soluble Cr(VI), as well as total Cr(VI) (a). The same data normalized to % Cr(VI), based on the total extractable Cr(VI) (b).

http://dx.doi.org/10.4314/wsa.v43i2.13
Available on website http://www.wrc.org.za
ISSN 1816-7950 (Online) = Water SA Vol. 43 No. 2 April 2017

water-insoluble fractions. As is evident from Fig. 5(b), there was no statistically significant difference in the extractable Cr(VI) at pH ≤ 9, with approximately 31% of the total Cr(VI) being extracted in this range. This represents the water-soluble Cr(VI) fraction. On average, approximately 65% of the total Cr(VI) was present as a combination of water-soluble and sparingly water-soluble compounds. The difference between these two factions, i.e. 34%, therefore represents the percentage of sparingly water-soluble Cr(VI) compounds. The difference between the total Cr(VI) (100%) and the combined water-soluble and sparingly water-soluble fractions (65%) revealed the presence of approximately 35% water-insoluble Cr(VI) compounds in the BFD samples evaluated.

The above-mentioned results and, in particular, the presence of substantial fractions of sparingly water-soluble and water-insoluble Cr(VI) compounds, contradict the general perception that total Cr(VI) extraction from ferrochrome BFD can be achieved by neutral or acidic aqueous extractions. For instance, Maine et al. (2005) indicated that > 100 h of extraction is required with neutral water to completely extract Cr(VI) from BFD. Gericke (1995) maintained that 24 h leaching with aqueous solutions of pH 2 to 6 is adequate for Cr(VI) extraction from BFD. Bulut et al. (2009) stated that only 30 min was required to dissolve all Cr(VI) present in BFD and that the solution pH did not play a significant role. However, none of these authors used buffers and extraction methods to ensure extraction of sparingly water-soluble and water-insoluble Cr(VI) compounds (Ashley et al., 2003).

Apart from the above-mentioned possible underestimation of the amount of Cr(VI) present in BFD by previous studies, the retention times applied in some studies (Maine et al., 2005; Gericke, 1995) are unpractical. Some FeCr producers pump their BFD sludge (BFD after being contacted with water) directly to a thickener to separate the solid particles from the process water, while others might have a small surge tank to regulate the pumping of the afore-mentioned BFD sludge to the thickener. Figure 6 indicates a simplified schematic illustration to demonstrate a typical process flow of BFD.

Typically, chemical Cr(VI) treatment takes place just prior to the BFD sludge entering the thickener. Currently, ferrous sulphate reduction of Cr(VI) is the most commonly applied treatment method (Beukes et al., 2012). However, Fe(II) that is not consumed to reduce Cr(VI) is oxidized within a couple of minutes to Fe(III), at the pH levels applicable to FeCr process water (Beukes et al., 2012; He et al., 2004; Buerge and Hug., 1997; Fendorf and Li, 1996). Therefore, the effective residence time of the BFD particles in the process water, during which Cr(VI) extraction can take place, is far less than the 2 h extraction time applied in this study. Considering the afore-mentioned description, it is evident that it is highly likely that the short extraction times associated with current Cr(VI) treatment

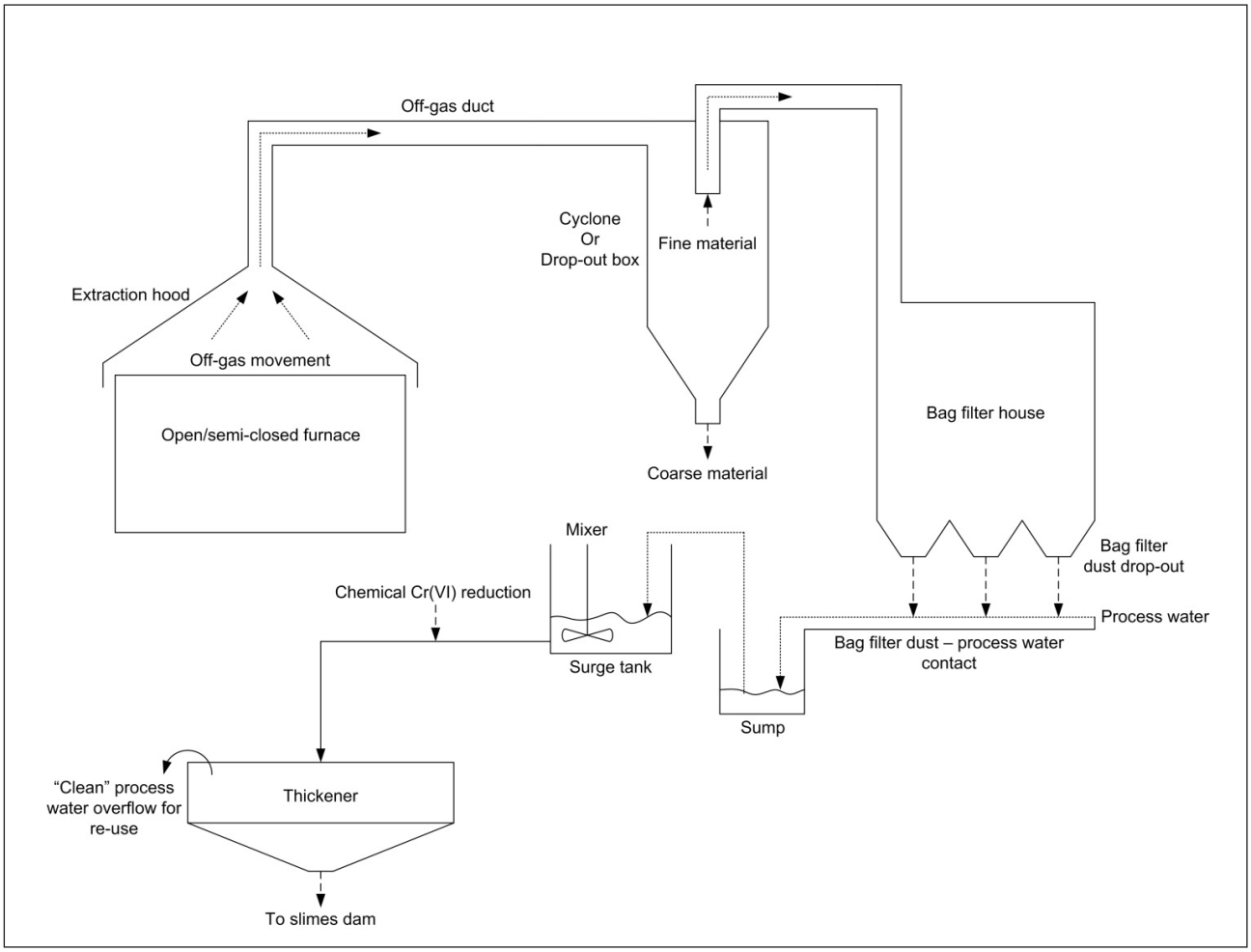

Figure 6

Schematic illustration to demonstrate a typical process flow of BFD

http://dx.doi.org/10.4314/wsa.v43i2.13
Available on website http://www.wrc.org.za
ISSN 1816-7950 (Online) = Water SA Vol. 43 No. 2 April 2017

strategies of FeCr producers only allow the extraction of the water-soluble Cr(VI) fraction.

Previously Maine et al. (2005) attempted to explain the slow release of Cr(VI), beyond the initial fast solubilisation of a certain fraction. These authors postulated that most of the Cr(VI) condenses onto the surface of the rounded fly ash type BFD particles, which can dissolve very rapidly in water. They further suggested that a small fraction of Cr(VI) might be trapped by the glassy surface of the BFD particles, which resulted in the slow release of the remaining Cr(VI). However, the results presented in this paper prove that the slow release, following the rapid initial dissolution of a fraction of the Cr(VI), can rather be attributed to the presence of substantial fractions of sparingly water-soluble and water-insoluble Cr(VI) compounds.

According to a survey conducted by Beukes et al. (2012) at various FeCr producers, the pH of FeCr process waters usually varies between 6.2 and 9.0. As indicated in Fig. 5(b), as well the discussions thereafter, approximately 31% of the total Cr(VI) is leached at pH ≤ 9, which correlates with the water-soluble Cr(VI) fraction. In order to confirm that the currently applied Cr(VI) treatment strategies extract only the water-soluble Cr(VI) fraction, even if extended extraction times are applied, the solid residue obtained from the evaporation of 4 successive 24 h extractions of the BDF samples at pH 7 were characterized with XAS and presented in Fig. 7. The pH level of 7 was chosen to avoid potential complications from pH adjustments (i.e. addition of CO_3^{2-} and/or OH^- altering cation association of CrO_4^{2-} at higher pH levels).

As is evident from Fig. 7, the XANES spectra of the solid residue of all four BFD samples investigated (A, B, C and D) indicated that the Cr present in the samples is dominated by Cr(VI) species. The spectra display a strong similarity to the spectrum of Na_2CrO_4, which is a water-soluble Cr(VI) species. This does not necessarily imply that Na_2CrO_4 was the sole source of Cr(VI) in the leachate precipitates of the BFD samples. Due to the low Cr concentrations, EXAFS spectra were not optimal and the results should therefore be regarded as qualitative, rather than quantitative. These results also did not permit modelling of the local coordination environment of the Cr(VI) species. Notwithstanding the afore-mentioned limitations, the presence of Cr(VI) in all BFD leachate precipitates is unequivocal; additionally, the Cr(VI) species were similar to Na_2CrO_4.

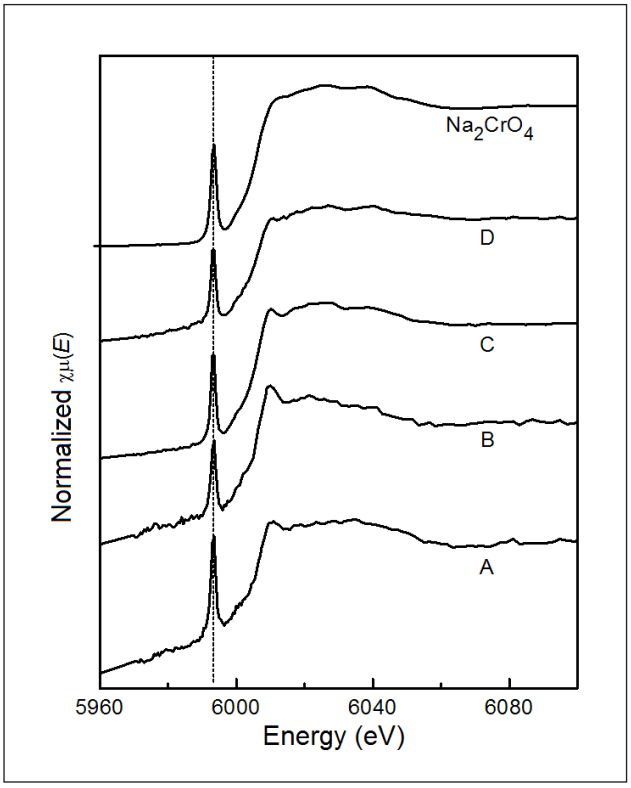

Figure 7

Normalized Cr K-edge XANES spectra of the solid residue extracted from BFD samples. The pre-edge peak characteristic of the Cr(VI) species is marked by the vertical dotted line at 5 993 eV.

CONCLUSIONS

The results presented in this paper indicate that the currently applied Cr(VI) treatment strategies of FeCr producer (with process water pH ≤9) only effectively extract and treat the water-soluble Cr(VI) compounds from the BFD, which represent approximately 31% of the total Cr(VI) present in the BFD samples evaluated. Extended extraction times of 4 consecutive 24 h extractions, proved futile in extracting sparingly water-soluble and water-insoluble Cr(VI) species within the afore-mentioned pH range, as confirmed with XAFS.

Considering the above-mentioned, it is critical that improved Cr(VI) treatment strategies be formulated that would extract all of the Cr(VI) from BFDs. The results presented in this paper suggest that extraction at pH 13 would be required to solubilise the sparingly water-soluble Cr(VI) species from BFD. This will ensure that sparingly water-soluble Cr(VI) compounds do not leach from the waste storage facilities (e.g. slimes dams). Otherwise, there is the potential of Cr(VI) releases over time, which has been proven to results in environmental Cr(VI) pollution (Loock-Hatting, 2016; Loock-Hatting et al., 2015; Loock et al., 2014). However, it is highly unlikely that such a high process-water pH would be economically feasible. Additionally, it is well known from literature that Fe(II), currently the most commonly employed chemical reductant of Cr(VI), oxidizes very quickly with dissolved oxygen at such high pH levels. Therefore, the effectiveness of this and other potential reductants at elevated pH levels needs to be investigated. Furthermore, the need to extract the water-insoluble Cr(VI) species prior to chemical reduction should be investigated in greater detail, in order to assess the likelihood of such species being mobilised over extended time periods relevant to waste disposal facilities.

ACKNOWLEDGEMENTS

The authors of this paper wish to thank the four FeCr production facilities that provided the BFD case study samples that were used in this study. The financial assistance of the National Research Foundation (NRF) towards the PhD study of SP du Preez (grant number: 101345) is hereby acknowledged. Opinions expressed and conclusions arrived at, are those of the authors and are not necessarily to be attributed to the NRF. XAS experiments were performed at the PNC-CAT beamline of the Advanced Photon Source, Argonne National Laboratory which is supported by the US Department of Energy under Contracts W-31-109-Eng-38 (APS) and DE-FG03-97ER45628 (PNC-CAT). The XAS experiments were also supported by the Natural Sciences and Engineering Research Council of Canada through a MRS grant to the Canadian Light Source.

REFERENCES

ANTONY M, TATHAVADKAR V, CALVERT C and JHA A (2001) The soda-ash roasting of chromite ore processing residue for the reclamation of chromium. *Metall. Mater. Trans. B*. **32** 987–995. https://doi.org/10.1007/s11663-001-0087-6

APTE AD, TARE V and BOSE P (2006) Extent of oxidation of Cr(III) to Cr(VI) under various conditions pertaining to natural environment. *J. Hazardous Mater.* **128** 164–174. https://doi.org/10.1016/j.jhazmat.2005.07.057

ASHLEY K, HOWE AM, DEMANGE M and NYGREN O (2003) Sampling and analysis considerations for the determination of hexavalent chromium in workplace air. *J. Environ. Monit.* **5** 707–716. https://doi.org/10.1039/b306105c

BEUKES JP, DAWSON NF and VAN ZYL PG (2010) Theoretical and practical aspects of Cr(VI) in the South African ferrochrome industry. *J. S Afr. Inst. Min. Metall.* **110** 743–750.

BEUKES JP, PIENAAR JJ and LACHMANN G (2000) The reduction of hexavalent chromium by sulphite in wastewater – An explanation of the observed reactivity pattern. *Water SA* **26** 393–395.

BEUKES JP, PIENAAR JJ, LACHMANN G and GIESEKKE EW (1999) The reduction of hexavalent chromium by sulphite in wastewater. *Water SA* **25** 363–370.

BEUKES JP, VAN ZYL PG and RAS M (2012) Treatment of Cr(VI)-containing wastes in the South African ferrochrome industry – a review of currently applied methods. *J. S. Afr. Inst. Min. Metall.* **112** 347–352.

BUERGE IJ and HUG SJ (1997) Kinetics and pH dependence of chromium (VI) reduction by iron (II). *Environ. Sci. Technol.* **31** 1426–1432. https://doi.org/10.1021/es960672i

BULUT VN, OZDES D, BEKIRCAN O, GUNDOGDU A, DURAN C and SOYLAK M (2009) Carrier element-free co-precipitation (CEFC) method for the separation, pre-concentration and speciation of chromium using an isatin derivative. *Anal. Chim. Acta.* **632** 35–41. https://doi.org/10.1016/j.aca.2008.10.073

CRAMER LA, BASSON J and NELSON LR (2004) The impact of platinum production from UG2 ore on ferrochrome production in South Africa. *J. S. Afr. Inst. Min. Metall.* **104** 517–527.

DHAL B, DAS NN, THATOI HN and PANDEY BD (2013) Characterizing toxic Cr(VI) contamination in chromite mine overburden dump and its bacterial remediation. *J. Hazardous Mater.* **260** 141–149. https://doi.org/10.1016/j.jhazmat.2013.04.050

DING Y, SONG Z, FENG R and GUO J (2014) Interaction of organic acids and pH on multi-heavy metal extraction from alkaline and acid mine soils. *Int. J. Environ. Sci. Technol.* **11** 33–42. https://doi.org/10.1007/s13762-013-0433-7

DIONEX CORPORATION (2003) Determination of hexavalent chromium in drinking water using ion chromatography. Application Update 144, LPN 1495. Dionex Corporation, Sunnyvale, CA.

DIONEX CORPORATION (2011) Sensitive determination of hexavalent chromium in drinking water. Application Update 179. Dionex Corporation, Sunnyvale, CA.

DU PREEZ SP, BEUKES JP and VAN ZYL PG (2015) Cr (VI) Generation during flaring of CO-rich off-gas from closed ferrochromium submerged arc furnaces. *Metall. Mater. Trans. B.* **46** 1002–1010. https://doi.org/10.1007/s11663-014-0244-3

FENDORF SE and LI G (1996) Kinetics of chromate reduction by ferrous iron. *Environ. Sci. Technol.* **30** 1614–1617. https://doi.org/10.1021/es950618m

GASIK M (2013) Handbook of ferroalloys: theory and technology, Butterworth-Heinemann.

GERICKE WA (1998) Environmental solutions to waste products from ferrochrome production. In: *Proceedings of the 8th International Ferroalloys*, Beijing, China. 51–58.

GERICKE WA (1995) Environmental aspects of ferrochrome production. In: *Proceedings of the 7th International Ferroalloys Congress*, Trondheim, Norway. 131–140.

HE YT, CHEN CC and TRAINA SJ (2004) Inhibited Cr(VI) reduction by aqueous Fe(II) under hyper-alkaline conditions. *Environ. Sci. Technol.* **38** 5535–5539. https://doi.org/10.1021/es049809s

HININGER I, BENARABA R, OSMAN M, FAURE H, ROUSSEL AM and ANDERSON RA (2007) Safety of trivalent chromium complexes: no evidence for DNA damage in human HaCaT keratinocytes. *Free Radic. Biol. Med.* **42** 1759–1765. https://doi.org/10.1016/j.freeradbiomed.2007.02.034

ICDA (INTERNATIONAL CHROMIUM DEVELOPMENT ASSOCIATION) (2012) *Statistical Bulletin*, 2012 edition. ICDA, Paris. 46 pp.

KASSEM TS (2010) Kinetics and thermodynamic treatments of the reduction of hexavalent to trivalent chromium in presence of organic sulphide compounds. *Desalination*. **258** 206–218. https://doi.org/10.1016/j.desal.2010.03.011

LEE PK, KANG MJ, JO HY and CHOI SH (2012) Sequential extraction and leaching characteristics of heavy metals in abandoned tungsten mine tailings sediments. *Environ. Earth Sci.* **66** 1909–1923. https://doi.org/10.1007/s12665-011-1415-z

LIND BB, FÄLLMAN, AM and LARSSON LB (2001) Environmental impact of ferrochrome slag in road construction. *Waste Manage.* **21** 255–264. https://doi.org/10.1016/S0956-053X(00)00098-2

LOOCK-HATTINGH MM (2016) Cr(VI) contamination of aqueous systems. PhD thesis, North-West University, South Africa.

LOOCK-HATTINGH MM, BEUKES JP, VAN ZYL PG and TIEDT LR (2015) Cr(VI) and conductivity as indicators of surface water pollution from ferrochrome production in South Africa: Four Case studies. *Metall. Mater. Trans. B.* **46** 2315–2325. https://doi.org/10.1007/s11663-015-0395-x

LOOCK MM, BEUKES JP and VAN ZYL PG (2014) A survey of Cr(VI) contamination of surface and drinking water in the proximity of ferrochromium smelters in South Africa. *Water SA* **40** 709–716. https://doi.org/10.4314/wsa.v40i4.16

MAINE C, SMIT, J and GIESEKKE E (2005) The solid stabilization of soluble wastes generated in the South African ferrochrome industry. Water Research Commission, Pretoria.

MARCH J (1992) *Advanced Organic Chemistry: Reactions, Mechanisms, and Structure*. John Wiley & Sons, New York.

MOLOKWANE PE, MELI KC and NKHALAMBAYAUSI-CHIRWA EM (2008) Chromium (VI) reduction in activated sludge bacteria exposed to high chromium loading: Brits culture (South Africa). *Water Res.* **42** 4538–4548. https://doi.org/10.1016/j.watres.2008.07.040

MURTHY YR, TRIPATHY SK and KUMAR CR (2011) Chrome ore beneficiation challenges & opportunities – a review. *Miner. Eng.* **24** (5) 375–380. https://doi.org/10.1016/j.mineng.2010.12.001

NIEMELÄ P and KAUPPI M (2007) Production, characteristics and use of ferrochromium slags. In: *Proceedings of the 11th International Ferro Alloys Conference*, New Delhi, India. 171–179.

NIEMELÄ P, KROGERUS H and OIKARINEN P (2004) Formation, characterization and utilization of CO-gas formed in ferrochrome smelting. In: *Proceedings of the 12th International Ferroalloys Congress*, Cape Town, South Africa. 68–77.

NOISH 7605 (2003) *Chromium, Hexavalent by Ion Chromatography Method 7605*. NIOSH Manual of Analytical Methods (NMAM). NOISH, Cincinnati.

PAKTUNC D (2004) A computer program for analyzing complex bulk XAFS spectra and for performing significance tests. *J. Synchrotron. Radiat.* **11** 295–298. https://doi.org/10.1107/S0909049504003681

PROCTOR DM, OTANI JM, FINLEY BL, PAUSTENBACH DJ, BLAND JA, SPEIZER N and SARGENT EV (2002) Is hexavalent chromium carcinogenic via ingestion? A weight-of-evidence review. *J. Toxicol. Env. Health* A **65** 701–746. https://doi.org/10.1080/00984100290071018

RAVEL B and NEWVILLE M (2005) ATHENA, ARTEMIS, HEPHAESTUS: data analysis for X-ray absorption spectroscopy using IFEFFIT. *J. Synchrotron. Radiat.* **12** 537–541. https://doi.org/10.1107/S0909049505012719

RIEKKOLA-VANHANEN M (1999) Finnish expert report on best available techniques in ferrochrome production. Finnish Environmental Institute, Helsinki. 51 pp.

SEAMAN JC, BERTSCH PM and SCHWALLIE L (1999) In situ Cr (VI) reduction within coarse-textured, oxide-coated soil and aquifer systems using Fe (II) solutions. *Environ. Sci. Technol.* **33** 938–944. https://doi.org/10.1021/es980546+

http://dx.doi.org/10.4314/wsa.v43i2.13
Available on website http://www.wrc.org.za
ISSN 1816-7950 (Online) = Water SA Vol. 43 No. 2 April 2017

SKOOG DA, WEST DM, HOLLER FJ and CROUCH SR (2013) *Fundamentals of Analytical Chemistry*, Nelson Education, Belmont.
THOMAS DH, ROHRER JS, JACKSON PE, PAK T and SCOTT JN (2002) Determination of hexavalent chromium at the level of the California Public Health Goal by ion chromatography. *J. Chromatogr. A.* **956** 255–259. https://doi.org/10.1016/S0021-9673(01)01506-0
VAN STADEN Y, BEUKES JP, VAN ZYL PG, DU TOIT JS and DAWSON NF (2014) Characterization and liberation of chromium from fine ferrochrome waste materials. *Miner. Eng.* **56** 112–120. https://doi.org/10.1016/j.mineng.2013.11.004
VENTER AD, BEUKES JP, VAN ZYL PG, JOSIPOVIC M, JAARS K and VAKKARI V (2016) Regional atmospheric Cr (VI) pollution from the Bushveld Complex, South Africa. *Atmos. Pollut. Res.* **7** 762–767. https://doi.org/10.1016/j.apr.2016.03.009
ZELIĆ J (2005) Properties of concrete pavements prepared with ferrochromium slag as concrete aggregate. *Cement Concrete Res.* **35** 2340–2349. https://doi.org/10.1016/j.cemconres.2004.11.019

http://dx.doi.org/10.4314/wsa.v43i2.13
Available on website http://www.wrc.org.za
ISSN 1816-7950 (Online) = Water SA Vol. 43 No. 2 April 2017

CHAPTER 4: ARTICLE 2

Silicon carbide production as an alternative approach to store energy associated with CO-rich off-gas combustion

4.1 Author list, contributions, and consent

Authors list

SP du Preez[a], JP Beukes[a*], PG van Zyl[a], and LR Tiedt[a]

[a]Chemical Resource Beneficiation, North-West University, Potchefstroom Campus, Private Bag X6001, Potchefstroom 2520, South Africa

Contributions

Contributions of the various co-authors were as follows:

Experimental work, data processing and interpretation, research, and writing of the scientific paper, was performed by the candidate, SP du Preez. Some analytical work was performed by LR Tiedt. JP Beukes (supervisor) and PG van Zyl (co-supervisor) made conceptual contributions.

Consent

All of the co-authors that contributed to the article presented in this chapter have been informed that the article will form part of the candidate's PhD, submitted in article format, and have granted permission that the article may be used for the purpose stated.

4.2 Formatting and current status of the article

The article presented in Chapter 4 has been prepared for submission to *Resources, Conservation and Recycling*. It is currently foreseen that the paper will be submitted to the journal before 10 December 2017. The journal details can be found at https://www.journals.elsevier.com/resources-conservation-and-recycling (Date of access: 16 November 2017).

Silicon carbide production as an alternative approach to store energy associated with CO-rich off-gas combustion

S.P. du Preez[a], J.P. Beukes[a,*], P.G. van Zyl[a] and L.R. Tiedt[a]

[a] Chemical Resource Beneficiation, North-West University, Potchefstroom Campus, Private Bag X6001, Potchefstroom, 2520, South Africa

* Corresponding author. E-mail address: paul.beukes@nwu.ac.za;
telephone: +27 82 460 0594; fax: +27 18 299 2350

ABSTRACT

Carbothermic smelting of ore, with ferrochrome (FeCr) considered as an example in this paper, results in large volumes of CO-rich off-gas being generated. FeCr is produced in alternating current open/semi-closed and closed submerged arc furnaces (SAFs), or in closed direct current (DC) furnaces. The majority of CO-rich off-gas from closed SAF and DC furnace is cleaned and flared on stacks, since the storing of large volumes thereof is problematic due to the toxic and explosive risks associated with it. Flaring CO-rich off-gas wastes massive quantities of energy. In this study an alternative method to partially store the thermal energy associated with off-gas combustion, in the form of silicon carbide (SiC) generated from waste materials (quartz and anthracite fines), is proposed. SiC can partially replace conventional carbonaceous reductants used to produce alloys such a FeCr. The influences of quartz and anthracite particle size, treatment temperature and gaseous atmosphere (nitrogen or air) on SiC formation were investigated. A quartz-anthracite mixture with 90% of the particles <350.9 µm carbothermically treated at 1600°C resulted in almost complete conversion of quartz to SiC in both nitrogen and air atmospheres. The work indicated significant potential for industrial application of the process.

Keywords: Silicon carbide (SiC); Silicon nitride (Si_3N_4); Quartz; anthracite; carbothermic smelting.

1. Introduction

Pyro-metallurgical smelting of ores are used to produce various metals and alloys. In this paper, ferrochromium (FeCr) will be considered as an example. FeCr, a crude alloy between chromium (Cr) and iron (Fe), is produced by the energy intensive carbothermic reduction of chromite (formula $[(Mg,Fe^{2+})(Al,Cr,Fe^{3+})_2O_4]$) or simplified formula $FeCr_2O_4$, ore (Haggerty, 1991). FeCr is mainly produced using open/semi-closed and closed submerged arc furnaces (SAFs), or direct current (DC) furnaces (Beukes et al., 2010; Beukes et al., 2017) and is primarily used as a source of new Cr units during stainless steel production (Basson and Daavittila, 2013).

Four prominent wastes are generated during FeCr production, i.e. slag, CO-rich off-gas, bag filter dust during the cleaning of open/semi-closed SAF off-gas, and sludge from wet venturi scrubbing of closed SAF or DC arc furnace off-gas (Van Staden et al., 2014). Each of these wastes are handled and/or treated separately. Any remaining FeCr is usually removed from slag with magnetic separation or jigging, where after the slag is either stockpiled or utilized in various commercial applications (Lind et al., 2001; Zelić, 2005; Niemelä and Kauppi, 2007). Bag filter dust and venturi sludge are usually stored in fit-for-purpose landfill sites, after being treated for hexavalent Cr, if required (Maine et al., 2005; Beukes et al., 2010; Beukes et al., 2012; Du Preez et al., 2017). CO-rich off-gas percolating through the feed material bed of open/semi-closed SAFs ignites as the gas reach the top of the material bed, due to air ingress into these types of furnaces. Thereafter the combusted off-gas is extracted and cleaned with bag filters, before being released into the atmosphere (Riekkola-Vanhanen, 1999: Beukes et al., 2010; Du Preez et al., 2017). Of specific relevance in this study is the CO-rich off-gas originating from closed SAF or DC furnaces, which does not combust on the furnace feed material bed, due to the closed nature of the afore-mentioned furnaces.

Closed SAF off-gas typically consists of 60-90% CO, 10-40% CO_2, 2-7% N_2, and 2-10% H_2 (Niemelä et al., 2004; Kapure et al., 2007), with 650-750 Nm^3 CO(g) typically being generated per ton FeCr produced (Niemelä et al., 2004). Gas composition of a FeCr DC furnace have been reported to be 58-64% CO, 2-6% CO_2, 26-34% H_2, 0-5% N_2 and <1% O_2 (Schubert and Gottschling, 2011). Between 30-35% of the CO-rich off-gas is typically utilized as an on-site energy source for e.g. heating ladles, raw material drying, pre-heating furnace charge and chromite pellet sintering/pre-reduction (Niemelä et al., 2004). Unused cleaned off-gas is typically flared on top of purposefully designed stacks (Du Preez et al., 2015). The main reasons why CO-rich off-gas is usually not stored in large volumes on-site are its toxicity to humans via inhalation (Hall et al., 2015) and explosive risk (Niemelä et al., 2004). However, off-gas flaring results in the loss of massive quantities of energy (Niemelä et al., 2004; Schubert and Gottschling, 2011).

Due to increase pressure on profitability (e.g. due to increasing electricity costs) and increased environmental concerns (e.g. reduction in carbon footprint, and carbon tax) methods have been developed in an attempt to utilize CO-rich off-gas. One such method includes the combustion of the cleaned off-gas in so-called CO-gens, which is defined as internal combustion engines utilizing CO- and H_2-containing off-gas as a fuel source to drive electrical power producing alternators (Schubert and Gottschling, 2011). However, these engines are susceptible to breakdowns caused by the fluctuating octane levels associated with varying CO and H_2 contents present in off-gas, significantly reducing the operational life-spans thereof. Additionally, solid matter present in off-gas may results in internal abrasion of engine components (Schubert and Gottschling, 2011). Another method of utilizing CO-rich off-gas is the combustion thereof to produce steam for steam turbine electricity generation.

In this paper the authors suggest an alternative approach to the utilize CO-rich off-gas. It is suggested that the thermal energy associated with the combustion of such off-gas can at

least partially be stored in the form of chemical energy, i.e. production of silicon carbide (SiC) from waste materials generated on-site. Traditionally, SiC is used as a ceramic material and is characterized as an extremely hard and tough compound, possessing high chemical and thermal stability (Šajgalík et al., 2016). However, it has also been reported that SiC can be used as a partial replacement of conventional carbonaceous reductants (e.g. coke, char and anthracite), to produce alloys such a FeCr (Demir, 2001; Pheiffer and Cookson, 2015), as well as platinum group metals (PGMs) (Malan et al., 2015). One of the main authors of this paper was also involved in a trial during which SiC was used as a partial replacement of carbonaceous reductants on a large commercial open/semi-closed FeCr SAF. During this trial, significant increases in FeCr production volumes were observed. However, after completing the trial continuous operation using SiC as a partial replacement for carbonaceous reductants was not implemented, due to the high unit cost of commercially available SiC. The use of SiC as a reductant during FeCr production result in the SiC being oxidised to form SiO_2, while the oxides in the ores are reduced, as illustrated in Reaction 1 and 2.

$$Cr_2O_3 + SiC \rightarrow 2Cr + SiO_2 + CO \quad (1)$$

$$3FeO + SiC + \rightarrow 3Fe + SiO_2 + CO \quad (2)$$

2. Materials and methods

2.1. Materials

Materials used in this study, i.e. quartz and anthracite fines, were obtained from a large FeCr producer that uses these materials during FeCr production. FeCr producers utilizing closed SAFs minimize the consumption of fine feed materials to prevent furnace bed sintering, which may lead to gas eruptions and dangerous bed turn-overs (Riekkola-Vanhanen, 1999). The afore-mentioned, quartz and anthracite fines were screened out from lumpy anthracite (serving as a reductant) and lumpy quartz (serving as a flux) on-site by the afore-mentioned FeCr producer. Such screening is common for FeCr producers (Basson and

Daavittila, 2013; Beukes et al., 2017). These materials can therefore at least partially be classified as waste materials, although the fine anthracite could be included as a carbon source in oxidative sintered pellets (Glastonbury et al., 2015) that are produced on-site. The fine quartz could be used in sand moulds for casting liquid FeCr to produce FeCr ingots (large dome shaped FeCr metal blocks); however, the fine quartz is typically not fine enough to have the required binding characteristics. Fine quartz could also be used as fine aggregate in concrete; however, the need for the last application on-site is finite.

Characterization of the fine quartz was performed with quantitative X-ray diffraction analysis (described in Section 2.4). It revealed a composition of 94.9% SiO_2, 2.7% illite ($K_{0.65}Al_2[Al_{0.65}Si_{3.35}O_{10}](OH)_2$) and 2.4% magnesioferrite (Fe_2MgO_4). A detailed characterization of the fine anthracite used in this study was previously presented by Kleynhans et al. (2012) and are therefore not presented in detail here. Of importance for this study were the fixed carbon content of the anthracite that was 75.08% and the volatile content of 6.87%. The fixed carbon content was required, since C (not anthracite) input into the SiC formation reaction needed to be known. When heated, the volatile compounds in the anthracite decompose and are released as *in-situ* formed H_2 (Kleynhans et al., 2016). Li et al. (2015) indicated that quartz reduction to SiC is accelerated by *in-situ* formed CH_4, which is generated by the reaction between C and H_2 (Li et al., 2015). Thus, although other screened out fine reductant may be available at a typical FeCr producer, only anthracite was considered as a reductant in this study, since its volatile content is usually higher than that of coke (the most common reductant used in FeCr smelting) and it is generally much less expensive than coke.

2.2. Sizing of quartz and anthracite

Since particle size was one of the parameters considered in this study, it was decided to prepare samples by two different methods, i.e. size partitioning and milling. Size

partitioning of as-received materials was achieved by screening it into several size fractions, i.e. <106, 106 to 150, 150 to 250, and 250 to 500 µm. Screening was performed using a Haver EML Digital Plus shaker and Haver & Boecker sieves. During milling 2g of quartz and 6g of anthracite was milled together for various times, i.e. 10, 20, 30 and 60 sec. A Siebtechnik pulverizer was used for milling purposes. All parts of the pulverizer that made contact with the mixtures were made of tungsten carbide to minimize possible Fe contamination, as Fe can promote SiC and silicon nitride (Si_3N_4) formation (Bandyopadhyay and Mukerji, 1991; Krishnarao et al., 1998; Wu et al., 2002). Laser diffraction particle sizing, using a Malvern Mastersizer 2000, was used to determine particle size distribution. In order to prevent the use of chemical dispersant, samples were ultra-sonicated prior to the particle size measurements. Mechanical stirring was set to 2000 rpm and laser obscuration was kept between 10 to 15%.

The equivalent particle sizes (µm) of which 90% of the particles are finer (d_{90}), as well as d_{50} and d_{10} (both defined in a similar manner as d_{90}) of the screened size fractions and milled mixtures, as described in the previous paragraph, are presented in Table 1.

Table 1: D_{90}, d_{50} and d_{10} (µm) of size fractioned quartz and anthracite, and milled mixtures

Size fractioned	Sieve apertures (µm)			
	<106	106 to 150	150 to 250	250 to 500
Quartz				
d_{90}	119.5	192.5	312.3	556.8
d_{50}	51.9	138.9	213.1	387.1
d_{10}	7.8	100.8	29.8	277.7
Anthracite				
d_{90}	105.3	211.2	351.8	682.6
d_{50}	39.0	136.2	217.5	445.5
d_{10}	6.6	15.3	24.0	290.1
Milled mixtures	Milling time (sec)			
	60	30	20	10
d_{90}	58.7	116.1	248.4	350.9
d_{50}	17.4	19.9	25.8	68.1
d_{10}	2.9	3.9	3.9	5.0

2.3. Experimental setup for SiC formation

The mixing ratio of all carbothermically treated (defined as high temperature treatment in the presence of a carbonaceous reductant) quartz and anthracite mixtures, obtained either from mixing size fractioned anthracite and quartz, or from co-milled quartz and anthracite (Section 2.2) was kept constant at C/SiO_2 mass ratio of 2.4. This mass ratio represents approximately 400% excess C, according to Reaction 3 representing the overall reduction formation reaction (Chen and Lin, 1997; Gupta et al., 2001; Li et al., 2015):

$$SiO_2(s) + 3C(s) \rightarrow SiC(s) + 2CO(g) \quad (3)$$

$$\Delta G° = 507.17 - 0.3288\ T\ (kJ)$$

Agarwal and Pad (1999) determined that an C/SiO_2 mass ration equal to approximately 520% excess C would be ideal for SiC formation, however, a more conservative (using less carbon, which is less expensive) approach was followed in this study. The afore-mentioned ΔG, as well as all such further values presented in this paper, were determined by the thermodynamic modelling software package HSC (Roine, 2009; Du Preez et al., 2015).

Carbothermic treatment were performed in a 18kW Lenton Elite tube furnace with a Schunk AluSIK type C610 ‘‘A’’ impervious mullite ceramic tube (75 mm x 65 mm x 1500 mm) with a chemical composition of 60% Al_2O_3 and 40% SiO_2. Figure 1 presents a simple schematic illustration of the furnace setup used.

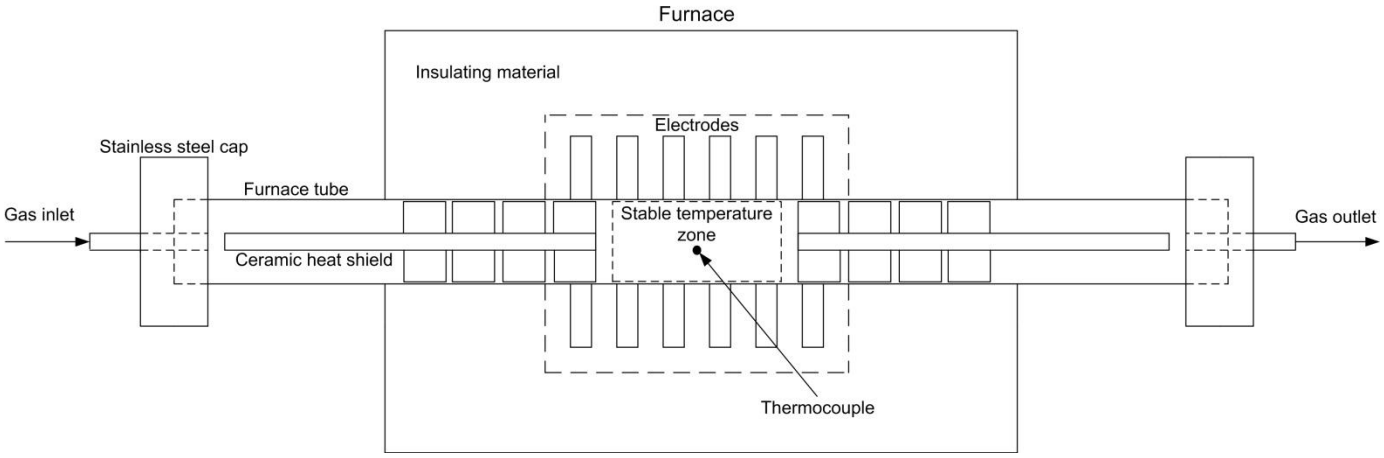

Figure 1: Schematic illustration of the furnace setup used.

As shown in Figure 1, ceramic heat shields were inserted at both ends of the furnace tube to increase the length of tube which could maintain a stable working temperature. In addition, these heat shields protected the stainless steel caps fitted to seal the furnace tube ends. The stainless steel caps had a gas inlet on the one side of the furnace tube, and a gas outlet on the other. The thermocouple used for temperature measurements was located at the centre of the stable workable temperature zone. The furnace was heated by twelve electrodes, which were located adjacent to the furnace tube. Samples were placed in ceramic boats and placed within the stable temperature zone.

Li et al. (2015) investigated the effects argon (Ar) and hydrogen (H_2) atmospheres on the carbothermic production of SiC from quartz and found that H_2 was a better (more productive) atmosphere than Ar. However, considering the nature of the suggested method to produce SiC using combustion of CO-rich off-gas, such atmospheres will not be realistic, or economically feasible. The intended combustion of CO-rich off-gas will require air as an oxidizer, which will result in large volumes of nitrogen (N_2) being introduced into the process (since normal atmosphere contains >78% N_2). Therefore, during this study carbothermic quartz reduction was mainly investigated in a N_2 atmosphere, with some CO_2 and CO being

generated *in-situ*. The N_2 atmosphere was maintained within the furnace tube by utilizing a 1 NL min^{-1} N_2 flow rate during all experiments. Prior to each experiment the furnace tube already loaded with samples, was flushed for 30 min with a 2 NL min^{-1} flow rate of N_2. During carbothermic treatment, the furnace temperature was increased at a rate of 17.8°C min^{-1} until the designated temperature was reached. Samples were exposed to the designated maximum temperature for 120 min. Subsequently, the furnace was turned off and allowed to cool down to room temperature, while a 1 NL min^{-1} flow of N_2 was maintained with the samples in the furnace tube. Samples were then collected and stored in an airtight container until further analysis.

Additionally, the temperature range investigated had to be established. Since the formation of SiC from quartz is an energy intensive reaction (Reaction 3), it will require a large amount of heat from CO-rich off-gas combustion. The $\Delta G°$ for Reaction 3 will reach equilibrium at approximately 1540 °C (calculated with the thermodynamic software package HSC; Roine, 2009). According to Niemelä et al. (2004), pure CO gas can burn in air at 2250°C. This value was confirmed by Du Preez et al. (2015) using the thermodynamic software program HSC to determine the adiabatic flame temperature of pure CO combustion (Roine, 2009; Du Preez et al., 2015). The afore-mentioned authors further determined that a gas composition of 60% CO and 40% CO_2, which is at the low end of the CO composition of CO-rich off-gas (Kapure et al., 2007; Niemelä et al., 2004; Schubert and Gottschling, 2011), will burn at an adiabatic flame temperature of approximately 1790°C. Therefore, the temperatures that could be attained by CO-rich off-gas combustion will be sufficient to sustain, or even surpass, the temperature required for SiC formation. Considering the afore-mentioned, the temperature range of 1400 to 1600°C was investigated. This range is much lower that the temperatures typically achieved in the Acheson type processes to commercially produce SiC and is similar to the temperature range proposed by Agarwal and Pad (1999) of

1200 to 1450°C for microwave production of SiC. For the formation of Si metal from SiO_2 and C much higher temperatures would be required Itaka et al. (2015); however, Si metal formation is beyond the scope of the current paper.

2.4. Scanning electron microscopy and X-ray diffraction analysis

Scanning electron microscopy (SEM) with energy dispersive X-ray spectroscopy (EDS) was used to perform surface characterisation of carbothermic treated samples. A FEI Quanta 200 scanning electron microscope with an integrated Oxford Instruments INCA 200 energy dispersive X-ray spectroscopy microanalysis system was used. Samples were prepared in two different manners prior to SEM analysis. Firstly, samples were mounted onto an aluminium (Al) specimen stub with adhesive carbon coated tape and subsequently coated with a thin layer (approximate 5nm) of gold-palladium in order to determine the particle morphologies. Secondly, in order to analyse the surface and sub-surface chemical composition, the samples were set in a carbon based resin and polished before the SEM-EDS analyses were conducted.

Phase analysis of bulk samples (overall sample) was performed by X-ray diffraction (XRD) using a Röntgen diffraction system (PW3040/60 X'Pert Pro) and a back loading preparation method to determine the crystalline phases and percentage thereof. The samples were scanned using X-rays generated by a copper (Cu) Ka X-ray tube. Measurements were carried out between variable divergence- and fixed-receiving slits. Phases were identified using X'PertHighscore plus software. The relative abundances of the detected phases were refined using the Rietveld method (Hill and Howard, 1987). Figure 2 indicates an example of observed and calculated XRD patterns, as well as the difference between the two patterns. The goodness-of-fit (GoF) value for the presented pattern was 1.91. The GoF value for all quantitative Rietveld refined XRD results presented in this study was ≤2.04.

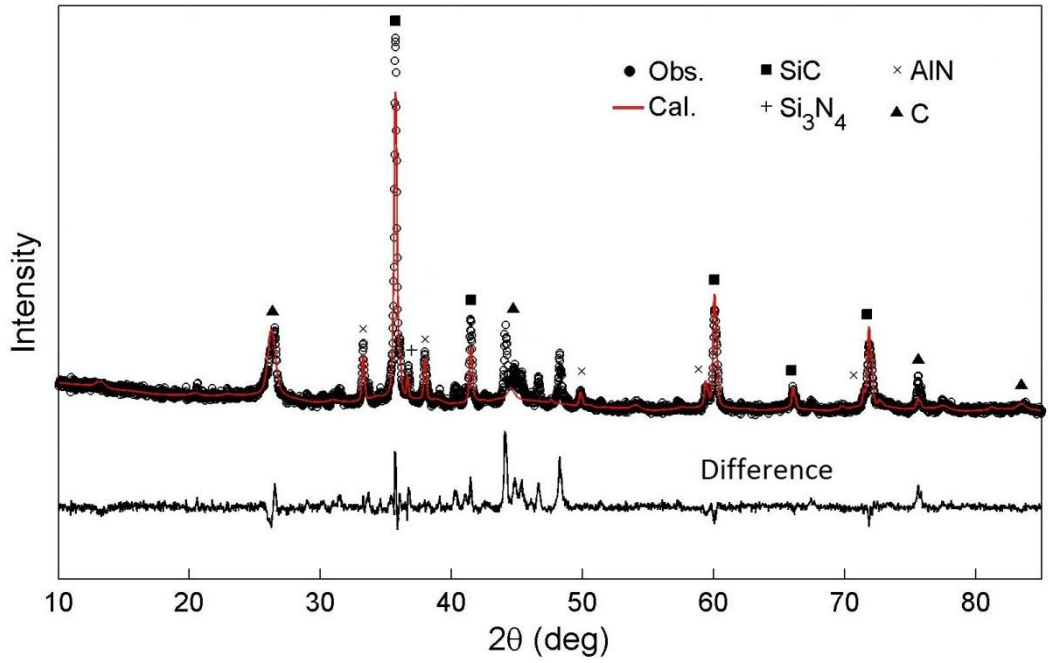

Figure 2: An example of a Rietveld refined XRD pattern of fine quartz carbothermically treated with anthracite.

2.5. TG analysis

Thermogravimetric (TG) analysis was performed using a Netzsch Model STA 449 F3 instrument with its high temperature rhodium furnace. Approximately 0.5 mg of powdered sample was place in the manufacture's Al_2O_3 crucible and enclosed using the crucible lid. Samples were then heated at a rate of 30°C min^{-1} to 1600°C. After which, the samples were allowed to cool down to room temperature. A N_2 atmosphere was maintained within the furnace chamber by continuously purging the chamber with a 20 mL min^{-1} N_2 flow. All TG results reported were corrected by a baseline obtained under identical conditions from an empty crucible.

3. Results and discussions

3.1. Effect of particle size

For a constant weigh of particulate matter a decrease in the particle size will result in an increase in surface area. Therefore, the intimate contact between quartz and anthracite particles will increase as a function of decreasing particle size. Intimate particle contact, promoted by finer particle size, is likely to be important to promote SiC formation, since solid-state reactions between SiO_2 and C (Reaction 4) are involved in the SiC formation reaction mechanism (Reaction 4 to 5) (Chen and Lin, 1997; Van Dijen and Metselaar, 1991):

$$SiO_2\,(s) + C(s) \rightarrow SiO(g) + CO(g) \quad (4)$$

$$\Delta G° = 582.30 - 0.3296\ T\ (kJ)$$

$$SiO(g) + 2C(s) \rightarrow SiC(s) + CO(g) \quad (5)$$

$$\Delta G° = -75.56 - 0.0012\ T\ (kJ)$$

Reaction 4 presents the endothermic initial solid-state reaction between SiO_2 and C, producing SiO(g) and CO(g). Subsequently, the volatile SiO(g) reacts with solid carbon in a CO/CO_2 atmosphere to produce SiC(s) and CO(g) according to the exothermic Reaction 5.

To investigate the effects of quartz and anthracite particle sizes, the finest quartz size fraction (d_{90} of 119.5 µm, Table 1) was carbothermically treated with increasingly larger anthracite particle size fractions (d_{90} of 105.3 to 682.6 µm, Table 1) at the maximum investigated temperature (1600°C), as indicated in Figure 3a. Subsequently, the finest anthracite size fraction (d_{90} of 105.3µm, Table 1) was carbothermically treated at 1600°C with increasingly larger quartz particle size fractions (d_{90} of 119.5 to 556.8 µm, Table 1) (Figure 3b). These and subsequent result figures only indicate the Si-containing compounds normalised to 100% (i.e. total of Si-containing compound is 100%). Non Si-containing compounds such as unreacted C, as well as other compounds that could be detected with the applied XRD method (Section 2.4), such as $MgAl_2O_4$ and AlN formed from impurities in the

quartz and anthracite, were not indicated. Also, since SiC can occur as various crystalline phases, it is important to specify which phase was observed. All XRD diffraction patterns (of which an example is indicated in Figure 2) indicated that the formed SiC occurred as cubic-SiC (β-SiC). This observation is in agreement with results published by (Muranaka et al., 2008), who indicated that β-SiC primarily forms at temperatures < 1700°C.

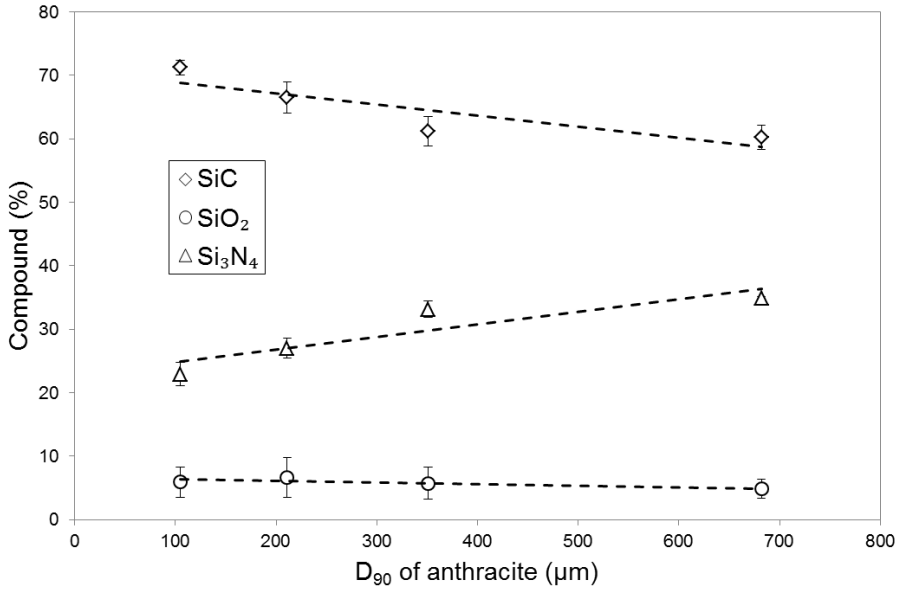

(a)

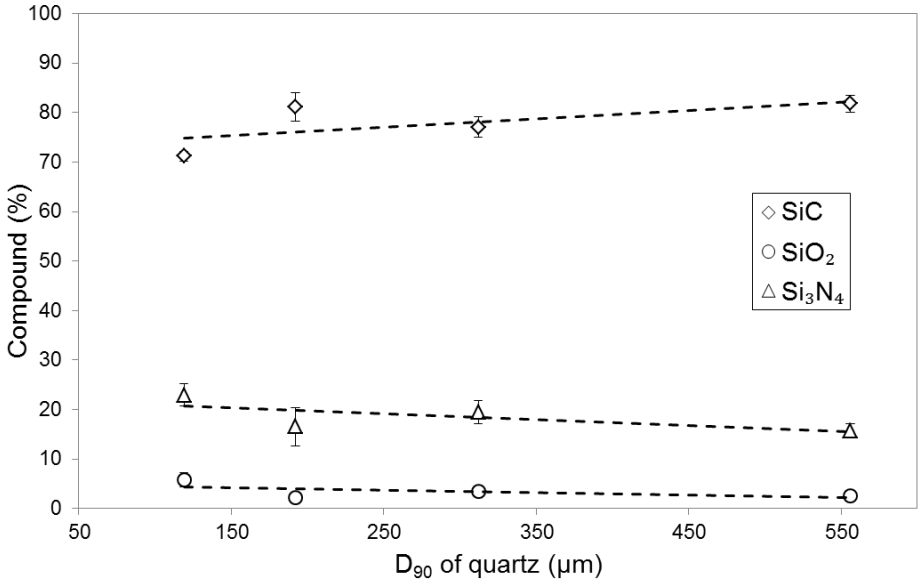

(b)

Figure 3: Average percentage (%) composition and standard deviation (based on three experimental repeats) of the finest quartz size fraction (d_{90} of 119.5 µm, Table 1) carbothermically treated with increasingly larger anthracite particle sizes fractions (a), as well as, the finest anthracite size fraction carbothermically treated with increasingly larger quartz particle size fractions (b). Both sets of experiment were conducted at a maximum temperature at 1600°C. The bars indicated the standard deviations from three experimental repeats.

The results presented in Figures 3a and 3b indicate that not only was SiC formed, but also Si_3N_4. This was expected, since carbothermic reduction of SiO_2 in the presence of N_2 result in Si_3N_4 formation (Arik, 2003):

$$3SiO_2(s) + 6C(s) + 2N_2(g) \rightarrow Si_3N_4(s) + 6CO(g) \quad (6)$$

$$\Delta G° = 1011.9 – 0.6406\ T\ (kJ)$$

According to the $\Delta G°$ of Reaction 6 (determined with HSC), the reaction will initiate at a temperature of approximately 1550°C, which is lower than the actual maximum temperature at which these tests were conducted (i.e. 1600°C). Thus, according to thermodynamic calculations some formation competitiveness is expected during the carbothermic treatment of quartz in a N_2 containing atmosphere, which could limit the application of the proposed SiC production method if Si_3N_4 formation precedes SiC formation.

As is evident from the results presented in Figure 3a, decreasing d_{90} of the screened size fractioned anthracite (decreasing from 682.6 to 119.5 µm) resulted in a SiC yield increase from 60.3 to 71.2%. An associated decrease in Si_3N_4 formation, i.e. from 34.9 to 22.9%, was also observed. The remaining unreacted quartz content was approximately 5.4 ± 0.6% in all cases.

Considering the results presented in Figure 3b, SiC formation was relatively insensitive to the screened fraction quartz particle size. Although the linear interpolated lines indicate increased SiC formation with larger size fractioned quartz, the %SiC formed was almost identical for the quartz size fractions with d_{90} of 556.8 and 192.5 µm, i.e. 81.76 and 81.17% SiC, respectively. The remaining unreacted quartz content was approximately 3.1 ± 1.2% for all cases.

In order to further investigate the effect of particle size, milled mixtures of quartz and anthracite (Table 1) were carbothermically treated at 1600°C. These results are presented in

Figure 4. Quartz and anthracite mixture milling was kept to a minimum to prevent *in-situ* SiC formation. Raygan et al. (2011) produced a small quantity of SiC from silica sand during 200 hrs of low energy ball milling, whereas Lu et al. (2013) completely converted silicon powder to SiC by 24 hrs of high energy stirred bead milling (Raygan et al., 2011; Lu et al., 2013). However, it is highly unlikely that any significant amount of SiC formed during the less than 60 sec milling applied in this study.

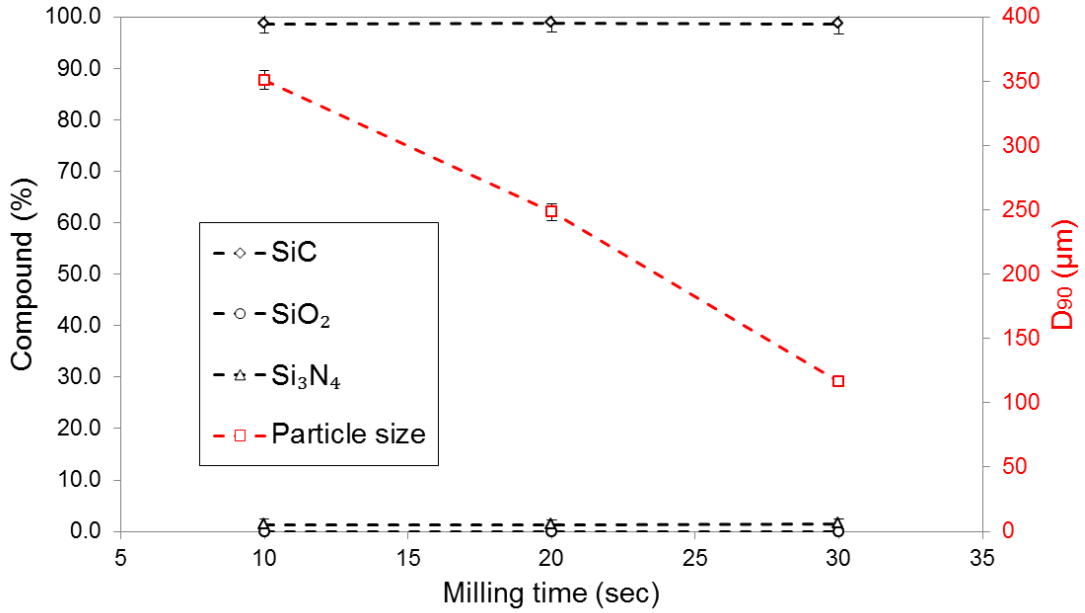

Figure 4: Percentage composition (formed SiC and Si_3N_4, as well as unreacted quartz) of milled mixtures carbothermically treated at 1600°C indicated on the primary y-axis, while the particle sizes (d_{90}) of these milled mixtures are indicated on the secondary y-axis. The bars indicated the standard deviations from three experimental repeats.

As is evident from the results presented in Figure 4, carbothermic treatment at 1600°C of milled quartz and anthracite mixtures, of which the $d_{90} \leq 350.9$ µm, resulted in almost complete conversion of quartz to SiC (> 98%), with very limited Si_3N_4 formation (≤ 1.4%). The results indicate that limited milling would be required to ensure sufficient inter-particle contact to promote the solid-state reaction between SiO_2 and C, as indicated in Reaction 4.

This result is very promising from a possible industrial application perspective, since limited milling requires less energy input (which is directly related to cost of production). To place these results in perspective, extensive milling to achieve d_{90} of 75 µm is specified for the composite pellet mixture used in the industrial solid state reduction of chromite (also known as chromite pre-reduction) (Kleynhans et al., 2012).

3.2 Effect of temperature

To determine the effects of reaction temperature on conversion of quartz, the milled mixture with d_{90} of 350.9 µm (Table 1, 10 sec milling) was carbothermically treated at various temperatures, i.e. 1400, 1450, 1500 and 1600°C, as indicated in Figure 5. Previously it was proven that quartz conversion to SiC, in the afore-mentioned milled particle size material, was almost complete after 1600°C treatment (Figure 4).

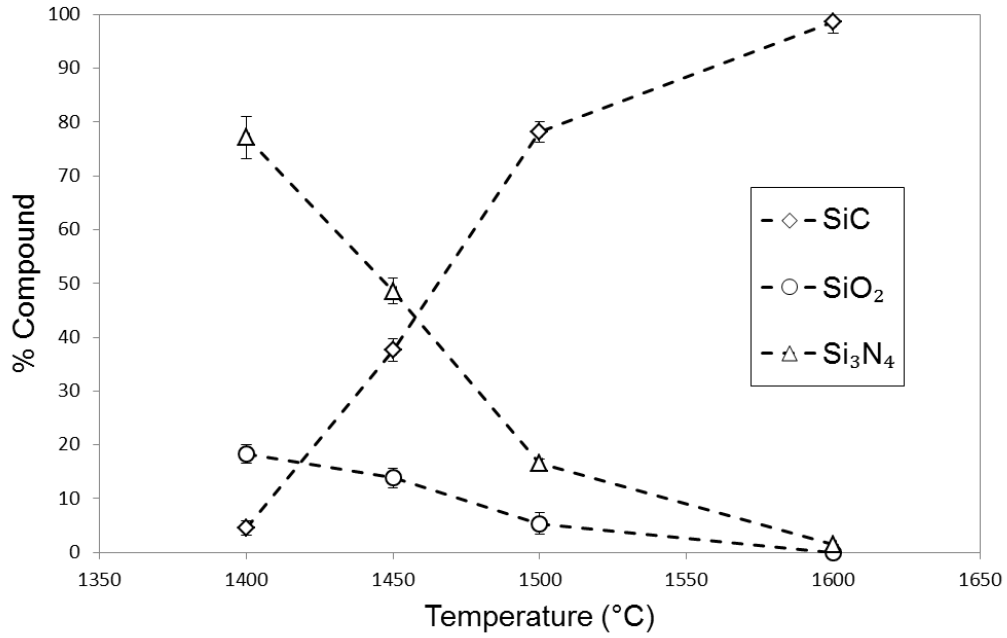

Figure 5: Effects of temperature on quartz conversions (average and standard deviation composition, based on three repeats) of the milled mixtures with a d_{90} of 350.9 µm. The bars indicated the standard deviations from three experimental repeats.

As is evident from the temperature dependency results (Figure 5), Si_3N_4 was the dominant Si-containing phase after 1400°C carbothermic treatment (77.1% Si_3N_4 and 4.6% SiC), while a significant fraction of unreacted quartz remained (18.3%). This indicated that Si_3N_4 formation occurred at temperatures lower than 1550°C, which was predicted from thermodynamic calculations with HSC (Reaction 6).

It is clear from Figure 5 that for the carbothermal treatment of quartz in a N_2 atmosphere, Si_3N_4 formation occurs before SiC, further emphasizing the importance of understanding Si_3N_4 formation and its possible conversion to SiC.

3.3 Mechanistic deductions

The mechanism for the reaction system considered in this paper, or at least identification of important aspects thereof, needed to be established. To initiate this, backscatter SEM and cross-sectional EDS-mappings of milled mixtures with d_{90} of 350.9 µm carbothermically treated were considered, as presented in Figure 6. Again, the milled mixtures with d_{90} of 350.9 µm was considered, due to its high quartz to SiC conversion % and the minimal milling energy required to achieve this particle size (Figure 4 and associated text).

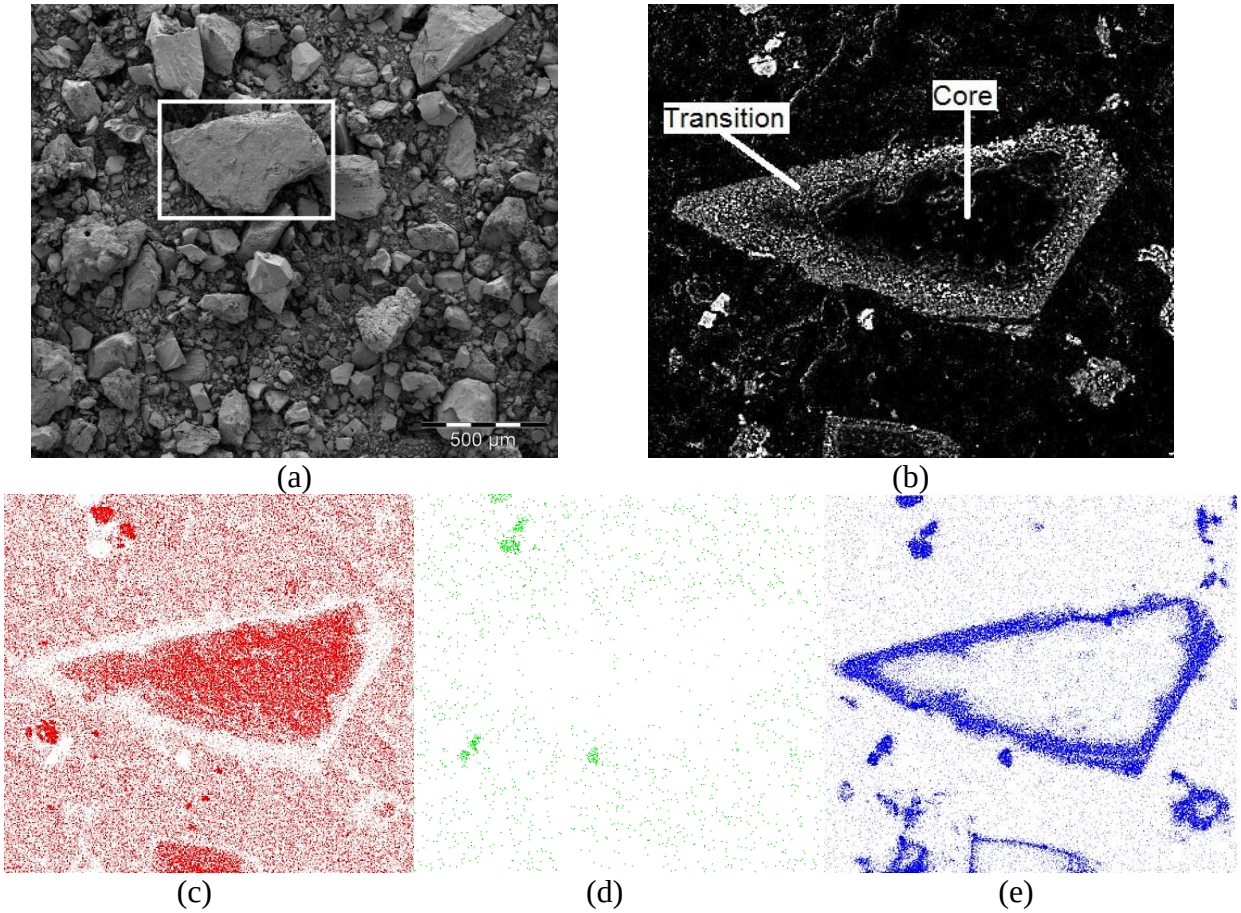

Figure 6: Backscatter SEM micrograph of SiC containing particles originating from a milled mixture with d_{90} of 350.9 µm that was carbothermically threated at 1600°C (a); a polished cross section of a SiC containing particle (b), and the corresponding EDS mapping for C (c), O (d) and Si (e).

SEM-EDS spot analyses were performed on the surface of a typical unpolished SiC containing particle (marked with a white block in Figure 6a), as well as areas towards the centre of a cross sectioned (polished) SiC containing particle in Figure 6b. These EDS results are presented in Table 2 and should be considered as semi-quantitative, with O content determined by difference. The areas selected for investigation are referred to as "Surface" (from unpolished sample as in Figure 6a), as well as "Transition" and "Core" (from polished sample as in Figure 6b), in Table 2.

Table 2: SEM-EDS analyses of SiC containing particles					
Area	Detected elements (at%)				
	C	Si	Al	O	Total
Surface	55.11	40.65	2.15	2.09	100
Transition	73.46	23.17	1.28	2.09	100
Core	89.14	7.51	0.31	3.04	100

Considering the carbon based resin used to prepare samples prior to polishing, the C content of the "Transition" and "Core" sampled areas may be a minor over-estimation, and the O continent may also originate at least partially from the resin used. Some Si detected at the core of the investigated particle (Figure 6b) might also be as a results of smearing (spreading of traces thereof) of elements during polishing. Notwithstanding these data limitations, the composition of the "Surface" and "Transition" areas confirm the combined enrichment of Si and C in these areas, which indicate SiC formation (pure SiC will have 70.04% Si and 29.96% C). The Al content, which likely originated from impurities in the anthracite and quartz, also decreased towards the core of the investigated particles.

Considering the results presented in Table 2, the decrease in Si content and associated C content increase towards the centre of the particles was of particular mechanistic interest. This is indicative of a shrinking core mechanism, where the C is non-mobile and the Si is the mobile element. This supports the commonly held mechanistic theory that the SiO_2 present in the quartz was reduced to form SiO(g) in the presence of C(s) at elevated temperatures (1600°C), as indicated in Reaction 4 (Chen and Lin, 1997; Van Dijen and Metselaar, 1991). The *in-situ* generated SiO(g) can then subsequently reacted with C(s) present on the anthracite surface to form SiC(s), as indicated in Reaction 5 (Chen and Lin, 1997; Van Dijen and Metselaar, 1991). SiO(g) can further penetrate the outer SiC(s) layer on the anthracite particle to react with underlying C(s), until either the SiO(g) reaches its penetration limit, or the supply of SiO(g) is depleted. It is also likely that SiC(s) formation is dependent on the availability of reaction surface on the anthracite, with smaller particle size implying larger

surface area. However, the effect of particle size (Figures 3 and 4) proved that after a critical particle size is achieved (which was established as $d_{90} \leq 350.9$ μm) quartz to SiC conversion was almost complete. Therefore the remaining C "Core" (Figure 5) is due to the excess C supply (400% excess C, Section 2.3), indicating that all Si have been converted to SiC, before a SiO(g) penetration limit had been achieved.

The above-mentioned reaction mechanism usually occurs in a CO/CO_2 atmosphere. However, in this study a N_2 atmosphere was applied (Section 2.3). Nevertheless, some *in-situ* formed CO and CO_2 will occur, due to the C reacting with oxygen in the material matrix. At a pressure of 1 atm and over the temperature range considered in this study (i.e. 1400 to 1600°C), the equilibrium of the Boudouard reaction (Reaction 7) is shifted towards the right, implying that almost all CO_2 will be converted to CO (Tangstad et al., 2017), which generate a more reducing environment favorable for SiC formation.

$$C + CO_2 \leftrightarrow 2CO \quad (7)$$

Although the afore-mentioned mechanistic discussion, within the context of commonly accepted mechanistic theory (Reactions 4 and 5; Van Dijen and Metselaar, 1991; Chen and Lin, 1997) and recognition of some *in-situ* formed CO/CO_2 is valid, it was proven beyond doubt that Si_3N_4 was the dominant Si-containing phase at maximum carbothermic reaction temperatures of approximately ≤ 1465°C (Figure 5). It is therefore likely that Si_3N_4 formation would precede SiC formation, as the milled mixtures were heated from room temperature to 1600°C (Figure 3 and 4). The mechanistic role of Si_3N_4 within this process therefore needed to be clarified.

Figure 7 present the surface morphologies of a milled mixture with d_{90} of 350.9 μm carbothermically treated at 1400 and 1450°C. From these SEM micrograms, thin, strand-like growths or whisker, are clearly visible for the 1400°C treated material (Figure 7a). EDS spot

analyses were performed on various areas, indicated by the white numbers 1 to 4 (Figure 7a and 7b), as presented in Table 3.

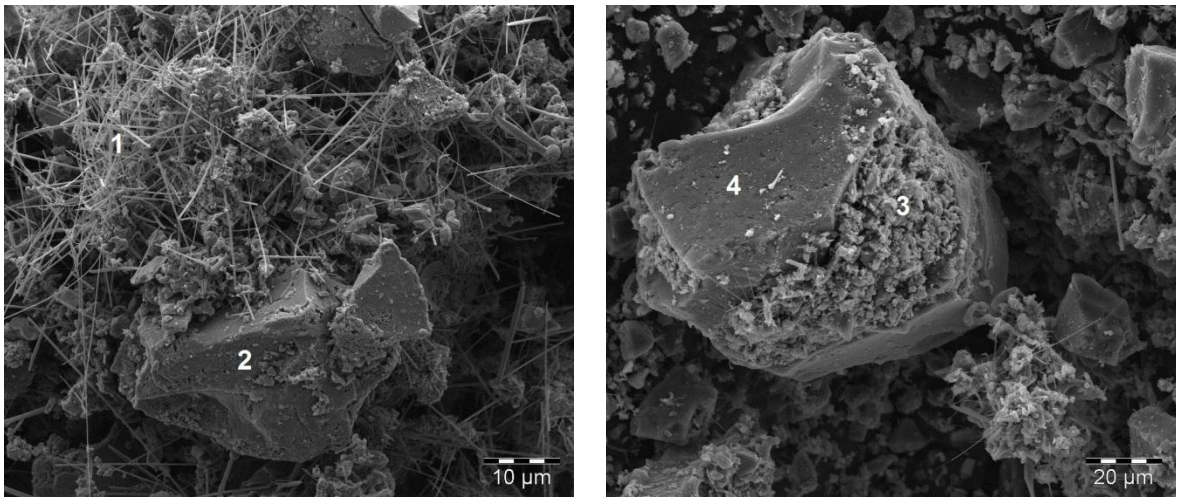

(a) (b)

Figure 7: SEM micrographs of milled mixture material with d_{90} of 350.9 µm carbothermically treated at 1400°C (a) and 1450°C (b). The compositions of the numbered areas were determined with EDS analyses, as indicated in Table 3.

Table 3: EDS analyses of numbered areas indicated in Figure 7 for milled mixture material with d_{90} of 350.9 µm carbothermically treated at 1400 and 1450°C.

Spot	Detected elements (at%)					
	C	Si	Al	O	N	Mg
1	21.65	20.44	2.64	7.3	47.61	0.37
2	99.29	0.33				
3	92.24	5.22	0.16	2.39		
4	99.07	0.81				

By jointly considering Figure 7a and "Spot" analysis 1 in Table 3, it is evident that the whiskers that are formed at 1400°C (Figure 7a, numbered area 1) consist mainly out of Si_3N_4. These Si_3N_4 whiskers sit on and around unreacted C particles (areas numbered 2 and 4 in Figure 7a and 7b, as well as Table 3). At 1450°C these whiskers lose their whisker-like morphology, as indicated by area number 3 in Figure 7b and Table 3. This morphology change may be ascribed to the dissociation of nitrogen from the Si_3N_4 molecule. The

observed morphology change for this dissociation was previously described to occur at 1600°C < temperature < 1800°C (Murray et al., 2006). However, Murray et al. (2006) referred to Si_3N_4 dissociation in a solar-thermal process where Si_3N_4 was obtained from purer sources of SiO_2 and C. Therefore, the lower temperature Si_3N_4 dissociation observed here may be due to possible catalytic effects of impurities present in quartz and anthracite. Notwithstanding the uncertainty regarding the cause of the lower temperature Si_3N_4 dissociation, this dissociation resulted in a very finely divided source of Si being deposited onto the anthracite particles. Subsequently, this resulted in almost complete conversion of Si to SiC at 1600°C, which is below the expected SiC formation temperature. Therefore, Si_3N_4 formation significantly enhanced SiC formation and should thus not be regarded as a competing, unwanted reaction.

In order to assess if the Si_3N_4 formation, its subsequent decomposition, and SiC formation occurred in distinct phases, TG analysis of milled mixture material with d_{90} of 350.9 µm was undertaken, as presented in Figure 8. From this data it is clear that up to approximately 800°C, very little mass loss occur, which is mainly explained by de-volatilization of the anthracite. However, from approximately ≥ 1200°C significant and continuous (not phased) mass loss occurs. The only deductions that can be made from this TG data, in conjunction with previous results, were that Si_3N_4 formation initiate at ≥ 1200°C, which is followed by its decomposition (that occur at ≤ 1450°C Figure 7b and Table 3) and formation of SiC that is complete at ≤ 1600°C (Figure 3 and 4). Therefore, the formation of Si_3N_4, its decomposition, and SiC formation did not occur in distinct separate temperature phases, but rather concurrently.

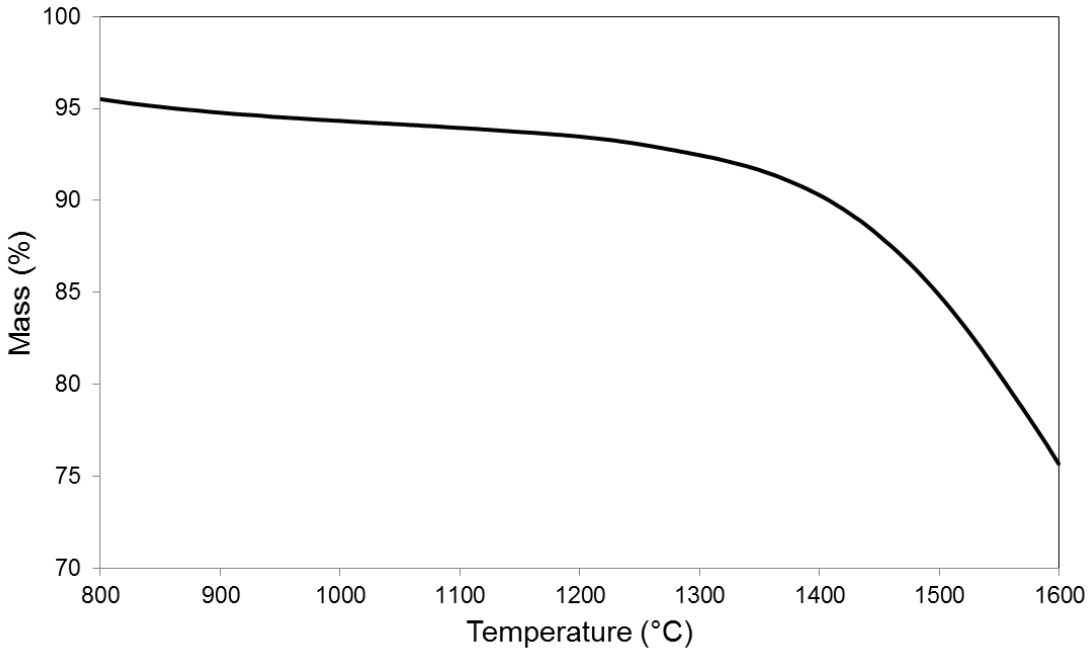

Figure 8: TG curve of milled mixture material with d_{90} of 350.9 µm that was carbothermically treated in a N_2 atmosphere at increasing temperature, with the range 800 to 1600°C presented here.

4. Possible practical applications of on-site SiC production

This paper was mainly focussed on exploring the fundamental possibility of producing SiC from waste materials (i.e. combustion of CO-rich off gas, as well as screened out quartz and anthracite fines). However, to guide future studies in this field of research, it is worth considering the limitations of the current study and the aspects that must still be considered, before process up-scaling is deliberated.

Possibly the most significant fundamental scientific concern is that all the results presented thus far were obtained in a N_2 gaseous environment. Such an environment will not be industrially feasible. When this study was initiated, it was thought that a N_2 atmosphere would be disadvantageous due to possible competing Si_3N_4 formation. However, as was indicated, Si_3N_4 formation actually enhanced SiC formation (Section 3.3). This indicates that N_2 in the ambient gaseous environment (with approximately 78% N_2) will not negatively

influence SiC formation. The approximately 21% oxygen (O_2) in the ambient environment could however be problematic, since oxidation of the carbonaceous source (anthracite in this case) could occur during CO combustion to supply the heat. To test if this will be a problem, milled material mixture with d_{90} of 350.9 µm (identified as being optimal, i.e. reducing milling cost, but maintaining SiC formation efficiency) was placed in a crucible and with a normal crucible lid on top. The mixture filled approximately 70% of the crucible's total volume and the crucible lid did not fit airtight onto the crucible sides, allowing air to enter the reaction vessel. After treatment with the same temperature profile applied to all previous samples (up to 1600°C), XRD analysis revealed a SiC and Si_3N_4 contents of 97.7 and 2.3%, respectively. No residual SiO_2 was detected. The high SiC content and lack of SiO_2, proved that oxidation that would interfere with SiC formation, can be prevented. Within the milled material *in-situ* generated CO_2 and CO (Reaction 7) will generate a partial positive pressure, preventing O_2 from entering the mixture. Additionally, it seems that a similar partial positive pressure within the crucible, combined with the 400% excess C (Section 2.3) also prevented oxidation on the surface of the material mixture. The proposed process therefore seems feasible, if some precautions are taken to prevent oxidation.

The availability of sufficient volumes of CO-rich off-gas, as well as fine quartz and anthracite, may also be considered as limiting factors for possible on-site SiC production. The availability and quality of off-gas is determined by two factors, i.e. (i) furnace operating conditions such as power input; and (ii) the metallurgical health of the furnace. A major benefit of the processed approach of storing energy in the form of SiC, would be that SiC can be produced when the waste materials (CO-rich off-gas, as well as fine quartz and anthracite) are available, and the process can be halted if this is not the case.

Selecting a proper furnace design for SiC production would be critical. Although rotary kilns are often used in pre-reduction processes, it would require pelletized material

feed, since un-pelletized material that tumbles in such a furnace would cause huge dust issues. Therefore, an alternative approach would be to use a rotary hearth furnace, wherein the material is stationary and the refractory line bed moves through several refractory line cambers. Such a furnace may contain several chambers, each with its own operation temperature, allowing a systematic increase in operational temperature. Figure 9 presents a simple schematic of a rotary hearth furnace and the suggested operational temperatures.

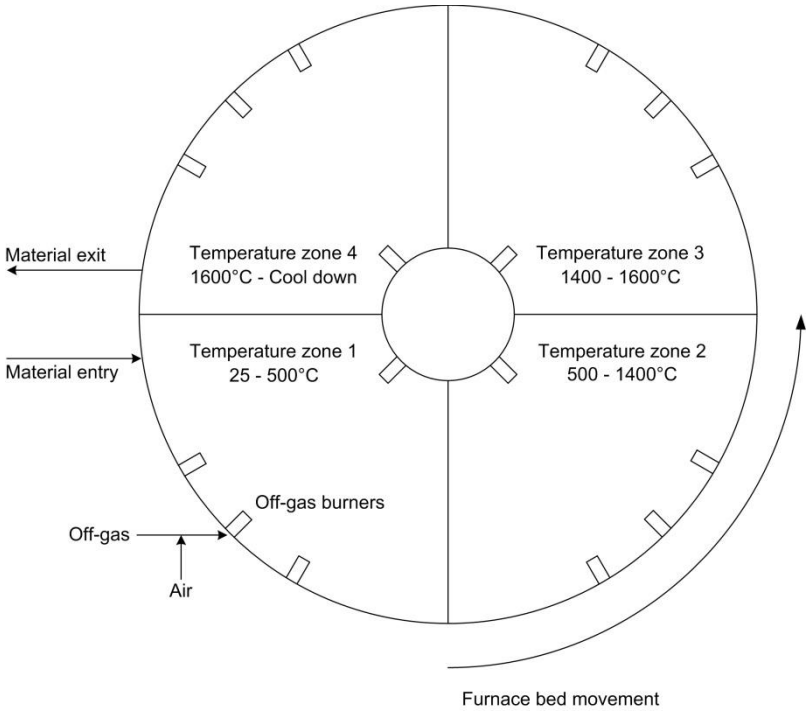

Figure 9: A simplified schematic of a rotary hearth furnace and the suggested operation temperatures for on-site SiC production.

It was previously mentioned that precaution should be taken to prevent oxidation on the surface of the material mixtures thermally treated and additionally, dust suppression should be considered. Obviously pelletization of the material can be considered. Alternatively, a sacrificial layer of coarse, low grade coal could be placed on top of the material in the rotary hearth, as indicated in Figure 10. This material will assist in the formation of a partial positive CO_2/CO atmosphere below the mixed material surface.

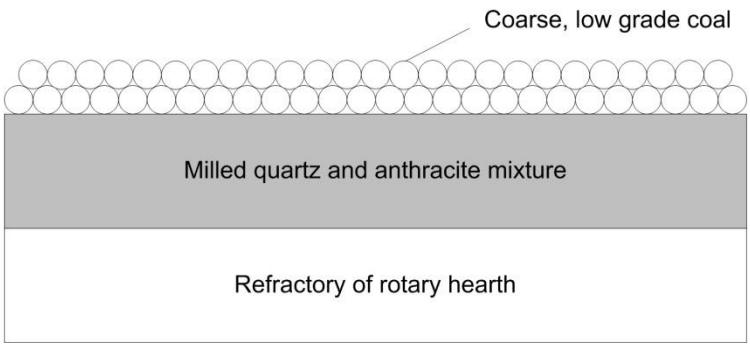

Figure 10: Schematic illustration of material in rotary heart furnace for the proposed SiC production route.

EDS mapping of C and Si (Figure 7) of the formed SiC indicated that C rich particles are coated with SiC. Therefore, unreacted C particles, which can be separated from the SiC, are unlikely to occur. It is therefore essential that actual reductive smelting of ores be conducted in future to assess the effectiveness of the unique SiC coated and unreacted C core type particles. Obviously, a techno-economic study should also be undertaken if all the afore-mentioned results are positive.

5. Conclusions

The results presented in this paper present a novel approach to store the energy associated with CO-rich off-gas combustion in the form of SiC, which can be used as a partial carbonaceous reductant replacement during the smelting process.

SiC formation was achieved using materials partially classified as waste (quartz and anthracite fines), from a large FeCr producer. Relatively little milling of the raw materials were required (minimizing milling energy) and carbothermic treatment of 1600°C allowed for the almost complete conversion of quartz to SiC. This temperature can be achieved without difficulty by CO-rich off-gas combustion. It was found that Si_3N_4 will form in a N_2 containing atmosphere, prior to SiC formation. However, Si_3N_4 decomposition actually

enhanced SiC formation. Therefore, Si_3N_4 formation should not be considered as a competing pathway or a competing/hampering product.

A quick assessment of the possible practical application of this process indicated that numerous practical aspects still have to be considered before this process can be implemented, but the work presented here indicate considerable potential.

Acknowledgements

The authors thank the FeCr producer that provided the materials that were used in this study. The financial assistance of the National Research Foundation (NRF) towards the PhD study of SP du Preez (grant number: 101345) is hereby acknowledged. Opinions expressed and conclusions arrived at, are those of the authors and are not necessarily to be attributed to the NRF. The authors would also like to thank Mr Kosie Oosthuizen from the Geology Subject Group for the use of their pulveriser, and Mr Nico Lemmer from the Faculty of Engineering for the use of their particle size analyser.

References

Agarwal, A., Pad, U., 1999. Influence of pellet composition and structure on carbothermic reduction of silica. Metallurgical and Materials Transactions B 30(2), 295-306.

Arik, H., 2003. Synthesis of Si_3N_4 by the carbo-thermal reduction and nitridation of diatomite. Journal of the European Ceramic Society 23(12), 2005-2014. https://doi.org/10.1016/S0955-2219(03)00038-4

Bandyopadhyay, S., Mukerji, J., 1991. Reaction sequences in the synthesis of silicon nitride from quartz. Ceramics International 17(3), 171-179. https://doi.org/10.1016/0272-8842(91)90064-7

Basson, J., Daavittila, J., 2013. High Carbon Ferrochrome Technology-Chapter 9, in: Gasik, M. (Ed.) Handbook of ferroalloys: theory and technology. Elsivier, United Kingdom. http://dx.doi.org/10.1016/B978-0-08-097753-9.00009-5

Beukes, J.P., Dawson, N.F., Van Zyl, P.G., 2010. Theoretical and practical aspects of Cr(VI) in the South African ferrochrome industry. The Journal of The Southern African Institute of Mining and Metallurgy 110(12), 743-750.

Beukes, J.P., du Preez, S.P., van Zyl, P.G., Paktunc, D., Fabritius, T., Päätalo, M., Cramer, M., 2017. Review of Cr (VI) environmental practices in the chromite mining and smelting industry–relevance to development of the Ring of Fire, Canada. Journal of Cleaner Production. https://doi.org/10.1016/j.jclepro.2017.07.176

Beukes, J.P., Van Zyl, P.G., Ras, M., 2012. Treatment of Cr(VI)-containing wastes in the South African ferrochrome industry – A review of currently applied methods. The Journal of The Southern African Institute of Mining and Metallurgy 112, 347-352.

Chen, S.H., Lin, C.I., 1997. Effect of contact area on synthesis of silicon carbide through carbothermal reduction of silicon dioxide. Journal of Materials Science Letters 16(9), 702-704. https://doi.org/10.1023/A:1018508525803

Demir, O., 2001. Ferroalloy production. Publication number: WO2001079572 A1. Google Patents.

Du Preez, S.P., Beukes, J.P., Van Dalen, W.P.J., Van Zyl, P.G., Paktunc, D., Loock-Hatting, M.M., 2017. Aqueous solubility of Cr(VI) compounds in ferrochrome bag filter dust and the implications thereof. Water SA 43(2), 298-309. http://dx.doi.org/10.4314/wsa.v43i2.13

Du Preez, S.P., Beukes, J.P., van Zyl, P.G., 2015. Cr (VI) Generation During Flaring of CO-Rich Off-Gas from Closed Ferrochromium Submerged Arc Furnaces. Metallurgical and Materials Transactions B 46(2), 1002-1010. https://doi.org/10.1007/s11663-014-0244-3

Glastonbury, R.I., Beukes, J., Van Zyl, P., Sadikit, L., Jordaan, A., Campbell, Q., Stewart, H., Dawson, N., 2015. Comparison of physical properties of oxidative sintered pellets produced with UG2 or metallurgical-grade South African chromite: A case study. Journal of the Southern African Institute of Mining and Metallurgy 115(8), 699-706. http://dx.doi.org/10.17159/2411-9717/2015/V115N8A6

Gupta, G.S., Vasanth Kumar, P., Rudolph, V.R., Gupta, M., 2001. Heat-transfer model for the acheson process. Metallurgical and Materials Transactions A 32(6), 1301-1308. https://doi.org/10.1007/s11661-001-0220-9

Haggerty, S.E., 1991. Oxide mineralogy of the upper mantle. Reviews in Mineralogy and Geochemistry 25(1), 355-416.

Hall, D., Donaldson, K., McAllister, J., Marrs, T., Ross, J.A., Anderson, D., Baker, D., Chen, L.-C., Baxter, P.J., Murray, V., 2015. Toxicology, Survival and Health Hazards of Combustion Products. Royal Society of Chemistry. ISSN: 1757-7179

Hill, R., Howard, C., 1987. Quantitative phase analysis from neutron powder diffraction data using the Rietveld method. Journal of Applied Crystallography 20(6), 467-474. https://doi.org/10.1107/S0021889887086199

Itaka, K., Ogasawara, T., Boucetta, A., Benioub, R., Sumiya, M., Hashimoto, T., Koinuma, H., Furuya, Y., 2015. Direct Carbothermic Silica Reduction from Purified Silica to Solar-Grade Silicon, Journal of Physics: Conference Series 596. IOP Publishing, 012015. doi:10.1088/1742-6596/596/1/012015

Kapure, G., Kari, C., Rao, S.M., Raju, K., 2007. Use of chemical energy in submerged arc furnace to produce ferrochrome: Prospects and limitations. In: *Proceedings of the 11th International Ferro Alloys Conference*, New Delhi, India. 165–170.

Kleynhans, E.L.J., Beukes, J.P., Van Zyl, P.G., Bunt, J.R., Nkosi, N.S.B., Venter, M., 2016. The Effect of Carbonaceous Reductant Selection on Chromite Pre-reduction. Metallurgical and Materials Transactions B, 1-14. https://doi.org/10.1007/s11663-016-0878-4

Kleynhans, E.L.J., Beukes, J.P., Van Zyl, P.G., Kestens, P.H.I., Langa, J.M., 2012. Unique challenges of clay binders in a pelletised chromite pre-reduction process. Minerals Engineering 34(0), 55-62. https://doi.org/10.1016/j.mineng.2012.03.021

Krishnarao, R.V., Mahajan, Y.R., Kumar, T.J., 1998. Conversion of raw rice husks to SiC by pyrolysis in nitrogen atmosphere. Journal of the European Ceramic Society 18(2), 147-152. https://doi.org/10.1016/S0955-2219(97)00093-9

Li, X., Zhang, G., Tang, K., Ostrovski, O., Tronstad, R., 2015. Carbothermal Reduction of Quartz in Different Gas Atmospheres. Metallurgical and Materials Transactions B 46(3), 1343-1352. https://doi.org/10.1007/s11663-015-0293-2

Lind, B.B., Fällman, A.M., Larsson, L.B., 2001. Environmental impact of ferrochrome slag in road construction. Waste Management 21(3), 255-264. https://doi.org/10.1016/S0956-053X(00)00098-2

Lu, Y., Wang, Y., Pan, Z., Shen, H., Wu, L., 2013. Preparation of carbon–silicon carbide composite powder via a mechanochemical route. Ceramics International 39(4), 4421-4426. https://doi.org/10.1016/j.ceramint.2012.11.033

Maine, C., Smit, J., Giesekke, E., 2005. The solid stabilization of soluble wastes generated in the South African ferrochrome industry. Water Research Commission.

Malan, W., Akdogan, G., Bradshaw, S., Bezuidenhout, G., 2015. The recovery of platinum group metals from low-grade concentrates to an iron alloy using silicon carbide as reductant. Journal of the Southern African Institute of Mining and Metallurgy 115(5), 375-383.

Muranaka, T., Kikuchi, Y., Yoshizawa, T., Shirakawa, N., Akimitsu, J., 2008. Superconductivity in carrier-doped silicon carbide. Science and Technology of Advanced Materials 9(4), 044204. doi:10.1088/1468-6996/9/4/044204

Murray, J.P., Flamant, G., Roos, C.J., 2006. Silicon and solar-grade silicon production by solar dissociation of Si3N4. Solar Energy 80(10), 1349-1354. https://doi.org/10.1016/j.solener.2005.11.009

Niemelä, P., Kauppi, M., 2007. Production, characteristics and use of ferrochromium slags. In: *Proceedings of the 11th International Ferro Alloys Conference*, New Delhi, India. 171–179.

Niemelä, P., Krogerus, H., Oikarinen, P., 2004. Formation, characterization and utilization of CO-gas formed in ferrochrome smelting. In: *Proceedings of the 12th International Ferroalloys Congress*, Cape Town, South Africa. 68–77.

Pheiffer, D.M., Cookson, K., 2015. Ferrochrome alloy production.Publication number: WO2015159268 A1. Google Patents.

Raygan, S., Kondori, B., Yangijeh, H.M., 2011. Effect of mechanical activation on the production of SiC from silica sand. International Journal of Refractory Metals and Hard Materials 29(1), 10-13. https://doi.org/10.1016/j.ijrmhm.2010.06.002

Riekkola-Vanhanen, M., 1999. Finnish expert report on best available techniques in ferrochromium production., Helsinki.

Roine, A., 2009. HSC Chemistry 7.0. Outotec Research, Pori, Finland.

Šajgalík, P., Sedláček, J., Lenčéš, Z., Dusza, J., Lin, H.-T., 2016. Additive-free hot-pressed silicon carbide ceramics—A material with exceptional mechanical properties. Journal of the European Ceramic Society 36(6), 1333-1341. https://doi.org/10.1016/j.jeurceramsoc.2015.12.013

Schubert, E., Gottschling, R., 2011. Co-generation: A challenge for furnace off-gas cleaning systems. Southern African Pyrometallurgy. In: *Jones, R.T. & den Hoed, P. (eds) Southern African pyrometallurgy*. Johannesburg: Southern African Institute of Mining and Metallurgy. 6–9.

Tangstad, M., Beukes, J.P., Steenkamp, J.E.R., 2017. In preparation. Coal-based reducing agents in ferroalloys and silicon production. To be updated with book details.

Van Dijen, F., Metselaar, R., 1991. The chemistry of the carbothermal synthesis of β-SiC: Reaction mechanism, reaction rate and grain growth. Journal of the European Ceramic Society 7(3), 177-184. https://doi.org/10.1016/0955-2219(91)90035-X

Van Staden, Y., Beukes, J.P., van Zyl, P.G., du Toit, J.S., Dawson, N.F., 2014. Characterisation and liberation of chromium from fine ferrochrome waste materials. Minerals Engineering 56(0), 112-120. https://doi.org/10.1016/j.mineng.2013.11.004

Wu, Z., Deng, S., Xu, N., Chen, J., Zhou, J., Chen, J., 2002. Needle-shaped silicon carbide nanowires: Synthesis and field electron emission properties. Applied physics letters 80(20), 3829-3831. http://dx.doi.org/10.1063/1.1476703

Zelić, J., 2005. Properties of concrete pavements prepared with ferrochromium slag as concrete aggregate. Cement and Concrete Research 35(12), 2340-2349. https://doi.org/10.1016/j.cemconres.2004.11.019

CHAPTER 5: ARTICLE 3

Recycling pre-oxidized chromite fines in the oxidative sintered pellet production process

5.1 Author list, contributions, and consent

Authors list

SP du Preez[a], JP Beukes[a*], D Paktunc[b], PG van Zyl[a], and A Jordaan[a]

[a]Chemical Resource Beneficiation, North-West University, Potchefstroom Campus, Private Bag X6001, Potchefstroom 2520, South Africa

[b]CanmetMINING, Natural Resources Canada, 555 Booth St., Ottawa, ON, K1A0G1, Canada

Contributions

Contributions of the various co-authors were as follows:

Experimental work, data processing and interpretation, research, and writing of the scientific paper, was performed by the candidate, SP du Preez. Some analytical work and assistance with the interpretation thereof was performed by D Paktunc and A Jordaan. JP Beukes (supervisor) and PG van Zyl (co-supervisor) made conceptual contributions.

Consent

All of the co-authors that contributed to the article presented in this chapter have been informed that the article will form part of the candidate's PhD, submitted in article format, and have granted permission that the article may be used for the purpose stated.

5.2 Formatting and current status of the article

The article presented in Chapter 5 has been prepared for submission to *Metallurgical and Materials Transactions B*. It is currently foreseen that the paper will be submitted to the journal before 10 December 2017. The journal details can be found at http://www.springer.com/materials/special+types/journal/11663 (Date of access: 16 November 2017).

Recycling pre-oxidized chromite fines in the oxidative sintered pellet production process

S.P. du Preez[a], J.P. Beukes[a,*], D. Paktunc[b], P.G. van Zyl[a] and A. Jordaan[a]

[a] Chemical Resource Beneficiation (CRB), North-West University, Potchefstroom Campus, Private Bag X6001, Potchefstroom, 2520, South Africa

[b] CanmetMINING, Natural Resources Canada, 555 Booth St., Ottawa, Canada

* Corresponding author. E-mail address: paul.beukes@nwu.ac.za;
telephone: +27 82 460 0594; fax: +27 18 299 2350

ABSTRACT

The chromium (Cr) content of stainless steel originates from recycled scrap and/or ferrochrome (FeCr), which is mainly produced by the carbothermic reduction of chromite ore. The oxidative sintered pellet production process is one of the most widely applied FeCr practises. The supplier of the afore-mentioned technology specifies that re-cycling of chromite containing dust collected from the pellet sintering off-gas and fines screened out from the sintered pellets (collectively referred to as pre-oxidized chromite fines) should be limited to a maximum of 4 wt% of the total pellet composition. However, the results presented in this paper prove that re-cycling of such fines up to a limit 32 wt% of the total pellet composition improve cured pellet compressive and abrasions strengths. In addition, electron microprobe and quantitative X-ray diffraction (XRD) analyses demonstrate that chromite grains present in the pre-oxidized chromite fines at least partially consist of crystalline phases/compounds that will improve the metallurgical efficiency and specific electricity consumption (i.e. MWh/ton FeCr produced) of the smelting process.

Keywords: Chromite, ferrochrome/ferrochromium, pre-oxidation, oxidative sintering, recycling

1. Introduction

Stainless steel is a vital modern day alloy that is well-known for its corrosion resistance, which is mainly due to the inclusion of chromium (Cr) (ICDA, 2013). Stainless steel is mostly produced from recycled scrap and ferrochrome (FeCr), a relatively crude alloy between Cr and iron (Fe). FeCr is predominantly produced by the carbothermic reduction of chromite ore, which is a mineral belonging to the spinel group minerals characterized by the formula unit $[(Mg,Fe^{2+})(Al,Cr,Fe^{3+})_2O_4]$ (Haggerty, 1991; Paktunc and Cabri, 1995; Tathavakar et al., 2005). Though Cr can occur in 82 different minerals, chromite is the only source of new Cr units that can be exploited in commercial volumes (Motzer and Engineers, 2004). Approximately 90% of mined chromite is used in the production of various FeCr grades, of which high-carbon and charge grade FeCr is the most common (ICDA, 2013).

A recent review presented a synopsis of FeCr production processes utilized (Beukes et al., 2017). According to this review, FeCr is principally produced by (i) conventional open/semi-closed submerged arc furnaces (SAFs) that are mainly fed with lumpy (typically, 6mm ≤ size ≤ 150 mm) chromite ore, fluxes and reductants, (ii) closed SAFs that are fed with oxidative sintered chromite pellets, as well as lumpy reductants and fluxes, (iii) closed SAFs fed with pre-reduced chromite pellets, as well as lumpy reductants and fluxes, and (iv) closed direct current (DC) arc furnaces fed with fine (typically, size ≤ 6mm) chromite ore, fluxes and reductants (Beukes et al., 2017). Of particular interest in this paper is the oxidative sintered pellet production process, which is commercially known as the Outotec steel belt sintering process (https://www.outotec.com/products/sintering-and-pelletizing/steel-belt-sintering-plant/, accessed 24/10/2017) – process (ii) in the afore-mentioned text.

Various authors have previously described the oxidative sintered pellet production process (Riekkola-Vanhanen, 1999; Beukes et al., 2010; Basson and Daavittila, 2013). Chromite fines (typically, size ≤ 1mm) are wet milled together with a small percentage of a

carbonaceous material that serves as an energy source during sintering. The grain size specification that must be obtained during milling is typically a d_{80} of 74 µm (80% of the particles smaller than 74 µm). Ceramic filters are used to dewater the milled slurry to a moisture content of below 9%. A fine clay binder (usually refined bentonite) is then mixed into the afore-mentioned filter cake with a high intensity mixer, where after the moist mixture is pelletized in a pelletizing drum. Thereafter, newly formed pellets are screened on a roller screen. Oversized pellets are broken down and recycled, together with undersized pellets. This leads to rather homogeneously sized green pellets (not yet cured), with an average diameter of approximately 12 mm. The green pellets are then layered on a perforated steel conveyer, which carries the pellets through a multi-compartment sintering furnace. The perforated steel conveyer is protected against excessive temperatures by a layer of already sintered pellets that are placed between the green pellets and the conveyer. The temperature of the pellet bed gradually increases as it passes through the sintering furnace, to a maximum temperature of approximately 1400 to 1500 °C. Sintered pellets are then cooled by blowing air through the pellet bed from below. Thereafter, the sintered pellets are discharged and screened to remove <6 mm material, but smaller aperture screening has also been observed. The overall process produce porous and mechanically strong pellets suitable for SAF smelting, which results in improved SAF stability and metallurgical efficiency, as well as lower energy consumption if compared with conventional SAF smelting of lumpy ore.

The suppliers of the above-mentioned technology indicated that chromite containing dusts collected from the pellet sintering scrubber, and fines screened out from the sintered pellets can be re-introduced into the moist material mixture that is pelletized (Basson and Daavittila, 2013). However, it is specified that this addition must be limited to a maximum of 4 wt% of the total pellet composition, since it is believed to adversely affect pellet quality (Basson and Daavittila, 2013). The fundamental reason(s) behind this limitation is not

known from information available in the public peer reviewed domain. Additionally, at some FeCr producers the generation of pre-oxidised fines, originating from the sintering scrubber and screening of the sintered pellet, are in excess of what can be recycled according to the afore-mentioned 4 wt% limitation. This has resulted in the accumulation of pre-oxidised fine chromite stockpiles at these producers. It was even observed that some FeCr producers mixed the pre-oxidised fines with metallurgical grade chromite ore, which is then sold as normal ore. However, pre-oxidized chromite requires less energy to metallize if compared to normal chromite (Kapure et al., 2010). Additional oxidation of oxidative sintered pellets also result in less energy being required during reduction (Zhao and Hayes, 2010). Furthermore, pre-oxidation of chromite fines significantly improves pre-reduction (solid state reduction) of chromite (Kleynhans et al., 2016 and 2017). Considering these energy related benefits, the authors believe that all pre-oxidised fine chromite should be recycled on-site at FeCr producers. With this in mind, the possible recycling of pre-oxidized chromite fines into oxidative sintered pellets beyond the current limitation of 4 wt% pellet composition was investigated in this paper, considering both fundamental and practical aspects.

2. Materials and methods

2.1. Materials

A metallurgical grade chromite ore sample was received from a large FeCr producer in South Africa, which served as the case study ore in this investigation. Previously Glastonbury et al. (2015) presented a detailed characterization of this case study ore, therefore, such a characterization is not repeated here. In short, the ore contained by weight 44.19% Cr_2O_3, 24.68% FeO, 14.71% Al_2O_3, 10.31% MgO and 2.96% SiO_2, and had a Cr/Fe ratio of 1.58 (Glastonbury et al., 2015). This composition is representative of a typical South African metallurgical grade chromite ore (Cramer et al., 2004). Additionally, it has to be considered that a substantial fraction of chromite smelted outside South Africa, originate

from South Africa. In 2012 for instance, 28% of chromite ore consumed in the rest of the world originated from South Africa (Kleynhans et al., 2016). Therefore, the results generated from the case study ore is of international relevance.

A sample of chromite fines screened out from industrially produced sintered pellets was collected at a large FeCr producer in South Africa that applies the oxidative sintered pellet production process. In the rest of this paper, this material is referred to as "pre-oxidized chromite". Refined bentonite (binder) and coke fines (carbon fuel source), which were used to produce oxidative sintered pellets at the afore-mentioned FeCr producer, were also obtained.

2.2 Material preparation and pelletization

In this study, material intended for pelletization experiments was prepared by dry milling a 50 g mixture, consisting of 1.5 wt% coke, with chromite the balance, for 2 min in a Siebtechnik laboratory disc mill. Prior to milling, all materials were dried in an oven overnight at 75 °C to remove moisture, to enable accurate and repeatable batching of the mixtures. A tungsten carbide grinding chamber was used to avoid possible Fe contamination. This milling procedure ensured a particle size distribution similar to that applied industrially, i.e. d_{80} of 74 µm (Basson and Daavittila, 2013; Glastonbury et al., 2015). After milling, refined bentonite was added to the material to obtain a mixture with a composition of 97.52 wt% ore, 1.49 wt% coke, and 0.99 wt% bentonite. The pelletization mixture was thereafter vigorously blended for 15 minutes using a laboratory scale Eirich-type mixer. As-received pre-oxidized chromite was subsequently added to the pelletization mixture to obtain mixtures containing 4, 8, 16, 32, and 64 wt% pre-oxidized chromite. No additional coke or bentonite was added to these mixtures to compensate for the addition of pre-oxidized chromite, since this is also the industrial practise.

Green pellets containing the various percentages of pre-oxidized chromite were generated using a laboratory scale disc pelletizer. The laboratory disc pelletizer consisted of a 600 mm diameter flat steel disc with a 150 mm deep rim. The entire disc and rim were pressed from a single steel plate and the connection area between the disc and rim was rounded to limit material build-up. The pelletizer rotated at a speed of 40 rpm and a constant angle of 60° to the horizon was maintained in all experiments. Fine water spray was introduced to the mixture with a handheld spray bottle to initiate pellet nucleation, i.e. formation of micro pellets. Thereafter, the micro pellets were grown by continuously wetting the surface of the micro pellets with water spray and introducing dry pelletization mixture onto it, until the desired pellet diameter was achieved. Material build-up on the bottom, side and the pelletizer's corner (rounded steel plate between the disc and rim) were continuously loosened with a fit-for-purpose handheld scraper, to facilitate the inclusion of this material into the pellets. This scraper had a flat edge to remove material build-up from the disc and the rim, as well as a rounded point to remove material build-up from the corner. Pellets with a diameter of >11 and <13 mm were collected by screening. Care was taken to ensure consistent pellet moisture content, with all pellet used in further experiments containing 5.5 ± 0.7 wt% moisture. Pellet moisture contents were determined with an ADAM PMB 53 moisture balance. Green pellets were allowed to dry in an ambient atmosphere after collection, before oxidative sintering experiments proceeded.

2.3 Pellet oxidative sintering

As previously stated, Basson and Daavittila (2013) indicated that industrially produced oxidative sintered pellets are heated up to maximum temperatures of between 1400 to 1500 °C. Glastonbury et al. (2015) mimicked the afore-mentioned industrially applied process on laboratory scale, with a temperature profile that attained a maximum temperature of 1400 °C. However, the afore-mentioned authors did not verify how deep into the pellets

oxidation altered chromite grains. Zhao and Hayes (2010) proved that only the outer chromite grains of industrially produced oxidative sintered pellets are partially oxidised, while the chromite grains deeper into the pellets were not oxidised. Heat transfer to pellets in laboratory conditions, where small amounts of pellets are sintered in batches with highly effective furnaces, will be significantly superior to industrial furnaces, where very large quantities have to be treated continuously. Therefore, rather than blindly selecting a maximum sintering temperature, or applying the temperature profile used by Glastonbury et al. (2015) the authors tested various sintering temperatures. A Lenton Elite camber furnace (UK, Model BRF 15/5) with a programmable temperature controller was used for sintering. Prior to sintering, the pellets (in a 99.7% Al_2O_3 ceramic crucible) and furnace were pre-heated to 100 and 900°C, respectively. Once the pellets were placed in the furnace, the temperature was ramped from 900°C to the designated maximum temperature at a rate of approximately 17°C/min. Once the designated maximum temperature was reached, the pellets were removed from the furnace and allowed to cool in the ambient atmosphere.

2.4 Analytical techniques

Scanning electron microscopy (SEM) equipped with an energy dispersive x-ray soectrometer (EDS) was used to perform surface characterisation of the sintered pellets in secondary electron mode. An FEI Quanta 250 FEG SEM incorporating an Oxford X-map EDS system operating at 15 kV and a working distance of 10 mm was used. Pellets were split in half and mounted on aluminium stubs, or were set in resin and polished with a SS20 Spectrum System Grinder polisher before being mounted on the stubs. The polished resin-embedded samples were coated with carbon in an Emscope TB 500 carbon coater prior to SEM analysis. Resin embedded polished pellets were imaged in backscattered electron mode and un-embedded pellets in secondary electrons mode.

Crystalline phase analysis of bulk samples was performed by X-ray diffraction (XRD) using two methods; (1) using a Rigaku D/MAX 2500 rotating-anode powder diffractometer with Cu Kα radiation at 50 kV, 260 mA, a step-scan of 0.02º, and a scan rate at 1/min in 2h from 5 to 70º. Phase identification was performed using JADE v.3.9 with the ICDD and ICSD diffraction databases; and (2) Röntgen diffraction system (PW3040/60 X'Pert Pro) and a back loading preparation method to determine the crystalline phases, and percentage thereof, present in materials. The samples were scanned using X-rays generated by a copper (Cu) Ka X-ray tube. Measurements were carried out between variable divergence- and fixed-receiving slits. Phases were identified using X'PertHighscore plus software. Phase refinement was performed using the Rietveld method (Hill and Howard, 1987).

Further analysis was undertaken by mounting cross-sectioned polished pellets on glass slides and carbon-coating them, prior to electron microprobe analysis (EMPA). Analysis was performed using a JEOL JXA-8900 electron microprobe fitted with five wavelength dispersive spectrometers at an accelerating voltage of 20 kV and beam current of 26 nA.

2.5 *Pellet compressive strength and abrasion resistance*

Sintered pellets compressive strengths were determined using an Ametek Lloyd Instruments LRXplus 5 kN strength tester. NEXYGENPlus material test and data analysis software was used to capture and process the generated data, as well as to control and monitor all aspects of the system. The speed of the compression plates was kept to 10 mm/min during compressive strength tests to apply an increasing force on the prepared pellets. The maximum load to induce pellet breakage was recorded. Standard deviations were calculated based on 10 experimental repetitions.

The abrasion resistance apparatus used in this study was based on a downscaled version of the European standard EN 15051 rotating drum, as indicated by Schneider and

Jensen (2008). The same drum was utilized in previous studies (Kleynhans et al., 2012; Neizel et al., 2013; Glastonbury et al., 2015; Kleynhans et al., 2016). During each experiment, 10 sintered pellets were abraded at 40 rotations/min rotational speed for 64 minutes. The pellets were screened at various time intervals, i.e. 1, 2, 4, 8, 16, 32 and 64 min, using a sieve with an aperture of 6.5 mm. This aperture was chosen, since <6mm material is generally classified as fines, which has to be limited in SAF feed material (Basson and Daavittila, 2013). The oversized materials were weighed and returned to the drum, together with the fines, for further abrasion until the full abrasion time, i.e. 64 min, was reached.

3. Results and discussion

3.1 Mimicking the industrial applied oxidative sintering process

As previously stated, Zhao and Hayes (2010) showed that only the outer chromite grains of industrially produced oxidative sintered pellets are partially oxidized, whilst the grains deeper into the pellet cores remain un-oxidized. Therefore, it was critical to establish the maximum temperature for the proposed laboratory sintering profile (Section 2.3). Consequently, batches of pellets were cured with sintering profiles that had maximum temperatures from 1000 to 1500ºC. SEM examination of cross-section polished sintered pellets revealed that the outer chromite grains of pellets sintered at <1200ºC do not indicate signs of oxidation, while oxidation penetrated deep into pellets sintered at >1200 ºC. A sintering profile (Section 2.3) with a maximum temperature of 1200ºC was therefore applied within the context of this paper, to mimic the industrially applied oxidative sintered pellets process. Figure 1 presents backscattered electron micrographs of a cross-sectioned polished pellet containing 0 wt% pre-oxidized chromite, which was sintered at a maximum temperature of 1200ºC. As is evident from Figure 1, oxidation induced differences (alteration being indicated by the lighter greyscale patterns), were evident between the outer chromite

grains and grains toward the centre of the pellet (Figure 1a). The higher magnification micrograph of outer chromite grains (Figure 1b) clearly shows an oxidation induced altered phase that formed on the rim of such grains, while the chromite grains toward the pellet centre were unaffected (Figure 1c). Similar oxidation induced phase patterns have been observed during investigations of the thermal oxidative decomposition of chromite relevant to the formation of sodium chromate during soda-ash roasting (Tathavakar et al., 2005), pre-oxidation of chromite prior to direct reduction (Kapure et al., 2010), laboratory oxidative sintering of chromite pellets (Glastonbury et al., 2015) and industrially produced oxidative sintered chromite pellets (Zhao and Hayes, 2010).

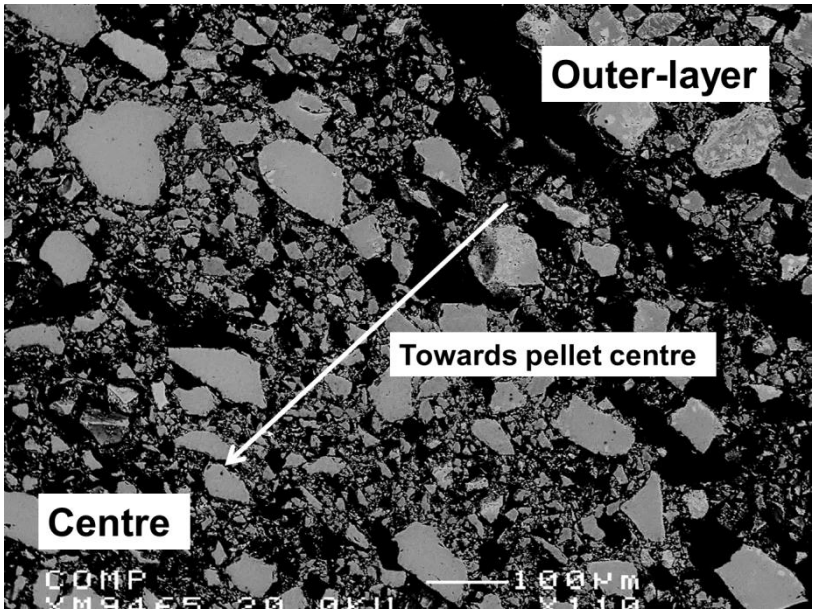

(a)

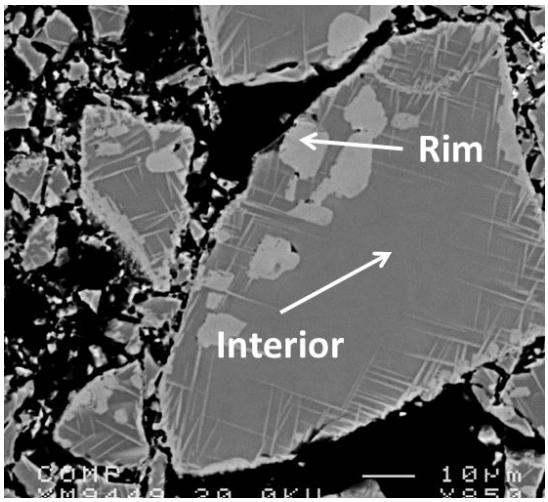

(b)

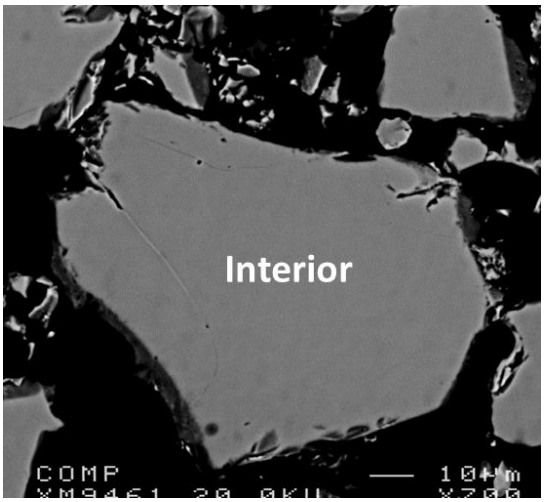

(c)

Figure 1: Backscattered electron (SEM) micrographs of a cross-sectioned and polished pellet containing 0 wt% pre-oxidized chromite sintered at a maximum temperature of 1200ºC. Oxidation induced differences (indicated by the lighter greyscale patterns) are evident between the outer chromite grains and grains toward the centre (a). These differences are better seen in the higher magnification images of the outer chromite grains (b) and grains toward the centre of the pellet (c).

3.2 Mechanism of chromite oxidation

In order to gain insight into the recycling of pre-oxidized chromite fines, it is vital to understand the mechanism(s) at play during the oxidative sintered pellet production process.

It was indicated in Figure 1 that oxidation induced alteration, which were indicated by lighter greyscale patterns in the SEM micrographs, were evident on the rims of the outer chromite grains of sintered pellets containing 0 wt% pre-oxidized chromite (Figure 1b). EMPA analysis was subsequently used to determine the chemical compositions of the transformation products, as indicated in Table 1. The areas analysed were indicated as "grain location" and "grain area" in Table 1, with "location" referring to the position of the chromite grain within the pellet (i.e. centre or outer-grains), and grain "area" referring to the zone within a specific grain (i.e. interior or rim of a specific grain, which was also indicated in Figure 1b). The Cr/Fe, and Mg/Fe elemental ratios, with Fe = (Fe^{2+} + Fe^{3+}), were also presented in Table 1.

Table 1: EMPA analysis (wt%) of different "Grain location" and "Grain areas", as well as Mg/Fe, and Cr/Fe ratios of the transformation products (chromite and M_2O_3 phase) in a sintered pellet (maximum temperature of 1200ºC) containing 0 wt% pre-oxidized chromite. Six to 10 analyses were conducted in similar locations and areas, with the averages thereof indicated.

Grain location	Grain area	wt%									Ratios	
		Cr_2O_3	Al_2O_3	FeO	Fe_2O_3	MgO	TiO_2	V_2O_3	MnO	NiO	Mg/ Fe	Cr/ Fe
Centre	Interior (chromite)	47.25	15.78	19.77	6.13	9.90	0.70	0.36	0.23	0.12	0.30	1.64
Outer-layer	Interior (chromite)	48.49	15.39	15.39	6.75	12.65	0.72	0.36	0.32	0.13	0.46	1.99
Outer-layer	Rim (M_2O_3 phase)	48.30	16.47	0.21	33.15	0.31	0.79	0.41	0.01	0.01	0.01	1.42

As is evident from Table 1, the grain interiors at the centre and outer-layer of the pellets had appreciable differences in the MgO and FeO contents, whereas no appreciable differences between trivalent cations (primarily Cr^{3+}, Al^{3+} and Fe^{3+}, indicated as Cr_2O_3, Al_2O_3 and Fe_2O_3, respectively) occupying the octahedral sites in chromite were observed. In contrast, relatively large differences in FeO, Fe_2O_3, and MgO contents were evident for grain interiors and rims located in the outer-layer of pellets.

Grain interiors in the centre of pellets had an MgO content of 9.90 wt%, compared to 12.65 wt% at the outer-layer. The FeO content of grain interiors at the centre and outer-layer of pellets were 19.77 and 15.93 wt%, respectively. Consequently, the Mg/Fe ratios for grain interiors at the pellet outer-layer were higher (0.46) than grains at the pellet centre (0.30). The Mg/Fe ratio difference of grain interiors as a function of location within the pellet was indicative of Mg^{2+}-enrichment at the expense of Fe^{2+} occurring in grains at the outer-layer. Fe^{2+} occupies the tetrahedral sites in normal (untreated) chromite spinel. High temperature oxidative treatment of chromite caused Fe^{2+} to oxidize and diffuse towards the grain rim, generating tetrahedral site vacancies within the particle interior. Vacancy formation occurs according to the following reaction (Lindsley, 1991; Tathavakar et al., 2005):

$$0.5\ O_2 \xrightarrow{T} O^{2-}{}_0 + V_{cat} + 2\ h \qquad (1)$$

where $O^{2-}{}_0$ represents oxygen anions on the cubic closed packed lattice, V_{cat} is the cation vacancies and *h* a "hole", respectively. Subsequently, these tetrahedral vacancies were filled by Mg^{2+} (originating from the particle rim) *via* a Mg-Fe exchange reaction, which resulted in the observed 0.31 wt% MgO content at the grain rim in the pellet outer-layer.

The above-mentioned Fe^{2+} that migrated to the grain rim in the pellet outer layer is subsequently oxidised to Fe^{3+}, or alternatively the Fe^{2+} is oxidised to Fe^{3+} which then migrate to the surface – currently it is impossible to say with certainty which occurs first. The generalized oxidative spinel phase decomposition is described by Reaction 2 (Alper, 1970; Tathavakar et al., 2005):

$$(A)[B]_2O_4 = (AO) + [B_2O_3] \qquad (2)$$

The decomposition products of chromite $(Mg,Fe)[Al,Cr,Fe]_2O_4$ at elevated temperatures would be FeO, MgO, Al_2O_3, Fe_2O_3 and Cr_2O_3. The chemical potentials for chromite decomposition (Reaction 2) are strongly dependent on the oxygen partial pressure and the chemical composition of chromite (Tathavakar et al., 2005). In the presence of

oxygen, Fe^{2+} will be oxidized to Fe^{3+} at sufficiently high temperatures. The afore-mentioned explains the decrease in FeO content of 15.39 to 0.21% and increase in Fe_2O_3 content of 6.75 to 33.15% at the grain interior and rim of the pellet outer layer, respectively. Ultimately, this results in the exsolution of a Fe_2O_3-rich sesquioxide phase along the chromite grain rims and cleavage planes, which was shown in Figure 1b and identified in Table 1. Such Widmänstatten intergrowth of sesquioxide phase (M_2O_3, with M representing a series of trivalent ions such as Cr^{3+}, Al^{3+}, and Fe^{3+}) during chromite oxidation have been identified by various authors (Tathavakar et al., 2005; Kapure et al., 2010; Zhao and Hayes, 2010; Glastonbury et al., 2015). It is believed that the sesquioxide Fe_2O_3 phase is initially present as metastable, intermediate maghemite (γ-Fe_2O_3) exsolved precipitate, which was formed by changing an ABC packing into an ABAB packing by dislocations along the (111) chromite spinel plane. The maghemite phase then decomposes to the more stable hematite (Fe_2O_3) phase at elevated temperatures (>600 ºC) in the presence of oxygen ($P_{O2} = 0.2$ atm) (Tathavakar et al., 2005; Pan et al., 2015). The presence of Al^{3+} cations increases the oxidative decomposition temperature as they can occupy vacancies present in the maghemite structure (Hellwege and Hellwege, 1970).

Furthermore, chromite oxidation resulted in Cr/Fe ratio variations at the grain interiors and rims as a function of grain location within the pellet. The un-oxidized chromite had a Cr/Fe ratio of 1.64, which correlated well with typical Cr/Fe ratios of South African chromite ore originating from the middle group 1 and 2 seams of the Bushveld Complex (Basson et al., 2007; Kleynhans, 2011). Chromite near the grain rim in the outer-layer of sintered pellets had a Cr/Fe ratio of 1.99 as opposed to 1.64 near the grain interior, which resulted from Fe diffusion from the grain interior towards the grain rim.

3.3 XRD characterization of pre-oxidized chromite fines

Quantitative Rietveld refined XRD analysis was performed on the as-received pre-oxidized chromite fines. These phases (indicated as a function of decreasing abundance) were chromite 39.9 wt%, chromian spinel 42.9 wt%, hematite 5.1 wt%, and enstatite 12.0 wt%. The chromite phase ($(Fe^{2+}_{0.50}Mg_{0.50})(Cr_{0.71}Al_{0.29})_2O_4$) represents residual chromite originating from the Bushveld Complex. The chromian spinel phase had the following stoichiometry, i.e. $(Mg_{0.540}Fe^{2+}_{0.416}Al_{0.041})(Cr_{1.202}Al_{0.674}Fe^{3+}_{0.088}Mg_{0.028})O_4$), which is a likely composition of chromite formed at 1200ºC in the presence of oxygen. Tathavakar et al. (2015) stated that South African chromite decomposes into two spinel phases upon heating, i.e. $(Mg_{1-x},Fe_x)(Cr_{1-y},Al_y)_2O_4$ and $(Fe_{1-a},Mg_a)(Cr_{1-b},Al_b)_2O_4$. The two observed chromite phases, i.e. chromite and chromian spinel, were in agreement with phases detected by Tathavakar et al. (2015). Furthermore, the detection of hematite (Fe_2O_3) indicated that free Fe_2O_3, which formed as described in Section 3.2, was present in the pre-oxidized chromite fines. The detected enstatite-phase likely originated from siliceous gangue minerals, clay that was added as a pellet binder, and ash from the coke (in-pellet carbon fuel source).

3.4. Pellet compressive and abrasion resistance strengths

If pre-oxidized chromite fines were to be recycled into oxidative sintered pellets beyond the current limitation of 4 wt% pellet composition (Basson and Daavittila, 2013), such pellets must be physically strong enough to prevent fines formation. Figure 2 and 3 present the cured compressive and abrasion resistance strengths of pellets containing 4, 8, 16, 32, and 64 wt% pre-oxidized chromite fines, compared to pellets containing 0 wt% pre-oxidized chromite fines (indicated by the y-axis).

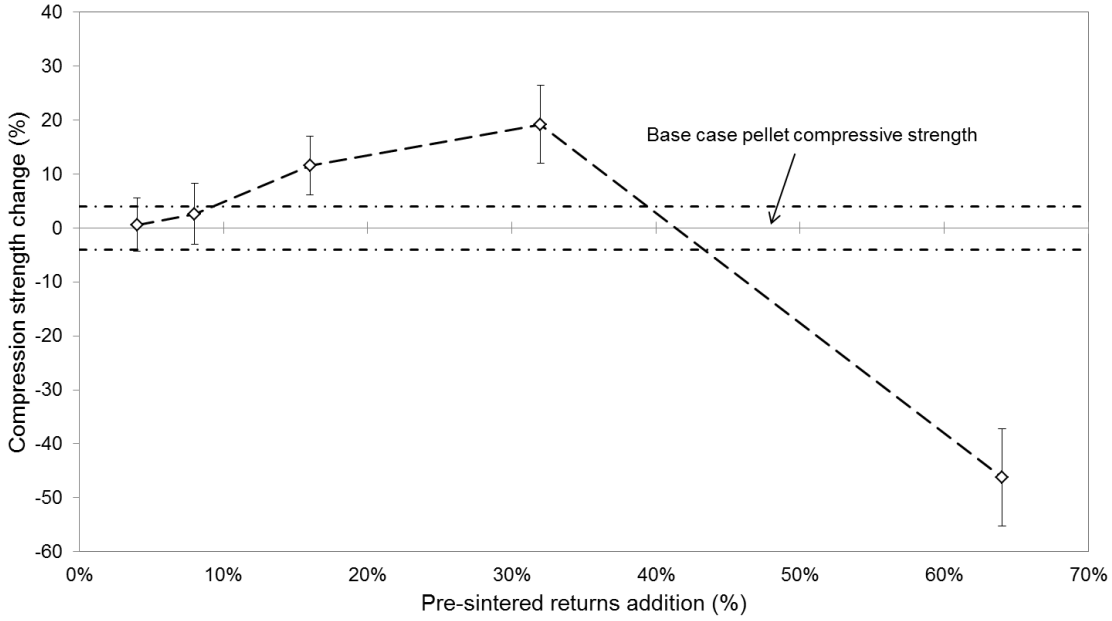

Figure 2: The effect of pre-oxidized chromite fines content on cured pellet compressive strength.

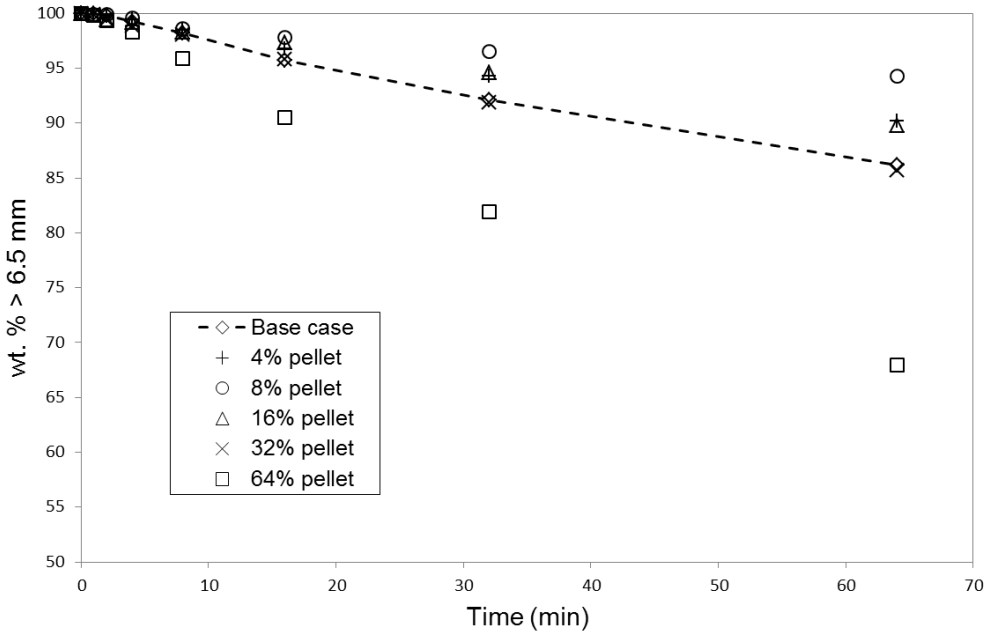

Figure 3: The effect of pre-oxidized chromite fines content on cured pellet abrasion strength.

From Figures 2 and 3, it is evident that pellet compressive and abrasion resistance strengths were the same, or improved if compared to the base case (0 wt% containing pre-oxidized chromite fines pellets), as the pre-oxidized chromite fines content increased from 4

to 32 wt% pellet composition. However, pellets containing 64 wt% pre-oxidized chromite fines were substantially weaker. It thus seems feasible to include up to 32 wt% pre-oxidized chromite fines in oxidative sintered pellet mixtures, without adversely affecting cured pellet strengths. However, it is unlikely that such large additions would ever be required.

There might be various reasons why the pre-oxidized chromite fines containing cured sintered pellets (at least up to 32 wt% containing pellets) were stronger than the base case (0 wt% containing pellets). However, the most obvious was that the pre-oxidized chromite fines containing cured sintered pellets had a larger proportion of the fine material, as is evident from Figures 4a and 4b. These fines, apparently filled inter-particle gaps and improved particle contact, which resulted in enhancement of the cured pellet strength. The reason for the presence of finer material in the pre-oxidized chromite fines can be related to the phase/chemical nature thereof. EMPA indicated that sesquioxide Fe_2O_3 phases were formed in outer-layer pellet chromite grains (Section 3.2, Table 1) during pellet oxidative sintering. Quantitative Rietveld refined XRD analysis even indicated the presence of hematite (Section 3.3) in the pre-oxidized chromite fines. It can be expected that the grains containing sesquioxide Fe_2O_3 phase included hematite will abrade relatively easily form cured sintered pellets, compared to un-oxidized chromite grains that were bonded together with clay. If recycled, these fragmented and/or whole grains present in the pre-oxidized chromite fines then acted to enhance cured pellet strength.

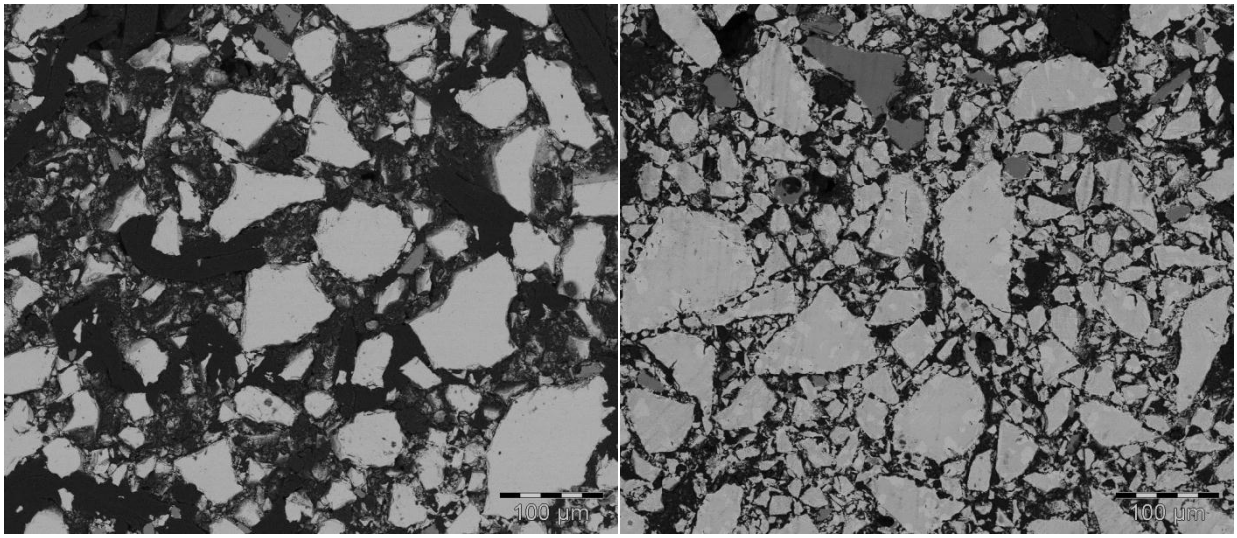

(a) (b)

Figure 4: Backscattered electron micrographs of a cross-sectioned cured pellet containing 0 wt% (a) and 32 wt% (b) pre-oxidized chromite fines.

In addition to the above-mentioned particle size related enhancement of cured pellet strength, particle surface morphology was also considered. Surface SEM micrographs of 0 and 16 wt% containing pre-oxidized chromite fines pellets, are presented in Figures 5a and 5b, respectively. The most notable difference in surface morphology was the enhanced inter-particle sintering of the pre-oxidized chromite fines containing cured pellet. This suggests that some additional degree of material melting occurred during sintering, probably due to the presence of pre-oxidized chromite fines. Obviously, this can at least in part be attributed to the better inter-particle contact and reduced inter-particle voids, but it was also important to investigate the chemical nature of the inter-particle bonding. SEM-EDS analyses of the areas indicated with the white blocks in Figures 5a and 5b indicated similar chemical compositions. This indicates that the siliceous gangue minerals, clay as the pellet binder, and ash from the coke (in-pellet carbon fuel source) contributed to binding the particles together via the formation of a molten phase. The presence of alumino-silicate type particles, which contribute to the formation of a molten phase that bind particles together, present in pre-

oxidized chromite fines were shown (Figure 6a and b). A SEM micrograph of a typical pre-oxidized chromite fines particle, while the white box in Figure 6b indicate the presence of a alumino-silicate type particle (SEM-EDS composition of 4.0 wt% Al, 8.0 wt% Si, 7.7 wt% Mg and 0.5 wt% Ca). Considering that the inter-particle bridges in the samples with and without the pre-oxidized chromite fines were compositionally similar, the difference in their responses can be attributed to the particle size distributions.

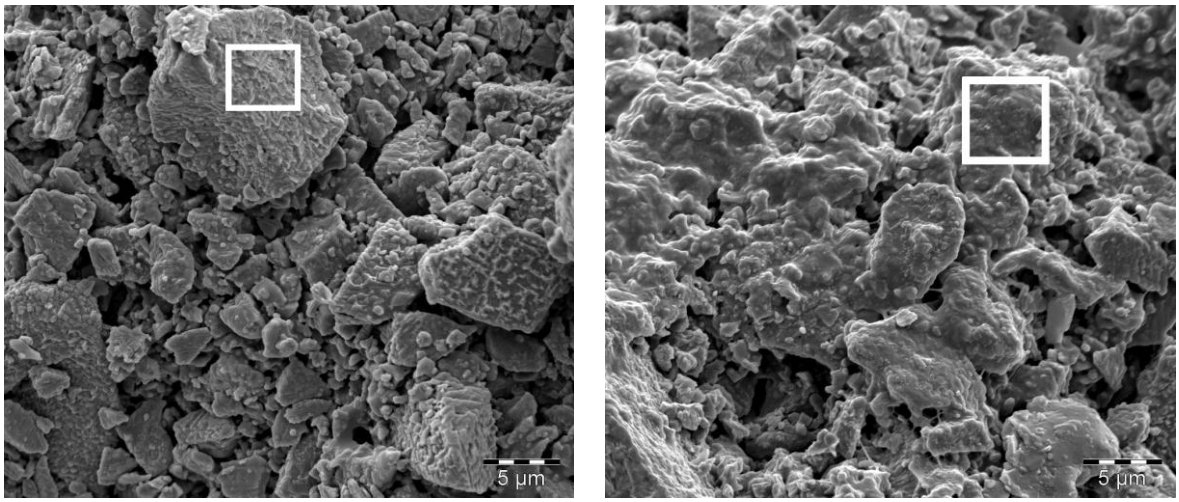

(a) (b)

Figure 5: Secondary electron SEM micrographs of the particle morphologies with surface features of 0 (a) and 16 wt% (b) pre-oxidized chromite fines containing pellets. The white boxes indicate areas analysed by SEM-EDS.

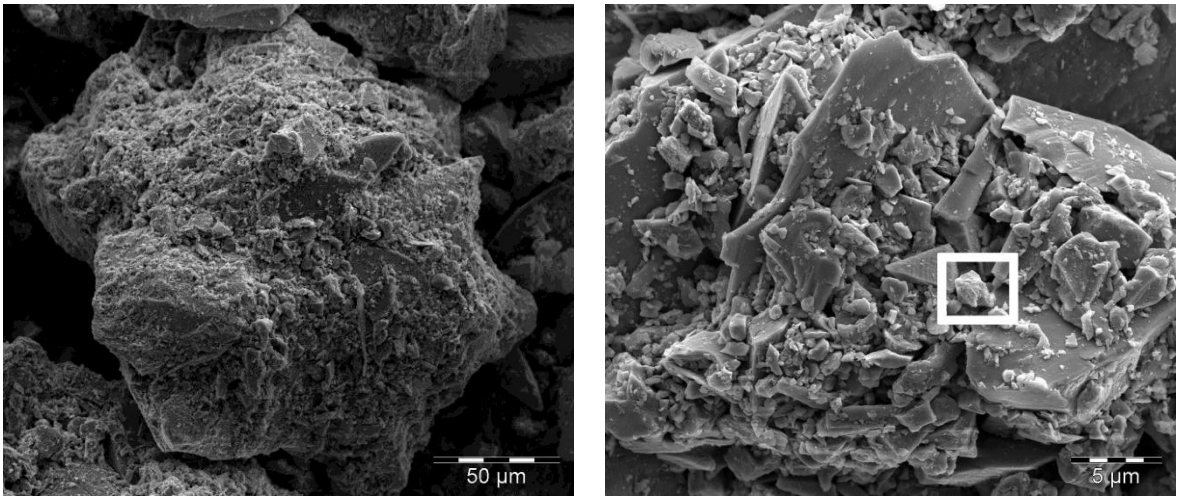

(a) (b)

Figure 6: Secondary electron SEM micrographs of a typical pre-oxidized chromite fines particle at two magnifications (a and b). The white box highlights an alumino-silicate particle that enables inter-particle binding due to the formation of molten phase.

4. Conclusions

The findings presented in this paper suggest that pre-oxidized chromite fines, originating from the oxidative pellet sintering scrubber, and fines screened out from oxidative sintered pellets may be re-introduced into the moist material mixture that is pelletized, in excess of the current 4 wt% limit indicated by the technology supplier (Basson and Daavittila, 2013). EMPA and quantitative XRD analysis verified the formation of Fe_2O_3-rich sesquioxide phases and/or liberated Fe_2O_3. Such phases will metalize at lower temperatures during smelting if compared to normal chromite; hence enhancing metallurgical efficiency and reducing electricity consumption. The authors therefore recommend that pre-oxidized chromite fines can be recycled in excess of the current 4 wt% limitation. Certain practical implications such as the crushing of oversized green pellets were not considered in this paper. Currently such pellets are crushed with a roller, before the moist material is re-fed to the pelletizing drum. It might be that this roller (which crushes the oversized green pellets) might be damaged by larger hard particles occurring in the pre-oxidized chromite fines.

However, this operational issue should be address to capitalize on the possible metallurgical and energy benefits associated re-cycling of pre-oxidized chromite fines.

Acknowledgements

The authors thank Mr Sarel Naude from the faculty of Mechanical Engineering for assistance provided during sample preparation. Thanks are also given to Derek Smith and Dominique Duguay at CANMET for XRD and electron microprobe analyses, respectively. The financial assistance of the National Research Foundation (NRF) towards the PhD study of SP du Preez (grant number: 101345) is hereby acknowledged. Opinions expressed and conclusions arrived at, are those of the authors and are not necessarily to be attributed to the NRF.

References

Alper, A.M. 1970. *High temperature oxides*, New York, Academic Press.

Basson, J., Curr, T., Gericke, W. South Africa's ferro alloys industry-present status and future outlook. Proceedings of the 11th International Ferro Alloys-Congress (INFACON XI). New Delhi, 2007. 3-24.

Basson, J., Daavittila, J. 2013. *High Carbon Ferrochrome Technology-Chapter 9*. In: Gasik, M. (ed.) Handbook of ferroalloys: theory and technology. United Kingdom: Elsivier. http://dx.doi.org/10.1016/B978-0-08-097753-9.00009-5

Beukes, J.P., Dawson, N.F., Van Zyl, P.G., 2010. Theoretical and practical aspects of Cr(VI) in the South African ferrochrome industry. The Journal of The Southern African Institute of Mining and Metallurgy 110, 743-750.

Beukes, J.P., Du Preez, S.P., Van Zyl, P.G., Paktunc, D., Fabritius, T., Päätalo, M., Cramer, M., 2017. Review of Cr (VI) environmental practices in the chromite mining and smelting industry–relevance to development of the Ring of Fire, Canada. Journal of Cleaner Production. https://doi.org/10.1016/j.jclepro.2017.07.176

Cramer, L.A., Basson, J., Nelson, L.R., 2004. The impact of platinum production from UG2 ore on ferrochrome production in South Africa. The Journal of The South African Institute of Mining and Metallurgy. 517-527.

Glastonbury, R.I., Beukes, J.P, Van Zyl, P.G, Sadikit, L.N, Jordaan, A., Campbell, Q.P, Stewart, H.M, Dawson, N.F, 2015. Comparison of physical properties of oxidative sintered pellets produced with UG2 or metallurgical-grade South African chromite: A case study. Journal of the Southern African Institute of Mining and Metallurgy. 115, 699-706. http://dx.doi.org/10.17159/2411-9717/2015/V115N8A6

Haggerty, S.E., 1991. Oxide mineralogy of the upper mantle. Reviews in Mineralogy and Geochemistry. 25, 355-416.

Hellwege, K.H., Hellwege, A.H., 1970. *Landolt–Bornsten Numerical Data and Functional Relation in Science and Technology*. Springer-Verlag. b52, a18-a20.

Hill, R., Howard, C., 1987. Quantitative phase analysis from neutron powder diffraction data using the Rietveld method. Journal of Applied Crystallography. 20, 467-474. https://doi.org/10.1107/S0021889887086199

ICDA 2013. *Statistical Bulletin 2013 Edition,* International Chromium Development Association, Paris, France.

Kapure, G., Tathavadkar, V., Rao, C., Rao, S., Raju, K. Coal based direct reduction of preoxidized chromite ore at high temperature. Proceedings of the 12th International Ferro-Alloys Congress (INFACON XII), 2010. 293-301.

Kleynhans, E.L.J., Beukes, J.P, Van Zyl, P.G, Fick, J.I.J., 2017. Techno-economic feasibility of a pre-oxidation process to enhance prereduction of chromite. Journal of the Southern African Institute of Mining and Metallurgy. 117, 457-468. http://dx.doi.org/10.17159/2411-9717/2017/v117n5a8

Kleynhans, E.L.J., Neizel, B.W., Beukes, J.P., Van Zyl, P.G., 2016. Utilisation of pre-oxidised ore in the pelletised chromite pre-reduction process. Minerals Engineering. 92, 114-124. https://doi.org/10.1016/j.mineng.2016.03.005

Kleynhans, E.L.J., 2011. Unique challenges of clay binders in a pelletised chromite pre-reduction process – a case study. Potchefstroom: North-West University (Dissertation - MSc.). 25.

Kleynhans, E.L.J., Beukes, J.P., Van Zyl, P.G., Kestens, P.H.I., Langa, J.M., 2012. Unique challenges of clay binders in a pelletised chromite pre-reduction process. Minerals Engineering. 34, 55-62. https://doi.org/10.1016/j.mineng.2012.03.021

Lindsley, D., 1991. Reviews in Mineralogy and Geochemistry. 25, 69-106.

Motzer, W.E., Engineers, T., 2004. Chemistry, geochemistry, and geology of chromium and chromium compounds, in: Guetin, J., Jacobs, J.A, Avakian, C.P. (Eds), Chromium(VI) Handbook, CRC Press, USA, pp. 23-91. ISBN 1-56670-608-4.

Neizel, B.W., Beukes, J.P, Van Zyl, P.G, Dawson, N.F., 2013. Why is CaCO 3 not used as an additive in the pelletised chromite pre-reduction process? Minerals Engineering. 45, 115-120.

Paktunc, A.D, Cabri, L., 1995. A proton-and electron-microprobe study of gallium, nickel and zinc distribution in chromian spinel. Lithos. 35, 261-282. https://doi.org/10.1016/j.mineng.2013.02.015

Pan, J., Yang, C., Zhu, D., 2015. Solid State Reduction of Preoxidized Chromite-iron Ore Pellets by Coal. ISIJ International. 55, 727-735. http://doi.org/10.2355/isijinternational.55.727

Riekkola-Vanhanen, M. 1999. Finnish expert report on best available techniques in ferrochromium production. Helsinki. ISSN 1238-7312

Schneider, T., Jensen, K.A., 2008. Combined single-drop and rotating drum dustiness test of fine to nanosize powders using a small drum. Annals of Occupational Hygiene. 52, 23-34. https://doi.org/10.1093/annhyg/mem059

Tathavakar, V.D., Antony, M., Jha, A., 2005. The physical chemistry of thermal decomposition of South African chromite minerals. Metallurgical and Materials Transactions B. 36, 75-84. https://doi.org/10.1007/s11663-005-0008-1

Zhao, B., Hayes, P. Effects of oxidation on the microstructure and reduction of chromite pellets. Proceedings of 12th International Ferro Alloys Congress (INFACON XII), 2010. 263-273.

CHAPTER 6: CONCLUSIONS AND PROJECT EVALUATION

The project evaluation is presented in Section 6.1. Therein the project is evaluated against the general aims and specific objectives, as presented in Chapter 1, Section 1.2. The main conclusions from the results are also discussed. Additionally, future prospectives for continued research is presented in Section 6.2.

6.1 Project evaluation and main conclusions

In order to do a self-evaluation, the candidate evaluated the study against the objectives that were set in Chapter 1. The points listed below correlate with the objectives set in Section 1.2. Main conclusions drawn from the results presented in each of the results chapters (Chapter 3, 4, and 5) are also briefly discussed.

a) Objective 1: Determine the solubility of Cr(VI) present in bag filter dusts (BFDs) as a function of solution pH, and possibly speciate the respective compounds. Ultimately, the efficiency of currently applied Cr(VI) treatment of BFD will be assessed.

Previous literature only indicated the leachability of Cr(VI) compounds present in BFDs in neutral and acidic aqueous phases, without considering the leachability thereof in a ultra-basic buffered aqueous phase (which is required to leach water-insoluble Cr(VI) compounds). Therefore, the leachability of Cr(VI) compounds present in four BFD samples were determined as a function of leach solution pH.

It was observed that the leach solution pH did not appreciable affect Cr(VI) solubilization at pH $\leq$ 9. The solubility of Cr(VI) compounds were categorized according to solubility, i.e. water-soluble, sparingly water-soluble, and water-insoluble, using buffers, as specified in literature. It was determined that

approximately 31 and 34% of the total Cr(VI) was present as a water-soluble and sparingly water-soluble compounds, respectively. Thus, the remaining approximate 35% of Cr(VI) is present as water-insoluble Cr(VI) compounds. The presences of substantial fractions of sparingly water-soluble and water-insoluble Cr(VI) compounds contradict the general perception that the total Cr(VI) extraction from BFDs can be achieved by neutral or acidic aqueous solutions. The pH of process water (e.g. water used to leach BFD) of FeCr producers typically varies from 6.2 to 9.0. Thus, in practice, only approximately 31% (the water-soluble Cr(VI) fraction) of the total Cr(VI) is leached form BFDs. The water-soluble fraction was speciated by X-ray absorption spectroscopy (XAS), indicating that Cr present therein was dominated by Cr(VI) species. Obtained spectra showed strong similarities to the spectrum of Na_2CrO_4. However, this did not necessarily imply that Na_2CrO_4 was the sole source of Cr(VI) present in the water-soluble fraction.

It was concluded that the currently applied Cr(VI) extraction procedures applied by industry does not effectively extract the total Cr(VI) content from BFDs, and that only the water-soluble (approximately 31%) fraction is extracted. In order to solubilize the sparingly water-soluble fraction, an extraction solution with a pH of 13 would be required. However, it is highly unlikely that such a high process-water pH would be economically feasible. Additionally, it is well known from literature that Fe(II), currently the most commonly employed chemical reductant of Cr(VI), oxidizes rapidly with dissolved oxygen at such high pH levels.

b) Objective 2: Test if it will not be possible to store thermal energy generated by CO-rich off-gas combustion as chemical energy, which can be used in the FeCr production process. Specifically it was evaluated if under-sized (too fine for SAF smelting) quartz (that is used as a flux) can be carbothermically treated with

under-sized anthracite to produce silicon carbide (SiC) within the temperature range achievable by closed SAF CO-rich off-gas combustion. Various authors have previously proven that SiC can be used as a reductant during chromite smelting. SiC formation will be investigated as a function of temperature required to convert quartz to SiC, as well as quartz and anthracite particle size. The reaction mechanism will also be considered and the possible on-site industrial application of such a process will be considered.

The formation of SiC from quartz is an energy intensive reaction and will require a large amount of heat from the combustion of the intended fuel source, i.e. CO-rich off-gas. The ΔG° for the carbothermic treatment of quartz (source of SiO_2) with anthracite (source of C) will reach equilibrium at approximately 1540°C. The off-gas composition will determine the combustion temperature. Typically, closed SAF off-gas consists of 60-90% CO, 10-40% CO_2, 2-7% N_2, and 2-10% H_2. The off-gas achievable combustion temperature was calculated using the thermodynamic modelling software package HSC Chemistry. It was determined that an off-gas composition of 60% CO and 40% CO_2, which is at the low end of the CO composition of off-gas, will burn at an adiabatic flame temperature of approximately 1790°C. Therefore, the temperatures that could be attained by off-gas combustion will be sufficient to sustain, or even surpass, the temperature required for SiC formation. Considering instrumental limitations, a maximum temperature of 1600°C was selected for all experiments. Furthermore, the intended CO-rich off-gas combustion will require air as an oxidizer, which will result in large volumes of nitrogen (N_2) being introduced into the process. Consequently, experiments were mainly conducted in a N_2 atmosphere.

Under-sized quartz and anthracite (both partially classified as wastes) were obtained from a large FeCr producer. To evaluate the effects of particle size on SiC formation, samples were prepared by two different methods, i.e. size partitioning and milling.

Size partitioned experiments were performed by carbothermically treating increasingly larger quartz with anthracite fines, and *vice versa*. The Si-products obtained after experimental work were unreacted SiO_2, Si_3N_4 (which was an unwanted product) and SiC. SiC yields did not exceed 82%, and in some cases, relatively large Si_3N_4 amounts were formed (34.9%).

Quartz and anthracite milled together for 10, 20, and 30 seconds had >98% SiC yields, and ≤1.4% Si_3N_4 yields. The effects of reaction temperature on a mixture with d_{90} (equivalent particle sizes (µm) of which 90% are finer) of 350.9 µm were determined by heat treatment at 1400, 1450, and 1500°C. A lower reaction temperature (1400°C) favoured Si_3N_4 as the primary Si-compound product. Increasing the reaction decreased Si_3N_4 formation and an increased SiC formation. At 1600°C almost only SiC (>98% SiC yield) was formed.

In order to test conditions that would be more realistic for industrial application, carbothermic treatment of the mixture with d_{90} of 350.9 µm was performed in an ambient atmosphere (i.e. air). The sample was placed in a crucible and enclosed with a crucible lid, which did not fit airtight on the crucible. Similar heat treatment, as applied to samples investigated in N_2 atmosphere was applied, yielding SiC and Si_3N_4 yields of 97.7% and 2.3% Si_3N_4, respectively. This indicated that it might be possible to apply this process in the real world, i.e. in the presence of oxygen.

c) Objective 3: Determine the effect of under-sized pre-oxidized material inclusion as a pellet constituent on pellet mechanical properties, i.e. compressive strength and abrasion resistance. Furthermore, the reasons (mechanism) behind the observations will be investigated.

Under-sized (screened out) pre-oxidized material was obtained from a large FeCr producer. To determine the effects of including under-sized pre-oxidized material in oxidative sintered pellet mixtures, pellets were prepared similarly to the industrial process.

Literature indicted that industrially produced oxidative sintered pellets primarily underwent oxidation at the pellet outer-layer, whilst the pellet centre remained relatively un-oxidized. The latter mentioned oxidation pattern was mimicked by sintering pellets at 1200°C.

The compressive and abrasion resistance strengths of pellets containing 4 and 8 wt% pre-oxidized materials were similar to pellets containing no pre-oxidized material (the base case), and pellets containing 16 and 32 wt% pre-oxidized materials had increased strengths compared to the base case. Further increasing the pre-oxidized material content to 64% drastically decreased pellet strengths.

The observed increased mechanical properties (compressive strength and abrasion resistance) were ascribed to the inclusion of fine particles originating from the under-sized pre-oxidized material. These particles filled the voids/gaps between larger chromite particles, promoting intimate inter-particle contact. Thus, the bonds between particles, caused by molten alumina silicates (from the gangue minerals, clay binder and ash from the carbon fuel source that was included in the pellet) were increased, due to the intimate inter-particle contact.

Metallurgical, the inclusion of larger fractions of recycled pre-oxidized chromite fines should be beneficial, since pre-oxidised chromite require less energy to reduce/metallize if compared to normal (un-oxidized) chromite.

6.2 Future prospects

The ineffectiveness of the currently applied Cr(VI) extraction from BFDs process was demonstrated in this study. It was indicated that approximately 69% of the total Cr(VI) content remains within BFDs, after Cr(VI) extraction was applied. It was also found that a pH $\geq$ 13 would be required to solubilize the sparingly water-soluble Cr(VI) content present in BFDs. It is therefore suggested to investigate if the use of such a high pH extraction would be feasible in practice, and to evaluate if the currently applied Cr(VI) reducing agent (i.e. ferrous sulphate or chloride) would still be effective, considering Fe(II) oxidation kinetics at such a high pH. Speciation of the sparingly water-soluble and water-insoluble Cr(VI) compounds present in BFDs should also be undertaken. This information will help formulate better Cr(VI) extraction and treatment processes.

It was determined that SiC could be produced from the carbothermic treatment of fine quartz using a laboratory scale furnace. Since the proposed heat source is CO-rich off-gas combustion, it would be prudent to test this process on a pilot scale, using CO(g) combustion as a the heat source. Another important future prospect would be to determine the effectiveness of the as-formed SiC (formed during carbothermic treatment of fine quartz) as a chromite reductant.

It was proven that up to 32 wt% pre-oxidized chromite fines, originating from the oxidative pellet sintering plant scrubbers and fines screened out from oxidative sintered pellets, can be included as a pellet constituent. Therefore, an important future prospect would be to test increased pre-oxidized chromite fines content in oxidative sintered pellets on an industrial

scale (i.e. at a FeCr smelter applying this process). It would also be important to assess if the proposed energy benefits associated with increased recycling of pre-oxidized chromite fines is realized.

BIBLIOGRAPHY

Abbasi, S., Soni, R., 1983. Stress-induced enhancement of reproduction in earthworm octochaetus pattoni exposed to chromium (vi) and mercury (ii)—implications in environmental management. International Journal of Environmental Studies. 22, 43-47.

Abubakre, O., Muriana, R., Nwokike, P., 2007. Characterization and beneficiation of Anka chromite ore using magnetic separation process. Journal of Minerals and Materials Characterization and Engineering. 6, 143.

Apte, A.D., Tare, V., Bose, P., 2006. Extent of oxidation of Cr(III) to Cr(VI) under various conditions pertaining to natural environment. Journal of Hazardous Materials. 128, 164-174.

Apte, A.D., Verma, S., Tare, V., Bose, P., 2005. Oxidation of Cr(III) in tannery sludge to Cr(VI): Field observations and theoretical assessment. Journal of Hazardous Materials. 121, 215-222.

Ashley, K., Howe, A.M., Demange, M., Nygren, O., 2003. Sampling and analysis considerations for the determination of hexavalent chromium in workplace air. Journal of Environmental Monitoring. 5, 707-716.

Bartlett, R.J., 1991. Chromium cycling in soils and water: links, gaps, and methods. Environmental Health Perspectives. 92, 17.

Basson, J., Curr, T., Gericke, W. South Africa's ferro alloys industry-present status and future outlook. The Eleventh International Ferro Alloys Congress. New Delhi, 2007. 3-24.

Basson, J., Daavittila, J. 2013. High Carbon Ferrochrome Technology-Chapter 9. In: Gasik, M. (ed.) Handbook of ferroalloys: theory and technology. United Kingdom: Elsivier.

Barnes, A., Muinonen, M., Lavigne, M.J. 2015. Reducing energy consumption by alternative processing routes to produce ferrochromium alloys from chromite ore. Paper presented at The Conference of Metallurgists.

Beaumont, J.J., Sedman, R.M., Reynolds, S.D., Sherman, C.D., Li, L.-H., Howd, R.A., Sandy, M.S., Zeise, L., Alexeeff, G.V., 2008. Cancer mortality in a Chinese population exposed to hexavalent chromium in drinking water. Epidemiology. 19, 12-23.

Beaver, L.M., Stemmy, E.J., Constant, S.L., Schwartz, A., Little, L.G., Gigley, J.P., Chun, G., Sugden, K.D., Ceryak, S.M., Patierno, S.R., 2009. Lung injury, inflammation and Akt signaling following inhalation of particulate hexavalent chromium. Toxicology and applied pharmacology. 235, 47-56.

Berner, T.O., Murphy, M.M., Slesinski, R., 2004. Determining the safety of chromium tripicolinate for addition to foods as a nutrient supplement. Food and Chemical Toxicology. 42, 1029-1042.

Beukes, J.P., Dawson, N.F., Van Zyl, P.G., 2010. Theoretical and practical aspects of Cr(VI) in the South African ferrochrome industry. The Journal of The Southern African Institute of Mining and Metallurgy 110, 743-750.

Beukes, J.P., Du Preez, S.P., Van Zyl, P.G., Paktunc, D., Fabritius, T., Päätalo, M., Cramer, M., 2017. Review of Cr (VI) environmental practices in the chromite mining and smelting industry–relevance to development of the Ring of Fire, Canada. Journal of Cleaner Production.

Beukes, J.P., Pienaar, J.J., Lachmann, G., 2000. The reduction of hexavalent chromium by sulphite in wastewater - An explanation of the observed reactivity pattern. Water SA. 26, 393-396.

Beukes, J.P., Pienaar, J.J., Lachmann, G., Giesekke, E.W., 1999. The reduction of haxavalent chromium by sulphite in wastewater. Water SA. 25, 363-370.

Beukes, J.P., Van Zyl, P.G., Ras, M., 2012. Treatment of Cr(VI)-containing wastes in the South African ferrochrome industry – A review of currently applied methods. The Journal of The Southern African Institute of Mining and Metallurgy. 112, 347-352.

Bielicka, A., Bojanowska, I., Wisniewski, A., 2005. Two Faces of Chromium - Pollutant and Bioelement. Polish Journal of Environmental Studies. 14, 5-10.

Bollinger, J.E., Bundy, K., Anderson, M.B., Millet, L., Preslan, J.E., Jolibois, L., Chen, H.-L., Kamath, B., George, W.J., 1997. Bioaccumulation of chromium in red swamp crayfish (Procambarus clarkii). Journal of Hazardous Materials. 54, 1-13.

Bulut, V.N., Ozdes, D., Bekircan, O., Gundogdu, A., Duran, C., Soylak, M., 2009. Carrier element-free coprecipitation (CEFC) method for the separation, preconcentration and speciation of chromium using an isatin derivative. Analytica chimica acta. 632, 35-41.

Cawthorn, R.G., 2010. The Platinum Group Element Deposits of the Bushveld Complex in South Africa. Platinum Metals Rev. 54, 205-215.

Cervantes, C., Campos-García, J., Devars, S., Gutiérrez-Corona, F., Loza-Tavera, H., Torres-Guzmán, J.C., Moreno-Sánchez, R., 2001. Interactions of chromium with microorganisms and plants. FEMS microbiology reviews. 25, 335-347.

Chang, D., Chen, T., Liu, H., Xi, Y., Qing, C., Xie, Q., Frost, R.L., 2014. A new approach to prepare ZVI and its application in removal of Cr (VI) from aqueous solution. Chemical Engineering Journal. 244, 264-272.

Cramer, L.A., Basson, J., Nelson, L.R., 2004. The impact of platinum production from UG2 ore on ferrochrome production in South Africa. The Journal of The South African Institute of Mining and Metallurgy. 517-527.

Creamer, M. 2013. South Africa's raw chrome exports soar as ferrochrome edge is lost [Online]. Creamer Media Editor. [Accessed 13 September 2017].

Cui, H., Fu, M., Yu, S., Wang, M.K., 2011. Reduction and removal of Cr(VI) from aqueous solutions using modified byproducts of beer production. Journal of Hazardous Materials. 186, 1625-1631.

Curr, T. The history of DC arc furnace process development. 2009. Mintek.

Darrie, G., 2001. Commercial Extraction Technology and Process Waste Disposal in the Manufacture of Chromium chemicals From Ore. Environmental Geochemistry & Health. 23, 187-193.

Demir, O. 2001. Ferroalloy production.

Denton, G., Bennie, J., De Jong, A. An improved DC-arc process for chromite smelting. Proceedings of the 10th International Ferro-Alloys Congress (INFACON X), 2004. 4.

Dhal, B., Thatoi, H.N., Das, N.N., Pandey, B.D., 2013a. Chemical and microbial remediation of hexavalent chromium from contaminated soil and mining/metallurgical solid waste: A review. Journal of Hazardous Materials. 250–251, 272-291.

Dhal, B., Das, N.N., Thatoi, H.N., Pandey, B.D., 2013b. Characterizing toxic Cr(VI) contamination in chromite mine overburden dump and its bacterial remediation. Journal of Hazardous Materials. 260, 141-149.

Dhal, B., Thatoi, H., Das, N., Pandey, B.D., 2010. Reduction of hexavalent chromium by Bacillus sp. isolated from chromite mine soils and characterization of reduced product. Journal of chemical technology and biotechnology. 85, 1471-1479.

Dong, X., Ma, L.Q., Gress, J., Harris, W., Li, Y., 2014. Enhanced Cr(VI) reduction and As(III) oxidation in ice phase: Important role of dissolved organic matter from biochar. Journal of Hazardous Materials. 267, 62-70.

Dos Santos, M. Meeting the challenge of sustainability through technology development and integration in ferroalloy submerged arc furnace plant design. Proceedings of 12th International Ferroalloys Conference/Sustainable Future, 2010. 71-80.

Døssing, L.N., Dideriksen, K., Stipp, S.L.S., Frei, R., 2011. Reduction of hexavalent chromium by ferrous iron: A process of chromium isotope fractionation and its relevance to natural environments. Chemical Geology. 285, 157-166.

Downing, J.H., Deeley, P.H., Fichte, R.M. 1986. Chromium and chromium alloys. In: Ullmans Encyclopedia of industrial chemistry. Germany: VCH: Verlagsgeschellschaft mbH.

Du Preez, S.P., Beukes, J.P., Van Dalen, W.P.J., Van Zyl, P.G., Paktunc, D., Loock-Hatting, M.M., 2017. Aqueous solubility of Cr(VI) compounds in ferrochrome bag filter dust and the implications thereof. Water SA. 43, 298-309.

Du Preez, S.P., Beukes, J.P., Van Zyl, P.G., 2015. Cr (VI) Generation During Flaring of CO-Rich Off-Gas from Closed Ferrochromium Submerged Arc Furnaces. Metallurgical and Materials Transactions B. 46, 1002-1010.

Dubey, C., Sahoo, B., Nayak, N., 2001. Chromium (VI) in waters in parts of Sukinda chromite valley and health hazards, Orissa, India. Bulletin of environmental contamination and toxicology. 67, 541-548.

Dwarapudi, S., Tathavadkar, V., Rao, B.C., Kumar, T.S., Ghosh, T.K., Denys, M., 2013. Development of cold bonded chromite pellets for ferrochrome production in submerged arc furnace. ISIJ international. 53, 9-17.

Eary, L., Rai, D., 1988. Chromate removal from aqueous wastes by reduction with ferrous ion. Environmental Science & Technology. 22, 972-977.

Eary, L.E., Davis, A., 2007. Geochemistry of an acidic chromium sulfate plume. Applied Geochemistry. 22, 357-369.

Eksteen, J., Frank, S., Reuter, M., 2002. Dynamic structures in variance based data reconciliation adjustments for a chromite smelting furnace. Minerals Engineering. 15, 931-943.

El-Shazly, A.H., Mubarak, A.A., Konsowa, A.H., 2005. Hexavalent chromium reduction using a fixed bed of scrap bearing iron spheres. Desalination. 185, 307-316.

Emsley, J. 2011. Nature's building blocks: an AZ guide to the elements, Oxford University Press.

Fendorf, S.E., 1995. Surface reactions of chromium in soils and waters. Geoderma. 67, 55-71.

Ferreira, M.J., Almeida, M.F., Pinto, T., 1999. Influence of temperature and holding time on hexavalent chromium formation during leather combustion. Society of Leather Technologists and Chemists. 83, 135-138.

Fowkes, K. 2014. Is there a limit to the market share of South African chrome units? [Online]. [Accessed 28 November 2017].

Gediga, J., Russ, M., 2007. Life cycle inventory (LCI) update of primary ferrochrome production. ICDA (International Chromium Development Association).

Gericke, W.A. Environmental aspects of ferrochrome production. Proceedings of the 7th International Ferro-alloys Congress (INFACON VII), 1995. 131-140.

Glastonbury, R.I., Beukes, J., Van Zyl, P., Sadikit, L., Jordaan, A., Campbell, Q., Stewart, H., Dawson, N., 2015. Comparison of physical properties of oxidative sintered pellets produced with UG2 or metallurgical-grade South African chromite: A case study. Journal of the Southern African Institute of Mining and Metallurgy. 115, 699-706.

Glastonbury, R.I., Van Der Merwe, W., Beukes, J.P., Van Zyl, P.G., Lachmann, G., Steenkamp, C.J.H., Dawson, N.F., Steward, H.M., 2010. Cr(VI) generation during sample preparation of solid samples – A chromite ore case study. Water SA. 36, 105-110.

Godgul, G., Sahu, K., 1995. Chromium contamination from chromite mine. Environmental Geology. 25, 251-257.

Gu, F., Wills, B.A. 1988. Chromite mineralogy and processing. Minerals Engineering. 1, 235-240.

Guertin, J., 2005. Toxicity and health effects of chromium (all oxidation states). Chromium (VI) handbook. 215-234.

Gupta, S., Yadav, A., Verma, N., 2017. Simultaneous Cr(VI) reduction and bioelectricity generation using microbial fuel cell based on alumina-nickel nanoparticles-dispersed carbon nanofiber electrode. Chemical Engineering Journal. 307, 729-738.

Haggerty, S.E., 1991. Oxide mineralogy of the upper mantle. Reviews in Mineralogy and Geochemistry. 25, 355-416.

Hall, D., Donaldson, K., Mcallister, J., Marrs, T., Ross, J.A., Anderson, D., Baker, D., Chen, L.-C., Baxter, P.J., Murray, V. 2015. Toxicology, Survival and Health Hazards of Combustion Products, Royal Society of Chemistry.

Hesketh, H.E., 1973. Atomization and cloud behaviour in venturi scrubbing. Journal of the Air Pollution Control Association. 23, 600-604.

Hininger, I., Benaraba, R., Osman, M., Faure, H., Roussel, A.M., Anderson, R.A., 2007. Safety of trivalent chromium complexes: no evidence for DNA damage in human HaCaT keratinocytes. Free Radical Biology and Medicine. 42, 1759-1765.

Howat, D.D., 1994. Chromium in South Africa. Journal of the South African Institute of Mining and Metallurgy. 86, 37-50.

Hutchinson, T.H., Williams, T.D., Eales, G.J., 1994. Toxicity of cadmium, hexavalent chromium and copper to marine fish larvae (Cyprinodon variegatus) and copepods (Tisbe battagliai). Marine Environmental Research. 38, 275-290.

IARC, 2012. International Agency for Research on Cancer. Agents Classified by the IARC Monographs. 100, 147-167.

ICDA 2013a. Chrome ore - Global overview of the chrome ore market. Paris, France. International Chromium Development Association.

ICDA 2013b. Ferrochrome. International Chromium Development Association.

ICDA 2013c. Statistical Bulletin, Paris, France. International Chromium Development Association.

Jin, R., Liu, Y., Liu, G., Tian, T., Qiao, S., Zhou, J., 2017. Characterization of Product and Potential Mechanism of Cr(VI) Reduction by Anaerobic Activated Sludge in a Sequencing Batch Reactor. Scientific Reports. 7, 1681.

Jones, D.L., Darrah, P.R., 1994. Role of root derived organic acids in the mobilization of nutrients from the rhizosphere. Plant and soil. 166, 247-257.

Jones, R. 2011. Pyrometallurgy in Southern Africa.

Kamolpornwijit, W., Meegoda, J.N., Hu, Z., 2007. Characterization of Chromite Ore Processing Residue. Practice Periodical of Hazardous, Toxic, and Radioactive Waste Management. 11, 234-239.

Kapure, G., Tathavadkar, V., Rao, C., Rao, S., Raju, K. Coal based direct reduction of preoxidized chromite ore at high temperature. Proceedings of the 12th International Ferro-Alloys Congress (INFACON XII), 2010. 293-301.

Kassem, T.S., 2010. Kinetics and thermodynamic treatments of the reduction of hexavalent to trivalent chromium in presence of organic sulphide compounds. Desalination. 258, 206-218.

Kimbrough, D.E., Cohen, Y., Winer, A.M., Creelman, L., Mabuni, C., 1999. A critical assessment of chromium in the environment. Critical reviews in environmental science and technology. 29, 1-46.

Kleynhans, E., Beukes, J., Van Zyl, P., Fick, J., 2017. Techno-economic feasibility of a pre-oxidation process to enhance prereduction of chromite. Journal of the Southern African Institute of Mining and Metallurgy. 117, 457-468.

Kleynhans, E.L.J. 2016a. Development and improvement of pre-reduced technologies to enhance ferrochrome production. PhD thesis. North-West University, South Africa.

Kleynhans, E.L.J., Beukes, J.P., Van Zyl, P.G., Bunt, J.R., Nkosi, N.S.B., Venter, M., 2016b. The Effect of Carbonaceous Reductant Selection on Chromite Pre-reduction. Metallurgical and Materials Transactions B. 1-14.

Kleynhans, E.L.J., Neizel, B.W., Beukes, J.P., Van Zyl, P.G., 2016c. Utilisation of pre-oxidised ore in the pelletised chromite pre-reduction process. Minerals Engineering. 92, 114-124.

Kleynhans, E.L.J., Beukes, J.P., Van Zyl, P.G., Kestens, P.H.I., Langa, J.M., 2012. Unique challenges of clay binders in a pelletised chromite pre-reduction process. Minerals Engineering. 34, 55-62.

Kleynhans, E.L.J., 2011. Unique challenges of clay binders in a pelletised chromite pre-reduction process – a case study. MSc dissertation. Potchefstroom, North-West University.

Lekatou, A., Walker, R.D., 1997. Effect of SiO_2 on solid state reduction of chromite concentrate. Iron and Steelmaking.

Li, H., Li, Z., Liu, T., Xiao, X., Peng, Z., Deng, L., 2008. A novel technology for biosorption and recovery hexavalent chromium in wastewater by bio-functional magnetic beads. Bioresource Technology. 99, 6271-6279.

Lind, B.B., Fällman, A.M., Larsson, L.B., 2001. Environmental impact of ferrochrome slag in road construction. Waste Management. 21, 255-264.

Loock-Hatting, M.M. 2016. Cr(VI) contamination of aqueous systems. North-West University, South Africa.

Loock-Hattingh, M.M., Beukes, J.P., Van Zyl, P.G., Tiedt, L.R., 2015. Cr(VI) and Conductivity as Indicators of Surface Water Pollution from Ferrochrome Production in South Africa: Four Case Studies. Metallurgical and Materials Transactions B. 46, 2315-2325.

Loock, M., Beukes, J., Van Zyl, P., 2014. A survey of Cr (VI) contamination of surface water in the proximity of ferrochromium smelters in South Africa. Water SA. 40, 709-716.

Maine, C., Smit, J., Giesekke, E. 2005. The solid stabilization of soluble wastes generated in the South African ferrochrome industry, Water Research Commission.

Makhoba, G., Hurman Eric, R. Reductant characterization and selection for ferrochromium production. In: Vartiainen, A. (ed.) Proceedings of the 12th International Ferroalloys Congress (INFACON XII), 2010. Helsinki. Finland: Outotec Oyj.

March, J. 1992. Advanced organic chemistry: reactions, mechanisms, and structure, John Wiley & Sons.

Maynard, R.L., Myers, I., Ross, J.A. 2015. Carbon monoxide. Toxicology, Survival and Health Hazards of Combustion Products. Royal Society of Chemistry.

Miller, R.B., Giai, C., Iannuzzi, M., Monty, C.N., Senko, J.M., 2016. Microbial reduction of Cr (VI) in the presence of chromate conversion coating constituents. Bioremediation Journal. 20, 174-182.

Mishra, A.K., Mohanty, B., 2008. Acute toxicity impacts of hexavalent chromium on behavior and histopathology of gill, kidney and liver of the freshwater fish, Channa punctatus (Bloch). Environmental Toxicology and Pharmacology. 26, 136-141.

Mohan, D., Pittman Jr, C.U., 2006. Activated carbons and low cost adsorbents for remediation of tri- and hexavalent chromium from water. Journal of Hazardous Materials. 137, 762-811.

Molitor, B., Richter, H., Martin, M.E., Jensen, R.O., Juminaga, A., Mihalcea, C., Angenent, L.T., 2016. Carbon recovery by fermentation of CO-rich off gases – Turning steel mills into biorefineries. Bioresource Technology. 215, 386-396.

Motzer, W.E., Engineers, T., 2004. Chemistry, geochemistry, and geology of chromium and chromium compounds. Chromium (VI) Handbook. 23-88.

Mukherjee, A.B., 1998. Chromium in the environment of Finland. Science of The Total Environment. 217, 9-19.

Murthy, Y.R., Tripathy, S.K., Kumar, C.R., 2011. Chrome ore beneficiation challenges and opportunities – A review. Minerals Engineering. 24, 375-380.

Naiker, O. The development and advantages of Xstrata's Premus Process. Proceedings of the 11th Ferro-alloys International Congress (INFACON XI), 2007. 112-119.

Namasivayam, C., Sureshkumar, M.V., 2008. Removal of chromium(VI) from water and wastewater using surfactant modified coconut coir pith as a biosorbent. Bioresource Technology. 99, 2218-2225.

Neizel, B., Beukes, J., Van Zyl, P., Dawson, N., 2013. Why is CaCO 3 not used as an additive in the pelletised chromite pre-reduction process? Minerals Engineering. 45, 115-120.

Niemelä, P., Kauppi, M. Production, characteristics and use of ferrochromium slags. Proceedings of the 11th Ferro-alloys International Congress (INFACON XI), 2007. New Delhi, India. 171-179.

Niemelä, P., Krogerus, H., Oikarinen, P. Formation, characterization and utilization of CO-gas formed in ferrochrome smelting. Proceedings of the 11th Ferro-alloys International Congress (INFACON XI), 2004. Cape Town, South Africa. 68-77.

Nriagu, J.O., Nieboer, E. 1988. Chromium in the natural and human environments, John Wiley & Sons.

Pan, X., 2013. Effect of South African chrome ores on ferrochrome production. ICMMMC, Johannesburg, Apr.

Pandey, P., Lobo, N.F., Kumar, P., 2012. Optimization of Disc Parameters Producing More Suitable Size Range of Green Pellets. International Journal of Metallurgical Engineering. 1, 48-59.

Peralta, R.J., Gardea-Torresdey, L.J., Tiemann, J.K., Gomez, E., Arteaga, S., Rascon, E., Parsons, G.J., 2001. Uptake and Effects of Five Heavy Metals on Seed Germination and Plant Growth in Alfalfa (Medicago sativa L.). Bulletin of Environmental Contamination and Toxicology. 66, 727-734.

Peterson, M.L., Brown, G.E., Parks, G.A., 1996. Direct XAFS evidence for heterogeneous redox reaction at the aqueous chromium/magnetite interface. Colloids and Surfaces A: Physicochemical and Engineering Aspects. 107, 77-88.

Pheiffer, D.M., Cookson, K. 2015. Ferrochrome alloy production. Google Patents.

Pöykiö, R., Perämäki, P., Niemelä, M., 2005. The use of Scots pine (Pinus sylvestris L.) bark as a bioindicator for environmental pollution monitoring along two industrial gradients in the Kemi–Tornio area, northern Finland. International Journal of Environmental Analytical Chemistry. 85, 127-139.

Rai, D., Sass, B.M., Moore, D.A., 1987. Chromium(III) hydrolysis constants and solubility of chromium(III) hydroxide. Inorg. Chem. 26, 345-349.

Rai, D., Zachara, J., Schmidt, R., Schwab, A. 1984. Chemical attenuation rates, coefficients, and constants in leachate migration. Volume 2. An annotated bibliography. Final report. Pacific Northwest Lab., Richland, WA (USA).

Riekkola-Vanhanen, M. 1999. Finnish expert report on best available techniques in ferrochromium production. Helsinki.

Rinehart, T.L., Schulze, D.G., Bricka, R.M., Bajt, S., Blatchley Iii, E.R., 1997. Chromium leaching vs. oxidation state for a contaminated solidified/stabilized soil. Journal of Hazardous Materials. 52, 213-221.

Roza, G. 2008. Understanding the Elements of the Periodic Table–Chromium. New York, USA: The Rosen Publishing Group, Inc. 49p.

Salem, F.Y., Parkerton, T.F., Lewis, R.V., Huang, J.H., Dickson, K.L., 1989. Kinetics of chromium transformations in the environment. Science of the Total Environment. 86, 25-41.

Sass, B.M., Rai, D., 1987. Solubility of amorphous chromium (III)-iron (III) hydroxide solid solutions. Inorganic Chemistry. 26, 2228-2232.

Schubert, E., Gottschling, R., 2011. Co-generation: A challenge for furnace off-gas cleaning systems. Southern African Pyrometallurgy.

Seigneur, C., Constantinou, E., 1995. Chemical kinetic mechanism for atmospheric chromium. Environmental science & technology. 29, 222-231.

Sethunathan, N., Megharaj, M., Smith, L., Kamaludeen, S.P.B., Avudainayagam, S., Naidu, R., 2005. Microbial role in the failure of natural attenuation of chromium(VI) in long-term tannery waste contaminated soil. Agriculture, Ecosystems & Environment. 105, 657-661.

Shanker, A.K., Cervantes, C., Loza-Tavera, H., Avudainayagam, S., 2005. Chromium toxicity in plants. Environment International. 31, 739-753.

Shen, Y.-S., Wang, S.-L., Tzou, Y.-M., Yan, Y.-Y., Kuan, W.-H., 2012. Removal of hexavalent Cr by coconut coir and derived chars – The effect of surface functionality. Bioresource Technology. 104, 165-172.

Soykan, O., Eric, R., King, R., 1991. Kinetics of the reduction of Bushveld complex chromite ore at 1416 C. Metallurgical Transactions B. 22, 801-810.

Testa, S.M., Guertin, J., Jacobs, J., Avakian, C. 2004. Sources of chromium contamination in soil and groundwater, CRC Press: Boca Raton, FL.

Tiwary, R., Dhakate, R., Rao, V.A., Singh, V., 2005. Assessment and prediction of contaminant migration in ground water from chromite waste dump. Environmental Geology. 48, 420-429.

Van Staden, Y., Beukes, J.P., Van Zyl, P.G., Du Toit, J.S., Dawson, N.F., 2014. Characterisation and liberation of chromium from fine ferrochrome waste materials. Minerals Engineering. 56, 112-120.

Visser, M., 2006. An overview of the history and current operational facilities of Samancor Chrome. Southern African Pyrometallurgy 2006. 285-296.

Wang, G., Zhang, B., Li, S., Yang, M., Yin, C., 2017. Simultaneous microbial reduction of vanadium (V) and chromium (VI) by Shewanella loihica PV-4. Bioresource Technology. 227, 353-358.

Wesseldijk, Q., Reuter, M., Bradshaw, D., Harris, P., 1999. The flotation behaviour of chromite with respect to the beneficiation of UG2 ore. Minerals Engineering. 12, 1177-1184.

Whittleston, R.A., Stewart, D.I., Mortimer, R.J.G., Tilt, Z.C., Brown, A.P., Geraki, K., Burke, I.T., 2011. Chromate reduction in Fe(II)-containing soil affected by hyperalkaline leachate from chromite ore processing residue. Journal of Hazardous Materials. 194, 15-23.

Williams, A.G., Scherer, M.M., 2001. Kinetics of Cr (VI) reduction by carbonate green rust. Environmental Science & Technology. 35, 3488-3494.

Xiao, Z., Laplante, A., 2004. Characterizing and recovering the platinum group minerals—a review. Minerals Engineering. 17, 961-979.

Zelić, J., 2005. Properties of concrete pavements prepared with ferrochromium slag as concrete aggregate. Cement and Concrete Research. 35, 2340-2349.

Zhang, B., Shi, P., Jiang, M., 2016. Advances towards a clean hydrometallurgical process for chromite. Minerals. 6, 7.

Zhang, J., Li, X., 1987. Chromium pollution of soil and water in Jinzhou. Chinese Journal of Preventive Medicine. 21, 262.

Zhao, B., Hayes, P. Effects of oxidation on the microstructure and reduction of chromite pellets. Proceedings of 12th International Ferro Alloys-Congress (INFACON XII), 2010. 263-273.

APPENDIX A

A.1 Introduction

As stated in Section 2.7.1, the candidate, co-authored a review paper related to Cr(VI) issues associated with the FeCr industry as part of his PhD work. The candidate was the second author of the afore-mentioned paper.

Journal of Cleaner Production 165 (2017) 874–889

Contents lists available at ScienceDirect

Journal of Cleaner Production

journal homepage: www.elsevier.com/locate/jclepro

Review

Review of Cr(VI) environmental practices in the chromite mining and smelting industry – Relevance to development of the Ring of Fire, Canada

J.P. Beukes [a, *], S.P. du Preez [a], P.G. van Zyl [a], D. Paktunc [b], T. Fabritius [c], M. Päätalo [d], M. Cramer [e]

[a] Chemical Resource Beneficiation, North-West University, Potchefstroom Campus, Private Bag X6001, Potchefstroom 2520, South Africa
[b] CanmetMINING, Natural Resources Canada, 555 Booth St., Ottawa, Canada
[c] University of Oulu, Laboratory of Process Metallurgy, PO Box 4300, Oulu, Finland
[d] Outokumpu Chrome Oy, 95490 Tornio, Finland
[e] Ferroalloy Smelting Technologies, Hatch, Ontario, L5K 2R7, Canada

ARTICLE INFO

Article history:
Received 28 April 2017
Received in revised form
21 July 2017
Accepted 21 July 2017
Available online 22 July 2017

Handling Editor: Cecilia Maria Villas Bôas de Almeida

Keywords:
Hexavalent chrome
Cr(VI)
Chromite
Ferrochrome
Ring of Fire
Canada

ABSTRACT

During stainless steel production, new chromium units are obtained from ferrochrome, a relatively crude alloy produced from chromite ore. Large chromite reserves have recently been discovered in the so-called Ring of Fire, Canada. Due to the strategic importance of uninterrupted stainless steel production in North America, it is highly likely that these reserves will be exploited in the foreseeable future. However, the Ring of Fire is located in an area that forms part of the largest peatland in the world, as well as the traditional territories of several First Nations (indigenous American communities), which highlights the environmental and social sensitive nature of the intended developments. In this review, relevant mining and/or smelting processes were considered within the context of possible prevention and mitigation of hexavalent chromium, Cr(VI), formation, and the treatment of possible Cr(VI) containing waste materials. Cr(VI) is classified as a carcinogen and it has several negative environmental impacts.

Prior to commencing chromite mining in the Ring of Fire, baseline studies should be undertaken to determine the possible natural occurrence of Cr(VI) in soils, untreated chromite ore and surface/groundwater, as well as sources thereof. During mining and ore processing, dry milling was identified as the only process step with the potential to generate Cr(VI); therefore, it should be avoided. Instead, wet milling should be used.

Assessments of all process steps associated with conventional ferrochrome production indicated that smelting will lead to the formation of unintended small amounts of Cr(VI) (mg.kg^{-1} concentration range), irrespective of the technology applied. However, this review proved that it will be possible to produce ferrochrome without causing occupational/community health issues related to Cr(VI), as well as environmental pollution, if appropriate preventative and mitigation measures are applied. Apart from Cr(VI) related considerations, it is acknowledged that factors such as physical and chemical characteristics of the ore, capital and operational costs, specific electricity consumption, carbon footprint, and availability of expertise will determine what process options will be implemented.

Contents

* Corresponding author.
E-mail address: paul.beukes@nwu.ac.za (J.P. Beukes).

http://dx.doi.org/10.1016/j.jclepro.2017.07.176
0959-6526/

1. Introduction

1.1. The Ring of Fire deposit

Various chromium (Cr) compounds, Cr metal and/or Cr-containing alloys are used in modern society. By volume the largest application for Cr is in the production of stainless steel (Murthy et al., 2011), which owes its corrosion resistance mainly to the inclusion of Cr. Cr can occur in 82 different ore types (Motzer and Engineers, 2004), but the only type that is mined in commercial volumes that can supply the required new units for the production of stainless steel is chromite (Motzer and Engineers, 2004). Chromite ($FeCr_2O_4$) is a mineral belonging to the spinel group of minerals characterized by the following formula $[(Mg,Fe^{2+})(Al,Cr,Fe^{3+})_2O_4]$ (Haggerty, 1991). The largest exploitable deposits of chromite occur in South Africa and Zimbabwe, with significant deposits in several other countries such as Finland, Kazakhstan and Turkey. Only 31,250 tons of chromite was produced in North America during 2012, which represented less than 0.13% of the more than 24.5 million tons of chromite produced internationally (ICDA, 2013). Fairly recently very large chromite reserves were discovered in the so-called Ring of Fire in Canada. Due to the strategic importance of uninterrupted stainless steel production in North America, it is highly likely that these deposits will be exploited in the foreseeable future.

The Ring of Fire is located in the relatively remote far north of Ontario in the James Bay Lowlands (Fig. 1a). It is approximately 1000 and 500 km from Toronto and Thunder Bay, respectively. Although the Ring of Fire has an approximate surface area of 5000 km^2, most of the mineral deposits discovered to date are located within a 20 km long strip (Fig. 1b).

The first commercially viable quantities of chromite in the Ring of Fire were discovered in 2008 (Chong, 2014). It has been estimated that the chromite reserves in the Ring of Fire could meet North American needs for several centuries. However, the Ring of Fire is located in an area that forms part of the largest peatland (a type of wetland) in the world (Warner and Rubec, 1997), which makes it environmentally and logistically challenging for mining operations. Developing chromite mining and/or processing, as well as building infrastructure in this sensitive ecosystem will require careful planning to mitigate environmental impacts. The Ring of Fire is also located within the traditional territories of several First Nations (Chong, 2014). Exploitation of the mineral deposits will therefore require adequate consultations with the First Nations.

1.2. Relevance of hexavalent chromium

Chromium can occur in several oxidation states, but only trivalent chromium, Cr(III), and hexavalent chromium, Cr(VI), are common in near surface environments, while metallic chromium, Cr(0), is mainly produced by human intervention (Motzer and Engineers, 2004; Bartlett, 1991).

Cr(VI) compounds are generally classified as carcinogenic, with specific ailments of the respiratory system being implicated (Beaver et al., 2009; IARC, 2012). Cr(VI) is also on the List of Toxic Substances under Schedule 1 of the Canadian Environmental Protection Act, 1999 (Environment Canada, 2014). Furthermore, Cr(VI) has been shown to have several negative environmental impacts, e.g. reduced germination and growth of some plants (Peralta et al., 2001), increased mortality and reproduction rates in earthworms (Abbasi and Soni, 1983), organ damage in crayfish (Bollinger et al., 1997), detrimental effects on survivability, growth and post-exposure reproduction of marine fish larvae and copepods (Hutchinson et al., 1994), toxic effects on gill, kidney and liver cells of fresh water fish (Mishra and Mohanty, 2008), and possible diatom demise (Loock-Hattingh et al., 2015). Therefore, it is important to prevent or at least mitigate the formation of such compounds, and to apply proper treatment strategies to Cr(VI) containing wastes. This is of particular importance within the context of the possible development of the Ring of Fire chromite ore deposits, considering the sensitive nature of the area.

Cr(III) and Cr(0) are not classified as carcinogenic. Cr(III) is in fact an important trace element in a balanced nutritional diet and is in certain circumstances specifically included as a dietary supplement (Hininger et al., 2007).

1.3. Methods

Considering the significant differences in the impact of Cr(VI) on human health and the environment, as opposed to Cr(III) and Cr(0),

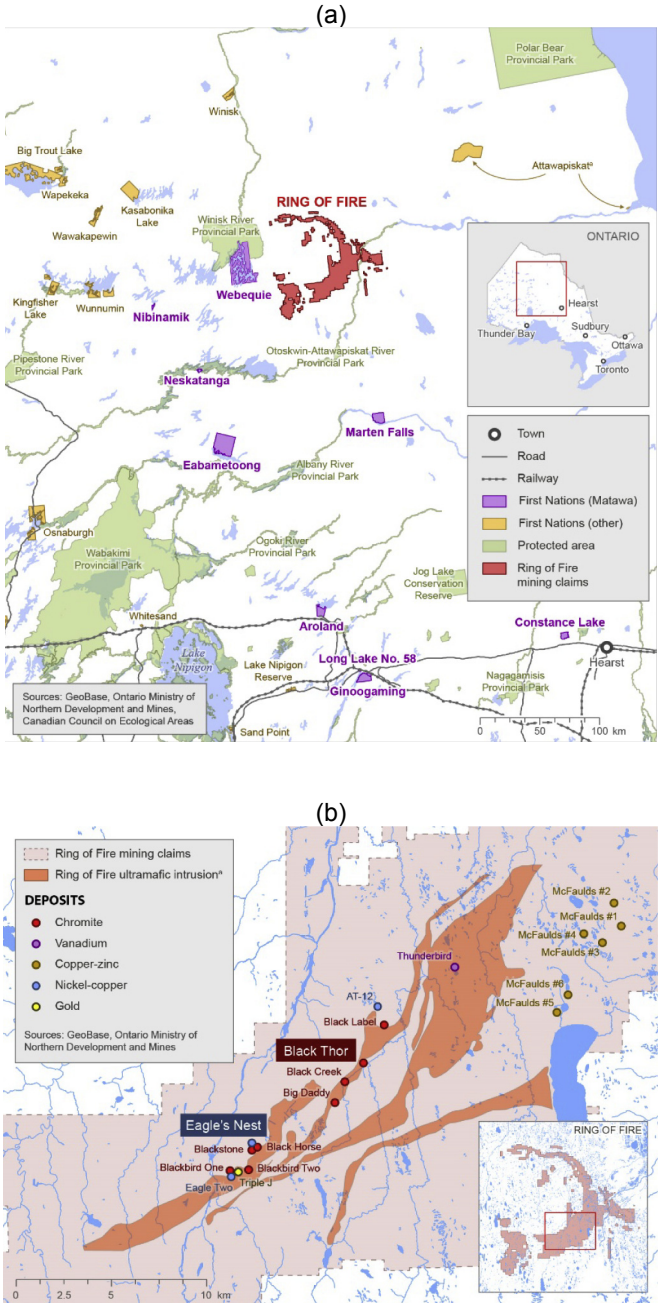

Fig. 1. Location of the Ring of Fire within a regional perspective (a), as well as an enlarged area showing the mineral deposits (b) (Chong, 2014).

it is important to consider the current knowledge base and the gaps therein, as well as best practices related to mining and smelting of chromite to produce ferrochrome (FeCr) within the context of the possible development of the chromite deposits in the Ring of Fire. Several aspects have to be considered: (1) the possible natural occurrence and/or natural formation of Cr(VI), (2) prevention and mitigation of Cr(VI) formation during mineral and metallurgical processing leading to the production of FeCr, and (3) treatment of possible Cr(VI)-containing waste materials originating from the afore-mentioned processes.

Although information (literature) and experience available internationally was considered in this review, where possible specific reference will be made to the Finnish mining, beneficiation and pyrometallurgical conversion of chromite, since the

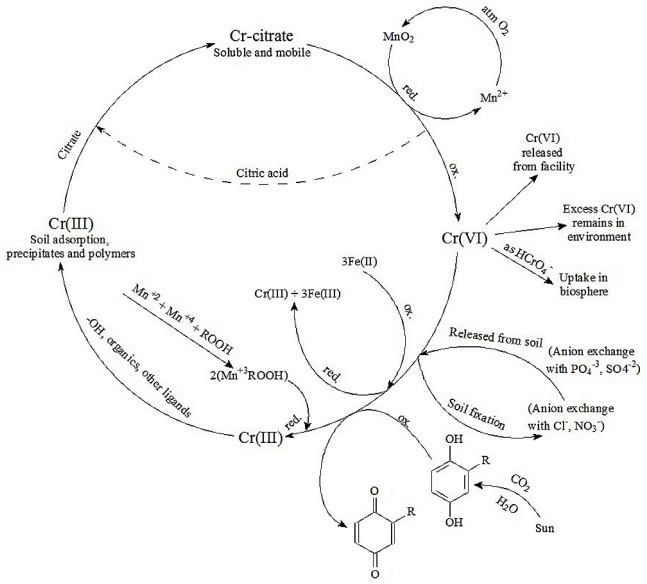

Fig. 2. The Cr cycle, adapted from Testa (2004) and Bartlett (1991).

environment in which these operations occur is somewhat similar to the Canadian conditions. The Finnish chromite/ferrochrome operations are also regarded as leaders in environmental practices (e.g. Riekkola-Vanhanen, 1999; Päätalo and Raiskio, 2015).

2. Natural occurrence and/or natural formation of Cr(VI)

In order to contextualize the possible natural occurrence and/or formation of Cr(VI), the basic Cr cycle in soil and water, as presented in Fig. 2 (Bartlett, 1991; Testa, 2004), needs to be considered first. Only a synopsis of this Cr cycle will be considered here, with detailed information available in the original text and references therein (Bartlett, 1991; Testa, 2004).

In essence, the soil/water Cr cycle (Fig. 2) indicates that Cr(III) is the dominant species under most near-surface environmental conditions. However, Cr(III) can be oxidized under ambient environmental conditions in the presence of MnO_2, which serves as a catalyst for the atmospheric oxidation of Cr(III) in surface or ground water. However, for this to take place Cr(III) must be in a soluble form (Bartlett, 1991). Cr(III) hydroxides are relatively insoluble over a wide pH range (see Fig. 3; Rai et al., 1987) and therefore usually do not contribute significantly to such oxidation. Cr(VI) can be reduced by various inorganic species, including aqueous Fe(II) (Eary and Rai, 1988), magnetite (Peterson et al., 1996), green rust (Williams and Scherer, 2001) and zero valent iron (Chang et al., 2014). Additionally, Cr(VI) can be reduced by numerous organic compounds (both synthetic and natural) and microorganisms (March, 1992; Dong et al., 2014; Miller et al., 2016; Jin et al., 2017; Gupta et al., 2017; Wang et al., 2017). However, some organic compounds could complex Cr(III) and in so doing solubilize it, which could facilitate the formation of Cr(VI) due to natural oxidation in the presence of MnO_2. Cr(VI) species primarily occur under oxidizing (Eh > 0) and alkaline (pH > 6) conditions (Motzer and Engineers, 2004 and references therein).

In the ambient atmosphere, Cr(VI) is associated exclusively with particulate matter and/or atmospheric water, since the vapor pressure of all Cr compounds at ambient conditions is negligible (Kimbrough et al., 1999; Seigneur and Constantinou, 1995). All atmospheric inter-conversion reactions leading to possible Cr(VI) formation and reduction to Cr(III) are therefore water-phase

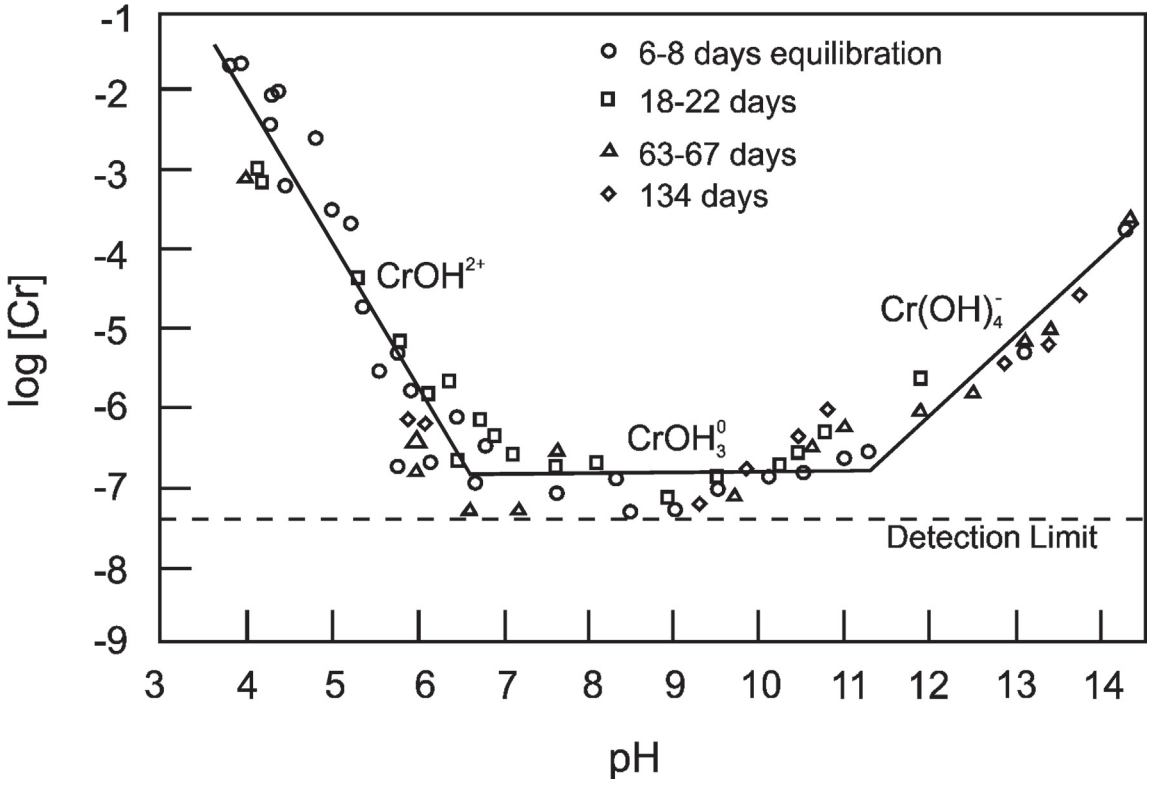

Fig. 3. The solubility of $Cr(OH)_3$ (s), adapted from Rai et al. (1987).

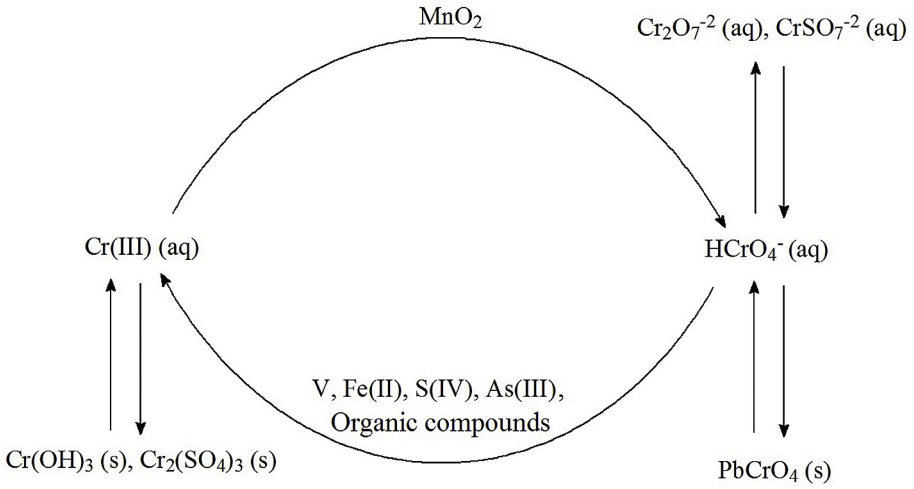

Fig. 4. The basic atmospheric cycle of Cr, adapted from Seigneur and Constantinou (1995).

reactions (Kimbrough et al., 1999; Seigneur and Constantinou, 1995). The basic atmospheric cycle of Cr, as presented in Fig. 4, has some similarities to the soil/water cycle previously presented (Fig. 2). Again, Cr(III) is the dominant species, with many compounds able to reduce Cr(VI) to Cr(III). In the atmosphere S(IV) is a relatively important species that can reduce Cr(VI) to Cr(III). S(IV) is basically SO_2, which is a common atmospheric anthropogenic pollutant, dissolved in water (Seigneur and Constantinou, 1995; Beukes et al., 1999, 2000). Cr(VI) formation is usually associated with the presence of MnO_2 (Kimbrough et al., 1999; Seigneur and Constantinou, 1995).

Notwithstanding the likely dominance of insoluble Cr(III) in natural environments, naturally occurring Cr(VI) and/or natural formation thereof have been reported for various locations. At least 24 known Cr(VI)-bearing minerals occur (Motzer and Engineers, 2004 and references therein), which could serve as a natural sources of Cr(VI). This includes minerals such as crocoite ($PbCrO_4$) that form in the oxidized zones of lead (Pb) deposits and Cr(VI) minerals in nitrate-rich evaporite deposits in arid environments such as the Chilean nitrate deposits in the Atacama Desert. Motzer and Engineers (2004) and references therein, also described Cr(VI) as occurring in groundwater due to natural formation/processes at various locations in the USA, including Paradise Valley (Arizona), the Presidio in San Francisco, Davis (California), the western Mojave

Desert (California) and Soquel Water District south of Santa Cruz (California). In general, it is believed that most of these natural occurrences of Cr(VI) in groundwater are linked to the hydrolysis of feldspar, some common mafic minerals such as Cr-bearing pyroxenes and chromite, together with calcite, which cause alkaline groundwater conditions. This, coupled with the absence of natural reducing agents, e.g. Fe(II), organic matter and reducing organisms (see Fig. 2), may have allowed oxidation of Cr(III) to Cr(VI).

Chromite is a stable non-soluble mineral, in which Cr occurs in the Cr(III) oxidation state. However, Cr(VI) contamination of ground and/or surface water has been reported as a direct result of chromite mining in India. Godgul and Sahu (1995) postulated that serpentinization and magnesium (Mg) ion release during deuteric alteration of ultramafic rocks (peridotites) and associated oxidation (laterization) created alkaline pore water in the chromite deposits of the Sukinda belt of Orissa (India), which resulted in conditions favorable for natural Cr(VI) formation. Dubey et al. (2001), Tiwary et al. (2005) and Dhal et al. (2010) subsequently reported on several aspects related to the Cr(VI) leaching from these deposits and/or mine dumps in the same area.

As far as the authors could ascertain, Cr(VI) has not been reported in surface and/or ground-waters in Finland as a result of natural occurrence/formation, or chromite mining. Pöykiö et al. (2005) did, however, show that Scots pine (Pinus sylvestris L.) bark used as a passive bio-indicator in the immediate vicinity of the FeCr and stainless steel works at Tornio and near the open-cast chromite mine at Kemi (both in northern Finland) indicated Cr pollution factors (PF i.e. ratio of heavy metal concentrations in the bio-indicators to those in the background area) of 81 and 5.3, respectively. However, this data does not imply that the Cr occurred as Cr(VI).

Considering that Cr(VI) has been reported to occur/form naturally in some environments, it is vital to properly assess the possible occurrences of natural Cr(VI) in surface and ground-waters, and soils before large-scale chromite mining commences in the Ring of Fire. Failure to do so will result in industry carrying the total burden if Cr(VI) contamination were to be reported later, even if natural processes are responsible in part, or wholly. Additionally, since chromite mining has been implicated in Cr(VI) pollution in India, the susceptibility of all Cr-bearing minerals (not only chromite) that will be exposed during chromite mining in the Ring of Fire to form Cr(VI) needs to be established in the presence of natural oxidants and/or catalysts for such oxidation. Preliminary results by Paktunc (2016) indicated that apart from chromite that would be the targeted mineral, various other Cr-bearing minerals occur in the Ring of Fire, e.g. clinochlore, phlogopite, amphibole and clinopyroxene, with traces of minor Cr content also occurring in orthopyroxene, olivine, serpentine and carbonates. Preliminary leach tests by the same authors indicated that Cr(VI) can be generated from these minerals in the presence of birnessite, a Mn-containing mineral. Although the afore-mentioned leach conditions were not necessarily realistic for chromite tailings disposal, it does indicate the need to evaluate the possible formation of Cr(VI) from chromite mining and/or process residue for the Ring of Fire deposits.

3. Cr(VI) formation, prevention and mitigation in various process options

Cr(VI) formation and mitigation need to be considered within the context of process options that are likely to be considered for the development of the Ring of Fire. As far as the authors could ascertain, a relatively detailed mineral processing strategy was developed for the chromite ore mining and processing activities that Cliffs was planning for their Ring of Fire development, by the research and development company Mintek (2016). However, Cliffs abandoned this development and the report was not available in the public domain by the time that this paper was prepared. Therefore, techniques generally associated with mining, beneficiation and conversion of chromite ore are considered further. Within the context of this paper, two categories will be considered: (1) mining and beneficiation of chromite ore and (2) pyrometallurgical conversion of chromite into FeCr.

3.1. Mining and beneficiation of chromite ore

Run-of-mine (ROM) chromite (mined ore, prior to beneficiation) is usually beneficiated with relatively simple processes. The most commonly applied processes include primary and secondary crushing, screening, milling, dense media separation and gravity separation methods (Murthy et al., 2011). More sophisticated processes such as flotation can also be used (Wesseldijk et al., 1999), but are usually not economically feasible.

In order to generate beneficiated lumpy, chip and/or pebble chromite ore (the coarser fractions, typically 6–150 mm) crushing, screening and dense media separation would be applied. The finer fraction (typically < 6 mm) of ROM chromite would normally be milled to approximately < 1 mm and then upgraded with a series of hydrocyclones and spiral concentrators to generate metallurgical and/or chemical grade chromite concentrate (Murthy et al., 2011). Fig. 5 presents a process flow diagram for the beneficiation of

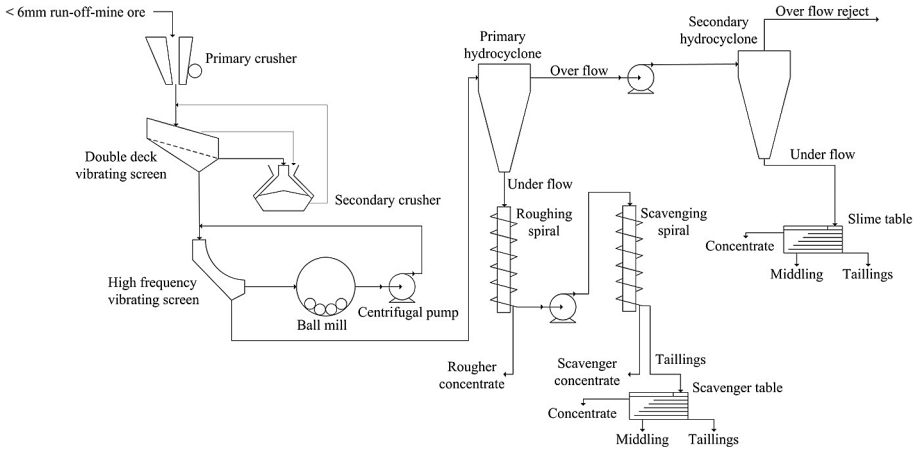

Fig. 5. General process flow diagram of a beneficiation circuit for chromite concentrate (typically < 1 mm), adapted from Murthy et al. (2011).

chromite concentrate (<1 mm) adapted from Murthy et al. (2011), who reviewed chromite beneficiation. The shaking tables (slime and scavenger tables) in this diagram would probably not be used in large-scale operations and the single spiral concentrators would probably consist of numerous banks of spiral concentrators operating in parallel.

Milling is the only process step applied during chromite beneficiation that has been implicated in the possible generation of Cr(VI). However, only dry milling of chromite has been proven to generate Cr(VI) (Beukes and Guest, 2001; Glastonbury et al., 2010). Extreme grinding (i.e. pulverization), which is not a typical comminution technique, was applied in both the afore-mentioned referenced studies and it could therefore be argued that Cr(VI) is less likely to be formed by industrial dry milling. However, Beukes and Guest (2001) also report relatively high levels of Cr(VI) in samples gathered from a dry ball mill circuit at a FeCr producer. In contrast, wet milling does not seem to generate Cr(VI) (Beukes and Guest, 2001). Wet milling would also be the obvious choice during chromite concentrate beneficiation, since hydrocyclones and spiral concentrators are wet processes. Also, during chromite concentrate beneficiation the milling step would be aimed only at liberating the chromite crystals from the gangue minerals. This is in contrast to the dry milling tests conducted by Beukes and Guest (2001) and Glastonbury et al. (2010), during which Cr(VI) was generated, where the intent was to obtain particle sizes fine enough for pelletization (which will be discussed in Section 3.2.2 and 3.2.3).

3.2. Ferrochrome production

There are four grades of FeCr that are produced commercially, i.e. High Carbon FeCr (typically > 60% Cr and 6–9% carbon, C), Charge Grade FeCr (typically 50–60% Cr and 6–9% C), Medium Carbon FeCr (typically 56–70% Cr and 1–4% C) and Low Carbon FeCr (typically 56–70% Cr and 0.015–1.0% C) (Goel, 1997). Due to the similarities of High Carbon FeCr and Charge Grade FeCr, it is common to refer to these two grades combined as High Carbon Charge

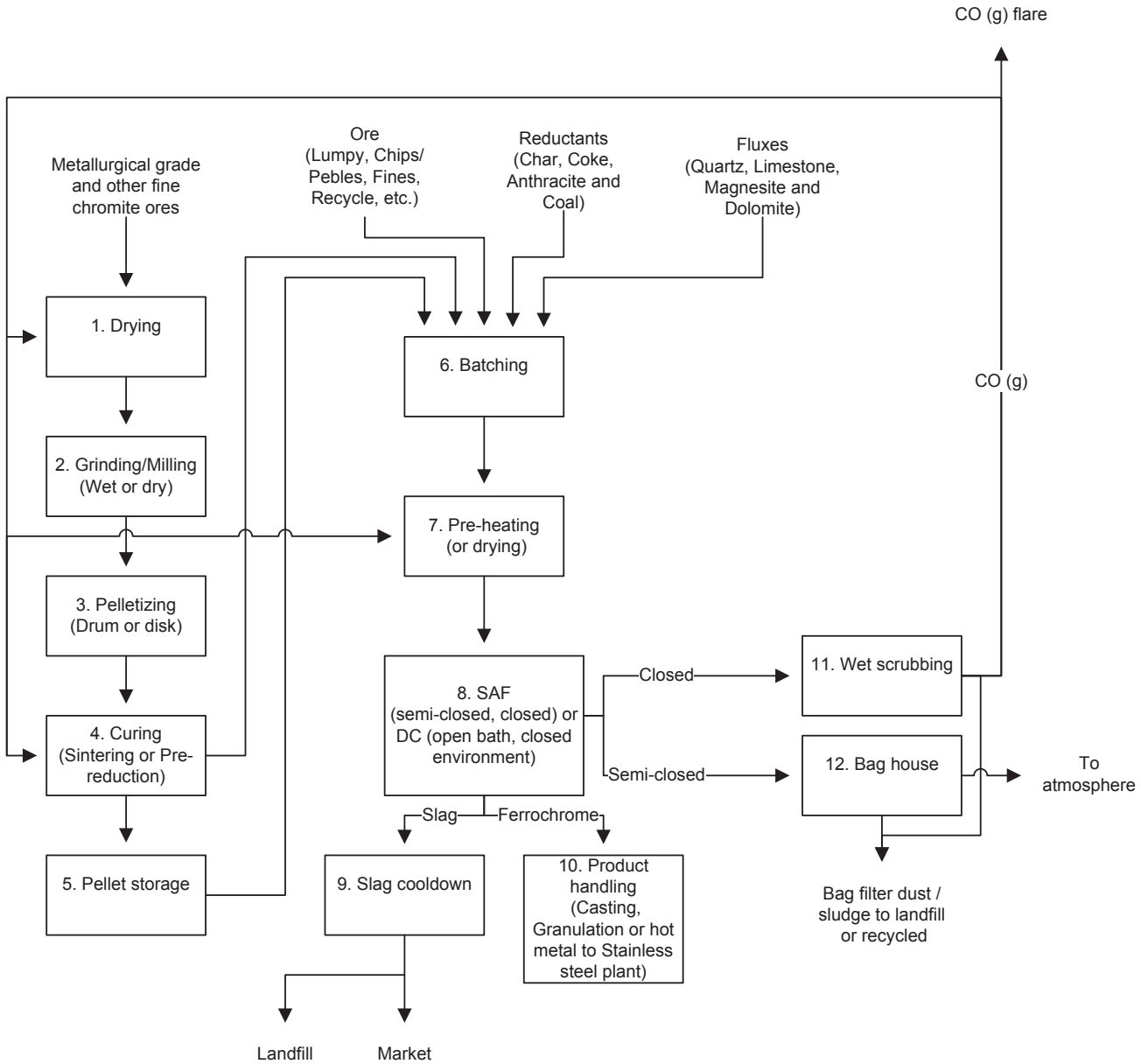

Fig. 6. A flow diagram adapted from Riekkola-Vanhanen (1999) and Beukes et al. (2010) indicating the most common process steps used for High Carbon Charge Grade FeCr production.

Grade FeCr (ICDA, 2013). The demand for low and medium grade carbon FeCr has decreased dramatically due to the development of processes such as argon oxygen decarburization (AOD) and vacuum oxygen decarburization (VOD), which allow for the removal of C from stainless steel with acceptable losses of Cr. In 2012, medium and low carbon FeCr accounted for less than 8.5% of the global annual FeCr production (ICDA, 2013). Therefore, in this paper the focus will be on Cr(VI) aspects related to High Carbon Charge Grade FeCr production, although certain aspects of other process options will also be explored.

High Carbon Charge Grade FeCr is produced with carbo-thermic reduction of chromite. Fig. 6 presents a generalized flow diagram indicating the individual process steps most commonly applied during High Carbon Charge Grade FeCr production.

Four relatively well-defined process combinations are used by most High Carbon Charge Grade FeCr producers (Beukes et al., 2010 and references therein). A brief description of each is presented below, within the context of Fig. 6.

A) Conventional open/semi-closed submerged arc furnace (SAF) operation. As the name implies, the roofs of these SAFs do not fit with a gas tight seal on the furnace sidewalls, with the subsequent unavoidable combustion of process-rich CO gas on top of the furnace bed. This is the oldest technology being applied, but internationally it still accounts for a substantial fraction of overall production (Gediga and Russ, 2007). In this type of operation, coarse (typically 6–150 mm) chromite is smelted in the presence of coarse carbonaceous reductants and coarse fluxes. The coarse nature of the feed material allows processed gas that emanates from the smelting process to permeate to the top of the bed and prevent the bed surface from sintering, which could cause dangerous blow-outs or bed turnovers (Riekkola-Vanhanen, 1999). A small fraction of fines (typically $\leq$ 6 mm) can be fed into an open/semi-closed SAF, but this increases the afore-mentioned risk. Due to the lack of sophisticated feed material pre-treatment, this process option requires the lowest capital investment. With reference to the process flow diagram (Fig. 6), the process steps followed are 6, 8, 9, 10 and 12. Some open/semi-closed SAFs do consume pelletized feed (it can also be other agglomerates such as briquettes), in which case all, or some of process steps 1–5 would also be included. Most open/semi-closed SAFs are operated on an acid slag, with a basicity factor (BF, defined in Equation (1)) smaller than 1.

$$BF = \frac{\%CaO + \%MgO}{\%SiO_2} \quad (1)$$

Some open/semi-closed SAFs operate with BF > 1. Such operations are sometimes only temporarily undertaken to either compensate for refractory linings being in poor condition (basic slag has a higher liquidus temperature than acidic slag), or if enhanced sulfur-removing capacity (through formation of sulfides in the slag) is required. Bag filter off-gas cleaning is typically applied with open/semi-closed SAF operation.

B) Closed furnace operation, using oxidative sintered pelletized feed together with coarse reductants and fluxes – commercially known as the Outotec process, which is applied at the Outokumpu smelter at Tornio in Finland (Outokumpu, 2016). This technology has been commonly applied in many countries, including South Africa where the majority of green and brown field expansions during the last two decades have utilized it. Process steps usually include steps 2, 3, 4, 5, 6, 8, 9, 10 and 11, with or without 7. In most green field FeCr developments, the pelletizing and sintering sections (steps 3 and 4) are combined with closed SAFs, in which case off-gas cleaning is achieved with wet venturi scrubbing. However, pelletizing and sintering sections have also been constructed to feed conventional open/semi-closed furnaces. SAFs consuming oxidative sintered pelletized feed are usually operated on an acid slag (BF < 1).

C) Closed furnace operation with pre-reduced pelletized feed, together with coarse reductants and fluxes – commercially known as the Premus Process, as applied by Glencore Alloys (previously Xstrata Alloys) in South Africa (Naiker, 2007). FeCr smelters applying this process are also being developed in China, but this information is not yet available in the public domain. The process steps include steps 1, 2, 3, 4, 6, 8, 9, 10 and 11, with or without 5. The pelletized feed differs substantially from the oxidative sintered type (Process Option B) since the pellets are pre-reduced and mostly fed hot, directly after pre-reduction, into the SAFs. The SAFs are closed and operate on a basic slag (BF > 1), with off-gas cleaning achieved with wet venturi scrubbing. A basic slag (which is conductive) is required, since not enough lumpy carbonaceous reductants can be added during the smelting process to facilitate burden conductivity, as a result of the chromite being pre-reduced. This process option is likely to have the highest capital requirement, but the lowest specific electricity consumption (SEC) (Kleynhans et al., 2016).

D) Direct current arc furnace (DCF) operation (Jones, 2014) – currently applied at several smelters in Kazakhstan and South Africa. For this type of operation, the feed (chromite, carbonaceous reductants and fluxes) can consist exclusively of fine material. Process steps include 6, 8, 9, 10 and 11, with or without step 7. The DCF typically utilizes a basic slag (BF > 1), with off-gas cleaning achieved with wet venturi scrubbing. Of all the process options, this process has the highest SEC. In order to reduce the SEC pre-reduction of the fine chromite ore prior to DCF smelting has been attempted (McCullough et al., 2010), but has not yet been implemented commercially.

In the subsequent sections, the individual process steps presented in Fig. 6 are discussed.

3.2.1. Drying of fine feed material prior to dry milling (Fig. 6, process step 1)

Process Option C requires that the chromite concentrate, as well as other fine feed materials, be dried prior to milling and pelletization. As far as could ascertained, no studies considering the formation of Cr(VI) during this process step have been published in the public domain. However, temperatures required to drive off moisture would typically not be high enough to facilitate oxidation of chromite to generate Cr(VI).

3.2.2. Milling (Fig. 6, process step 2)

The friability of many chromite ores, e.g. the Bushveld Complex in South Africa, necessitated the implementation of agglomeration processes prior to SAF smelting to ensure a permeable bed. This applies to Process Options B and C. The most commonly applied agglomeration technique is pelletization (both with drum and disk), although briquetting is also used. Pelletization of chromite requires milling prior to agglomeration. Milling and subsequent pelletization also increase the effective surface area for reduction during smelting, which have been linked with improved SEC (Zhao and Hayes, 2010).

Currently dry milling is applied in the pre-reduced pelletized feed process (Process Option C), with a targeted particle size of d_{90}

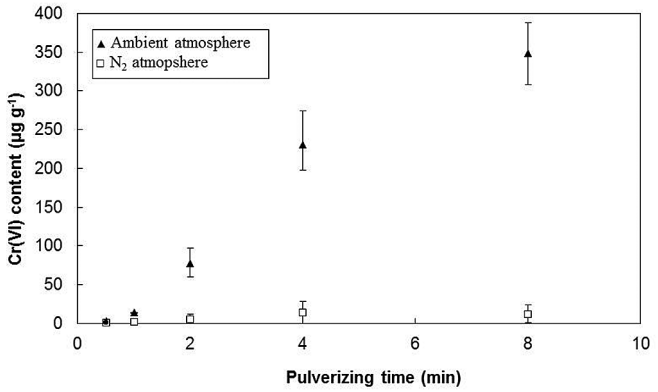

Fig. 7. Cr(VI) formation during dry milling with a Siebtechnik pulverizer under ambient and inert atmospheric conditions (adapted from Glastonbury et al., 2010).

equal to 75 μm (90% of the particles smaller than 75 μm) prior to pelletization (Kleynhans et al., 2012). Previously it was proven that dry milling of chromite ore (and other Cr containing materials) leads to Cr(VI) formation (Beukes and Guest, 2001; Glastonbury et al., 2010). Although not common, some chromite ores, e.g. chromite of the Sukinda belt of Orissa (India) might contain Cr(VI) that occurs naturally (Section 2) (Godgul and Sahu, 1995; Dubey et al., 2001; Tiwary et al., 2005; Dhal et al., 2010). However, as indicated in Fig. 7 (Glastonbury et al., 2010), Cr(VI) is formed during dry milling and not merely liberated from the mineral matrix, since no Cr(VI) was formed with dry milling under a nitrogen (N_2) atmosphere. The generation of Cr(VI) during dry milling was also acknowledged in the health, safety and environmental guidelines document compiled by the International Chromium Development Organization (ICDA) (ICDA, 2007).

No previously published data (Beukes and Guest, 2001; Glastonbury et al., 2010) can be used to quantify the generation of Cr(VI) by dry milling, since Cr(VI) generation is likely to depend on various factors, e.g. chromite composition, initial ore particle size, targeted particle size, milling equipment design, milling intensity and retention time.

Wet milling does not seem to generate Cr(VI) (Beukes and Guest, 2001). Therefore, ignoring all other aspects (e.g. capital investment, operational costs, integration with other process steps), it can be stated that wet milling has an advantage with regard to Cr(VI) formation. Currently wet milling is used in conjunction with the oxidative sintered pelletized process (Process Option B), with a targeted d_{80} of 74 μm.

Presently there seems to be conflicting views with regard to the human health hazards associated with Cr(VI) ingestion. Numerous studies (e.g. Proctor et al., 2002; Guertin, 2004) have indicated that ingested Cr(VI) is not problematic. However, all literature agrees that airborne Cr(VI) is hazardous. Therefore, if dry milling of chromite cannot be prevented, dust prevention, extraction and suppression must be applied. Captured dust must be contacted with water to immediately reduce the risk of human respiratory exposure and such captured dust must be recycled, since it consists of fine feed material. Process water utilized for contacting/capturing milling dust must be treated to reduce Cr(VI), which will be discussed later (Section 4). The wearing of appropriate dust masks must also be made compulsory for operational personnel in the dry-milling section(s).

3.2.3. Pelletization (Fig. 6, process step 3)

The formation of green (uncured/newly-formed) pellets and briquettes are not known to generate Cr(VI) in any manner, since the materials usually contain moisture (for enhanced green pellet strength) and the processes typically take place at ambient temperatures. However, curing of these green agglomerates, which will be discussed in the next section, could lead to Cr(VI) formation.

3.2.4. Curing of green pellets (Fig. 6, process step 4)

Curing of green pellets takes place in Process Options B and C. Since both these curing steps are high-temperature processes in which oxygen is not totally excluded, Cr(VI) could be generated. These two process options are therefore discussed separately.

As previously stated, the oxidative sintered pelletized process (Process Option B) is commonly applied, since it is a proven technology. It also originated from Finland, which is internationally regarded as a leader in FeCr technology and environmental aspects (Riekkola-Vanhanen, 1999). In this process, chromite concentrate (<1 mm) together with 1–2 wt % carbonaceous reductant (e.g. coke), is wet milled and thereafter de-watered. Fine refined clay (e.g. activated bentonite) is then mixed into the moist milled ore-carbon blend. The mixture is then pelletized with a pelletizing drum. The over- and undersized green pellets are recycled, while the appropriate-sized green pellets are layered on a stainless steel sintering belt, which is protected by a layer of already sintered pellets. The green pellets are then heated in a furnace, while air is pulled through the pellet bed to sinter the pellets. The amount of carbon in the green pellets is limited to supply just enough exothermic energy to sinter the pellets to the correct hardness. This process produces evenly-sized, hard and porous furnace pelletized feed material, which result in reduced furnace instabilities, lower SEC and improved Cr recovery efficiencies, if compared to the conventional open/semi-closed SAF operation (Process Option A). However, the sintering step is in essence an oxidizing process and a small amount of Cr(VI) might therefore form. The levels of Cr(VI) that form will depend on the raw material composition, particle size, plant layout, green pellet carbon content, reaction temperature, residence times, etc. Mandiwana et al. (2007) reported Cr(VI) concentrations of 2270–7070 $\mu g\ g^{-1}$ in dust collected in the proximity of such sintering furnaces. However, these values are likely to be over-estimations, since Glastonbury et al. (2010) proved that the sample preparation techniques applied by the aforementioned authors were prone to *in situ* generation of Cr(VI). It should therefore be an important future research objective to quantify Cr(VI) in off-gas particulates originating from such a sintering plant.

In the pre-reduced pelletized process (Process Option C) the chromite concentrate (<1 mm) is dry-milled together with 12–16 wt % carbonaceous reductant (fine coke, char or anthracite) and a clay binder (bentonite, or attapulgite). As is evident, substantially more carbon is added to the mixture than in the oxidative sintered process (Process Option B). Water is then added during the mixing step to obtain the desired moisture content, after which the moist material is pelletized on a pelletizing disk. The green pellets are then dried and pre-heated in a grate, after which they are cured in a counter-current rotary kiln. Such kilns are usually fired with pulverized coal, although CO-rich off-gas from closed SAFs (Du Preez et al., 2015) and crude oil can also be used. In essence, this is a reducing process. CO gas concentrations of 1–15% are common in the gas exiting the kiln and entering the grate. The high pellet carbon content also results in a partial positive CO gas pressure inside the pellets. This partial positive pressure prevents oxygen from entering the core of the pellets. Due to its reductive nature, less Cr(VI) is expected to be generated during the pre-reduced pellet curing process than is generated during an oxidizing pellet-curing process (Process Options B). However, since firing of these counter-current rotary kilns takes place from within the kiln, oxygen must be available for the combustion of the pulverized coal, CO

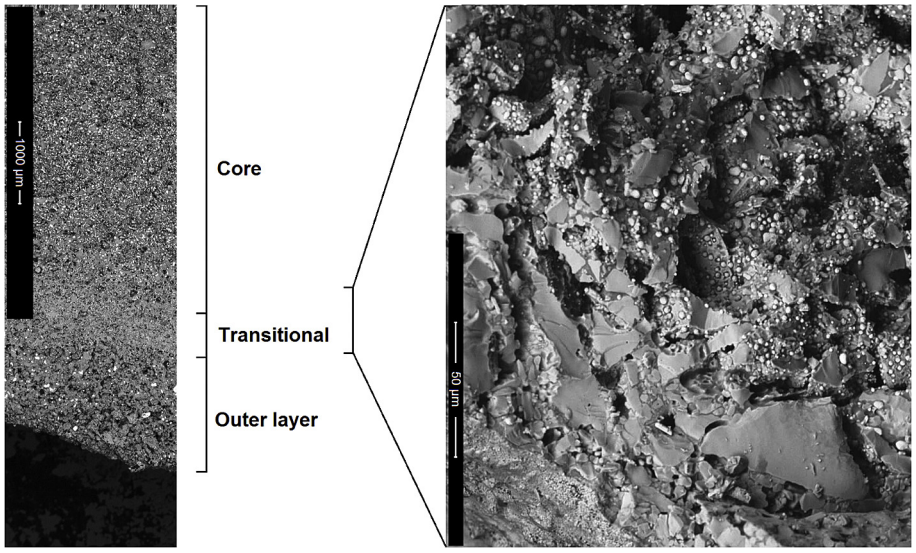

Fig. 8. SEM micrograph of a polished section of a pre-reduced pellet (left), as well as a micrograph of an unpolished section zoomed-in on the transitional zone and a portion of the pre-reduced core, with metallized droplets clearly visible (right) (Kleynhans et al., 2012).

gas or the crude oil. This results in the cured pellets usually having a thin oxidized outer layer (as indicated in Fig. 8, Kleynhans et al., 2012) in addition to the reduced core, suggesting that small amounts of Cr(VI) might also be formed.

As far as the authors could assess, a direct comparison of Cr(VI) generation between the curing steps of Process Options B and C has yet to be undertaken and it can therefore not be stated with confidence which process option generates less Cr(VI). This comparison should therefore be an important future research objective. However, both these processes represent a huge improvement in terms of the overall Cr(VI) footprint, if compared to conventional open/semi-closed FeCr production (Process Option A).

3.2.5. Pellet storage (Fig. 6, process step 5)

Assessments of possible Cr(VI) leaching from cured pellets produced by Process Options B and C have not yet been published. Therefore, leaching tests performed on such pellets should be considered as an important study aspect prior to selecting smelting process options for the Ring of Fire. Such results will indicate whether any preventative measures should be taken during pellet storage, e.g. storing of cured pellets on a lined surface.

As previously mentioned (Section 2), the possible natural occurrence and/or formation of Cr(VI) under ambient conditions for the Canadian ores needs to be assessed. In the unlikely event that liberation and/or formation of Cr(VI) from such ores is/are possible, the area where the lumpy chromite ore stockpiles are located prior to batching would also need to be lined to prevent possible surface and ground water pollution. This would also apply to chromite concentrate consumed by the pelletization section of the plant (i.e. storage prior to process step 1).

3.2.6. Batching (Fig. 6, process step 6)

The action of batching (i.e. weight proportioning of pellets, as well as lumpy chromite, reductants and fluxes according to a predetermined metallurgical recipe) does not hold any dangers of Cr(VI) generation. However, spillages of possible Cr(VI) containing materials during batching and conveying should be avoided with appropriate engineering solutions and subsequent maintenance procedures.

3.2.7. Pre-heating (Fig. 6, process step 7)

As far as the authors could ascertain, the possible Cr(VI) formation during pre-heating of batched material mixtures, prior to smelting of these materials in a furnace has not yet been evaluated and presented in the public domain. The pre-heating temperatures would be considerably lower than the temperatures required during pellet curing (process step 4), and the likelihood of Cr(VI) formation is therefore substantially lower. Typical pre-heating temperature achieved at the Outokumpu smelter in Finland is 500 °C.

3.2.8. Furnace smelting (Fig. 6, process step 8)

Many factors will affect the possible formation of Cr(VI) during smelting, of which the most important are likely to be the availability of oxygen, slag composition, presence of very fine ore and the temperature above the material bed (i.e. area above material bed and below furnace roof). These factors are therefore discussed separately.

Since oxygen is required for the oxidation of Cr(III) to Cr(VI), the availability of oxygen during smelting will influence the formation of Cr(VI). In practice, this implies that a closed furnaces (SAF or DCF) will generate less Cr(VI) than an open/semi-closed SAF, with all other factors being equal (e.g. production capacity, bed temperature, composition of feed material, slag basicity). Although both open/semi-closed and closed furnaces have a reducing environment below the burden material, a closed furnace also has a reducing CO-rich atmosphere above the burden material, while an open/semi-closed furnace has a partially oxidizing environment due to ambient air entering below the furnace roof. These basic principles are demonstrated by the simple pictorial representations of an open/semi-closed SAF and a closed SAF presented in Fig. 9.

During smelting, Cr(VI) is likely to form in the area above the bed material, since the feed material bed itself contain carbonaceous reductants (e.g. coke, char and anthracite) that reduce Cr(III) in the ore to Cr(0) in the FeCr product. Table 1 presents data from Gericke (1995), who indicated the differences in water soluble Cr(VI) contents (not total Cr(VI)) of particulate matter obtained from the off-gas from semi-closed and closed FeCr SAFs. The significance of the slag regimes (acid or basic) will be discussed later in this section, while the relevance of the water soluble contents referred to in this data (Table 1) will be discussed in Section 4.

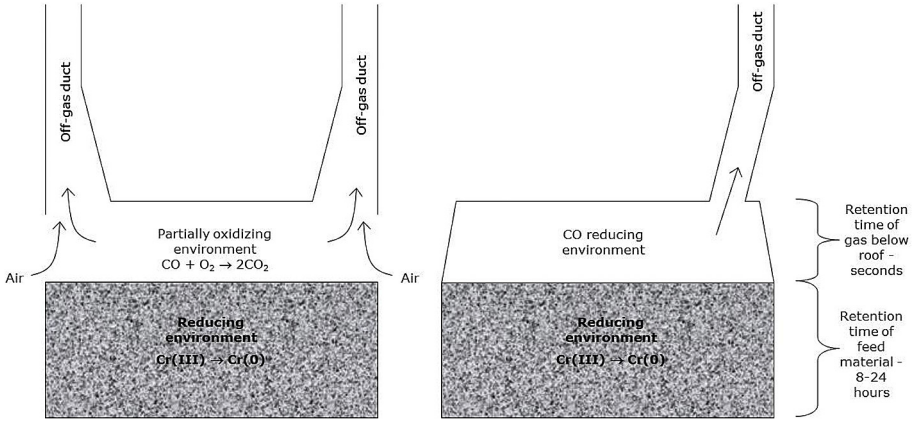

Fig. 9. Simplified representation of an open/semi-closed SAF (left) and a closed SAF (right) to demonstrate the availability of oxygen and the effect on Cr(VI) formation.

Table 1
Water soluble Cr(VI) contents of off-gas particulate matter from various types of FeCr SAFs fed with South African chromite ore (Gericke, 1995).

Furnace and slag description	Cr(VI) ($\mu g.g^{-1}$)
Closed furnace, with acid slag operation	5
Closed furnace, with basic slag operation	100
Semi-closed furnace, with acid slag operation	1000
Semi-closed furnace, with basic slag operation	7000

Considering all the afore-mentioned, and assuming comparative operating characteristics (furnace capacities, bed temperature, composition of feed material, slag basicity, etc.), it is strongly recommended that only closed furnace designs, which generates less Cr(VI) than open/semi-closed furnaces, should be considered for the Ring of Fire developments.

From the data presented in Table 1 it is also evident that a FeCr smelting furnace operated on a basic slag regime will generate more Cr(VI) than a similar furnace operated on an acid slag regime. This is due to the presence of higher concentrations of alkali and/or alkaline earth metal containing compounds in basic slag, which is achieved by the addition of fluxes such as limestone, magnesite and dolomite, in addition to the acid flux component (quartz). In contrast to FeCr production, Cr(VI) chemicals are produced *via* alkali roasting of chromite ore, by purposefully oxidizing the Cr(III) in the ore to Cr(VI) in the presence of soda ash (e.g. Antony et al., 2001). The alkali and/or alkaline earth content of FeCr feed materials is obviously only a fraction of that encountered during alkali roasting of chromite, but fundamental aspects that stimulate oxidation of Cr(III) to Cr(VI) are the same. Therefore, with all other factors being equal, a FeCr furnace operated on an acid slag generates less Cr(VI) than a comparable furnace operated on a basic slag. In a similar manner, the use of binders, catalysts, accelerants and any other compounds containing alkali and/or alkaline earth containing compounds should be avoided or minimized in all high temperature process steps applied during FeCr production. For instance it is known that several alkali and/or alkaline earth containing compounds enhance the degree of pellet pre-reduction obtained during Process Option C (e.g. Neizel et al., 2013 and references therein).

As previously stated, it is not preferred to feed fine materials directly into a FeCr SAF, since it makes the furnace bed impermeable that could result in so-called bed turnovers and blowing of the furnace. Apart from the obvious safety risks associated with the afore-mentioned instabilities, bed material disruptions also result in more fine material being suspended off the bed. Such suspended fines could be extracted with the furnace off-gas. Fig. 10 presents a

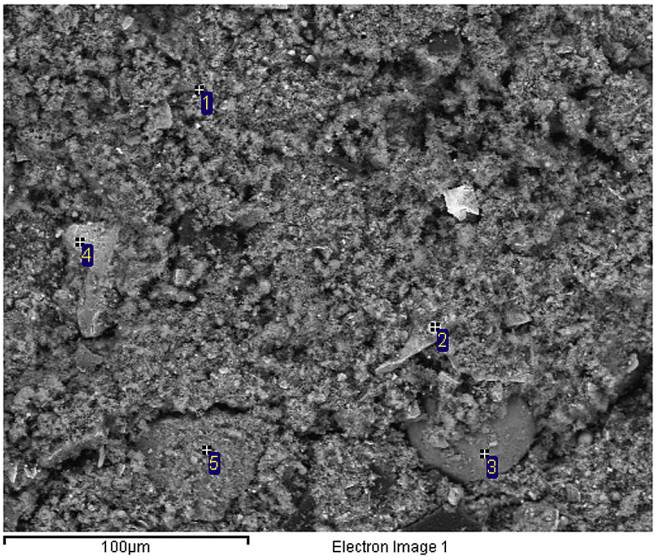

Fig. 10. A SEM micrograph of a typical bag filter dust sample originating from a semi-closed FeCr SAF.

SEM micrograph of a typical bag filter dust sample from a semi-closed FeCr SAF. The larger unevenly shaped particles that can be seen (numbers 2 to 5 in the figure) are un-reacted feed materials (chromite, fluxes and reductants). During the process of suspension and extraction, the fine Cr-containing particles will be exposed to partially oxidizing conditions above the bed material (see Fig. 9, with the associated text) in open/semi-closed furnaces (Process Option A), leading to a possible increase in Cr(VI) generation. Data to quantify the correlation between increased fines content of the feed material and possible Cr(VI) generation have not been presented in the public domain, but as a general rule of thumb it can be recommended that the content of Cr-bearing material that is fine enough to be ejected off the furnace bed must be kept as low as possible. In practice this can be achieved by screening feed materials before it is consumed in a FeCr SAF. Currently, Outokumpu in Finland (applying Process Option B) screens the FeCr smelter feed to remove the < 4 mm material.

The stability of a SAF bed, as referred to in the previous paragraph, depends on various factors. The fine material content has already been discussed. However, electrode length also plays a significant role. The oxidation of Cr(III) to Cr(VI) is dependent on temperature and oxygen partial pressure. Under normal operating

conditions on a particular SAF, the carbon content of the feed is adjusted in accordance with the metallurgical balance, targeting specific alloy and slag chemistry. However, the length of the electrodes will determine the distribution of heat in the furnace bed material. Short electrodes will result in a hotter surface layer, while long electrodes will result in a cooler surface layer. In an open/semi-closed FeCr SAF, a hotter partially oxidizing environment above the furnace bed will increase Cr(VI) generation. These deductions were made by Glastonbury et al. (2010) based only on logical assumptions and practical experience. As far as could be ascertained, no data quantifying the possible increased Cr(VI) formation during short electrode periods have been published. Short electrodes are not a design issue, but more an indication of operational stability.

3.2.9. Tapping, slag cool down and product handling (Fig. 6, process steps 9, 10)

As far as the authors could assess, there is no data available in the public domain that quantify the formation of Cr(VI) during tapping. However, it stands to reason that Cr-containing slag and metal that are tapped at > 1600 °C in ambient atmospheric conditions (with oxygen available) could result in some Cr(VI) formation. This notion is supported by the Health Safety and Environment Guidelines for Chromium report of the ICDA (2007), which states that "*hexavalent chromium compounds are found in small amounts in the highly oxidizing fumes from the melting/smelting processes, particularly the tapping process*". The key to reducing the potential Cr(VI) occupational health effects during this process step is to minimize splashing of liquid slag (decreased reaction area between the atmosphere and melt) and to have an effective taphole and runner fume extraction system, which will limit the exposure of operational personnel to possible Cr(VI) containing fumes. Additionally, fumes/dust captured by the extraction system must be contacted with water (e.g. in a wet scrubber), since this will immediately reduce the occupational health risk. Contact with water also eliminates the possible risk of wind dispersal. Maintaining operational availability of the taphole fume extraction system should be one of the highest priorities. Therefore, the design of the taphole fume extraction system should receive significant attention for any Ring of Fire developments. Cleaning of the runner, i.e. the furrow in which metal and slag are tapped from the furnace is usually a mechanized action. This is typically achieved with a front-end-loader/excavator, or with an overhead crane, during which the taphole fume extraction system can easily be damaged.

After solidification of the FeCr metal, it is unlikely that it could serve as a source of Cr(VI). However, slag is by volume the largest waste product produced during chromite smelting (Beukes et al., 2010) and it therefore requires additional attention. According to Beukes et al. (2010) in early period FeCr production, mono-product type disposal of FeCr slag was not rigorously applied and it was common to encounter the co-disposal of Cr(VI) containing bag filter dusts, together with FeCr slag. Within the context of possible future Ring of Fire FeCr developments, historic slag issues are irrelevant since new operations in Canada could prevent such mistakes. With regard to the tapping practice associated with hot current arising slag, two main hot slag handling practices are usually applied, i.e. (1) air cooling with limited water addition to enhance the cooling rate and (2) water granulation of the liquid slag.

Most of the South African FeCr smelters allow liquid slag to run into a designated slag bay, where it is air-cooled and spayed with a limited amount of water to accelerate the cooling process. However, this method is prone to the formation of additional Cr(VI), since the liquidus temperature of acid slag is in the order of > 1600 °C, while that of basic slag is > 1700 °C. According to Riekkola-Vanhanen (1999), FeCr slag contains 3–15% Cr_2O_3, mainly as unreduced, or partly reduced ore. Exposure of Cr-containing materials at the afore-mentioned temperatures to ambient atmospheric conditions will result in some Cr(VI) formation. Although data do not exist to quantify the Cr(VI) formation in this slag cooling process, preventative measures such as including a reducing agent, e.g. Fe(II), in the water that is used during slag cooling and capturing of aqueous drainage from slag bay areas should be considered. Additionally, any remaining FeCr metal in the slag can be recovered with physical separation techniques such as water-borne jigging, which can facilitate the effective treatment of Cr(VI) (Shen and Forssberg, 2003; Mashanyare and Guest, 1997; Coetzer et al., 1997). Properly treated air-cooled slag can be used as a replacement for building agglomerate (stone) in various applications, including cement bricks, concrete and road construction.

In contrast to the above-mentioned, 80% of the hot liquid slag at the Outokumpu FeCr smelter in Finland is granulated (Riekkola-Vanhanen, 1999). This process entails that the liquid slag is directed down a runner with water jets into a larger water pool. There are two advantages to this process, if compared to the above-mentioned air cooling of slag: (1) the exposure time of hot slag to the ambient atmosphere is substantially reduced, since granulation takes place within seconds after the liquid slag exits the tap hole, (2) the crystalline structure of the granulated slag consists of glassy-like phases (Riekkola-Vanhanen, 1999), which will limit/prevent leaching of compounds from it. The granulated slag is used in various applications, including road-building, under-building filling, paving, as a sand blasting grit and for the production of refractory castables (Riekkola-Vanhanen, 1999), with under-building filling and road-building being the most common in Finland (Niemelä and Kauppi, 2007). However, during slag granulation extreme caution should be taken to avoid liquid FeCr metal accidentally entering the slag runner, since this could results in an explosion. Therefore, plant design should prevent run-away taps from entering this area.

3.2.10. Wet scrubbing and flaring of CO-rich off-gas (Fig. 6, process step 11)

The volume and composition of the off-gas formed by a closed FeCr furnace (SAF or DCF) depend on various factors such as the feed materials, feed pre-treatment methods, design of the furnace, furnace operating philosophy and metallurgical condition of the process (Beukes et al., 2010). Gas volumes generated by closed SAF FeCr have been reported to be 220 to 250 $Nm^3.h^{-1}$ per MW or 650 to 750 $Nm^3.ton^{-1}$ FeCr, consisting of 75–90% CO, 2–15% H_2, 2–10% CO_2 and 2–7% N_2 (Niemelä et al., 2004). The solid content of the uncleaned furnace off-gas is typically 35–45 g. Nm^{-3} and depends on the operational conditions and the production technology (Niemelä et al., 2004). Cleaning of this off-gas is usually achieved with wet venturi scrubbing. The cleaning efficiency of wet scrubbers can be as high as 99.9%, after which the cleaned off-gas typically contains less than 50 mg. Nm^{-3} particulates (Niemelä et al., 2004). The particles remaining in the cleaned off-gas are very fine, with particles smaller than 1 μm being very difficult to remove with a wet venturi scrubber. At the Outokumpu FeCr operations in Finland, the cleaned off-gas is cleaned further by filtering the gas with a sintered plate filter to reduce particulate levels to <5 mg. Nm^{-3} (Niemelä et al., 2004; Päätalo and Raiskio, 2015). As far as the authors could assess, the sintered plate filters after wet venturi scrubbers are not used by the South African FeCr producers that apply Process Option B, C and D, and it is unlikely that it is used in other FeCr producing countries such as China, India and Kazakhstan. However, application thereof should be compulsory for the Ring of Fire developments, in order to ensure application of best practice.

The first study available in the peer-reviewed public domain to quantified the possible formation of Cr(VI) in the flaring of CO-rich off-gas from closed FeCr furnaces, was recently published (Du Preez

et al., 2015). These authors found that Cr(VI) formation during flaring was dependent on flaring temperature, size of the particles passing through the flare, and retention time within the flame. However, if no Cr-containing particles pass through the flare, no Cr(VI) can be formed. Therefore, the importance of implementing additional measures, such as the above-mentioned filtering of the off-gas after the wet venturi scrubbers with a sintered plate filter, is obvious. Burning of un-cleaned off-gas in the raw gas stack should be avoided as far as possible, since this will result in a significant amount of Cr-containing particles passing through the flare. Cleaned CO-rich off-gas should be utilized as an energy source at the plant, keeping the toxicity and explosive nature of CO gas in mind (Niemelä et al., 2004). Excess CO-rich off-gas could be combusted to generate hot water for the workforce/community, generating electricity to minimize the carbon footprint of the plant, or as fuel in rolling mills for reheating slabs in integrated stainless steel plants.

Du Preez et al. (2015) formulated an empirical model that can be used to predict Cr(VI) generation during flaring, which is indicated in Equation (2).

$$\%\ \mathrm{Cr(VI)}\ \text{conversion} = -3.78\text{x}10^{-3} + (1.51\text{x}10^{-6}\ \text{x Temp}) + (1.07\ \text{x}\ 10^{-2}\ \text{x}\ d_{90}^{-0.3203}) + (0.94\ \text{x}\ 1.08\ \text{x}\ 10^{-3}\exp^{(2.75475)(\text{Retention time})}) \quad (2)$$

In Equation (2), "Temp" is the flaring temperature (K), "d_{90}" the d_{90} particle size (μm) of the particulate matter passing through flare and "Retention time" the retention time (seconds) of particles within the flare. The afore-mentioned equation was used to predict formation of Cr(VI), which compared relatively well with laboratory results (Fig. 11).

3.2.11. Bag filter dust (Fig. 6, process step 12)

As was indicated in Table 1, bag filter dust from open/semi-closed FeCr SAFs is likely to be the FeCr waste material with the highest Cr(VI) content. As with dry milling dust, captured bag filter dust must be contacted with water to immediately reduce the risk of human respiratory exposure and environmental dispersion.

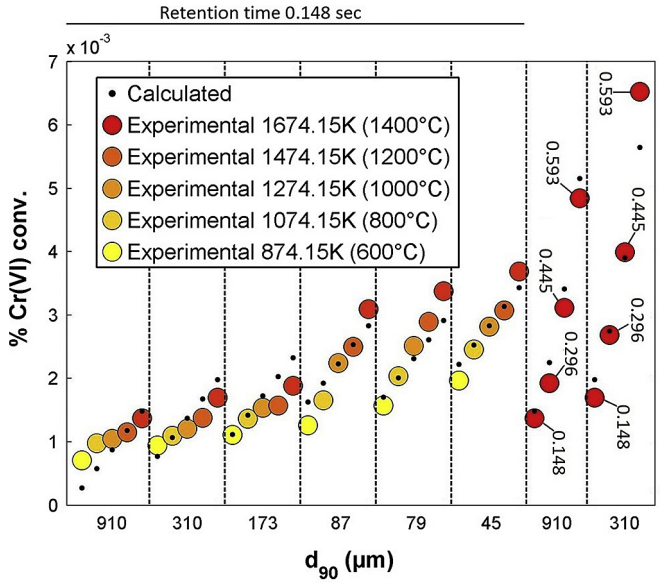

Fig. 11. Calculated % Cr(VI) conversion values using Equation (2) compared to experimental values for metallurgical grade South African ore chromite. All data presented in the figure were for particles spending 0.148 s in the heated area of a furnace to simulate a flare, except for the last two columns which also indicate retention times of up to 0.593 s (Du Preez et al., 2015).

Process water utilized for contacting bag filter dust must be treated to reduce Cr(VI) (discussed in Section 4). The wearing of appropriate dust masks must also be compulsory for operational personnel in the bag filter section.

Quantifying the atmospheric lifetimes of Cr(VI) containing particles that might be emitted (e.g. bag filter particles or particles passing through CO-rich off-gas flare) by future Canadian FeCr developments should be an important future research objective, since such values must be considered in atmospheric modeling studies to evaluate the wider regional impact. As far as could assess, there is currently no such assessment available in the public domain for the Finnish conditions. As was indicated in Section 2 (Fig. 4 and associated text), all atmospheric inter-conversion reactions leading to the possible Cr(VI) formation and reduction to Cr(III) are water-phase reactions (Kimbrough et al., 1999; Seigneur and Constantinou, 1995). During the humid Canadian summer conditions, Cr(VI) reduction will dominate and result in likely shorter atmospheric lifetimes, while in winter when moisture is frozen out of the atmosphere the situation might be different. Current estimates of the atmospheric half-life of Cr(VI) range from 16 h to 4.8 days (Kimbrough et al., 1999 and references therein), but this might not be valid for Canadian conditions. Recently Venter et al. (2016) detected Cr(VI) in ambient particulate matter that was sampled 105 km downwind of the nearest pyro-metallurgical smelter in the western Bushveld Complex, South Africa.

3.2.12. Disposal of bag filter dust and scrubber sludge (Fig. 6, process step 11 and 12)

According to the authors, bag filter dust originating from open/semi-closed SAFs and scrubber sludge originating from wet venturi scrubber cleaning the off-gas of closed SAFs or DCFs should be treated to reduce Cr(VI) and thereafter be disposed of in hazardous waste storage facilities (e.g. lined slimes dams). The reason for this recommendation will become evident in Section 4, where Cr(VI) treatment is discussed.

3.3. Additional processes

Hot liquid High Carbon Charge Grade FeCr can be refined in a converter to produce Medium and/or Low Carbon FeCr. In essence, this process is somewhat similar to stainless steel processes, during which argon oxygen decarburization (AOD) and vacuum oxygen decarburization (VOD) are used to remove C from stainless steel; however, in this case the objective would be to remove C from FeCr. Outokumpu's operations in Finland currently use such a conversion process (i.e. CRC, to remove silicon and some C from the liquid FeCr). During the CRC process, oxygen is blown into the liquid metal, which reduces the silicon content from 4–5 to less than 0.5 wt %, and the C content from approximately 7 to 3 wt % (Heikkinen, 2013). The heat released during the process is used for scrap melting. Since FeCr in all the afore-mentioned converter processes is in the hot liquid form and some oxidation has to take place to remove C (and silicon), small amounts of Cr(VI) might form. Also, limestone is typically added as a flux on top of the liquid FeCr in some of these processes, which as explained in Section 3.2.8 can enhance Cr(VI) formation. As far as could be ascertained, Cr(VI) formation and content of the lime-rich slag of such convertors have not yet been presented in the public domain. Therefore, if any Canadian development want to adopt such processes, it must assess Cr(VI) formation and develop appropriate preventative measures.

Within the Canadian context, the possible production of a FeCr-like alloy by direct solid state reduction without smelting, has received significant attention (Winter, 2014). It is not the intention of the current paper to evaluate the operability of this process, therefore only Cr(VI) related aspects are considered. Also, since no

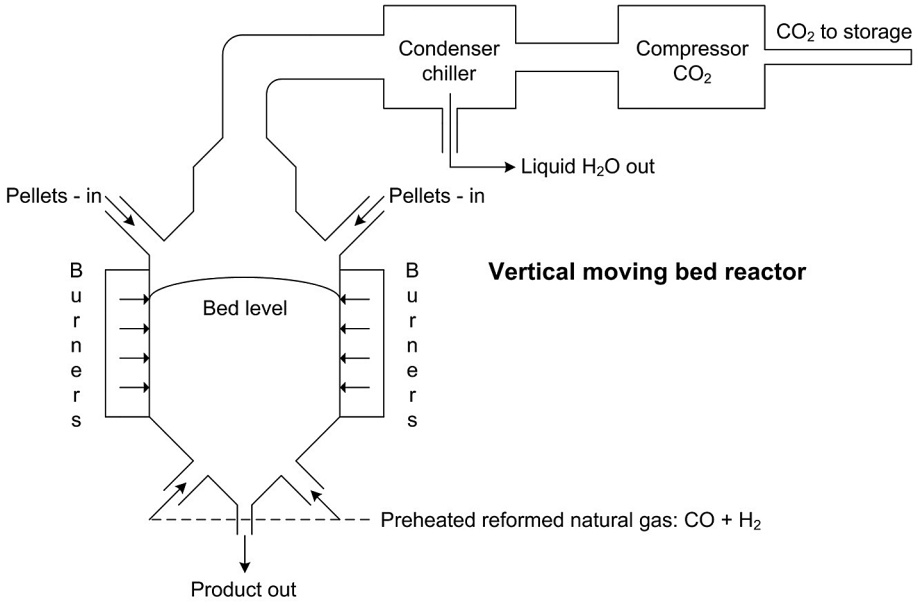

Fig. 12. Schematic outline indicating the proposed new process to produce Cr-containing alloy without smelting (adapted from Winter, 2014).

such operations exist, the evaluation is based solely on documentation available in the public domain (Winter, 2014). Fig. 12 presents the schematic outline of the proposed process. In essence, the process entails that chromite agglomerates (e.g. pellets) containing a carbonaceous reductant and an alkaline accelerant are reduced in a reaction vessel to such an extent that Cr-containing alloy can be recovered with physical separation after being liberated with milling, without the need for smelting. The most significant aspect of this proposed process is that firing of the process (indicated as "Burners" in Fig. 12) is proposed to be external to the reaction vessel. This is in contrast to the curing of green pellets produced during the pre-reduced pelletization process (Process Option C, Section 3.2.4) where pellets are cured within the same reaction vessel in which firing occurs (counter-current rotary kiln). External firing, as proposed in this new process, will reduce the tendency of the cured chromite agglomerates to form an oxidized outer layer as previously indicated (Fig. 8 and associated text). Based on this, the Cr(VI) formation potential of this process seems to be lower than the currently applied pre-reduction process (Process Option C). However, the use of an alkaline accelerant may have detrimental consequences, as previously indicated (Section 3.2.8).

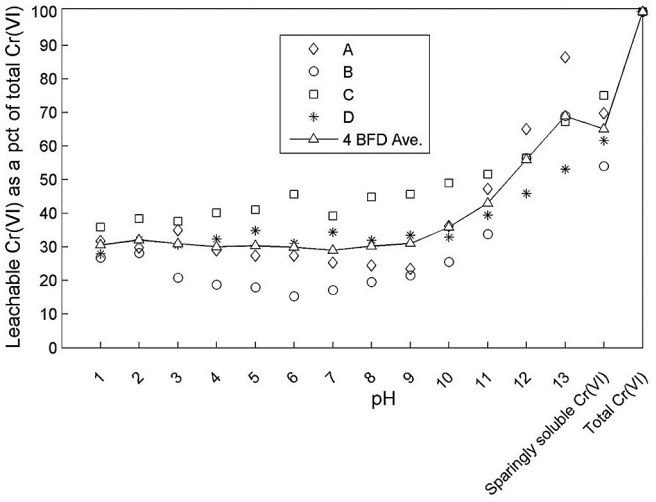

Fig. 13. Percentage leachable Cr(VI) as a function of solution pH (adapted from Du Preez et al., 2017).

4. Treatment of Cr(VI) containing waste

Prevention and waste minimization are obvious waste management options for Cr(VI). However, if Cr(VI) containing wastes are produced, recycling or treatment of such wastes must be applied. Treatment would involve capturing of the Cr(VI)-bearing materials, their leaching, and reduction in the aqueous phase. Beukes et al. (2012) reviewed the use of chemical reduction of Cr(VI) containing waste of the FeCr industry and this review is therefore not repeated here. The most important aspects that Beukes et al. (2012) pointed out were that an appropriate inorganic reducing agent should be used to reduce Cr(VI), so that insoluble Cr(III) hydroxide species form (Fig. 3 and associated text). Currently in South Africa, most FeCr producers use Fe(II) containing reducing agents to treat Cr(VI) containing process water (Beukes et al. 2012 and references therein). Some organic compounds can form water-soluble Cr(III)-complexes that are undesirable (Figs. 2 and 4 and associated text) and should therefore be avoided. Although soluble Cr(III) species may not be toxic or carcinogenic, potential exists for the soluble Cr(III) coming into contact with MnO_2 that is a naturally occurring oxidant for Cr(III) (Figs. 2 and 4).

From the above-mentioned discussion, it is evident that Cr(VI)-containing waste water can be dealt with in an acceptable manner. However, Maine et al. (2005) reported Cr(VI) leaching from FeCr wastes for days. Additionally, the authors also know from personal experience that properly treated Cr(VI) containing waste that has been stored in a purposefully designed waste facility (e.g. slimes dams) could leach small amounts of Cr(VI) over a prolonged period. Initially, it was thought that this slow leaching was due to some Cr(VI) containing waste (e.g. bag filter dust) containing glassy phases, which prevented the Cr(VI) in the core of such particles from leaching out quickly (Beukes et al., 1999). However, recent results by Du Preez et al. (2017) proved that the leachability of Cr(VI) from typical FeCr bag filter dust is dependent on pH. Even more significant is that within the pH range in which most FeCr waste waters occur (up to pH 9) only approximately 31% of total

Cr(VI) is released (Fig. 13). The reason for this is because Cr(VI) compounds can be classified as water-soluble (e.g. K_2CrO_4, Na_2CrO_4, $Na_2Cr_2O_7$), sparingly water-soluble (e.g. $SrCrO_4$) and water-insoluble (e.g. $BaCrO_4$ and $PbCrO_4$) (Ashley et al., 2003). By using appropriate buffer solutions Du Preez et al. (2017) proved that the afore-mentioned bag filter dusts contained approximately 34% sparingly water-soluble Cr(VI) compounds. The possible occurrences of sparingly-soluble Cr(VI) compounds in FeCr wastes are very problematic and new methods to dissolve both the water-soluble and sparingly water-soluble Cr(VI) fractions from such wastes should be a priority for researchers and FeCr producer alike. Ideally, to address this, the cation associations of the anion (chromate) in which the Cr(VI) occurs should be established for all Cr(VI)-containing wastes, since this directly determines the solubility characteristics. The inability to leach the Cr(VI) sparingly water-soluble fraction from FeCr wastes currently prevents optimal Cr(VI) treatment. The possible occurrence of water-insoluble Cr(VI) compounds are less problematic, since the solubilization of these compounds under conditions likely to occur during storage of waste material is unlikely.

From the literature review and discussions in this paper the authors believe that Cr(VI) containing wastes generated by chromite mining and FeCr production can be classified into three broad categories, i.e. wastes that should be i) recycled within the process (e.g. captured dust that mainly contain feed materials), ii) repurposed or re-used in other applications (e.g. granulated slag, or air cooled slag that has been treated to effect Cr(VI) reduction) and iii) considered as hazardous (e.g. open/semi-closed SAF bag filter dust that has been treated to reduce Cr(VI), closed SAF/DCF scrubber sludge that has been treated to reduce Cr(VI), mining tailings/wastes that are prone to Cr(VI) formation through atmospheric oxidation). The latter group, i.e. hazardous wastes, should be stored in appropriately designed lined waste facilities (e.g. lined slimes dam) that comply with the country specific legislation and international best practice. Such waste facilities should also be monitored to detect possible failure (e.g. leakage detection system indicating that liner have failed). However, metallurgical process performance, as well as occupational health and environmental practices should also be monitored, and continuous improvements undertaken to address shortcomings that are observed.

5. Conclusions

The conclusions and recommendations from this paper are summarized in Fig. 14. Prior to the development of the Ring of Fire reserves, baseline studies (Step 1, Fig. 14) needs to be conducted. The possible natural occurrences of Cr(VI) and the potential natural oxidation of Cr-containing minerals should be investigated. Additionally, existing anthropogenic sources that emit/release Cr(VI) and/or environmentally mobile Cr(III) species, should be identified. Failure to conduct the afore-mentioned baseline studies will result in the chromite and FeCr industries carrying the total burden if Cr(VI) contamination were to be reported later, even if natural or existing anthropogenic processes are responsible in part, or wholly.

The only process options that is known to generate Cr(VI) during mining and ore beneficiation is dry milling, which should therefore be avoided if possible (Step 2, Fig. 14).

The literature review proved that FeCr production, using recognized processes, will lead to the formation of small amounts of Cr(VI). The Cr(VI) quantities formed are usually in the $mg.kg^{-1}$ concentration range (or lower) and cannot be compared to the manufacturing of Cr(VI) chemicals (e.g. chromate or dichromate). From the assessment of the various process steps, an overall process can be chosen to minimize the formation of Cr(VI) (Step 3, Fig. 14). However, even the most ideal process will still lead to some Cr(VI) being generated. Although the operability of process option was not discussed in this review, it is important to state that individual process steps cannot merely be strung together to find the best overall process to limit Cr(VI) formation, since certain processing steps are not compatible with others. Therefore, a holistic view should be applied, which recognizes that many factors (e.g. physical and chemical characteristics of the ore, capital and operational costs, SEC, carbon footprint, availability of expertise) and not only Cr(VI) will dictate what process options will be chosen.

Since Cr(VI) formation cannot be totally eliminated, some Cr(VI) containing waste will be generated. Therefore, optimum waste treatment (e.g. chemical reduction to effect Cr(VI) reduction), reuse (e.g. slag that has been treated or verified as safe for use) and hazardous waste storage (e.g. slimes dams containing treated bag filter dust and/or scrubber sludge) should be applied (Step 4, Fig. 14).

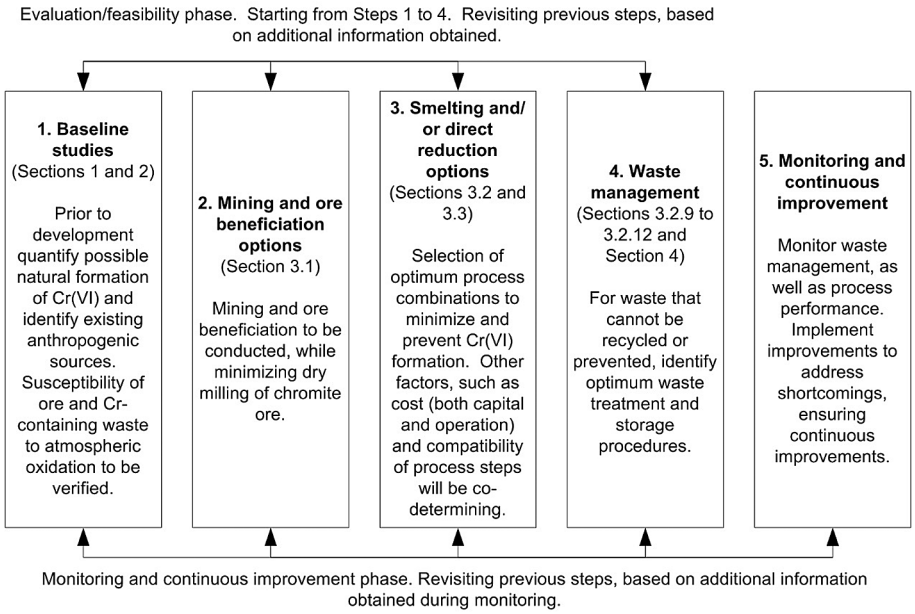

Fig. 14. Iterative steps that need to be considered for the possible development of the ROF to prevent and mitigate Cr(VI) impacts.

During the evaluation/feasibility phase, Step 1 to 4 (Fig. 14) should be considered in an iterative manner. For instance results obtained during the baseline studies (Step 1, Fig. 14) might influence the selection of process options (Step 2 to 3, Fig. 14), or waste management strategies (Step 4, Fig. 14). Alternatively, evaluation of different process options or waste management strategies, might give new insight into additional baseline studies that need to be undertaken. This iterative evaluation should be repeated until a satisfactory overall approach to the development of the ROF is obtained.

Ultimately if the chromite and FeCr industries are established, the effectiveness of preventative and mitigation measures identified during the evaluation/feasibility phase (Steps 1 to 4, Fig. 14) should be monitored (Step 5, Fig. 14). If shortcomings are observed, improvements to selected process options and/or waste management strategies should be applied as required. This again leads to an iterative approach, which results in continuous improvement.

Overall it can be stated that it is possible to produce FeCr without causing Cr(VI) occupational and community health issues, as well as environmental pollution. For instance, Huvinen and Pukkala (2013, 2016) conducted a cohort study of personnel employed by the Finnish FeCr and stainless steel industries during the period 1967–2004 and found that these workers did not have an increased mortality or cancer risk, when compared with the general population. Also, no significant Cr(VI) environmental pollution have been reported for the Finnish chromite mining and smelting industries.

Acknowledgements

The financial assistance of the National Research Foundation (NRF, South Africa, grant number: 101345) towards this PhD bursary of S.P. du Preez is hereby acknowledged. Opinions expressed and conclusions arrived at, are those of the authors and are not necessarily to be attributed to the NRF. The financial assistance and support of Natural Resources Canada under contract Number 3000603956 as part of the Canadian Rare Earth Elements and Chromite R&D Program is hereby acknowledged. All copyrights to this paper are held by the Government of Canada.

References

Abbasi, S., Soni, R., 1983. Stress-induced enhancement of reproduction in earthworm octochaetus pattoni exposed to chromium (vi) and mercury (ii) – implications in environmental management. Int. J. Environ. Stud. 22, 43–47. http://dx.doi.org/10.1080/00207238308710100.

Antony, M., Tathavadkar, V., Calvert, C., Jha, A., 2001. The soda-ash roasting of chromite ore processing residue for the reclamation of chromium. Metall. Mater. Trans. B 32, 987–995. http://dx.doi.org/10.1007/s1166300100876.

Ashley, K., Howe, A.M., Demange, M., Nygren, O., 2003. Sampling and analysis considerations for the determination of hexavalent chromium in workplace air. J. Environ. Monit. 5, 707–716. http://dx.doi.org/10.1039/b306105c.

Bartlett, R.J., 1991. Chromium cycling in soils and water: links, gaps, and methods. Environ. Health Perspect. 92, 17–24.

Beaver, L.M., Stemmy, E.J., Constant, S.L., Schwartz, A., Little, L.G., Gigley, J.P., Chun, G., Sugden, K.D., Ceryak, S.M., Patierno, S.R., 2009. Lung injury, inflammation and Akt signaling following inhalation of particulate hexavalent chromium. Toxicol. Appl. Pharm. 235, 47–56. http://dx.doi.org/10.1016/j.taap.2008.11.018.

Beukes, J.P., Dawson, N.F., Van Zyl, P.G., 2010. Theoretical and practical aspects of Cr(VI) in the South African ferrochrome industry. J. South. Afr. Inst. Min. Metall. 110, 743–750.

Beukes, J.P., Guest, R.N., 2001. Cr(VI) generation during milling. Min. Eng. 14, 423–426. http://dx.doi.org/10.1016/S0892-6875(01)00022-X.

Beukes, J.P., Pienaar, J.J., Lachmann, G., 2000. The reduction of hexavalent chromium by sulphite in wastewater - an explanation of the observed reactivity pattern. Water SA 26, 393–396.

Beukes, J.P., Pienaar, J.J., Lachmann, G., Giesekke, E.W., 1999. The reduction of hexavalent chromium by sulphite in wastewater. Water SA 25, 363–370.

Beukes, J.P., Van Zyl, P.G., Ras, M., 2012. Treatment of Cr(VI)-containing wastes in the South African ferrochrome industry – a review of currently applied methods. J. South. Afr. Inst. Min. Metall. 112, 347–352.

Bollinger, J.E., Bundy, K., Anderson, M.B., Millet, L., Preslan, J.E., Jolibois, L., Chen, H.-L., Kamath, B., George, W.J., 1997. Bioaccumulation of chromium in red swamp crayfish (Procambarus clarkii). J. Hazard. Mater 54, 1–13.

Chang, D., Chen, T., Liu, H., Xi, Y., Qing, C., Xie, Q., Frost, R.L., 2014. A new approach to prepare ZVI and its application in removal of Cr (VI) from aqueous solution. Chem. Eng. J. 244, 264–272. http://dx.doi.org/10.1016/j.cej.2014.01.095.

Chong, J., 2014. Resource Development in Canada: a Case Study on the Ring of Fire. http://www.lop.parl.gc.ca/content/lop/ResearchPublications/2014-17-e.htm#a3. (Accessed 22 March 2016).

Coetzer, G., Giesekke, E., Guest, R., 1997. Hexavalent chromium in the recovery of ferrochromium from slag. Can. Metall. Q. 36, 261–268.

Dhal, B., Thatoi, H.N., Das, N.N., Pandey, B.D., 2010. Reduction of hexavalent chromium by Bacillus sp. isolated from chromite mine soils and characterization of reduced product. J. Chem. Technol. Biotechnol. 85, 1471–1479. http://dx.doi.org/10.1002/jctb.2451.

Dong, X., Ma, L.Q., Gress, J., Harris, W., Li, Y., 2014. Enhanced Cr(VI) reduction and As(III) oxidation in ice phase: important role of dissolved organic matter from biochar. J. Hazard. Mater 267, 62–70.

Du Preez, S.P., Beukes, J.P., Van Dalen, W.P.J., Van Zyl, P.G., Paktunc, D., Loock-Hatting, M.M., 2017. Aqueous solubility of Cr(VI) compounds in ferrochrome bag filter dust and the implications thereof. Water SA 43, 298–309. http://dx.doi.org/10.4314/wsa.v43i2.13.

Du Preez, S.P., Beukes, J.P., Van Zyl, P.G., 2015. Cr (VI) generation during flaring of CO-rich off-gas from closed ferrochromium Submerged Arc furnaces. Metall. Mater. Trans. B 46, 1002–1010. http://dx.doi.org/10.1007/s11663-014-0244-3.

Dubey, C., Sahoo, B., Nayak, N., 2001. Chromium (VI) in waters in parts of Sukinda chromite valley and health hazards, Orissa. India. B. Environ. Contam. Toxicol. 67, 541–548. http://dx.doi.org/10.1007/s00128-001-0157-0.

Eary, L., Rai, D., 1988. Chromate removal from aqueous wastes by reduction with ferrous ion. Environ. Sci. Technol. 22, 972–977. http://dx.doi.org/10.1021/es00173a018.

Environment Canada, 2014. Proposed Amendments to the Chromium Electroplating, Chromium Anodizing and Reverse Etching Regulations. https://www.ec.gc.ca/lcpe-cepa/208517F9-6423-4E9F-86FC-F74D6E0F4E71/Modifications_R%E8glement_Amendments_Regulations-eng.pdf. (Accessed 10 May 2016).

Gediga, J., Russ, M., 2007. Life Cycle Inventory (LCI) Update of Primary Ferrochrome Production. ICDA (International Chromium Development Association).

Gericke, W.A., 1995. Environmental aspects of ferrochrome production. In: Proceedings of 7th International Ferroalloys Congress, Trondheim, Norway, pp. 131–140.

Glastonbury, R.I., Van Der Merwe, W., Beukes, J.P., Van Zyl, P.G., Lachmann, G., Steenkamp, C.J.H., Dawson, N.F., Steward, H.M., 2010. Cr(VI) generation during sample preparation of solid samples – a chromite ore case study. Water SA 36, 105–110.

Godgul, G., Sahu, K., 1995. Chromium contamination from chromite mine. Environ. Geol. 25, 251–257.

Goel, R.P., 1997. Smelting technologies for ferrochromium production - recent trends. In: Vaish, A.K., Singh, S.D., Goswami, N.G., Ramachandraroa, P. (Eds.), Ferro Alloy Industries in the Liberalized Economy. NML Jamshedpur, pp. 37–50.

Guertin, J., 2004. Toxicity and Health Effects of Chromium (All Oxidation States). In: Guetin, J., Jacobs, J.A., Avakian, C.P. (Eds.), Chromium(VI) Handbook. CRC Press, USA, pp. 215–234. ISBN 1-56670-608-4.

Gupta, S., Yadav, A., Verma, N., 2017. Simultaneous Cr(VI) reduction and bioelectricity generation using microbial fuel cell based on alumina-nickel nanoparticles-dispersed carbon nanofiber electrode. Chem. Eng. J. 307, 729–738.

Haggerty, S.E., 1991. Oxide mineralogy of the upper mantle. Rev. Mineral. Geochem 25, 355–416.

Heikkinen, E.P., 2013. On the Role of Computational Thermodynamics in Research and Development of AOD and CRC Processes. PhD. University of Oulu, Finland, p. 106.

Hininger, I., Benaraba, R., Osman, M., Faure, H., Roussel, A.M., Anderson, R.A., 2007. Safety of trivalent chromium complexes: no evidence for DNA damage in human HaCaT keratinocytes. Free Radic. Biol. Med. 42, 1759–1765. http://dx.doi.org/10.1016/j.freeradbiomed.2007.02.034.

Hutchinson, T.H., Williams, T.D., Eales, G.J., 1994. Toxicity of cadmium, hexavalent chromium and copper to marine fish larvae (Cyprinodon variegatus) and copepods (Tisbe battagliai). Mar. Environ. Res. 38, 275–290.

Huvinen, M., Pukkala, E., 2013. Cancer incidence among Finnish ferrochromium and stainless steel production workers in 1967–2011: a cohort study. BMJ open 3, e003819. http://dx.doi.org/10.1136/bmjopen-2013-003819.

Huvinen, M., Pukkala, E., 2016. Cause-specific mortality in Finnish ferrochromium and stainless steel production workers. Occup. Med. 66, 241–246. http://dx.doi.org/10.1093/occmed/kqv197.

IARC (International Agency for Research on Cancer), World Health Organization, 2012. IARC Monographs on the Evaluation of Carcinogenic Risks to Humans, Arsenic, Metals, Fibers and Dust, Vol. 100C, Chromium(VI) Compounds. International Agency for Research on Cancer, Lyon, France, pp. 147–167. ISBN 978 92 832 1320 8.

ICDA, 2007. International Chromium Development Association, Health Safety and Environment Guidelines for Chromium Edition, Paris, France.

ICDA, 2013. International Chromium Development Association, Statistical Bulletin 2013 Edition, Paris, France.

Jin, R., Liu, Y., Liu, G., Tian, T., Qiao, S., Zhou, J., 2017. Characterization of product and potential mechanism of Cr(VI) reduction by anaerobic activated sludge in a

sequencing batch reactor. Sci. Rep. 7, 1681.
Jones, R.T., 2014. DC arc furnaces—Past, present, and future. In: Mackey, P.J., Grimsey, E.J., Jones, R.T., Brooks, G.A. (Eds.), Celebrating the Megascale, Proceedings of the Extraction and Processing Division Symposium on Pyrometallurgy in Honor of David GC Robertson. Wiley, TMS, California, pp. 16–20. http://dx.doi.org/10.1002/9781118889657.ch10.
Kimbrough, D.E., Cohen, Y., Winer, A.M., Creelman, L., Mabuni, C., 1999. A critical assessment of chromium in the environment. Crit. Rev. Env. Sci. Tec. 29, 1–46. http://dx.doi.org/10.1080/10643389991259164.
Kleynhans, E.L.J., Neizel, B.W., Beukes, J.P., Van Zyl, P.G., 2016. Utilisation of pre-oxidised ore in the pelletised chromite pre-reduction process. Min. Eng. 92, 114–124. http://dx.doi.org/10.1016/j.mineng.2016.03.005.
Kleynhans, E.L.J., Beukes, J.P., Van Zyl, P.G., Kestens, P.H.I., Langa, J.M., 2012. Unique challenges of clay binders in a pelletised chromite pre-reduction process. Min. Eng. 34, 55–62. http://dx.doi.org/10.1016/j.mineng.2012.03.021.
Loock-Hattingh, M.M., Beukes, J.P., Van Zyl, P.G., Tiedt, L.R., 2015. Cr(VI) and conductivity as indicators of surface water pollution from ferrochrome production in South Africa: four case studies. Metall. Mater. Trans. B 46, 2315–2325. http://dx.doi.org/10.1007/s11663-015-0395-x.
Maine, C.F., Smit, J.P., Giesekke, E.W., 2005. The Solid Stabilization of Soluble Wastes Generated in the South African Ferrochrome Industry. Final report to the Water Research Commission (of South Africa), WRC Report no 942/1/05.
Mandiwana, K.L., Panichev, N., Ngobeni, P., 2007. Electrothermal atomic absorption spectrometric determination of Cr(VI) during ferrochrome production. J. Hazard. Mater 145, 511–514. http://dx.doi.org/10.1016/j.jhazmat.2007.01.077.
March, J., 1992. March's Advanced Organic Chemistry: Reactions, Mechanisms, and Structure, sixth ed. John Wiley & Sons, New Jersey.
Mashanyare, H., Guest, R., 1997. The recovery of ferrochrome from slag at Zimasco. Min. Eng. 10, 1253–1258.
McCullough, S., Barcza, N., Hockaday, S., Johnson, C., 2010. Pre-reduction and Smelting Characteristics of Kazakhstan Ore Samples. Mintek.
Miller, R.B., Giai, C., Iannuzzi, M., Monty, C.N., Senko, J.M., 2016. Microbial reduction of Cr (VI) in the presence of chromate conversion coating constituents. Bioremed. J. 20, 174–182.
Mintek, 2016. http://www.mintek.co.za/. (Accessed 23 March 2016).
Mishra, A.K., Mohanty, B., 2008. Acute toxicity impacts of hexavalent chromium on behavior and histopathology of gill, kidney and liver of the freshwater fish, Channa punctatus (Bloch). Toxicol. Pharmacol. 26, 136–141.
Motzer, W.E., Engineers, T., 2004. Chemistry, geochemistry, and geology of chromium and chromium compounds. In: Guetin, J., Jacobs, J.A., Avakian, C.P. (Eds.), Chromium(VI) Handbook. CRC Press, USA, pp. 23–91. ISBN 1-56670-608-4.
Murthy, Y.R., Tripathy, S.K., Kumar, C.R., 2011. Chrome ore beneficiation challenges and opportunities – a review. Min. Eng. 24, 375–380. http://dx.doi.org/10.1016/j.mineng.2010.12.001.
Naiker, O., 2007. The development and advantages of Xstrata's Premus Process. In: Proceedings Ferroalloys 11th International Congress, pp. 112–119.
Neizel, B.W., Beukes, J.P., Van Zyl, P.G., Dawson, N.F., 2013. Why is $CaCO_3$ not used as an additive in the pelletised chromite pre-reduction process? Min. Eng. 45, 115–120. http://dx.doi.org/10.1016/j.mineng.2013.02.015.
Niemelä, P., Kauppi, M., 2007. Production, characteristics and use of ferrochromium slags. In: Proceedings of 11th International Ferroalloys Congress, New Delhi, India, pp. 171–179.
Niemelä, P., Krogerus, H., Oikarinen, P., 2004. Formation, Characterization and Utilization of CO-gas Formed in Ferrochrome Smelting. In: Proceedings of 10th International Ferroalloys Congress, Cape Town, South Africa, pp. 68–77.
Outokumpu, 2016. http://www.outokumpu.com/en/company/outokumpu-in-europe-middle-east-and-africa/production-sites/Tornio/Pages/Outokumpu-production-site-Tornio-Works-Finland.aspx (accessed 23 March 2016).
Päätalo, M., Raiskio, J., 2015. Dust Emission Minimizing, Measuring and Monitoring in FeCr-production in Tornio Works. In: Proceedings of 14th International Ferroalloys Congress, Kiev, Ukraine, pp. 703–708.
Paktunc, D., 2016. Chromite: Update on Progress. Presentation Presented at the Chromite Processing and Environment Technical Committee.
Peralta, R.J., Gardea-Torresdey, L.J., Tiemann, J.K., Gomez, E., Arteaga, S., Rascon, E., Parsons, G.J., 2001. Uptake and effects of five heavy metals on seed germination and plant growth in alfalfa (Medicago sativa L.). B. Environ. Contam. Toxicol. 66, 727–734.
Peterson, M.L., Brown, G.E., Parks, G.A., 1996. Direct XAFS evidence for heterogeneous redox reaction at the aqueous chromium/magnetite interface. Colloids Surf. A Physicochem. Eng. Asp. 107, 77–88. http://dx.doi.org/10.1016/0927-7757(95)03345-9.
Pöykiö, R., Perämäki, P., Niemelä, M., 2005. The use of Scots pine (Pinus sylvestris L.) bark as a bioindicator for environmental pollution monitoring along two industrial gradients in the Kemi–Tornio area, northern Finland. Int. J. Environ. An. Ch 85, 127–139.
Proctor, D.M., Otani, J.M., Finley, B.L., Paustenbach, D.J., Bland, J.A., Speizer, N., Sargent, E.V., 2002. Is hexavalent chromium carcinogenic via ingestion? A weight-of-evidence review. J. Toxicol. Environ. Health A 65, 701–746. http://dx.doi.org/10.1080/00984100290071018.
Rai, D., Sass, B.M., Moore, D.A., 1987. Chromium(III) hydrolysis constants and solubility of chromium(III) hydroxide. Inorg. Chem. 26, 345–349.
Riekkola-Vanhanen, M., 1999. Finnish Expert Report on Best Available Techniques in Ferrochromium Production. Helsinki.
Seigneur, C., Constantinou, E., 1995. Chemical kinetic mechanism for atmospheric chromium. Environ. Sci. Technol. 29, 222–231.
Shen, H., Forssberg, E., 2003. An overview of recovery of metals from slags. Waste Manag. 23, 933–949.
Testa, S.M., 2004. Sources of chromium contamination in soils and groundwater. In: Guetin, J., Jacobs, J.A., Avakian, C.P. (Eds.), Chromium(VI) Handbook. CRC Press, USA, pp. 143–163. ISBN 1-56670-608-4.
Tiwary, R., Dhakate, R., Rao, V.A., Singh, V., 2005. Assessment and prediction of contaminant migration in ground water from chromite waste dump. Environ. Geol. 48, 420–429. http://dx.doi.org/10.1007/s00254-005-1233-2.
Venter, A.D., Beukes, J.P., Van Zyl, P.G., Josipovic, M., Jaars, K., Vakkari, V., 2016. Regional atmospheric Cr (VI) pollution from the Bushveld complex, South Africa. Atmos. Pollut. Res. 7, 762–767. http://dx.doi.org/10.1016/j.apr.2016.03.009.
Wang, G., Zhang, B., Li, S., Yang, M., Yin, C., 2017. Simultaneous microbial reduction of vanadium (V) and chromium (VI) by Shewanella loihica PV-4. Bioresour. Technol. 227, 353–358.
Warner, B.G., Rubec, C.D.A., 1997. The Canadian Wetland Classification System, second ed. Wetlands Research Centre, University of Waterloo, Waterloo, Ontario. ISBN: 0-662-25857-6.
Wesseldijk, Q., Reuter, M., Bradshaw, D., Harris, P., 1999. The flotation behavior of chromite with respect to the beneficiation of UG2 ore. Min. Eng. 12, 1177–1184.
Williams, A.G., Scherer, M.M., 2001. Kinetics of Cr (VI) reduction by carbonate green rust. Mar. Environ. Res. 35, 3488–3494. http://dx.doi.org/10.1021/es010579g.
Winter, F. 2014. Production of chromium iron alloys directly from chromite ore. PCT patent number PCT/US2014/054644, International filing date: 9 September 2014, Priority date: 21 October 2013.
Zhao, B., Hayes, P., 2010. Effects of Oxidation on the Microstructure and Reduction of Chromite Pellets. In: Proceedings of 12th International Ferroalloys Congress, Helsinki, Finland, pp. 263–273.

APPENDIX B

B.1 Introduction

As stated in Section 2.7.2, the candidate published an article related to the formation of Cr(VI) in fine chromite particulate matter during CO-rich off-gas flaring. Although not part of this study *per se* this article is presented here, so that the reader can understand the total contribution the candidate have made to the field of study.

Cr(VI) Generation During Flaring of CO-Rich Off-Gas from Closed Ferrochromium Submerged Arc Furnaces

S.P. DU PREEZ, J.P. BEUKES, and P.G. VAN ZYL

Ferrochromium (FeCr) is the only source of new Cr units used in stainless steel production, which is a vital modern day alloy, making FeCr equally important. Small amounts of Cr(VI) are unintentionally formed during several FeCr production steps. One such production step is the flaring of CO-rich off-gas from closed submerged arc furnaces (SAF), for which Cr(VI) formation is currently not quantified. In this study, the influence of flaring temperature, size of the particles passing through the flare, and retention time within the flame were investigated by simulating the process on laboratory scale with a vertical tube furnace. Multiple linear regression (MLR) analysis was conducted on the overall dataset obtained, which indicated that retention time had the greatest impact on pct Cr(VI) conversion, followed by particle size and temperature. The MLR analysis also yielded an optimum mathematical solution, which could be used to determine the overall impact of these parameters on pct Cr(VI) conversion. This equation was used to determine realistic and unrealistic worst-case scenario pct Cr(VI) conversions for actual FeCr SAFs, which yielded 2.7×10^{-2} and 3.5×10^{-1} pct, respectively. These values are significantly lower than the current unsubstantiated pct Cr(VI) conversion used in environmental impact assessments for FeCr smelters, *i.e.*, 0.8 to 1 pct.

DOI: 10.1007/s11663-014-0244-3

I. INTRODUCTION

ALTHOUGH chemical oxidation states for chromium (Cr) range from −4 to +6,[1], only Cr(III) and Cr(VI) are stable in the ambient environment.[2–4] Cr(III) is considered an essential micro-nutrient that is essential for protein, carbohydrate, and lipid metabolism in animals and humans,[5] while Cr(VI) is generally considered to be carcinogenic, mutagenic, and teratogenic.[6,7]

Cr(VI) can be generated and/or released into the environment through various anthropogenic activities, *e.g.*, chromate chemical manufacturing,[8,9] electroplating,[10] leather tanning,[11] cement manufacturing,[12] paint industries,[13] stainless steel welding,[14] and stainless steel production.[15] Of relevance in this paper is the generation of Cr(VI) during ferrochrome (FeCr) production. FeCr is produced from chromite ore and is a relatively crude alloy that consists mainly of Cr and iron (Fe). FeCr is the only source of new Cr units used during stainless steel production for which 80 to 90 pct of all produced FeCr is used.[16] Stainless steel is a vital alloy in the modern society, making FeCr equally important.

Ma characterized off-gas dust from a FeCr smelter in South Africa, but did not specifically consider all the production steps that could lead to Cr(VI) formation.[17] Beukes *et al.*[18] reviewed the generation of Cr(VI) during FeCr production. According to this paper and references therein, several ferrochrome production steps can lead to Cr(VI) formation. This review[18] also highlighted uncertainties with regard to certain production steps that need to be further investigated in order to enhance the current understanding of Cr(VI) generation during FeCr production. One such process is the flaring of CO-rich off-gas from closed submerged arc furnaces (SAF). In Figure 1, an example of a typical off-gas flare from a closed FeCr SAF burning on a stack is presented.

Off-gas from a closed FeCr SAF is usually cleaned with wet venturi scrubbing, which removes 99.9 pct of particulate matter in the off-gas, reducing particulate matter from 35 to 45 g/Nm^3 to 50 to 100 mg/Nm^3.[19] In certain first-world countries, the remaining particulate matter is further removed with sintered filters leaving less than 1 mg/Nm^3 particulate matter in the cleaned furnace off-gas.[19] However, in most developing countries, this last step, *i.e.*, sintered filtering after wet venturi cleaning, has not been implemented. This implies that some Cr-containing particulate matter will pass through the CO-rich off-gas stack flare, which could lead to the possible formation of Cr(VI). This release of Cr(VI) is of great concern, since Cr(VI) is considered to be carcinogenic, particularly for the respiratory track. Currently, almost no data exist in the peer-reviewed public domain to quantify the conversion of Cr(III), *i.e.*, the oxidation state of Cr in the chromite ore, to Cr(VI) during the flaring process. As far as the authors could assess, only a personal communication has been cited in an environmental impact assessment (EIA),[20] which indicated that approximately 0.8 to 1 pct of Cr(III) is converted to Cr(VI) during flaring. This conversion factor has since been used in various EIAs, although it is largely

S.P. DU PREEZ, Post graduate student, J.P. BEUKES, Chief Research Scientist and Lecturer, P.G. VAN ZYL, Lecturer, are with Chemical Resource Beneficiation, North-West University, Potchefstroom Campus, Private Bag X6001, Potchefstroom, 2520, South Africa. Contact e-mail: paul.beukes@nwu.ac.za
Manuscript submitted May 29, 2014.
Article published online November 21, 2014.

Fig. 1—A typical CO-rich off-gas flare on top a closed FeCr SAF stack.

unverified since no supporting data were supplied in the afore-mentioned personal communication.

In order to partially address the uncertainty relating to Cr(III) to Cr(VI) conversion during flaring of CO-rich off-gas from closed FeCr SAFs, the influence of flaring temperature, size of the particles passing through the flare, and retention time within the flame were investigated in this paper. Although the oxidation of Cr(III) to Cr(VI) depends on various factors,[21,22] these three factors are likely to be important within this context. Multiple linear regression was also used to combine the effect of the three parameters investigated to estimate the overall impact.

II. MATERIALS AND METHODS

A. *Materials*

Two case study chromite ores were used, *i.e.*, a metallurgical grade chromite ore and an upgraded upper group 2 (UG2) ore that originated from platinum group metal (PGM) processing. Both these ores were obtained from a large FeCr producer in South Africa that used these ores as feedstock for the production of FeCr. A detailed characterization of these two ore samples was recently presented by Glastonbury *et al.*[23] Of importance for this study is the Cr_2O_3 contents of these ores, which were 44.19 and 41.82 pct for the metallurgical grade and UG2 ores, respectively. These values were used to determine the conversion of Cr(III) to Cr(VI).

All chemicals used in this study were of analytical grade. Calibration of the Cr(VI) analytical instrument was performed using a chromate reference standard (Spectroscan) with a certified concentration of 1009 ± 5 μg/mL CrO_4^{-2}. Ammonium sulfate (Merck) and a 25 pct ammonia solution (Ace) were used to prepare the eluent utilized for Cr(VI) analysis. Post-column reagent was prepared using 1,5-diphenylcarbazide (Fluka Analytical), 98 pct sulfuric acid (Rochelle Chemicals), and HPLC grade methanol (Ace). Sodium hydroxide (Promark chemicals) and sodium carbonate (Minema) were used to prepare a Na_2CO_3-NaOH buffer to extract Cr(VI) from samples. Deionized water (resistivity 18.2 MΩ/cm) produced by a Milli-Q water purification system was used in all procedures that required dilution, as well as to clean glassware. Self-indicating silica gel (Labchem) was placed in desiccators used in procedures where samples had to be dried. 99.999 pct pure nitrogen (N_2) (AFROX) was used to purge all Cr(VI) extraction solutions and the headspace of extraction containers during leaching procedures.

B. *Milling and Partitioning of Ore into Size Fractions*

Since Cr(III) occurs in the spinel mineral structure in chromite, it is unlikely that any Cr(VI)/Cr(III) interconversions will take place in chromite ore samples in the ambient environment. However, Mandiwana *et al.*[24] indicated that small amounts of Cr(VI) might occur in South African chromite ore, although this was questioned by Glastonbury *et al.*[25] Fine chromite ores, such as metallurgical grade and UG2, are commonly upgraded in wet gravity separation methods (*e.g.*, spiral). Atmospheric SO_2 can dissolve in moisture, which can result in Cr(VI) reduction.[26,27] Therefore, as a precautionary measure, the received ore samples were dried in desiccators prior to further use.

Since particle size was one of the parameters considered in this study, it was decided to separate ore particles into several size fractions, *i.e.*, >250, 125 to 250, 75 to 125, 63 to 75, 45 to 63, and <45 μm. For the >250, 125 to 250, and 75 to 125 μm size fractions, the as-received dried metallurgical grade and UG2 chromite ores were screened into these factions with a Haver EML Digital Plus shaker and Haver & Boecker sieves. Since only a small weight percentage of both the case study ores contained particles <75 μm,[23] the ores were milled to generate finer particles. A Siebtechnik pulverizer was used for this purpose. Milling time was kept to approximately 4 minutes to minimize Cr(VI) formation during milling.[25] All parts of the pulverizer that made contact with the ore were made of tungsten carbide, preventing possible iron contamination. Five 100 g batches of both ores were milled. The mill was thoroughly cleaned after milling each batch in order to prevent contamination of the different ore types with each another. Thereafter, each milled 100 g ore batch was sieved for 30 minutes in the previously described shaker with the appropriate screen sizes to yield size fractions of 63 to 75, 45 to 63, and <45 μm. All the size-fractioned ore samples were collected, sealed in individual plastic containers, and stored in a desiccator for future use.

C. *Particle Size Analysis*

Particle size distribution analyses were performed on the size-fractioned chromite ores samples with laser diffraction particle sizing using a Malvern Mastersizer 2000. In order to prevent the use of chemical dispersant, samples were ultra-sonicated prior to the particle size measurements. Mechanical stirring was set to 2000 rpm and laser obscuration was kept between 10 and 15 pct.

D. *Experimental Setup for Cr(VI) Generation*

In order to investigate the rapid heat exposure associated with FeCr SAF off-gas flaring, a tube furnace was placed vertically, allowing ore fines to be exposed to heat as they were dropped through the tube. A 18kW Lenton Elite tube furnace with a Schunk AluSIK type C610 "A" impervious mullite ceramic tube (75 mm × 65 mm × 1500 mm) with a chemical composition of 60 pct Al_2O_3 and 40 pct SiO_2 was used. This experimental setup had a maximum operational temperature of 1774.15 K (1500 °C). During each experiment, 5 g of a specific sample, *i.e.*, a specific ore type and particle size fraction, was dropped through the furnace that was set at a predetermined temperature and collected at the bottom. The top end of the tube was closed off with a piece of flat ceramic material and only briefly opened to drop the sample down the tube, where after it was again closed off immediately to prevent ultra-fine particles being dragged upward due to the chimney effect. Samples were then allowed to cool down to room temperature. Cooled samples were then placed in sample containers that were sealed and stored in a desiccator until future use.

In order to evaluate the effect of retention time of particulate matter within the FeCr SAF off-gas flare on the formation of Cr(VI), specific samples were dropped multiple times through the furnace tube. However, only 950 mm of the 1500 mm furnace tube is insulated within the furnace housing of which only approximately the middle third of the isolated tube is accurately heated to the desired temperature. This implies that particulate matter dropped through the tube furnace was only exposed to the targeted temperature for 320 mm, which correlated to approximately 0.148 seconds. Samples that were dropped multiple times through the tube were not allowed to cool down between drops.

Since Cr(III) oxidation is dependent on temperature, the temperature range relevant to closed FeCr SAF off-gas flaring had to be established. According to Niemelä *et al.*, the minimum ignition temperature of CO in air is 904.15 K (630 °C) and the theoretical burning temperature of pure CO in air is 2524.15 K (2250 °C). This range, *i.e.*, 904.15 K to 2524.15 K (630 °C to 2250 °C), can therefore be used as an estimate of the relevant temperature range that had to be investigated experimentally. In addition to this literature-based information, the temperature range was also calculated using the thermodynamics software program HSC.[28] Off-gas burns at a range of temperatures, depending on the composition of the gas. Typical gas compositions for a closed FeCr SAF have been reported to be CO 60 to 90 pct, CO_2 10 to 40 pct, N_2 2 to 7 pct, and H_2 2 to 10 pct.[19] The adiabatic flame temperatures of various gas mixtures within the range of these gas compositions were subsequently calculated with HSC. Results indicated that a maximum temperature of 2525.35 K (2251.2 °C) was calculated for a gas composition of 100 pct CO, which correlated almost perfectly with the theoretical burning temperature reported by Niemelä *et al.* Considering the literature-based and thermodynamically calculated flaring temperatures of FeCr SAF off-gas, it was decided to expose particulate matter to temperatures ranging from 874.15 K to 1674.15 K (600 °C to 1400 °C). Higher temperatures could not be investigated due to instrumental limitations of the tube furnace utilized.

E. *Cr(VI) Extraction from Heat-Treated Ores Fines*

Total Cr(VI) had to be extracted from a solid matrix into an aqueous phase without causing any interconversions between Cr(VI) and Cr(III). Cr(VI) compounds can be classified as water soluble and water insoluble.[29] Therefore, to accurately determine the total Cr(VI) concentrations, both water soluble and water insoluble compounds had to be extracted. This was achieved by conducting hotplate digestion extraction with a sodium carbonate and sodium hydroxide buffer solution, as suggested by Ashley *et al.* This buffer was prepared by dissolving 60 g sodium carbonate and 40 g sodium hydroxide in a 2 L volumetric flask. A hot alkaline extraction solution saturated with air could lead to *in situ* formation of Cr(VI) in the presence of Cr(III).[29] Therefore, in order to prevent the unwanted oxidation of Cr(III), extraction solutions and the headspace of the extraction container were purged with N_2 prior to, during, and after Cr(VI) extraction. After extraction, the solutions were purged until the solution cooled down to room temperature. 0.5 g of each sample was leached in 50 mL buffer solution for 60 minutes during hotplate extraction. Thereafter, the aqueous solution was filtered using a 0.45 μm Whatman filter. The filtrate was then placed in an airtight glass container and stored until Cr(VI) analysis was conducted.

F. *Cr(VI) Analysis*

The analytical method utilized in this study was adapted from DIONEX Application updates 144 and 179,[30,31] and Thomas *et al.*,[32] as described by Loock *et al.*[33] The Cr(VI) content of extracted solutions was determined using an ion chromatograph (IC) with a post-column 1,5-diphenylcarbazide (DPC) colorant delivery system (AXP pump) coupled to a UV–visible absorbance detector. The Thermo Scientific DIONEX ICS-3000 ion chromatograph system consists of a Dionex IonPac AG7 4 × 50 mm guard column, Dionex IonPac AS7 4 × 250 mm analytic column, a 1000 μL injection coil, and two 375 μL reaction coils fitted in series. An isocratic pump was used to transport injected samples with the eluent through the system. Flow rates utilized for DPC and eluent were 0.5 and 1.0 mL/min, respectively. Additional polyetherketone tubing was installed between the AXP pump and the back pressure tubing to reduce the pulse caused by the AXP pump,

which minimized the baseline noise of the chromatograms. This produced a smoother baseline and ensured more accurate analyses, especially for lower Cr(VI) concentrations. A six-point calibration line (between 5 and 75 μg/L) was used, which had a relative standard deviation ≤1.8 pct and a correlation coefficient ≥99.96 pct. The detection limit for this analytical setup was 1 μg/L.[30] In addition to the excellent detection limit, the analytical procedure utilized also prevented false positive Cr(VI) values, which is common with the direct DPC UV–visible method.[29]

The IC eluent was prepared by dissolving 66 g ammonium sulfate and 15.08 g ammonium hydroxide in 2 L deionized water. The DPC colorant was prepared by adding 28 mL 98 pct sulfuric acid to approximately 100 mL deionized water in a 1 L volumetric flask. The solution was then cooled down to room temperature. 0.5 g DPC was placed in a 100 mL volumetric flask with approximately 80 mL methanol. After most of the DPC had dissolved, the solution was diluted to 100 mL with methanol. Thereafter, the DPC methanol solution was steadily added to the sulfuric acid solution, which was then left to cool down to room temperature. Before the DPC solution was used for analysis, it was filtered with a 0.45 μm milli-pore filter to ensure that no solid particles were present that could block the fine tubes of the IC.

G. *Expressing Cr(VI) Conversion*

Since the percentage of Cr(VI) converted from Cr(III) during FeCr SAF off-gas flaring is currently utilized in EIAs for FeCr smelters,[20] all results were expressed as percentage Cr(VI) conversion, *i.e.*, pct Cr(VI) conversion. As explained later, expressing the results in this format enables the calculation of actual Cr(VI) emissions from individual FeCr smelters, which makes the results both scientifically significant and practically usable. All results reported are mean values calculated from triplicate repetition of particular experimental conditions and subsequent Cr(VI) analysis. Since it is well known that Cr(VI) can be generated during the milling of chromite,[25,34] the Cr(VI) contents of the size-fractioned ores samples were determined to establish a baseline. These baseline values were subtracted from the Cr(VI) contents determined after exposure to heat, to reflect the real Cr(VI) conversion.

H. *Multiple Linear Regression Analysis*

Linear regression is denoted by constants or known parameters (c), an independent variable (x) and a dependent variable (y). Multiple linear regression (MLR) is characterized by more than one independent variable (x). In MLR, the relationship between the dependent variable (y) and independent variables (x) is denoted by the equation:

$$y = c_0 + c_1x_1 + c_2x_2 + c_3x_3 + \ldots c_zx_z \qquad [1]$$

In this study, MLR was used to determine an equation for the dependent variable, *i.e.*, pct Cr(VI) conversion (y in Eq. [1]), expressed in terms of the independent variables, *i.e.*, flaring temperature, particle size, and retention time (x in Eq. [1]). This was achieved by utilizing a fit-for-purpose Matlab program.

III. RESULTS AND DISCUSSION

A. *Particle Size Analysis of Size-Fractioned Samples*

Various size-fractioned particle samples were generated from both case study ores, *i.e.*, >250, 125 to 250, 75 to 125, 63 to 75, 45 to 63, and <45 μm. D_{90} (defined as the equivalent particle size of which 90 pct of the particles are finer), d_{50}, and d_{10} values for both ores, as a function of all size fractions, were determined and are presented in Table I. In the rest of the paper, d_{90} will mostly be used as a reference for particle size for the various size fractions.

B. *Influence of Temperature on Pct Cr(VI) Conversion*

The effects of temperature on the pct Cr(VI) conversion observed for metallurgical grade and UG2 chromite ore fines are presented in Figures 2(a) and (b), respectively. The retention time of the particles in the hot zone of the tube furnace was kept constant at 0.148 seconds, *i.e.*, a single pass. Minimum, maximum, and/or standard deviation values are not indicated for the experimental results presented in these and subsequent figures, in order to prevent cluttering of the graphs. However, the maximum standard deviation observed in all experiments was approximately two orders of magnitude lower than the actual pct Cr(VI) conversion values, indicating very good repeatability of the results.

As is evident from the results presented in Figure 2(a), metallurgical grade chromite ore fines exposed to the lowest experimentally investigated temperature (874.15 K, 600 °C) had the lowest pct Cr(VI) conversion with conversion percentages ranging from 7.1×10^{-4} pct for the size fraction with the largest particles (d_{90} of 910 μm) to 1.97×10^{-3} pct for the size fraction with the smallest particles (d_{90} of 45 μm). The pct Cr(VI) conversion thereafter increased with an increase in temperature for all size fractions. At the maximum experimentally investigated temperature, *i.e.*, 1674.15 K (1400 °C), pct Cr(VI) conversion reached the highest levels. The size fraction with the largest particles had a pct Cr(VI) conversion of 1.37×10^{-3} pct, whereas the size fraction with the smallest particles had a conversion of 3.69×10^{-3} pct.

Results obtained for UG2 ore fines (Figure 2(b)) exposed to the different temperatures were very similar to that obtained for the metallurgical grade ore fines (Figure 2(a)). At 874.15 K (600 °C), the size fraction with the largest particles (d_{90} of 985 μm) had a pct Cr(VI) conversion of 7.6×10^{-4} pct, while the size fraction with the smallest particles (d_{90} of 45 μm) had a conversion of 1.83×10^{-3} pct. Percent Cr(VI) conversions reached 1.48×10^{-3} pct for the size fraction with the largest particles and 3.81×10^{-3} pct for the size fraction with the smallest particles at 1674.15 K

Table I. d_{90}, d_{50}, d_{10} Values of Metallurgical Grade Chromite and UG2 Ores as a Function of Sieved Size Fractions

	Sieve Sizes (μm)					
	>250	125 to 250	75 to 125	63 to 75	45 to 63	<45
Metallurgical Grade						
d_{90}	910.5	310.9	173.9	87.8	79.7	45.6
d_{50}	582.3	220.4	122.6	19.7	28.4	18.5
d_{10}	363.4	156.1	86.2	1.6	2.3	1.6
UG2						
d_{90}	985.4	310.3	161.8	87.1	60.4	45.3
d_{50}	587.8	219.5	113.6	17.8	18.3	22.1
d_{10}	337.5	155.4	79.7	0.9	1.1	2.1

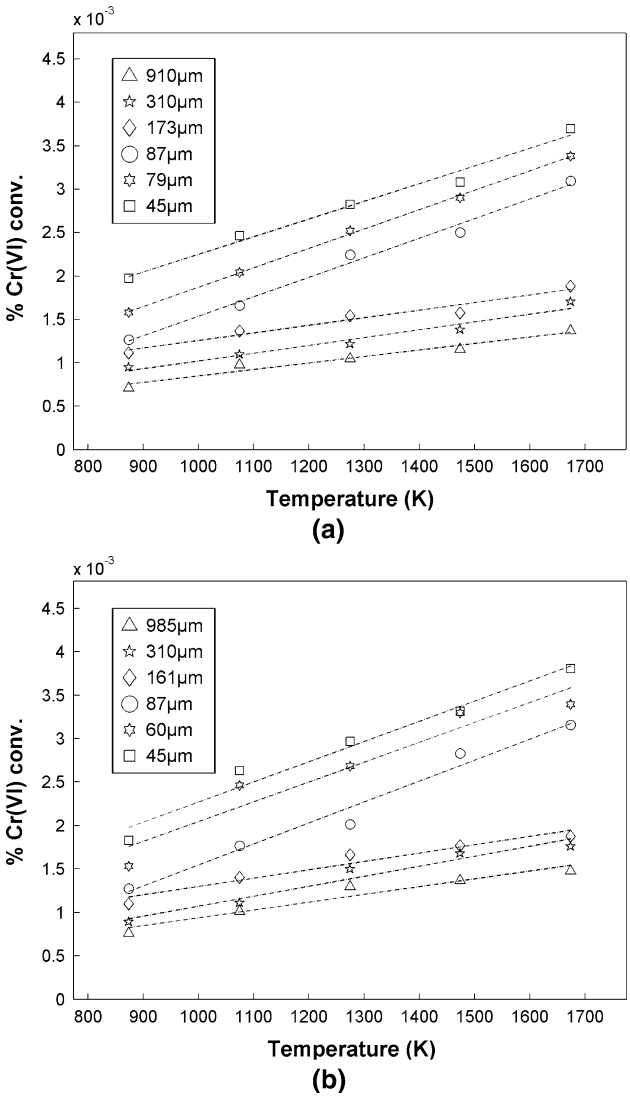

Fig. 2—The influence of temperature on pct Cr(VI) conversion for all particle size fractions (indicated with d_{90} values) of (*a*) metallurgical grade chromite and (*b*) UG2 ore fines. The retention time of the particles in the hot zone of the tube furnace was kept constant at 0.148 s, *i.e.*, a single pass.

(1400 °C). From Figure 2, it is also clear that the pct Cr(VI) conversion increased linearly with an increase in exposure temperature for the metallurgical grade and the UG2 ores.

As is evident from the results presented in both Figures 2(a) and (b), the slope, *i.e.*, pct Cr(VI) conversion increase per temperature unit, was different for the as-received, sieved size fractions (>250, 125 to 250, 75 to 125 μm), if compared to the slope for the milled size fractions (63 to 75, 45 to 63, and <45 μm). Milling could have resulted in some chromite crystalline damage, which might make these particles more susceptible to oxidation. However, more research needs to be conducted to postulate a reasonable explanation.

C. *Influence of Particle Size on Pct Cr(VI) Conversion*

For a constant amount of particulate matter, the surface area will increase as the particle size decreases. For smaller particles, this implies a larger surface area that can be oxidized within the off-gas flare. The effects of d_{90} particle size on pct Cr(VI) conversion for metallurgical grade chromite and UG2 ore fines are presented in Figures 3(a) and (b), respectively.

As is evident from the results (Figure 3(a)), metallurgical grade ore fines with a d_{90} of 910 μm had the lowest pct Cr(VI) conversion at each of the temperatures investigated, with pct Cr(VI) conversions ranging from 7.1×10^{-4} pct for samples exposed to 874.15 K (600 °C) to 1.37×10^{-4} pct for samples exposed to 1674.15 K (1400 °C). Thereafter, pct Cr(VI) conversion increased almost in an exponential manner as the d_{90} particle size decreased. The smallest particles (size fraction with d_{90} of 45 μm) had the highest Cr(VI) conversions of 1.97×10^{-3} pct for samples exposed to 874.15 K (600 °C) and 3.69×10^{-3} pct for samples exposed to 1674.15 K (1400 °C). Results obtained for all size fractions of UG2 ore fines (Figure 3(b)) showed a similar trend when compared to metallurgical grade chromite fines (Figure 3(a)). Fitting of the afore-mentioned results indicated that the relationship between pct Cr(VI) conversion and particle size had a power factor dependence with the general format of $d_{90}^{-0.3203}$.

D. *Influences of Retention Time on Pct Cr(VI) Conversion*

To investigate the influence of retention time on pct Cr(VI) conversion, the two size fractions with the largest particles (d_{90} of 910 and 310 μm for metallurgical grade and d_{90} of 985 and 310 μm for UG2) were exposed to

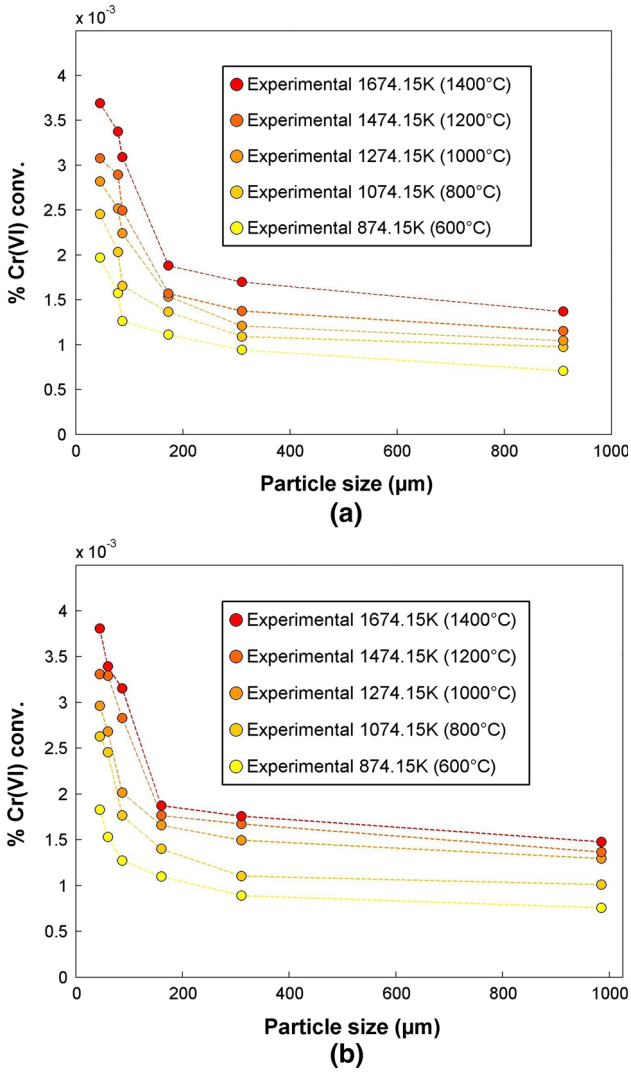

Fig. 3—The influence of particle size (indicated with d_{90} values) on pct Cr(VI) conversion for all temperature ranges of (*a*) metallurgical grade chromite and (*b*) UG2 ore fines. The retention time of the particles in the hot zone of the tube furnace was kept constant at 0.148 s, *i.e.*, a single pass.

the highest temperature 1674.15 K (1400 °C) in consecutive multiple drop experiments through the tube furnace. These larger particles were less prone to the chimney effect, making consecutive multiple drop experiments feasible. The effects of retention time on pct Cr(VI) conversion for the metallurgical grade chromite and UG2 ore fines are shown in Figure 4.

It is evident from these results (Figure 4) that increased retention times led to higher pct Cr(VI) conversions. Cr(VI) conversions ranged from 1.34×10^{-3} to 1.74×10^{-3} pct at the shortest evaluated retention time, *i.e.*, 0.148 seconds, for both ore types and the two sized fractions. At the longest evaluated retention time, *i.e.*, 0.594 seconds, the pct Cr conversions ranged from 4.185×10^{-3} to 6.53×10^{-3} pct. Fitting of the afore-mentioned results indicated that the relationship between pct Cr(VI) conversion and retention time had an exponential dependence with the general format of $0.001075e^{(2.75754)(\text{Retention time})}$.

E. *Multiple Linear Regression to Calculate Overall Pct Cr(VI) Conversion*

In Figure 5, the relationship between the number of independent variables included in the optimum MLR analysis solution (*x*-axis) and the root mean square error (RMSE) (*y*-axis) difference between the calculated and experimental pct Cr(VI) conversions is presented. In this statistical analysis, all possible independent variable combinations of temperature, particle size after being converted to $d_{90}^{-0.3203}$ and retention time after being converted to $0.001075e^{(2.75754)(\text{Retention time})}$, were considered to calculate the dependent variable, *i.e.*, pct Cr(VI) conversions. The data for both case study ore types were combined in the MLR analysis, since the intention was to determine a single MLR equation that could be applied to any Cr-containing off-gas particulate material and not only specific ores.

According to the MLR analysis conducted, statistically, retention time was the independent variable that had the most significant impact on minimizing the difference between the experimental pct Cr(VI) conversion and MLR calculated value. This is graphically illustrated in Figure 5, which shows that an MLR equation containing only the retention time had an RMSE difference between the calculated and experimental pct Cr(VI) conversion of approximately 7.9×10^{-4}. Addition of particle size, *i.e.*, d_{90}, which was found to be the second most significant independent variable, to the optimum MLR solution decreased the RMSE further. When all three investigated independent variables were included in the MLR solution, the RMSE decreased to approximately 2.83×10^{-4}.

From the above-mentioned MLR analysis, the optimal equation, containing all three the investigated independent variables, was determined as follows:

$$\begin{aligned}\text{Pct Cr(VI) conversion} &= -3.78 \times 10^{-3} \\ &+ \left(1.51 \times 10^{-6} \times \text{Temp}\right) + \left(1.07 \times 10^{-2} \times d_{90}^{-0.3203}\right) \\ &+ \left(0.94 \times 1.08 \times 10^{-3} e^{(2.75475)(\text{Retention time})}\right),\end{aligned} \quad [2]$$

where Temp is the exposure temperature (K), d_{90} the d_{90} particle size (μm) of the particulate matter passing through the tube furnace, and Retention time the retention time (seconds) of particles within the hot zone of the furnace.

From Eq. [2], it was possible to calculate pct Cr(VI) conversions for both case study ores and compare these mathematically calculated values to experimental values, which are presented in Figures 6(a) and (b) for metallurgical grade chromite and UG2 ore fines, respectively. In these figures, all experimentally investigated independent variable (exposure temperature, retention time and particle size) conditions are presented in one figure for each ore type. The first six columns indicate pct Cr(VI) conversions as a function of varying particle size (indicated in *x*-axis) and temperature (indicated with color) for a fixed retention time, *i.e.*, 0.148 seconds, while the last two columns indicate pct Cr(VI) conversions as a function of longer retention times, *i.e.*, from

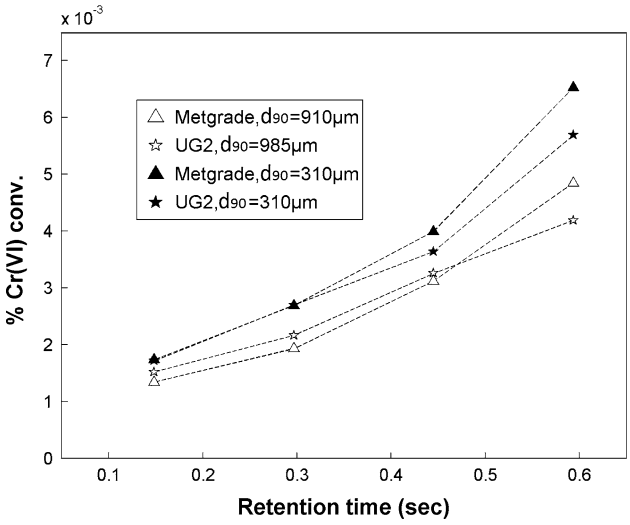

Fig. 4—The influence of retention time on pct Cr(VI) conversion for metallurgical grade chromite and UG2 ore fines at 1674.15 K (1400 °C).

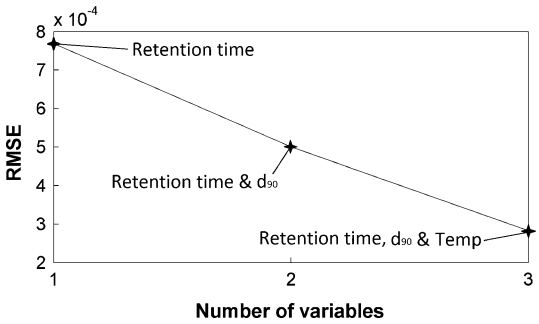

Fig. 5—RMSE difference between calculated pct Cr(VI) conversion for the combined dataset determined for metallurgical grade chromite and UG2 ore fines as a function of the independent variables included in the MLR solution.

0.148 to 0.593 seconds, at a constant temperature [1674.15 K (1400 °C)]. Although there are some differences between the experimentally determined pct Cr(VI) conversions and values calculated with the MLR Eq. [2], it is evident from Figures 6(a) and (b) that Eq. [2] can be used relatively effectively to determine pct Cr(VI) conversions.

F. *Industrial Relevance and Practical Application*

The optimum MLR Eq. [2], which was determined in Section II–E, can be used by specific FeCr smelters to estimate pct Cr(VI) conversion more accurately than the present estimations. Since three independent variables were included in the optimum MLR solution, *i.e.*, retention time, $d_{90,}$ and temperature, these parameters have to be determined or estimated for such application.

Retention time will depend on the length of the flare and the exit velocity of the off-gas. The length of the flare will depend on the operating conditions of a particular SAF—an SAF running at full power input (MWh) will produce more off-gas than an SAF operating at reduced power input. In practice, the flare

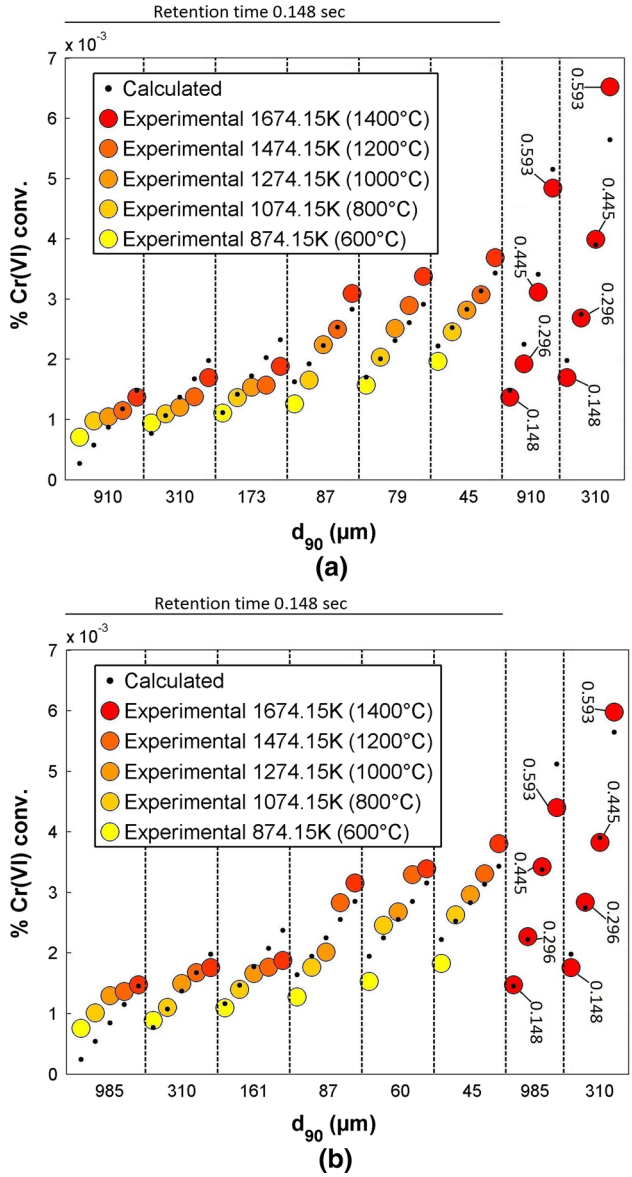

Fig. 6—Calculated pct Cr(VI) conversion values using Eq. [2] compared to experimental values for (*a*) metallurgical grade chromite and (*b*) UG2 ore fines.

length can be determined using a photo of the stack flare (such as Figure 1), with the diameter of the furnace flare stack serving as the scale to calculate the flare length. For the flare indicted in Figure 1, for instance, the flare length was calculated to be approximately 6.05 m. The off-gas velocity of this particular stack was also known to the authors, *i.e.*, 6 m/s. From these two parameters, the retention time of particulate matter in the flare can be determined. For the flare shown in Figure 1, it was calculated to be 1.01 seconds.

The d_{90} particle size of actual particles can be determined by collecting and analyzing particles from piping/equipment after the wet venturi scrubber. It would not be advisable to collect such particles during operation, since CO gas is very poisonous and can also result in a CO gas explosion. However, some particles tend to collect/build up within the off-gas piping and/or

the blades of the venturi fan, which can be accessed during plant maintenance periods. The d_{90} size of these particles can be determined by performing laser diffraction particle size analysis, as discussed in Section II–C.

The off-gas flare temperature can be determined using an infrared thermometer or infrared camera to visually determine the temperature, or alternatively it can be calculated with thermodynamic software based on the actual off-gas composition, as was indicated in Section II–D.

As an example of the practical application, the pct Cr(VI) conversion for a typical closed SAF can be considered. In this example, the retention time of the particulate matter is 1.01 seconds (for 6 m flare and exit velocity of 6 m/s, derived from Figure 1). According to Niemelä *et al.*, it is theoretically difficult to remove particles smaller than 1 μm from the off-gas stream with a wet venturi scrubber; therefore, the d_{90} was assumed to be 1 μm. The flaring temperature was assumed to be 2274.15 K (2000 °C), which is less than the burning temperature of pure CO due to typical dilution from other gases present in the off-gas, *e.g.*, CO_2 and N_2. Replacing these values into Eq. [2] yielded a pct Cr(VI) conversion of 2.7×10^{-2} for this specific FeCr SAF.

For an unrealistic worst-case scenario, it can be assumed that the retention time is 2.02 seconds (which represents a 12 m flare with an exit velocity of 6 m/s), the d_{90} particle size is 0.005 μm (which is an unrealistic small d_{90} particle size), and the flaring temperature is the highest temperature obtained from literature/thermodynamic calculations for pure CO combustion, *i.e.*, 2525.35 K (2251.2 °C). Equation [2] yielded a pct Cr(VI) conversion of 3.5×10^{-1} for this scenario. These calculated values indicate that the realistic and unrealistic worst-case scenarios pct Cr(VI) conversions are significantly lower than the pct Cr(VI) conversion values currently used in EIAs to determine the Cr(VI) emissions from FeCr smelters.

If the pct Cr(VI) conversion for a specific closed FeCr SAF is calculated as indicated above with Eq. [2], the total amount of Cr(VI) released from it can also be calculated if the average Cr(III) content of the off-gas and total off-gas volume is known or estimated.

IV. CONCLUSIONS

As far as the authors could assess, this is the first investigation published in the peer-reviewed public domain on the formation of Cr(VI) during the flaring of off-gas from closed FeCr SAFs. Three parameters considered to be critical during flaring were experimentally investigated in a tube furnace, *i.e.*, retention time of the particles in the hot zone, size of particulate matter passing through the hot zone (d_{90}), and temperature of the hot zone. MLR analysis indicated that retention time had the greatest impact on pct Cr(VI) conversion, followed by particle size and temperature. From the MLR analysis, an optimal equation, *i.e.*, Eq. [2], containing all three the investigated independent variables was determined, which reflected the overall impact of these parameters on pct Cr(VI) conversion. Equation [2] was subsequently used to calculated pct Cr(VI) conversions, which compared well to the experimentally determined values. Thereafter, this equation was used to determine pct Cr(VI) conversions for closed FeCr SAFs, which yielded 2.7×10^{-2} and 3.5×10^{-1} for realistic and unrealistic worst-case scenarios, respectively. In this practical application of Eq. [2], it was necessary to extrapolate to smaller particles sizes, higher temperatures, and longer retention times than the conditions that could be experimentally investigated. However, the overall pct Cr(VI) conversions obtained from Eq. [2] represent a much more reliable representation than the unsubstantiated pct Cr(VI) conversion currently being used in EIAs for FeCr smelters, *i.e.*, 0.8 to 1 pct. In future, the Cr(VI) conversion of a specific FeCr smelter can be calculated utilizing Eq. [2]. This conversion factor can then be included as an emission factor in an atmospheric dispersion model applied during an EIA to determine the Cr(VI) levels to which communities will be exposed. These exposure levels can then be related directly to possible health impact. Additionally, FeCr producers should be encouraged to flare less CO-rich off-gas, considering the international drive to reduce flaring,[35] as well as the increasing pressure on FeCr producer to reduce their carbon footprint and electricity consumption.

ACKNOWLEDGMENTS

The authors would like to thank Mr Nico Lemmer from the Faculty of Engineering for the use of the particle size analyzer and Mr Kosie Oosthuizen from the Geology Subject Group for the use of the pulverizer.

REFERENCES

1. M. Gheju and A. Iovi: *J. Hazard. Mater.*, 2006, vol. 135, pp. 66–73.
2. D. Mohan and C.U. Pittman: *J. Hazard. Mater.*, 2006, vol. 137, pp. 762–811.
3. L.E. Eary and A. Davis: *Appl. Geochem.*, 2007, vol. 22, pp. 357–69.
4. L.N. Døssing, K. Dideriksen, S.L.S. Stipp, and R. Frei: *Chem. Geol.*, 2011, vol. 285, pp. 157–66.
5. T.O. Berner, M.M. Murphy, and R. Slesinski: *Food Chem. Toxicol.*, 2004, vol. 42, pp. 1029–42.
6. A. Bielicka, I. Bojanowska, and A. Wisniewski: *Pol. J. Environ. Stud.*, 2005, vol. 14, pp. 5–10.
7. H. Li, L. Zhao, L. Ting, X. Xiao, P. Zhihui, and L. Deng: *Technol.*, 2008, vol. 99, pp. 6271–79.
8. G. Darrie: *Environ. Geochem. Health*, 2001, vol. 23, pp. 187–93.

9. R.A. Whittleston, D.I. Steward, R.J.G. Mortimer, A.P. Brown, K. Geraki, and I.T. Burke: *J. Hazard. Mater.*, 2011, vol. 194, pp. 15–23.
10. H. Cui, M. Fu, S. Yu, and M.K. Wang: *J. Hazard. Mater.*, 2011, vol. 186, pp. 1625–31.
11. A.D. Apte, S. Verma, V. Tare, and P. Bose: *J. Hazard. Mater.*, 2005, vol. 121, pp. 215–22.
12. S.S. Potgieter, N. Panichev, J.H. Potgieter, and S. Panicheva: *Cem. Concr. Res.*, 2003, vol. 33, pp. 1589–93.
13. T.S. Kassem: *Desalination*, 2010, vol. 258, pp. 206–18.
14. P.T.J. Scheepers, G.A.H. Heussen, P.G.M. Peer, K. Verbist, R. Anzion, and J. Willems: *Toxicol. Lett.*, 2008, vol. 178, pp. 185–90.
15. B. Dhal, H.N. Thatoi, N.N. Das, and B.D. Pandey: *J. Hazard. Mater.*, 2013, vols. 250–251, pp. 272–91.
16. E.L.J. Kleynhans, J.P. Beukes, P.G. van Zyl, P.H.I. Kestens, and J.M. Langa: *Miner. Eng.*, 2012, vol. 34, pp. 55–62.
17. G. Ma: PhD dissertation, University of Pretoria, South Africa, 2006.
18. J.P. Beukes, P.G. Van Zyl, and M. Ras: *J. S. Afr. Inst. Min. Metall.*, 2012, vol. 112, pp. 347–52.
19. P. Niemelä, H. Krogerus, and P. Oikarinen: *Proceedings of 10th International Ferroalloys Congress*, Cape Town, South Africa, February 2004, pp. 68–77.
20. C. Venter, and H. Liebenberg-Enslin: *Air Quality Impact Assessment Study for the Proposed Xstrata Lion Project*, Steelpoort, Report No. APP/04/METAGO-2 Rev 2, Airshed Planning Professionals (Pty) Ltd, South Africa, October 2004, pp. 1–86.
21. M.J. Ferreira, M.F. Almeida, and T. Pinto: *J. S. Leath. Tech. Ch.*, 1999, vol. 83, pp. 135–38.
22. J. Chen, M. Wey, B. Chiang, and S. Hsieh: *Chemosphere*, 1998, vol. 36, pp. 1553–64.
23. R.I. Glastonbury: MS dissertation, North-West University, Potchefstroom Campus, North West, South Africa, 2013.
24. K.L. Mandiwana, N. Panichev, and P. Ngobeni: *J. Hazard. Mater.*, 2007, vol. 145, pp. 511–14.
25. R.I. Glastonbury, W. van der Merwe, J.P. Beukes, P.G. van Zyl, G. Lachmann, C.J.H. Steenkamp, N.F. Dawson, and H.M. Steward: *Water SA*, 2010, vol. 36, pp. 105–10.
26. J.P. Beukes, J.J. Pienaar, G. Lachmann, and E.W. Giesekke: *Water SA*, 1999, vol. 25, pp. 363–70.
27. J.P. Beukes, J.J. Pienaar, and G. Lachmann: *Water SA*, 2000, vol. 26, pp. 393–96.
28. A. Roine: *HSC Chemistry*, 7th ed, Outotec Research, Pori, 2009, pp. 11-1–11-25.
29. K. Ashley, A.M. Howe, M. Demange, and O. Nygren: *J. Environ. Monit.*, 2003, vol. 5, pp. 707–16.
30. Dionex Corporation: *Determination of Hexavalent Chromium in Drinking Water Using Ion Chromatography*, Application Update 144, LPN 1495, Sunnyvale, CA, 2003.
31. Dionex Corporation: *Sensitive Determination of Hexavalent Chromium in Drinking Water*, Application Update 179, Sunnyvale, CA, 2011.
32. D.H. Thomas, J.S. Rohrer, P.E. Jackson, T. Pak, and J.N. Scott: *J. Chromatogr. A*, 2002, vol. 956, pp. 255–59.
33. M.M. Loock, J.P. Beukes, and P.G. van Zyl: *Water SA*, 2014, vol. 40, pp. 709–16.
34. J.P. Beukes and R.N. Guest: *Miner. Eng.*, 2001, vol. 14, pp. 423–26.
35. UN Sustainable Development Knowledge Platform. http://sustainabledevelopment.un.org/index.php?page=view&type=1006&menu=1348&nr=997, 2014. Accessed 22 October 2014.